BIOFUELS FROM LIGNIN AND NOVEL BIODIESEL ANALYSIS

A Dissertation
Presented to
The Academic Faculty

By

Máté Nagy

In Partial Fulfillment for the Degree
Doctor of Philosophy in the
School of Chemistry and Biochemistry

Georgia Institute of Technology

December, 2009

BIOFUELS FROM LIGNIN AND NOVEL BIODIESEL ANALYSIS

Approved by:

Dr. Arthur J. Ragauskas, Advisor
School of Chemistry and Biochemistry
Georgia Institute of Technology

Dr. Preet Singh
School of Materials Sci. and Eng.
Georgia Institute of Technology

Dr. Jake D. Soper
School of Chemistry and Biochemistry
Georgia Institute of Technology

Dr. Yulin Deng
School of Chemical and
Biomolecular Engineering
Georgia Institute of Technology

Dr. Uwe H. F. Bunz
School of Chemistry and Biochemistry
Georgia Institute of Technology

Date Approved: November 13, 2009

We do not inherit the earth from our ancestors, we borrow it from our children.

Native American song

Only those who will risk going too far can possibly find out how far one can go.

Thomas S. Eliot (1915-1965)

ACKNOWLEDGEMENTS

It is always hard to look back and try to remember all of those kind individuals who have helped me during my graduate studies. I would like to say ‘thank you’ to all of them.

First, I would like to express my sincere gratitude to my advisor, Dr. Arthur J. Ragauskas, for his instruction, encouragement, advice, and support throughout my graduate education. Thanks for trusting me and my capabilities. Thanks for forming my knowledge, and for instilling in me the engineering way of thinking.

I would also like to thank my thesis committee, Dr. Jake D. Soper, Dr. John Cairney, Dr. Preet Singh, Dr. Uwe H. F. Bunz, Dr. Yulin Deng, and Dr. George J. P. Britovsek for their insightful comments and support throughout this project.

I am grateful to my martial art coach, Mike Mobley who kept my spirits high even when I felt that as I were failing in my projects and when I questioned the validity of the great sacrifices that my family and I had to make to finish my graduate studies. Thanks, Renshi!

I would especially like to thank my senior co-workers for training me during my freshmen year. I also thank my current co-workers here in the United States and overseas for discussing those ‘simple problems’ with me and for keeping me driven throughout my research.

I am also grateful to my former supervisors, Dr. Kati Réczey, Dr. Ilona Sárvári Horváth and Dr. Zsolt Szengyel. Thank you for starting my scientific life and for introducing me to the ‘secrets and challenges’ of the scientific field of bioenergy and

biomaterials. Thanks you for giving me the educational foundation and the opportunities that will result in my accomplishment of a Ph.D. overseas.

A great deal of appreciation goes to Major White, who kept me safe during those long, overnight experiments, and who always told me cheerful stories and checked on me every night before he left the building. Thanks, Major!

Köszönettel tartozom szuleimnek hogy mindvégig bíztak bennem. Gondoskodásotokért, kitartásotokért, lelki és anyagi segítségetekért mindig is hálás maradok! Köszi Fatherka és Mutherka!

TABLE OF CONTENTS

LIST OF TABLES

LIST OF FIGURES

LIST OF EQUATIONS

LIST OF ABBREVATIONS

Atm	Atmospheric
bbl	Oil Barrel (42 US gallons)
BL	Black liquor
BTU	British thermal unit (1.06 kilojoules)
CO_2	Carbon dioxide
DAD	Diode-array detector
DMC	Direct microbial conversion
DMSO	Dimethyl sulfoxide
DOP	2-chloro-1,3,2-dioxaphospholane
DP	Degree of polymerization
DSC	Differential scanning calorimetry
DW	Deionized water
EDTA	Ethylenedinitrilotetraacetic acid
EOL	Ethanol organosolv lignin
ESI	Electrospray ionization
F	Filtrate fraction
FER	Fossil energy-replacement ratio
gal	Gallon
GC	Gas chromatography
GPC	Gel permeation chromatography
h	Hour

HMF	5-hydroxymethyl furfural
HPLC	High pressure liquid chromatography
HW	Hardwood
LLBL	Lignin-lean black liquor
LLC	Lignin-carbohydrate complexes
M_n	Number average molecular weight
MALDI	Matrix-assisted laser desorption ionization
min	Minute
MMT	Million metric tons
MS	Mass spectroscopy
M_w	Weight average molecular weight
MW	Molecular weight
MWD	Molecular weight distribution
MWL	Mill wood lignin
NIRS	Near infrared spectroscopy
NOE	Nuclear overhauser effect
NM	Non measured fraction
NMR	Nuclear magnetic resonance
P	Precipitate fraction
PD	Polydispersity
PFB	Pentafluorobenzaldehyde
ppm	Part-per-million
PPO	Pure plant oil

Pur	Purified sample
PVP	Polyvinylpyrrolidone
OS-MWL	Organosolv treated mill wood lignin
QM	Quinone methide
T	Temperature
TDS	Total dissolved solids
RT	Room temperature
s	Second
SEC	Size exclusion chromatography
SF	Salt fraction
SHF	Separated hydrolysis and fermentation
SSF	Simultaneous saccharification and fermentation
SW	Softwood
T_1	Spin-lattice relaxation time
T_g	Glass transition temperature
THF	Tetrahydrofuran
TMDP	2-chloro-4,4,5,5-tetramethyl-1,3,2-dioxaphospholane
TMP	Thermomechanical pulping
TOA	Tri-*n*-octylamine
TOF	Time of flight mass spectrometer
TPPMS	Sodium diphenyl(*m*-sulfonatophenyl)phosphine
UHP	Ultra high purity
UV	Ultraviolet

VIS	Visible light
VPO	Vapour pressure osmometry
wt. %	Weight percentage
WVO	Waste vegetable oil

SUMMARY

The forest biorefinery concept involves converting a pulp mill into a multi-purpose biofuels, biomaterials, and biopower production facility in which these products are produced in an environmentally compatible and sustainable manner. A key challenge in this process is the recovery of lignin from process streams such that it can be utilized in a variety of innovative green chemistry processes.

The first part of this thesis presents a study based on green prospects for the paper industries current (black liquor) and future (ethanol organosolv) lignin rich solutions. The first study examines the fundamental chemical structure of LignoBoost derived lignin recovered from Kraft pulping streams using an acid precipitation/washing methodology. Functional group analysis and molecular weight profiles were determined by nuclear magnetic resonance (NMR) and size exclusion chromatography. These findings gave valuable insight into the physical properties and the determining chemical properties of this currently underutilized, renewable bioresource. A known chemical structure and composition provided valuable data to optimize a subsequent controlled catalytic deoxygenation and liquefaction step for high yield biooil production.

The second study is based on the future second generation bioethanol production process, where ethanol produced from lignocellulosic materials will bring about the co-production of significant amounts of under-utilized lignin. The study examines the potential of conventional heterogeneous and novel homogeneous catalysts for the selective cleavage of the aryl-O-aryl and aryl-O-aliphatic linkages of ethanol organosolv lignin to convert it from a low grade fuel to potential fuel precursors or other value added

chemicals. The experimental data demonstrated that aryl-O-aryl and aryl-O-aliphatic linkages could be cleaved and the hydrogenated lignin had a decrease in oxygen functionality and the formation of products with lower oxygen content.

The second part of this thesis reports the development and optimization of a novel qualitative method for the determination of the various types of hydroxyl groups present in biodiesel production streams. In the first study, the use of 2-chloro-4,4,5,5-tetramethyl-1,3,2-dioxaphospholane (TMDP) as a phosphitylation reagent for quantitative ^{31}P-NMR analysis of the hydroxyl groups in biodiesel process samples has been developed. Subsequently a characteristic chemical shifts library is developed with model compounds to provide quantitative data on the concentration of alcohol, free glycerol, partially hydrolyzed triglycerides and free fatty acids in a rapid manner.

The last part of this thesis depicts the results of an industrial trial based on the novel biodiesel analytical method developed earlier. Due to optimized sample preparation and signal acquisition, the novel TMDP/^{31}P–NMR method can handle samples through the whole production line regardless of process step or feedstock used, becoming a novel research tool for process step optimization and for the characterization of biodiesel and its processing components.

CHAPTER 1

1 INTRODUCTION

1.1 Introduction

1.1.1 Biorefinery Project

Sustainability is undoubtedly one of the most important cornerstones of energy independence, rendering it desirable to utilize all biomaterial in the most efficient manner. Society's challenge is to not only develop new green technologies and products, but also to help establish commercial practices to become green industrial practices. For these reasons, the forest biorefinery is an evolving vision of wood utilization in an environmentally sustainable and economically viable manner; it is used to convert paper mills that currently produce primarily pulp and paper to biorefineries which produce biopower, biofules and biomaterials in addition to pulp and paper.[1] In this dissertation (Chapter 4) a novel green industrial method was tested at commerce practices following the methodology described above.

During chemical pulping, lignin is chemically degraded and extracted from wood in an aqueous environment in a pressure reactor.[2] The approach when NaSH is used in the cooking process along with caustic (NaOH) to delignify wood is referred to as Kraft pulping.[3] In turn, the paper industry produces residual lignin in a form of a caustic side stream. Currently, this material is burned in a low efficiency Thompson recovery furnace to recover energy and cooking chemicals.[2] A continuing interest in this field is the desire

to recover fractions of lignin from the Kraft cooking liquors for biopower, biochemical and biomaterial utilization.[1]

In the case of a future commercial cellulitic ethanol plant, since only the carbohydrate fraction is utilized during the fermentation step, the production of ethanol based on lignocellulosic materials will bring about the coproduction of significant amounts of under-utilized lignin. Due to these reasons the second study (Chapter 5) examines the potential to convert ethanol organosolv lignin from a low grade fuel to potential fuel precursors or other value added chemicals.

1.1.2 Biodiesel Project

In the case of a conventional commercial biodiesel process, regardless of source the conversion of triglycerides and/or fatty acids to biodiesel involves a transesterification step. The transesterification step is required to impart favourable fuel properties since direct use of plant oils with conventional diesel engines has been reported to result in coking and trumpet formation on the fuel injectors, carbon deposits, gelling of lubricating engine oil and incomplete combustion.[4] The efficiency of the production steps and the quality of the products is monitored by measuring the concentration of free, mono and disubstituted glycerols, methanol and free fatty acids. Along with the chemical and biochemical developments done in the last decade, there is a constant need for new and improved analytical techniques to monitor the quality of incoming feedstocks and their respective conversion products. Current analytical methods include HPLC,[5] GC ,[6] spectroscopic (i.e., MS,[7] NIR,[8]) and wet chemical techniques[9] (i.e., potentiometric, iodometric titration) which are often time-consuming typically due to

sample preparation, extended analysis time and/or complicated data analysis. The second part of this thesis describes our effort to invent (Chapter 6) and later to fully develop (Chapter 7, Chapter 8) a novel analytical method, to provide quantitative information on biodiesel constituents through the whole biodiesel production line in a rapid manner, regardless of feedstock or process step employed.

2.1 Objectives

2.1.1 Biorefinery Project

To address the challenges described above and meet with our goal to utilize lignin in the most efficient manner given the established commercial practice (Kraft pulping) and the future industrial process (cellulitic ethanol), the following major objectives were set:

- Determine the fundamental chemistry during LignoBoost lignin precipitation from black liquor.
- Characterize the fundamental chemical structure of the recovered lignin by functional group analysis and molecular weight profiles.
- Determine the optimal reaction conditions for ethanol organosolv lignin (EOL) hydrogenation.
- Select conventional heterogeneous and design novel homogeneous catalysts for the selective cleavage of the aryl-O-aryl and aryl-O-aliphatic linkages in the lignin biopolymer.

- Find catalyst systems with high lignin hydrogenolysis yield, and follow the changes in physical and chemical properties of the EOL during hydrogenation.
- Determine/propose fundamental hydrogenation/hydrogenolysis reaction mechanisms.

2.1.2 Biodiesel Project

Our goal was to develop a novel analytical method that will provide quantitative information on biodiesel constituents through the whole biodiesel production line in a rapid manner, regardless of feedstock or process step employed. To address these challenges described above, the following major objectives were set:

- Invent a rapid quantitative analytical technique for the determination of substitution patterns on partially esterified glycerols.
- Establish an NMR chemical shift data library, to be able to follow all major biodiesel constituents through the entire production line.
- Optimize the reaction mixture and physphitylation protocol so that the analytical method will be able to handle samples from all major process streams from a commercial industrial process.
- Tailor the pulse program for biodiesel constituents and reduce the analysis time to a minimum, so the method will be able to provide quantitative data quickly.
- Test the developed analytical protocol on industrial trials utilizing different feed stocks and process conditions.

CHAPTER 2

2 LITERATURE REVIEW

2.1 Fossil Fuels vs. Biofuels

Due to the increasing global energy demand and limited fossil fuel reserves, one of the most daunting challenges facing science in the 21st century is to deliver solutions for addressing global energy needs in the future in a sustainable manner.[1] There is also an increasing awareness that the utilization of fossil raw materials and fuels increase the net discharge of carbon dioxide (CO_2) in the atmosphere and contribute to the "green house effect".[10] Thus, beside the energy problem, the other important challenge is to predict how Earth's ecosystems will respond to global climate change. CO_2 is considered to be the most prevalent greenhouse gas, and the build up of CO_2 causes global climate change.[11,] The desire to maintain sustainable development has led to an increasing interest in society for biofuels and the conversion of renewable biomass resources to liquid fuels.[12]

Biofuels are biomass-based components for transport fuels, which are an interesting sustainable option for the transport sector. Unlike the combustion of fossil fuels which releases CO_2 that was captured several hundred million years ago, CO_2 released by during the utilization of a biomass based fuel is balanced by CO_2 captured in the recent growth of the biomass, resulting in far less net impact on greenhouse gas levels.[13] (Figure 1) Since biomass utilization can be considered as a closed carbon cycle, the production and usage of biofuels is expected to reduce the net CO_2 emission significantly.[14]

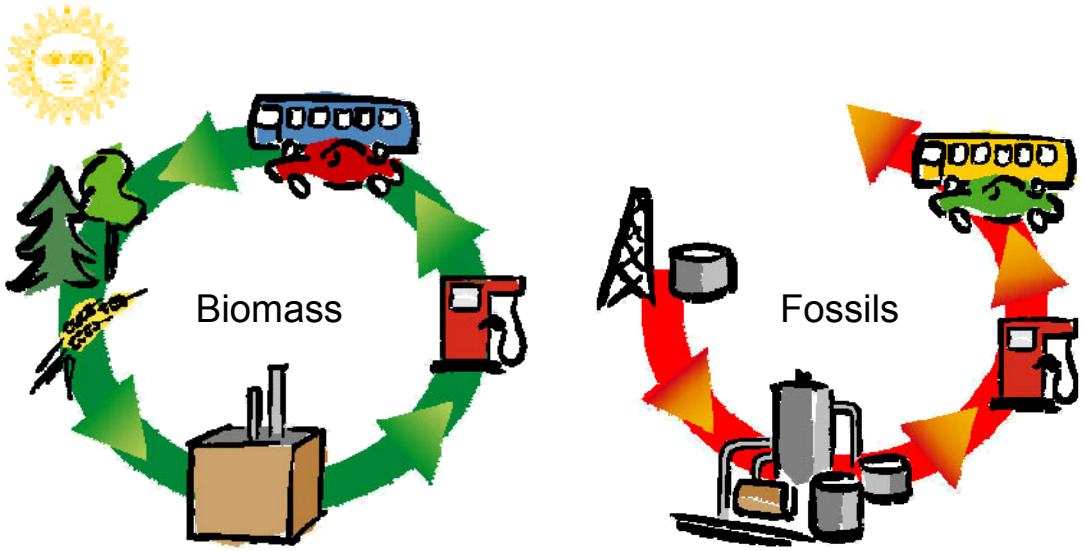

Figure 1. Carbon cycle for utilizing fuels from biomass - and fossils based production.

Until recently, the need for biofuels remained generally a low priority, as petroleum supply and demand curves were satisfactorily addressed.[12] Nonetheless, global petroleum demands have increased steadily from 56.2 x 10^6 barrels/day in 1975 to 85.9 x 10^6 barrels/day in 2007.[15] The impact of this growth in demand, and limited global production capacity has been foretold by several organizations and individuals.[1,16] Coupled with these concerns, the contribution of combustion CO_2 from fossil fuels to climate change has been noted in several recent reviews.[17,18] The relationship between the greenhouse gas emission produced by human activity and the increase of their average saturation levels in the atmosphere is obvious. Figure 2 depicts the changes in the atmospheric CO_2 levels and the fossil fuel carbon emission through the last millennia.[19,20]

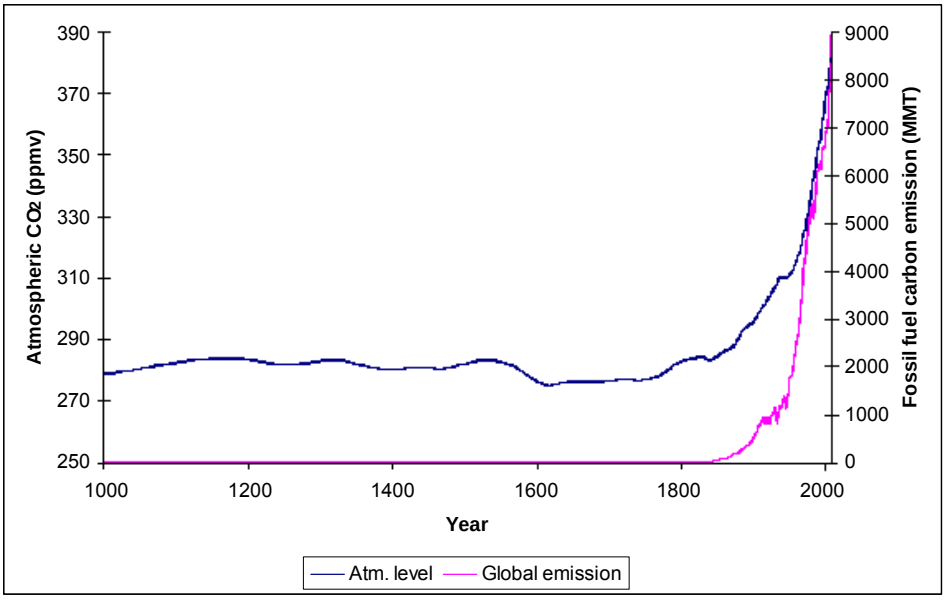

Figure 2. Changes in the atmospheric CO_2 levels and the anthropogenic fossil fuel related carbon emission through the last millennia.

As described by Hoffert et al., future reductions in the ecological footprint of energy generation will reside in multi-faceted approach that includes the use of hydrogen, wind, nuclear, solar power, and fossil fuels (from which carbon is sequestered) and biofuels.[21] In addition to the need to develop novel green technologies to reduce our carbon emission in the future, existing green and low impact energy generation technologies should be implemented in existing industrial practices. A review by Pacala and Socolov shed light on a portfolio of existing technologies capable of meeting the world's energy needs over the next 50 years and of limiting atmospheric CO_2 to a trajectory that avoids a doubling of the preindustrial concentration.[22] By upgrading current industrial practices while implementing already existing green technologies at an industrial scale or increasing the amount and quality of implementation in industry, it is proposed that over the next fifty years the atmospheric CO_2 concentration can be limited on 500±50 ppm to prevent most damaging climate change.[22]

In the short term, the market-place and societal concerns suggest that biofuels are one of the most attractive solutions for our transportation energy needs. Given that ~70% of United States' petroleum consumption is transportation related and that ~25% is for materials, it is clear that efficient production of biofuels and biomaterials will become one of this generation's greatest challenges. [23]

2.2 Problem Statement

The global primary energy production was 460 quadrillion British thermal unit (BTU) in 2005 wherein fossil fuels accounted for 86% of all energy produced worldwide.[15] In 2007 the world crude oil production totaled 74 million barrels per day, and by 2025 projected economic growth is anticipated to increase global demands for liquid fuels by another 50%.[24] The impact of this growth in demand and the dwindling supply of our geological reserves has led to an increased interest in renewable resources.[12] To be able to fulfill a sustainable and environmentally friendly method to cover our increasing energy requirements, there is a need for a new renewable carbon resource.

In 2008, 62.1% of the United States' petroleum consumption is covered by imports, which cost 354 billion dollars.[24] Thus, besides the obvious environmental benefits, the use of renewable raw materials to replace fossil fuels will have tremendous economic benefits, including the reduction of the crude oil dependency[25], trade deficit reduction[26]and the development of a strong biomass industry which will lead to the creation of jobs and the strengthening of agricultural markets.[27]

Biomass is an abundant resource with an annual global production rate of 170 x 10^9 metric tons.[28] Even though biomass is the oldest known renewable resource and has been used ever since man learned how to make fire, it currently contributes only 3.6% of the United States' primary energy supplies.[24] There is a wide variety of industrial[29,30], agricultural[31,32,33,34], and communal[35] resources available, which could provide suitable raw material for biofuel production. These potential renewable resources mentioned above are summarized under Section 2.3.

To be able to cover our global energy needs, the chosen renewable resources must have high energy content, be available in high volumes and be easily accessible at a low cost. Without the fulfillment of these four requirements the economical viability of the proposed renewable resource is questionable.[1]

2.3 Potential Renewable Resources

In nature, energy is mainly stored in the form of carbohydrates or hydrocarbons. As an abundant bio-renewable resource, carbohydrates can be found as; cellulose, hemicellulose and starch. Hydrocarbons are found as; fatty acids and triglycerides. Carbohydrates are easily accessible in the form of lignocellulosic materials whereas hydrocarbons are in the form of plant vegetable oils and animal fats.

Utilizing changes in agricultural and forest land use with existing novel techniques and with the future implementation of promising -but currently lab-scale industrial methods-- the estimated amount of biomass sustainably removable from forest lands is 368 million dry tons and from agricultural lands is close to 1 billion dry tons

annually in the United States.[36] Figure 3 and Figure 4 summarizes the potential forest and agricultural reserves in the United States.

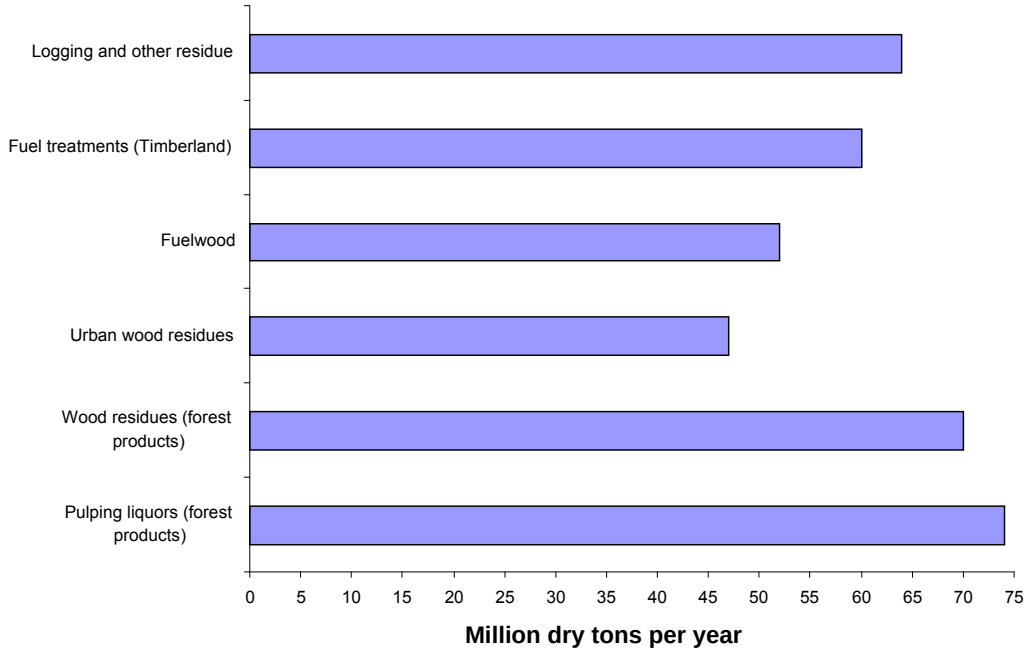

Figure 3. Summary of potentially available forest resources in the United States.

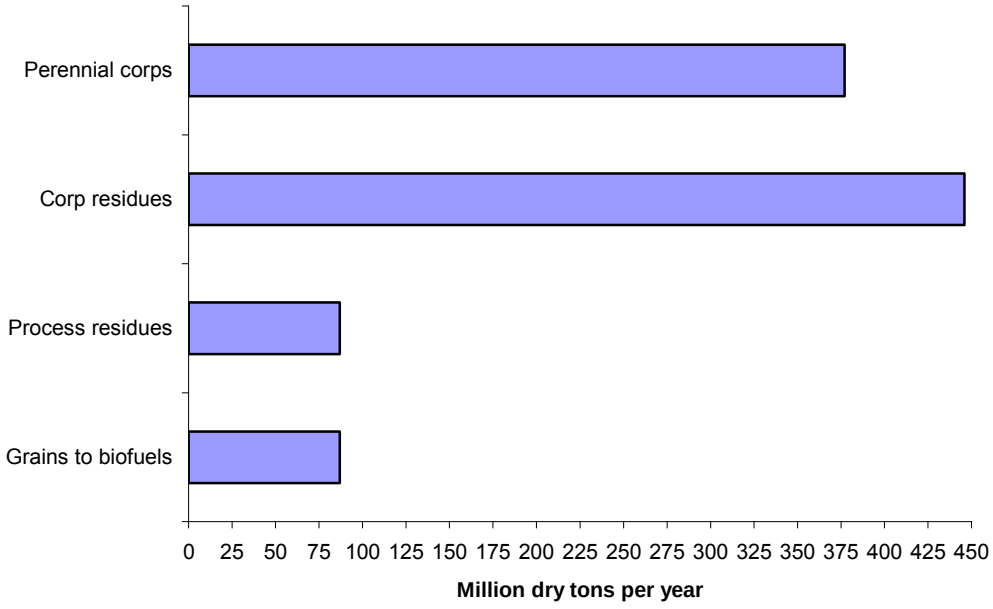

Figure 4. Summary of potentially available agriculture resources in the United States.

2.3.1 Lignocelluloses

Lignocellulosic materials are one of the world's largest renewable biochemical resources with 77 x 10^9 metric tons annual biosynthesis rate which may be available for large scale biofuel production.[37] Lignocellulosic materials could provide a rich sustainable feedstock for several biorefinery technologies.[1] Wood, or in general lignocellulosic material, contains cellulose, hemicellulose, lignin and extractives. The term "holocellulose" is often used to describe the total carbohydrate contained in a plant or microbial cell. Holocellulose is therefore comprised of cellulose and hemicellulose. Table 1 summarizes the typical distribution of major chemical constituents for several dominant wood resources.[38,39,40,41]

Table 1. Mayor chemical constituents of different softwood and hardwood species.

	Wood Macromolecules[a]		
Wood Species	**Cellulose (%)**	**Lignin (%)**	**Hemicelluloses (%)**
Softwoods			
Picea glauca	41	27	31
Abies balsamea	42	29	27
Pinus strobes	41	29	27
Tsuga canadensis	41	33	23
Norway spruce	46	28	25
Loblolly pine	39	31	25
Thuja occidentalis	41	31	26
Hardwoods			
Eucalyptus globulus	45	19	35
Acer rubrum	45	24	29
Ulmus americana	51	24	23
Populus tremuloides	48	21	27
Betula papyrifera	42	19	38
Fagus grandifolia	45	22	29

[a]all samples were analyzed extractives free

These three biopolymers are not just individual units in a plant cell wall but are intimately interrelated. Lignin-carbohydrate complexes (LCC) in wood have been extensively investigated and have been shown to be associated with hemicelluloses.[42,43] Figure 5 provides a schematic illustration of the integration of lignin, hemicellulose and cellulose at the cell wall level. [44,45,46]

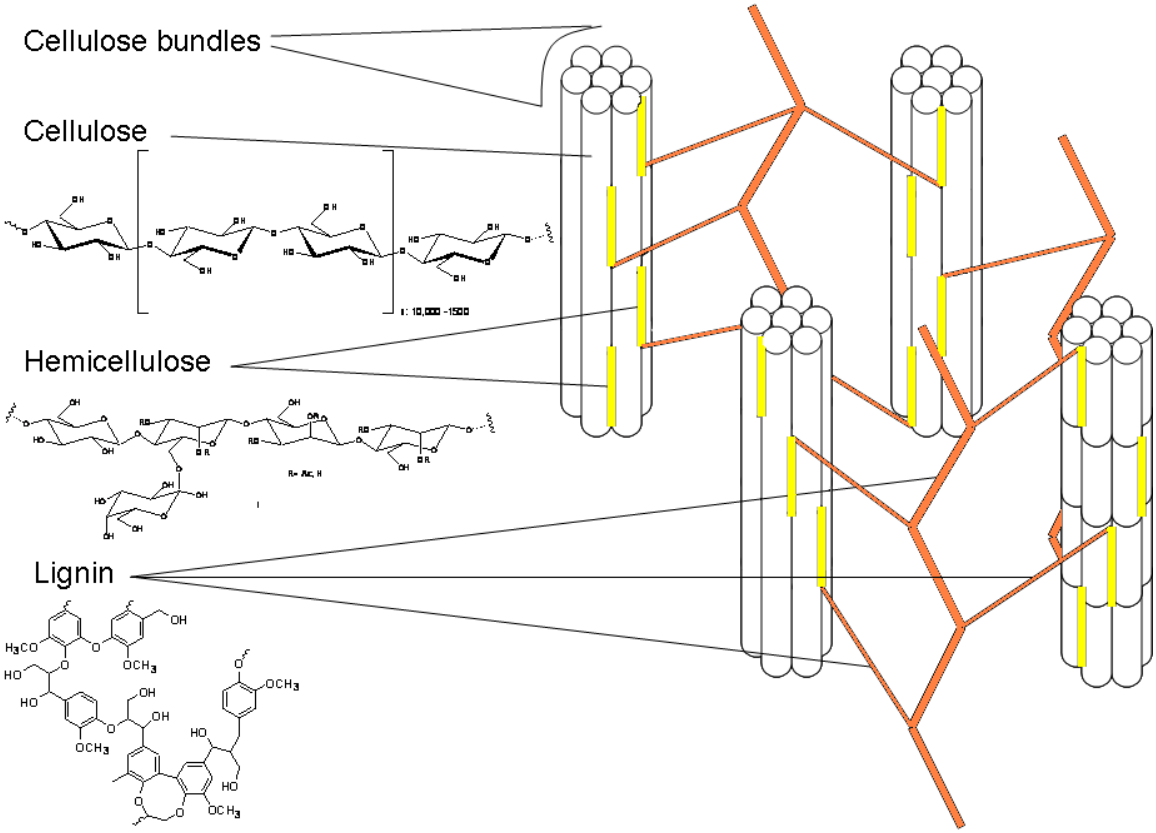

Figure 5. Schematic of plant cell wall utilization of lignin, hemicellulose and cellulose.

2.3.1.1 Cellulose

Cellulose is the most abundant biopolymer on Earth with a 100 x 10^9 metric tons annual biosynthesis rate.[1] It is the predominant polysaccharide in wood which is a homopolymer of (1→4)-linked β-D-glucopyranosyl units with a degree of polymerization (DP) ranging from a couple of hundred up to several thousand. Table 2 summarizes the number of polymer units in different cellulose containing materials.[47,48,49,50,51]

Table 2. Degree of polymerization (DP) in different cellulose containing materials.

Material	**DP**
Native form	
Algae	20.000
Cotton (unprocessed)	15.000
Loblolly pine (SW)	12000
Jack pine (SW)	10.300
Aspen (HW)	7900
Corn stover	7000
Eucalyptus (HW)	6000
Poplar (HW)	5500
Wheat straw	4000
Bacterial cellulose	2000-5000
Manmade	
Cotton (processed)	2000
Kraft pulp (Unbleached)	1600
Kraft pulp (Bleached)	1300
Sulfite pulp (Bleached)	1255
Raylon	305

In their native form, the glucopyranose units in the cellulose chain are in their thermodynamically most stable chair form with the -CH_2OH and -OH groups in equatorial position; only ~2% is in other forms.[52] Due to the cellulose highly organized structure, in its native form it reaches a relatively high-degree of crystallinity averaging 50-70% (see Figure 6).[53]

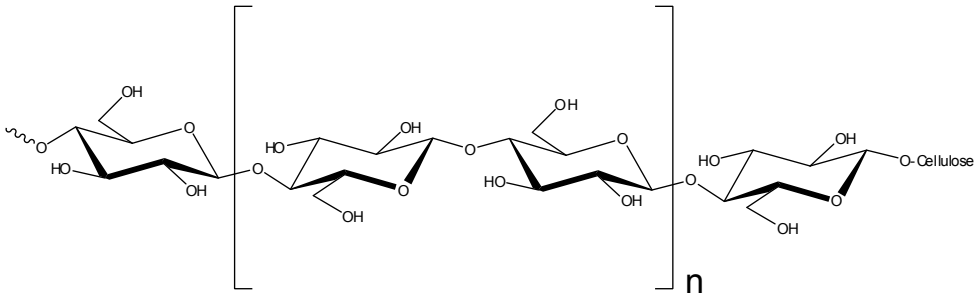

Figure 6. Cellobioside building unit in the cellulose polymer.

Cellulose can exhibit several different supra-molecular structures, including amphorous, para-crystalline and crystalline.[54,55] Native cellulose has been shown to be composed of two different crystalline forms, referred to as I_α and I_β.[56,57,58,59,60] Cellulose I_α is dominant in bacterial and algal cellulose. I_β crystalline form is dominant in higher plants such as cotton, ramie and wood.

Studies by Iversen and Larsson have proposed the occurrence of a para-crystalline component in cellulose which is less ordered than crystalline I_α and I_β allomorphs, but more ordered than amorphous domains.[61,62] These differences in crystalline packing forces and order have a broad impact on a variety of chemical[63,64] and enzymatic reactions with cellulose that can effect possible future industrial applications. Table 3 summarizes the relative amounts of crystallinity and para-crystallinity in different cellulose containing materials and the effect of a chemical or a mechanical treatment in its relative abundance.[65]

Table 3. The relative amounts (%) of different cellulose forms estimated from solid-state cross-polarization/magic angle spinning ^{13}C nuclear magnetic resonance spectra.

Material	Cristalline cellulose I.	Para-crystalline	Accessible fibril surface
	Native form		
Valonia (Algae)	81.0	12.0	nd
Cladophora (Algae)	63	17.4	0.7
Birch wood (HW)	3.8	19.1	4.3
	Manmade		
Birch pulp (Kraft)	7.1	33.3	1.6
Birch pulp (hydrolysed* 24 h)	31.9	25.6	6.6
Cladophora (hydrolysed* 4h)	75.4	7.4	1.7
Cladophora (milled 10** min)	27.6	26.1	4.3

* 2.5 M HCl at 100°C.
** Ball milled.

2.3.1.2 Hemicelluloses

The major hemicelluloses in softwoods are galactoglucomannans, and arbinoglucuronoxylan and minor amounts of arabinogalactan, xyloglucan and other glucans. The predominant hemicelluloses for hardwoods are glucomannan and glucuronoxylan with lesser amounts of galactans and glucans.

Hardwood glucuronoxylan and softwood arabinoglucuronoxylan both have a backbone of (1→4)-linked β-D-xylopyranosyl units, but exhibit differences in branching and substitution patterns. In the former, the C_2-OH and C_3-OH are partially acetylated (i.e., 3.5 – 7.0 acetyl groups/10 xylose) and are lesser amounts of (1→2)-linked pyranoid 4-O-methyl-α-D-glucuronic acid units. For softwoods, the xylan polymer is not acetylated and typically is branched with (1→2)-linked pyranoid 4-O-methyl-α-D-glucuronic acid and (1→3)-linked α-L-arabinofuranosyl units with an arabinose:uronic acid:xylose ratio of ~1:2:8.

Galactoglucomannan is far more important than arabinoglucuronoxylan to the hemicellulose chemistry of softwoods contributing 15-20% of the dry wood mass. This polysaccharide is comprised of (1→4)-linked β-D-glucopyranosyl and D-mannopyranosyl units that are partially acetylated at the C_2-OH and C_3-OH and partly substituted by (1→6)-linked α-D-galactopyranosyl units. Softwoods generally have two different types of galactoglucomannans: one being highly branched with a ~1:1:3 ratio of galactose:glucose:mannose and another that is less branched with a ~0.1:1:3 ratio galactose:glucose:mannose. In hardwoods, the glucomannan polymer has little or no branching with a typical glucose:mannose ratio of ~1:1.5.[66]

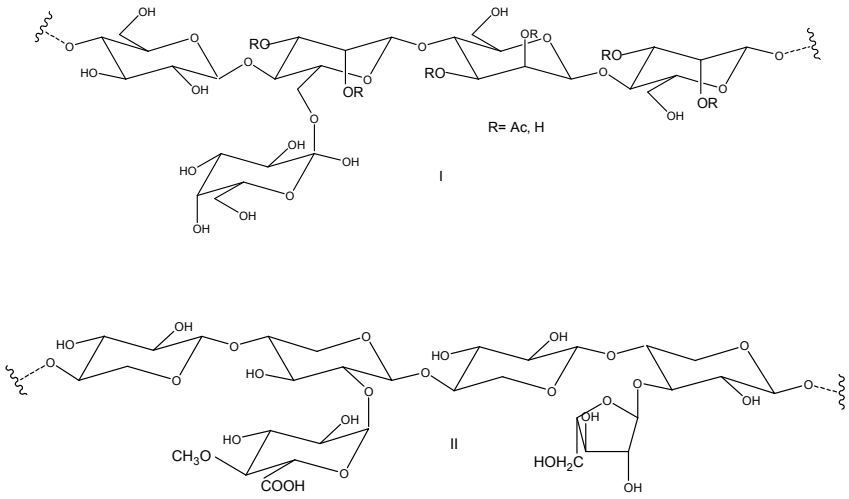

Figure 7. Representative plant hemicelluloses, I:galactoglucomannans and II: arabinoglucoronoxylan

A series of publications by Willfoer et al. have provided one of the most definitive analyses of carbohydrates present in industrially important wood resources.[67,68] Representative data from this study are summarized in Table 4 The hemicellulose

content, the main heteropolysaccharides and their degree of polymerization (DP) is summarized in Table 5 in case of hardwoods (HW) and softwood (SW).[69,70]

Table 4. Relative distribution of hemicellulose sugars in select wood resources.

Wood Species*	Ara	Xyl	Gal	Glc	Man	Rha	GlcA	GalA	4-O-MeGlcA	Total** %
Softwood										
Picea abies										
sapwood	0.14	0.61	0.17	0.37	**1.00**	0.02	0.03	0.16	0.10	24.6
heartwood	0.17	0.69	0.28	0.35	**1.00**	0.03	0.04	0.20	0.12	24.9
Pinus banksiana										
sapwood	0.18	0.57	0.18	0.40	**1.00**	0.02	0.05	0.13	0.10	27.2
heartwood	0.22	0.75	0.37	0.43	**1.00**	0.03	0.06	0.17	0.14	29.3
Hardwood										
Betula Pendula										
stemwood	0.02	**1.00**	0.06	0.08	0.04	0.02	0.01	0.10	0.16	33.6%
Populus tremuloides										
sapwood	0.03	**1.00**	0.04	0.11	0.05	0.03	0.01	0.12	0.13	29.1
heartwood	0.03	**1.00**	0.04	0.12	0.09	0.03	0.01	0.12	0.13	28.8

* Salmen and Olsson 1998; Ebringerova et. al 2005.
** mass sugar units/mass dry wood.

Table 5. Relative amount (%), distribution and degree of polymerization of major hemicelluloses in case of different softwood and hardwood species.

Material	Hemicellulose content	Degree of polymerization
Softwood		
Loblolly pine	15.3	---
Black Spruce	17.4	---
Galactogucomannan	~20	40-100
Gluconoxylan	5-10	50-185
Hardwood		
Birch	33	---
Gluconoxylan	15-30	~200
Gluconomannan	2-5	~70

2.3.1.3 Lignin

Of the three major biopolymers that constitute wood, lignin is distinctly different from the other macromolecular polymers. Lignin is one of the most complex natural polymers in regards its chemical structure and composition. It is formed by oxidative coupling of 4-hydroxyphenylpropanoids (monolignols) that differ in their degree of methoxylation.[71] Figure 8 depicts the three phenyl propane precursors of lignin and the carbon numbering in lignin. Because of its chemical composition, lignin is hydrophobic and acts like a coating around the cellulose fibrils. After cellulose, lignin is the second most abundant biopolymer on earth. Biosphere has an estimated 300 x 10^9 metric tons of lignin with a 20 x 10^9 metric tons annual biosynthesis rate.[9]

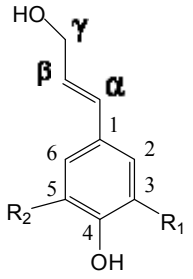

Coniferyl alcohol/guaiacyl: R_1= OMe, R_2= H
Sinapyl alcohol/ syringyl: R_1= R_2= OMe
p-Coumaryl alcohol: R_1= R_2= H

Figure 8. The three building blocks of lignin.

This polyphenolic polymer is synthesized by enzymatic dehydrogenative polymerization of 4-hydroxyphenyl propanoid units.[72] Figure 9 depicts the radical resonance structures of coniferyl alcohol after dehydrogenated by peroxidase.[73]

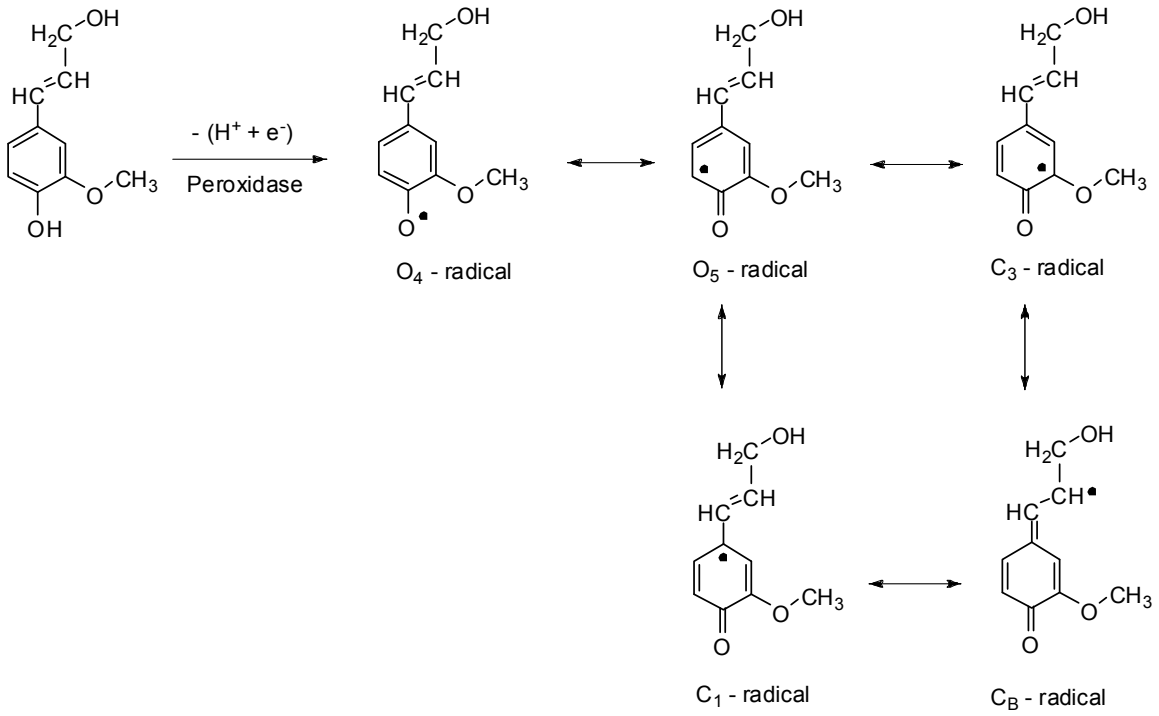

Figure 9. Radical resonance structures of coniferyl alcohol after dehydrogenated by peroxidase.

There are two main theories on lignin biosynthesis: one belief is that the assembly of lignin is controlled biochemically by dirigent proteins, while the other is that after the enzymes dehydrogenate the monoligols to radicals, they randomly couple each other and the growing lignin polymer.[74,75] The dominant linkages in softwood lignin are depicted in Figure 10. As an example, Figure 11 and Figure 12 show the mechanism for the formation of two predominant linkages in lignins: the oxidative coupling of 4-hydroxyphenylpropanoid units to form β-O-4 ether isomers and dibenzodioxocin respectively.[76]

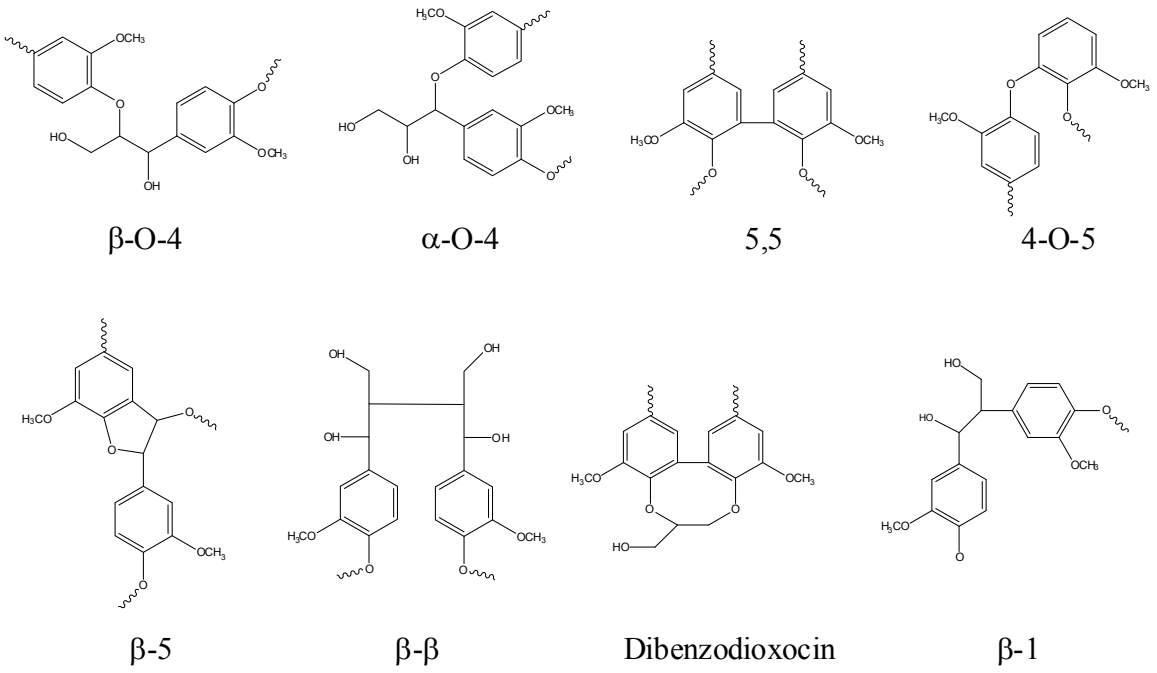

Figure 10. The dominant linkages in softwood lignin.

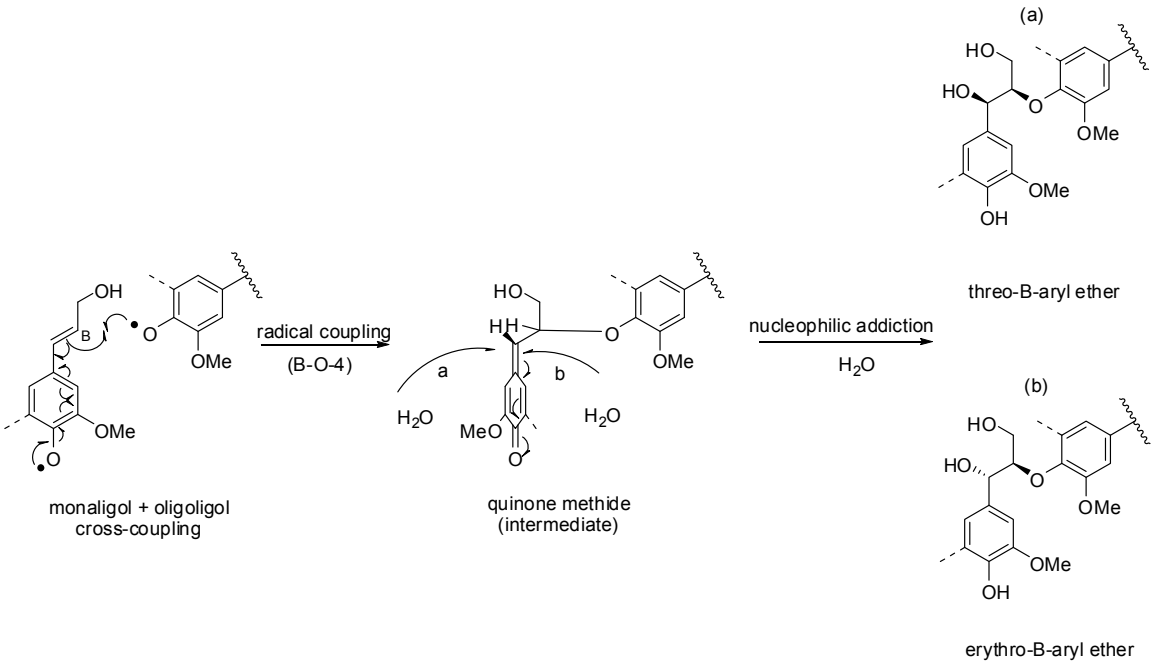

Figure 11. The formation of β-O-4 ether isomers in lignin.

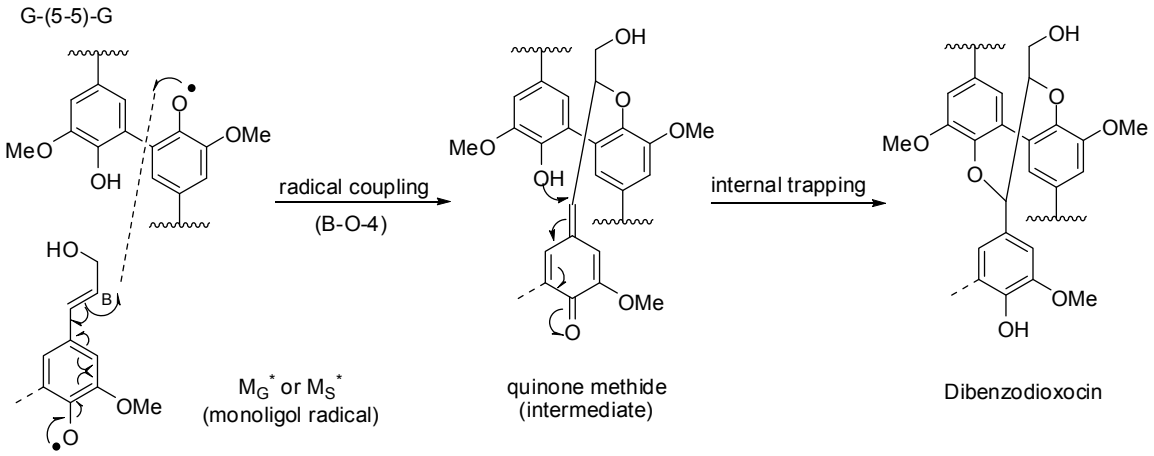

Figure 12. The formation of dibenzodioxocin units in lignin.

In a recent publication by Laurence et al. numerous facts for the proposed model of absolute structural control versus sole random chemical coupling were reviewed.[77] Biosynthesis of lignin based on random coupling would not result in completely irregular lignin as various positions of the radicals have different reactivity and the supply of monomers is well controlled.[78] The phenylpropanoids are linked to each other by various ether and carbon-carbon inter unit linkages creating a three-dimensional highly cross-linked polymer. The dominant linkages and the abundance of some of the functional groups found in softwood lignin are summarized in Table 6 and Table 7 respectively.[79] The schematic representation of a proposed softwood lignin structure is depicted in Figure 13.[3]

Table 6. Proportions of different types of linkages connecting the phenylpropane units in softwood lignin.

Linkage type	Dimer structure	Approximate percentage
β-O-4	Phenylpropane β-aryl ether	45-50
α-O-4	Phenylpropane α-aryl ether	6-8
β-5	Phenylcoumaran	9-12
5-5	Biphenyl and dibenzodioxocin	18-25
4-O-5	Diaryl ether	4-8
β-1	1,2-Diaryl propane	7-10
β-β	β-β-Linked structures	3

Table 7. Functional groups in softwood lignin (per 100 C_9 units).

Functional Group	Softwood Lignin
Methoxyl	92-97
Phenolic hydroxyl	15-30
Benzyl alcohol	30-40
Carbonyl	10-15

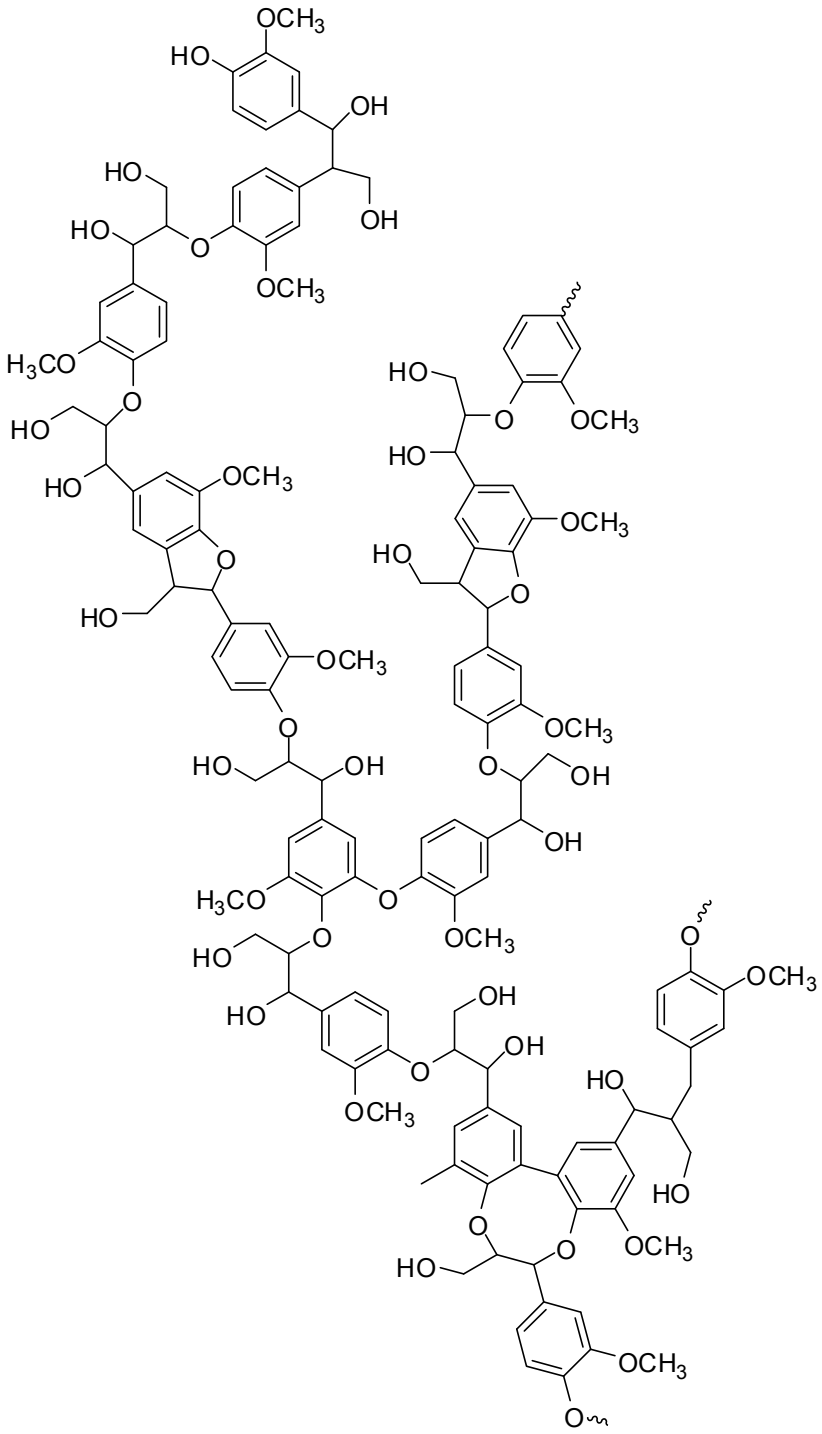

Figure 13 Example for structure of native softwood lignin.

Current review by Argyropoulos et al. suggested that most likely the lower limit for the DP for native softwood lignin is approximately 60 yielding a molecular weight (MW) of ~11.000, while the higher limit is 90 -100 phenyl propanoid units.[80] Table 8 summarizes several commercially available technical lignin resources and their measured MW with different analytical methods.[81,82,83]

Table 8. Molecular weight of technical lignin samples with different analytical methods.

Raw material	Lignin extraction method	Analytical method	M_w	M_n	M_w/M_n
Mixed softwood	Kraft lignin	SEC	9735	2755	3.5
Bagasse	Soda pulping	SEC	8481	2684	3.2
Mixed hardwood	Sulfite pulping	SEC	4317	2173	2.0
Mixed hardwood	Organosolv	SEC	3959	511	7.7
Aspen	Steam explosion	SEC	22876	2977	7.7
Spruce	Dioxane extracted	SEC	3800	---	---
Spruce	Dioxane extracted	VPO	---	2400	---
Spruce	Dioxane extracted	ESI-MS	2500	---	---
Spruce	Oxygen-organosolv	SEC	3700	---	---
Spruce	Oxygen-organosolv	VPO	---	1700	---
Spruce	Oxygen-organosolv	ESI-MS	1900	---	---
Eucalyptus	Dioxane extracted	VPO		2150	---
Eucalyptus	Dioxane extracted	ESI-MS	2400	---	---
Eucalyptus	Kraft lignin	VPO	---	650	---
Eucalyptus	Kraft lignin	ESI-MS	800	---	---
Loblolly pine	MWL	GPC	13500	7590	1.8
Loblolly pine	OS-MWL	GPC	16800	6530	2.6
Loblolly pine	EOL	GPC	2440	1191	1.7
Mixed Softwood	LignoBoost (pH 9.5)*	SEC	2979	1795	1.7
Mixed Softwood	LignoBoost (pH 10.5)**	SEC	2939	1694	1.7

* BL pH lowered to 9.5 during LignoBoost lignin precipitation.
** BL pH lowered to 10.5 during LignoBoost lignin precipitation.

2.3.2 Triglycerides and Fatty Acids

Triglycerides and fatty acids are starting feed stocks for the biodiesel production. The method widely used to produce biodiesel is transterification which involves triglycerides from vegetable oils or animal fats and an alcohol in the presence of a catalyst, yielding glycerol and the corresponding alkyl fatty ester. Figure 14 shows the structure of a typical triglyceride, a saturated and an unsaturated fatty acid.[84]

a/

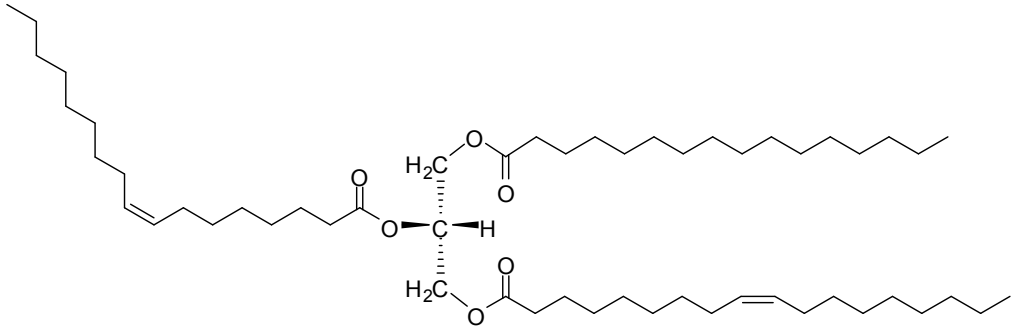

b/

Fatty acid	Chemical structure	C:D
Lauric acid	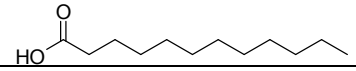	12:0
Myristic	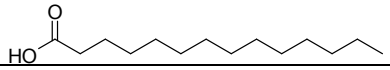	14:0
Palmitic	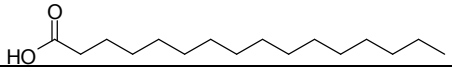	16:0
Stearic	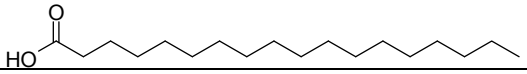	18:1
Oleic	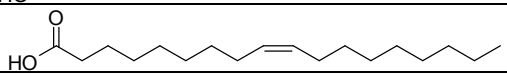	18:1
Linoleic	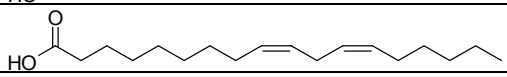	18:2
Linolenic	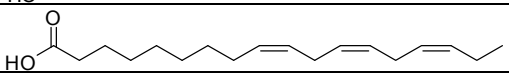	18:3
Arachidic	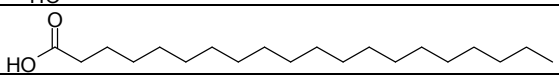	20:0
Eicosenoic	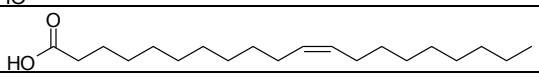	20:1
Erucic	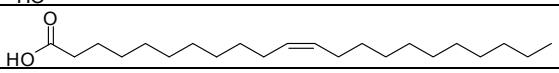	22:1

Figure 14. (a) Chemical structure of an unsaturated fat triglyceride, where substituting fatty acids from top to bottom: palmitic acid, *cis*-oleic acid and *trans*-oleic acid. (b) Common fatty acids in oil crops used for biodiesel production.

As shown in Figure 14, triglycerides are basically esterified glycerol with three fatty acids. Fat in food as well in body fat exists in the form of triglycerides, making it the main constituent of vegetable oil and animal fats. Today's multi-feedstock facilities can produce high quality biodiesel by utilizing fats from various origins.[85] Depending on the source, biodiesel feedstocks can be categorized into three groups: pure plant oil (PPO), waste vegetable oil (WVO) and animal fat. [86] These various feedstocks and their main properties will be reviewed.

2.3.2.1 Pure Plant Oil

Since the chain length of the fatty acids in naturally occurring triglycerides can vary in length, most natural fats contain a complex mixture of individual triglycerides. Depending on the specie utilized, the difference in chemical composition can result in changes in a wide variety of physical behaviors (i.e. viscosity, melting point) which can affect the reaction conditions used through the biodiesel production and also the properties of the final biodiesel product. Table 9 shows the fatty acid composition of some major pure plant oils.[87]

Table 9. The fatty acid profiles of various pure plant oils (PPO).

PPO	12:0*	14:0*	16:0*	18:0*	18:1*	18:2*	18:3*	20:0*	20:1*	22:1*
Soybean	trace	trace	6-10	2-5	20-30	50-60	5-11			
Hi oleic rapeseed			4.3	1.3	59.9	21.1	13.2			
Hi erucic rapeseed			3.0	0.8	13.1	14.1	9.7	7.4		50.7
Corn		1-2	8-12	2-5	19-49	34-62	trace			
Palm	trace	1.0	42.8	4.5	40.5	10.1	0.2			
Peanut			8-9	2-3	50-65	20-30				
Olive			9-10	2-3	73-84	10-12	trace			
Cottonseed		0-2	20-25	1-2	23-35	40-50	trace			
Coconut	46.5	19.2	9.8	3.0	6.9	2.2				
Linseed oil			4-7	2-4	25-40	35-40	25-60			
Tung oil			3-4	0-1	4-15		75-90			

* Fatty acids designated (carbon chain length : unsaturation) i. e; (18:1) stands for Oleic acid.

Virgin oil feedstock, rapeseed and soybean oils are most commonly used. Soybean oil alone accounts for about ninety percent of all fuel stocks in the United States.[84] At the same time, the positive attributes of PPO need to be balanced against the limited global production of plant oils since the production of vegetable oils for use as fuels is limited by the agricultural capacity of a given economy.

It is important to note that soybeans are also a food resource thus; from the soybeans used to produce biodiesel, 81% of the soybean's yield is protein that enters the market for either human consumption or animal feed.[85] Due to these production limitations, there is a constant search for next generation technologies that may address these problems by technological advances and/or increase soybean yields from existing acreage.[88]

2.3.2.2 Waste Vegetable Oil

In contrast to PPO, WVO is a byproduct of other industries thus; its prospects for use as fuel are limited by the capacities of other industries. Since the available supply is drastically less than the amount of petroleum-based fuel that is burned for transportation and home heating, this local solution does not scale well.[85]

In 2001, the United States was producing in excess of 2.9 billion U.S. gallons of waste vegetable oil annually, primarily from industrial deep fryers in potato processing plants, snack food factories and fast food restaurants.[89] It is proposed that if all 2.9 billion gallons could be collected and used to replace the energetically equivalent amount of petroleum, almost 1% of US oil consumption could be offset. Since the use of waste vegetable oil as a fuel competes with some other uses of the commodity, this can have a negative effect on its price as a fuel; and as an input, it may increases its cost of other uses as well. Yellow grease is distinct from brown grease; as yellow grease is typically used-frying oils from deep fryers, whereas brown grease is sourced from grease interceptors. Table 10 shows the representative fatty acid composition of yellow and brown grease feasible for biodiesel production.[90]

Table 10. The fatty acid profiles of various animal fats.

Feedstock	**14:0***	**16:0***	**18:0***	**18:1***	**18:2***	**18:3***	**20:0***	**22:1***
Yellow grease	1.3	17.3	12.4	54.7	8.0	0.7	0.3	0.5
Brown grease	1	24	10	50	15			

* Fatty acid designated (carbon chain length : unsaturation) i. e; (18:1) stands for Oleic acid.

2.3.2.3 Animal Fats

Animal fats used as a feedstock for the biodiesel industry include the white greases such as tallow, lard, chicken fat and fish oils.[85] Animal fats usually are by-products of the meat industry. Although it would not be efficient to raise animals simply for their fat, utilizing product streams for biodiesel production that would otherwise be discarded, adds value to the livestock industry. Currently, even multi-feedstock biodiesel facilities can produce biodiesel from a wide variety of feedstocks, all the biodiesel produced from animal fats could only replace a small percentage of the petroleum diesel usage. Table 11 shows the fatty acid composition of some animal fat based feedstock proposed for biodiesel production.[87]

Table 11. The fatty acid profiles of various animal fats.

Animal fat	14:0*	16:0*	18:0*	18:1*	18:2*	18:3*	20:0*	22:1*
Lard	1-2	28-30	12-18	40-50	7-13	0-1		
Chicken	0-1	26-33	7-10	32-36	16-21	0-1	1-2	0-1
Tallow	3-6	24-32	20-25	37-43	2-3			

* Fatty acid designated (carbon chain length : unsaturation) i. e; (18:1) stands for Oleic acid.

2.4 Current major biofuels

The interest and development of biofuels has grown exponentially over the last few years in response to the need to develop sustainable energy resources and to address climate change.[1] Currently the two major biofuels available on the market are bioethanol and biodiesel. Henry Ford and Rudolph Diesel are well known for their contribution to the industrial revolution and modern automotive history. What is frequently over-looked is that they both envisaged, at one time, that their engines would be powered by biofuels, such as bioethanol and peanut oil, respectively.[91,92] Bioethanol currently contributes ~7% to the total U.S. transportation fuels mix and another ~1.3% is based on biodiesel.[24,93] Currently, bioethanol and biodiesel are the most successful fossil fuel supplements. The absolute annual biodiesel potential of the U.S. is estimated to be 3.2 billion gallons.[36] The current biodiesel production capacity in the U.S. is 400 million gallons and is projected to double within the next two years.[1] Although this is less than the current bioethanol production, recent research efforts in algae-oil production could significantly change this outlook.[84] To make a substantial contribution to this nation's energy portfolio, biofuels production needs to grow substantially over the next decade by a factor 10 or more.

In December, 2007, the U.S. government signed comprehensive energy legislation, the Energy Independence and Security Act, into law which amends the renewable fuel standards and sets a goal to increase U.S. production up to 36 billion gallons by 2022.[94] The positive economic impact of reaching this goal is proposed to add $1.7 trillion to the gross domestic products, generate an additional $436 billion to U.S. household income and $209 billion in federal tax receipts while creating 1.1 million new

jobs in all sectors of the economy between now and 2022.[93] Beside the obvious economic benefits, renewable fuels are also offering environmental benefits by reducing the greenhouse gas emission and increase the energy security of the nation by reducing dependence on foreign oil.[1] Figure 15 depicts the annual biofuel production in the U.S. from 1981 and the projected growth based on the renewable fuels act.

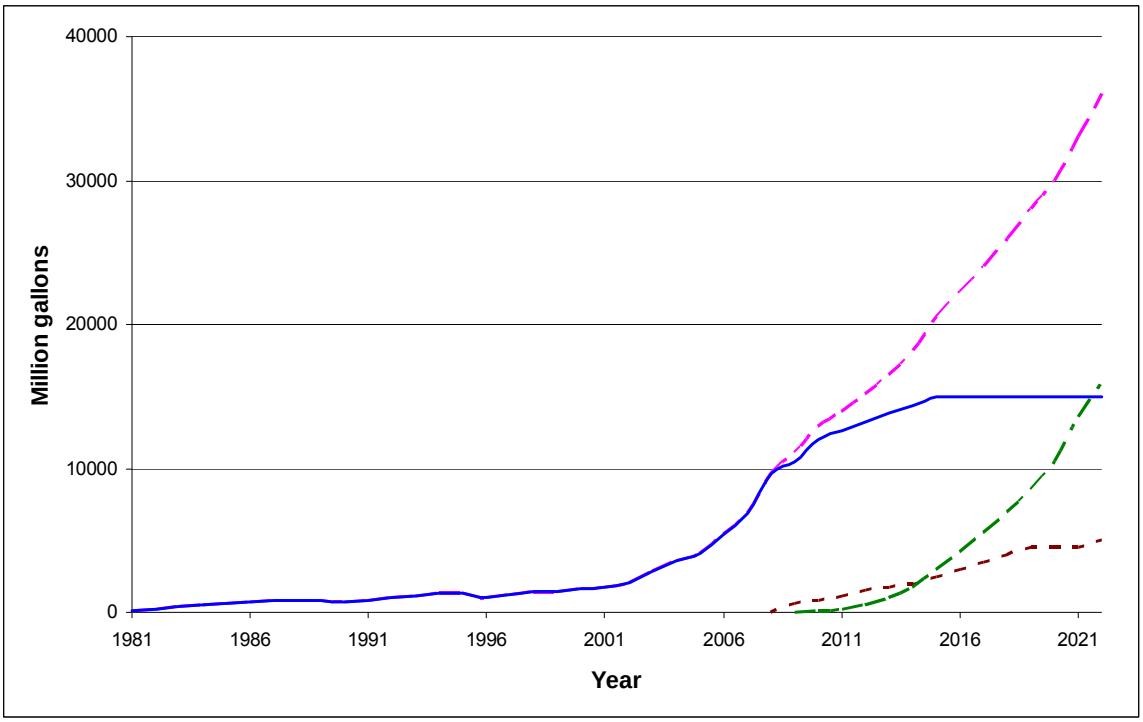

* Sissine 2007.

Figure 15. The annual U.S biofuel production from 1981; starch based first generation bioethanol (blue), cellulosic second generation bioethanol (green), biodiesel and undifferentiated advanced biofuels (brown) and the projected USA growth according to the Renewable Fuels Act* up to 2022 (pink).

2.4.1 Bioethanol

2.4.1.1 Starch Based Bioethanol

Current interest in bioethanol mainly lies in first generation bioethanol wherein ethanol is produced from starch or sugar found in a wide variety agricultural crops by fermentation.[1] First generation bioethanol production today is most often based on grains such as wheat, barley, corn or sugar cane. [95] During the last decade advances in biotechnology have reduced the cost of the first generation bioethanol by nearly 25%.[24] However, the economy and technology of fuel-ethanol production is strongly linked to the locally available raw material.

The first step of the bioethanol production is the conversion of the starting biomass resource to a feedstock for fermentation, i.e. some form of fermentable sugar. In case of the first generation bioethanol production, the process involves a biomass feedstock that already contains free fermentable sugars. Sugarcane in Brazil or sugar beets in France are examples of biomass containing substantial amounts of directly fermentable sugars, in the mentioned cases sucralose.[95] In most plant materials, however, sugars are found in the form of polysaccharides such as starch cellulose or hemicellulose. These polymer molecules must first be processed to liberate the sugar monomers for fermentation.

The ethanol production of the U.S. is based almost entirely on the degradation of starch from corn.[24] Processing starch to yield free sugars is a well-established process with the usage of enzymes, like α-amylases, glucoamylases and glucose isomerases.[96] The change in the U.S. ethanol production capacity through the last decade is shown in Figure 16.

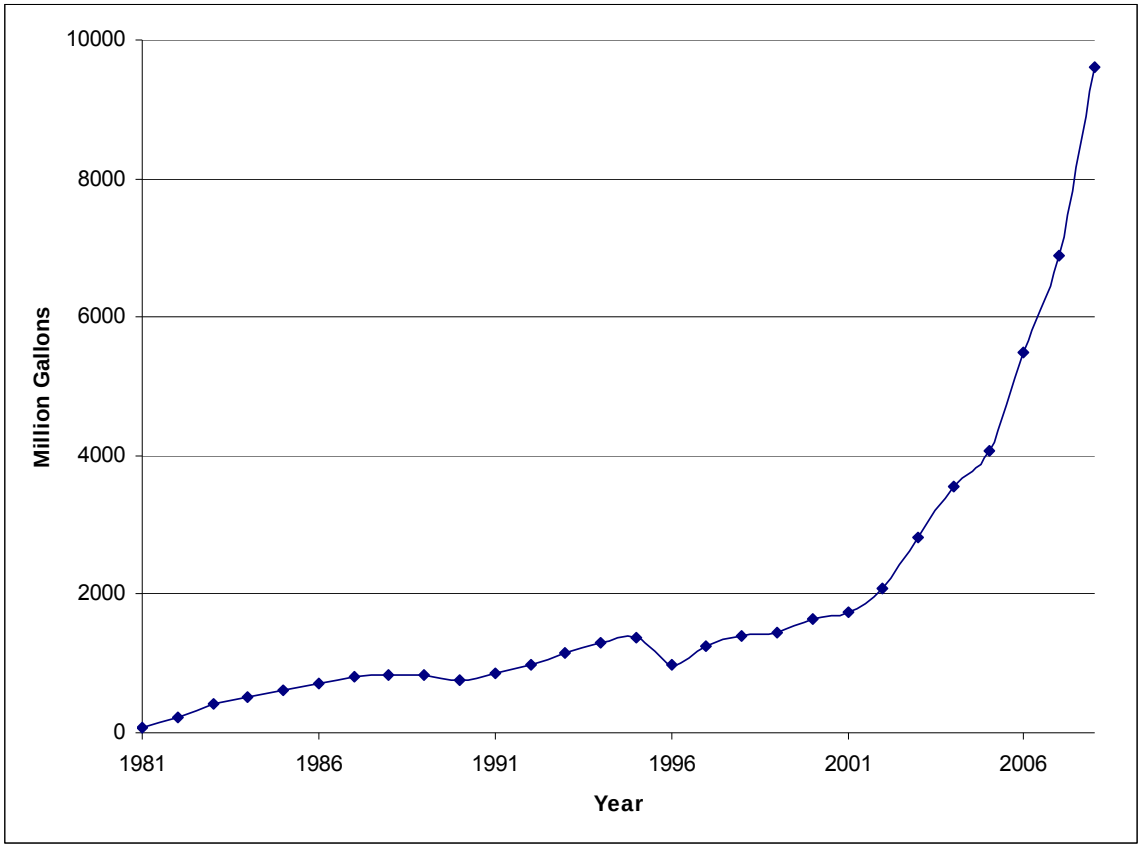

* Energy Information Administration 2007.

Figure 16. The annual U.S starch based fuel ethanol production from 1981 to 2008.*

In 2004, 3.41 Bgal of starch ethanol fuel were produced from 1.26 billion bushels of corn by 81 ethanol plant, utilizing 11% of all corn grain harvested in the U.S.[93] By the end of 2005, with the completion of 16 additional plants, the production increased to 4.4 Bgal. Although the capacity more than doubled between 2000 to 2004 and later almost doubled again from 2004 to 2008, ethanol only satisfied less than 8% of the U.S. transportation-energy demand in 2009.[24]

In the U.S., ethanol is processed in a corn wet or in a corn dry mill.[97] Corn wet mills fractionate the corn grain for oil and germ before converting the starch to fermentable sugars or for other valuable food products such as maltodextrins or high-

fructose corn syrup. The corn fiber by-product is ususlly sold for animal feed. In corn dry mills, the grain is first ground, then broken into sugars--monomers by enzymes--before fermentation. Unlike in the wet mill, the grain is not fractionated thus, the only by-product is the remaining solids which are a highly nutritious protein source and used in livestock feed.

With the modern first generation bioethanol processes utilized in the U.S., a bushel of corn yields about 2.5 gal ethanol from wet-mill processing and about 2.8 gal from dry grind.[98] Some 75% of corn ethanol production is from dry mill facilities and 25% from wet mills.

It has been debated considerably about how useful bioethanol will be in replacing fossil fuels in vehicles utilizing feedstocks from potential food resources. Beside concerns related to the large amount of arable land required for crops, the energy and pollution balance of the whole cycle of ethanol production is also debated. Recent developments with cellulosic ethanol production and commercialization may allay some of these concerns.

2.4.1.2 Cellulosic Ethanol

Cellulosic ethanol is considered the second generation bioethanol.[97] Compared to the first generation bioethanol which utilizes free fermentable sugars and starch which are a potential food resource, the second generation bioethanol is produced from non-food carbohydrates such as cellulose and hemicellulose. The process of making alcohol from lignocellulosic biomass, in principle, is relatively simple: after hydrolysis and a subsequent fermentation, the ethanol can be refined by distillation (see Figure 17).[99]

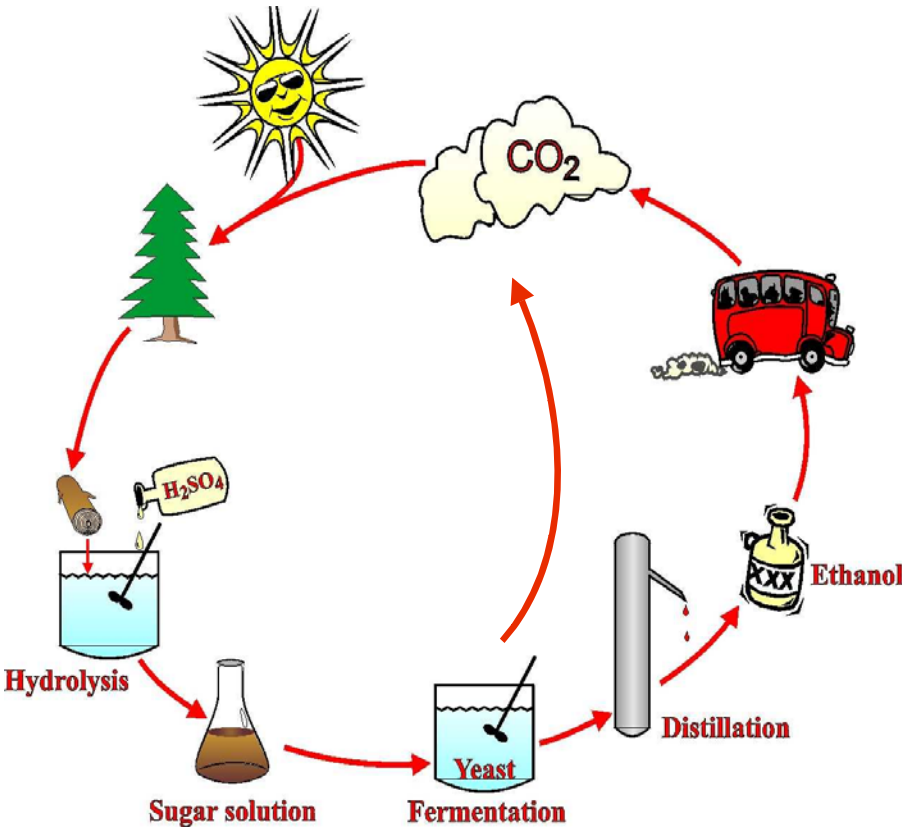

http://www.baff.info/english/
(2004)

Figure 17. Cellulosic fuel ethanol production using dilute acid hydrolysis and its closed carbon cycle.

2.4.1.2.1 Conversion of Lignocellulosic Biomass to Fermentable Sugar Solution

Bioethanol is made by fermentation, which implies the need for a fermentable resource for the microorganism. There are basically three techniques available for the conversion of the sugar content in lignocellulosic biomass into fermentable sugar solution. These are the one-step acid hydrolysis, the two steps dilute acid hydrolysis and the enzymatic hydrolysis.[100]

An important drawback of the acid hydrolysis is that in addition to the sugars, several by-products are formed or released during the hydrolysis process. The most important by-products are inhibitors such as furans, carboxylic acids and phenolic compounds.[101,102] When hemicellulose depolymerized, xylose, mannose, acetic acid, galactose and glucose are liberated. The degradation product of cellulose is glucose. At high temperature and pressure, xylose and other pentoses can be further degraded to furfural. Similarly, the hexose degradation leads to the formation of 5-hydroxymethyl furfural (HMF). These two furan derivates can, in turn, react further. HMF can be broken down to formic acid and levulinic acid, while furfural can be further degraded to formic acid or it can polymerize. Furthermore, partial breakdown of lignin can generate phenolic compounds. The nature, composition and concentration of these compounds are dependent on the hydrolysis conditions and have a profound influence on the production rate of biofuels from the hydrolyzate.[103,104] Table 12 summarizes the main compounds and their concentration in a hydrolyzate produced by two steps dilute acid hydrolysis from Spruce.

Table 12. Compounds determined in a Spruce hydrolyzate produced by two steps dilute acid hydrolysis for bioethanol fermentation.

Group of compounds	Compounds**	Concentration [g/L]
Sugars		
	Glucose	25.7
	Mannose	6.5
	Galactose	3.7
	Xylose	3.5
	Cellobiose	0.7
	Arabinose	0.6
Furan derivatives		
	5-Hydroxy-methyl-furfural	5.9
	Furfural	1.0
Aliphatic acids		
	Levulinic acid	2.6
	Acetic acid	2.4
	Formic acid	1.6
Phenolic compounds		
	Vanilin	0.12
	Dihydroconiferylalcohol	0.098
	Coniferyl aldehyde	0.035
	Vanillic acid	0.034
	Hydroquinone	0.017
	Catechol	0.009
	Acetoguaiacone	0.007
	Homovanillic acid	0.005
	4-Hydroxy-benzoic acid	0.005
Hibbert's ketones		
	G*-$CHOHCOCH_3$	0.048
	G*-$COCOCH_3$	0.029
	G*-CH_2COCH_2OH	0.028
	G*-$COCHOHCH_3$	0.025
	G*-CH_2COCH_3	0.016

* G*, Guaiacyl = 4-hydroxy-3-methoxyphenyl.

** Produced with residence time, 7 min; reaction temperature, 222°C; and 0.5% sulfuric acid (w/w).

There are several strategies for reducing the negative effects of the inhibitors in the hydrolyzate. First, the hydrolysis conditions can be optimized not only with respect to maximum sugar yields but also to low inhibitor formation.[104] Detoxification prior to fermentation is another option. If the natures of the inhibitors are known, a detoxification method can be chosen for a particular type of hydrolyzate such as alkali, sulfite, evaporation, anion exchange or enzymatic treatments.[105,106]

Genetic engineering of the fermenting micro-organism is a third possibility.[107] As a fourth option, one may select specific strains of micro-organisms based on evolutionary changes--after adaptation of the micro-organism to inhibitory hydrolyzate.[108] Alternative fermentation strategies, such as fed-batch techniques also could be employed to decrease the effect of the inhibitors.[109]

2.4.1.2.2 The Fermentation Stage

After the hydrolysis, the produced sugar solution undergoes a subsequent fermentation step and the biofuel can be later refined. For bioethanol production the widely used microorganisms that are able to ferment sugars to ethanol can be either yeasts or bacteria.[110] The production yield is obviously a crucial role in determining the feasibility of a large-scale industrial production, thus all of the available sugars in the hydrolyzate must be converted to ethanol. For a long time, microbiologists thought that many of the sugars contained in biomass were unfermentable. Over the past decades, new methods in molecular biology, protein chemistry and genetic engineering have led to an increasing number of new strains, exhibiting improved characteristics to ferment the full spectrum of sugars available in hydrolyzates.[111,112,113]

To be able to decrease the production cost of biofuels and make it competitive with gasoline, there is a great need for enhanced glucohydrolysis, pretreatments and fermentation technologies. When enzymatic hydrolysis is used, depending on the connection between the hydrolysis and the subsequent fermentation step, four different fermentation strategies can be distinguished.

SHF (Separated Hydrolysis and Fermentation)

In this process the hydrolysis and the fermentation goes in two separated reactors. With this technology, optimal reaction circumstances can be set for the enzymatic hydrolysis, and for the fermentation. The drawback of this system is the high capital cost derived by the two reactors.[114]

SSF (Simultaneous Saccharification and Fermentation)

This approach involves enzymatic hydrolysis and the ethanol production from the synthesized sugar which goes in the same reactor. By the SSF, a higher yield can be achieved compared to the SHF; but, the reaction time is longer because of the different temperature optimum of the hydrolysis and fermentation. The SSF fermentation runs approximately 50°C, thus thermo tolerant yeast strains are required for this technique.[115]

Biostil:

Biostil is a continuous ethanol production system by fermentation which is an SHF with a distillation stage.[116]

DMC (Direct Microbial Conversion)

In this process enzymes are produced by the same microbe that is involved with the fermentation. The enzyme production, the cellulose hydrolysis and the fermentation go in the same reactor. By the available technology with this fermentation strategy the yields are still low and the byproducts formation is substantial. It is proposed that by the usage of genetic modification, compatible fermentation yields could be achieved with DMC.[117]

2.4.1.3 Corn Ethanol vs. Cellulosic Ethanol

Both corn-derived ethanol and cellulosic ethanol are renewable liquid transportation fuels that can be readily integrated with petroleum based fuels and their infrastructure. This provides a strong incentive for the development of innovative new bioethanol technologies. This existing infrastructure and capability suggest that once a practical/profitable bioethanol-related technology is developed, the technology could be quickly implemented. The deciding factor of its success on the marketplace will be the benefits to the nation's economic growth and to the quality of the environment.

Beside its biorenewable nature, the attractiveness of bioethanol as a potential substance for replacement of conventional fossil fuel lies on its low net carbon dioxide release compared to that of burning fossil fuels.[97] Unfortunately, when the whole biofuel production cycle is analyzed, it is noted that several process steps still require the utilization of energy provided from fossil origins.[118] Even if energy corps requires energy inputs for production, processing and transportation, a future successful bioethanol industry must have a substantial positive energy balance. This balance has been described by the fossil energy-replacement ratio (FER), which compares the energy yielded from the source with the amount of energy from fossil fuels used to produce it. Figure 18 compares the FER in case of four energy sources.[119]

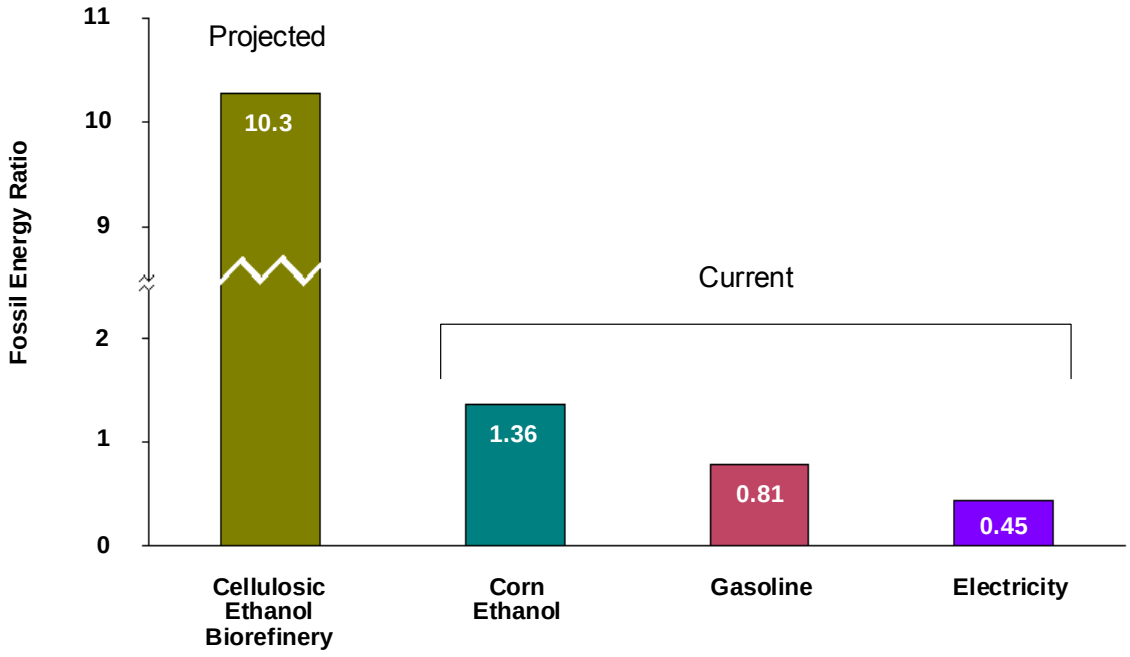

Figure 18. Comparison of energy yields with energy expenditures.
(Fossil energy-replacement ratio = Energy delivered / Fossil energy used)

Figure 18 shows the main benefit of using a second generation bioethanol over the first generation bioethanol; that is to say, bioethanol derived from lignocellulosic resources has a much higher FER ratio than when corn starch is used. It is also shown that the FER ratios in case of the biomass derived fuels are higher than both conventional energy resources, demonstrating their better sustainability. In addition to time, a mature bioenergy economy will substitute biomass-derived energy sources for fossil fuel, further reducing its net emissions.[120] Even ethanol derived from lignocellulosic biomass has a higher FER ratio and can be produced cost competitively with the market price of corn-starch ethanol; the economical competitiveness with gasoline still remains an issue.

2.4.2 Biodiesel

Although bioethanol represents the predominant first generation biofuel, biodiesel continues to garner regional support and in the U.S. it represents approximately 6.5% of the biofuels market.[121] Despite this limited market share, biodiesel has several strong attributes which suggest that its usage will continue to grow in the future. Attractive properties of biodiesel include ease of incorporation into existing fuels distribution systems, ready utilization in modern diesel combustion engines, growing demand and favourable exhaust emission profiles.[86]

Unfortunately these positive attributes need to be balanced against the limited global production of plant oils and animal renderings needed to propel growth in this industry. Table 13 summarizes the proposed main biodiesel feedstocks and their produced annual amounts for potential biodiesel production in the U.S. by 2016.[122]

Table 13. Projected biodiesel feedstocks and their proposed annual production in the U.S. by 2016.

Feedstock *	Resource	U.S. Potential [million gallons]***
PPO	Refined vegetable oil	1700
	Natural expansion of feedstocks by 2016	1800
	Corn oil from ethanol production **	750
WVO	Recycled restaurant oil (yellow grease)	380
	Recycled trap grease (brown grease)	525
Animal fats	(white grease)	300
Total feedstocks for biodiesel production by 2016		**5455**

* Pure plant oil (PPO), Waste vegetable oil (WVO).
** Based on proposed U.S. ethanol production by 2015.
*** Calculated as biodiesel equivalent volume from feedstock weight.

As summarized in Table 13, the prospective available feedstock for biodiesel production will be over 5 billion gallons--which is almost 10% of the 60 billion gallon diesel marketplace.[123] In contrast the U.S. produced only 500 million gallons of biodiesel in 2007, less than 1% of the diesel pool.[88] Table 14 summarizes the available oil crops, their typical oil yield and cultivation area needed to cover 50% of the U.S transportation oil needs.[124]

Table 14. Comparison of several available oil corps for biodiesel production to meet 50% of the United States' transportation oil needs.

Crop	Oil yield [L/ha]	Land area needed [M ha]	Percent of existing U.S. cropping area*
Corn	172	1540	846
Soybean	446	594	326
Canola	1190	223	122
Jatropha	1892	140	77
Coconut	2689	99	54
Oil palm	5950	45	24
Microalgae**	58.700	4.5	2.5
Microalgae***	136.900	2	1.1

* For meeting 50% of all transport fuel needs of the United States.
** 30% oil (by wt) in biomass.
*** 70% oil (by wt) in biomass.

Table 14 demonstrates that even in the case of a high-yielding oil crop such as oil palm, 24% of the total U.S. cropland will need to be devoted to its cultivation to meet only 50% of the U.S. transportation oil needs. This data clearly shows that oil crops cannot scientifically contribute to replacing fossil fuels in the near future. One of the most promising next generation of technologies that may address current production limitations is the development of algae energy farms for the efficient production triglycerides for biodiesel. Regardless of source, the conversion of triglycerides to biodiesel involves a transesterification step as shown in Figure 19.

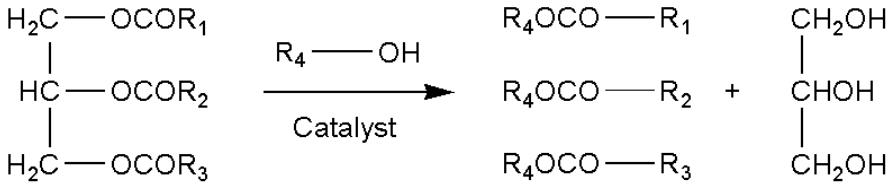

Figure 19. Transesterification reaction for biodiesel production $R_{1\text{-}4}$ are hydrocarbon groups.

The transesterification step is required to impart favourable fuel properties as direct use of plant oils with conventional diesel engines results in; coking and trumpet formation on the fuel injectors, carbon deposits, gelling of lubricating engine oil and incomplete combustion.[125] Transesterification of triglycerides, as shown in Figure 19, has been shown to mitigate these problems yielding a valuable, renewable biofuel resource. Many alcohols have been used in this reaction and influence final biodiesel properties; the most commonly employed alcohol used commercially is methanol.[126,127] Table 15 shows the change in melting point and cetane number of fatty acids and their methyl esters.

Table 15. Formula, molecular weight and properties of fatty acids and their methyl esters.

Fatty acid ***Methyl ester***	**Formula**	**Acronym**	**Molecular weight**	**Melting point [°C]**	**Cetane number**
Palmitic acid	$C_{16}H_{32}O_2$	C16:0	256.4	63-64	---
Methyl palmitate	$C_{17}H_{34}O_2$		*270.5*	*30.5*	*74.5*
Stearic acid	$C_{18}H_{36}O_2$	C18:0	184.5	70	---
Methyl stearate	$C_{19}H_{38}O_2$		*198.5*	*39*	*86.9*
Oleic acid	$C_{18}H_{34}O_2$	C18:1	282.5	16	---
Methyl oleate	$C_{19}H_{36}O_2$		*296.5*	*-20*	*47.2-55*
Linoleic acid	$C_{18}H_{32}O_2$	C18:2	280.5	-5	---
Methyl linoleate	$C_{19}H_{34}O_2$		*294.5*	*-35*	*28.5-42.2*
Linolenic acid	$C_{18}H_{30}O_2$	C18:3	278.4	-11	---
Methyl linolenate	$C_{19}H_{32}O_2$		*292.5*	*-52/-57*	*20.6-22.7*

The data in Table 15 indicates that the two important properties of fatty compounds of fuel vary with the chain of the fatty acid or ester. Cetane number of the methyl ester increases with increasing chain length and increasing saturation. Melting point also rises with augmenting chain length and increasing saturation. Therefore, the fatty acid profile is the major factor influencing the fuel properties of a biodiesel fuel; analytical methods for its determination are of great significance.[87,89]

Although commonly manufactured from natural gas, gasification of biomass in the future could yield a bio-based source of methanol.[128] A host of catalysts and conditions have been used to accomplish the transesterification step including assorted acids, bases, enzymes and physical treatments.[129,130] The base- and acid-catalyzed

transesterification reaction conditions are summarized in Table 16, and their reaction mechanism is depicted in Figure 20 and in Figure 21.[87]

Table 16. Reaction conditions for general base- and acid-catalysed transesterification conditions for biodiesel production.

Catalyst	Homogeneous catalysts	Heterogeneous catalysts	Alcohol/TriGly [mol/mol]	Catalyst/Oil [wt. %]	Reaction rate
Base	NaOH, KOH, NaOMe, KOMe, Na, NaH	Metal oxides, ion exchange resins, fixed bed	6 : 1	0.3-1.5	Fast
Acid	H_2SO_4, HCl, H_3PO_4, ion exchange catalyst	---	10-40 : 1	5-25	100 times slower than base

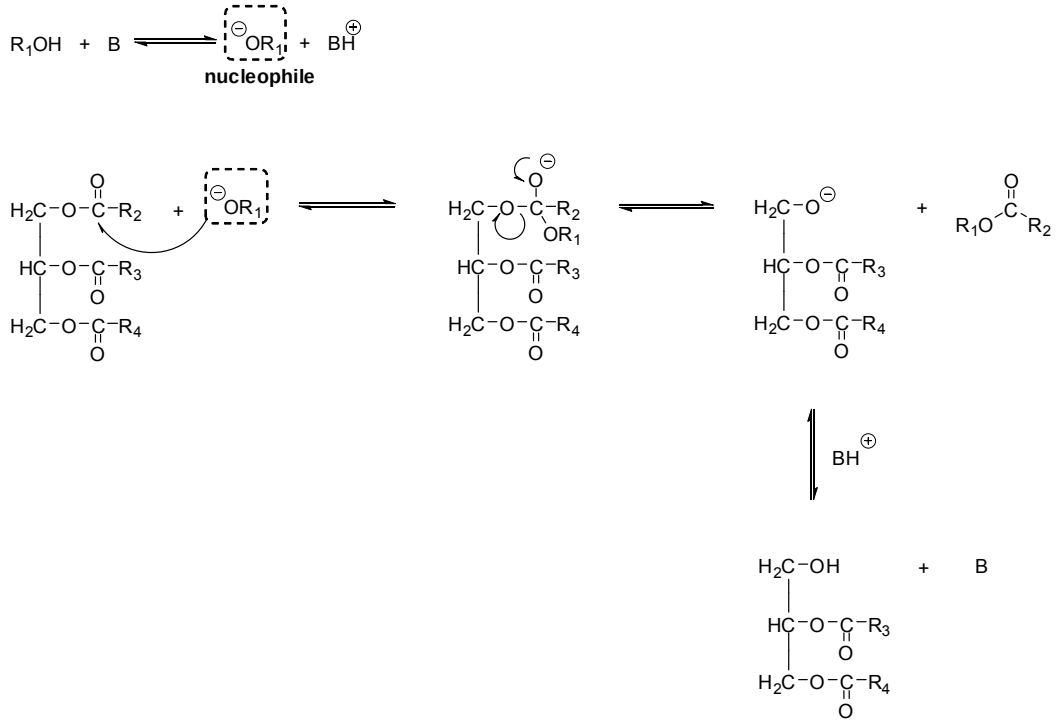

Figure 20. Reaction mechanism for base-catalyzed transesterification during biodiesel production. Where B is a base and $R_{1\text{-}4}$ are hydrocarbon groups.

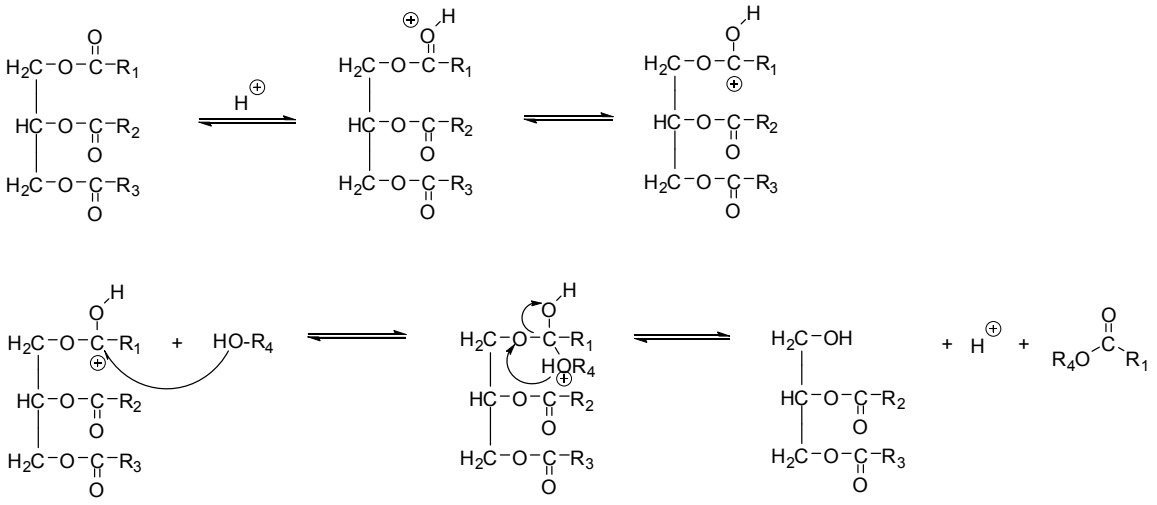

Figure 21. Reaction mechanism for acid-catalyzed transesterification during biodiesel production. Where $R_{1\text{-}3}$ are hydrocarbon groups.

Mono-alkyl esters and glycerin are the main products of the catalytic transesterification step. Glycerin is denser than the mono-alkyl esters and can be gravity-separated with the use of a settling vessel. After the glycerin is separated, the supernatant is washed with water to remove contaminants. The wash water is heavier than the mono-alkyl esters and during the washing sequence it absorbs contaminants, such as excess methanol, catalyst, soap, free and partial glycerols.[131] A common biodiesel production sequence utilizes several washing cycles to lower the concentration of process containments before the methanol recovery.[86] (Figure 22)

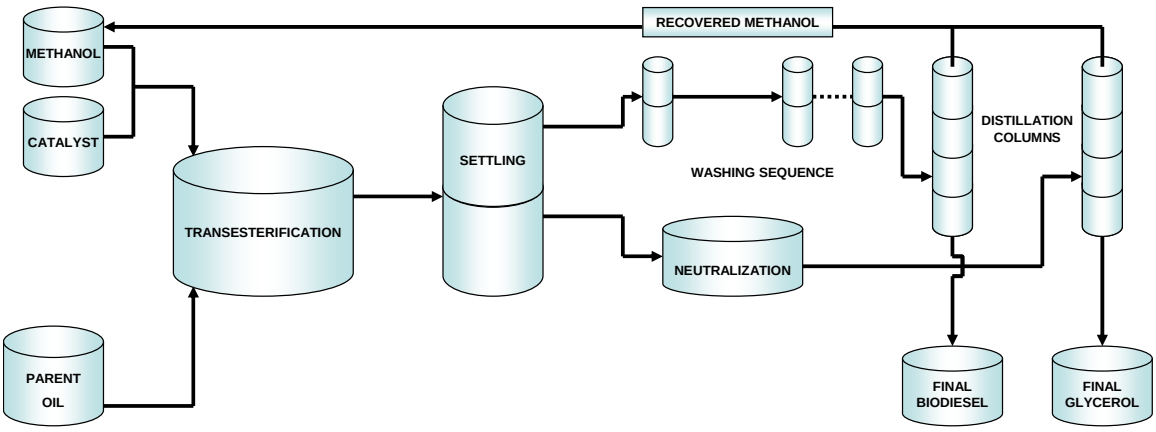

Figure 22 Outline of a commercial biodiesel production line.

After the washing sequence, the mono-alkyl ester stream enters into a subsequent alcohol recovery stage, where the remaining excess alcohol is removed through distillation and recycled for reuse. After the washing sequence and the alcohol recovery, the purified product is the desired biodiesel. To carry the designation "biodiesel fuel" the final purified fatty acid ester product must meet specifications set by the latest American (ASTM D 6751-08) and European (DIN EN 14214) standards.[132,133] To meet these standards, a common biodiesel production line utilizes downstream alcohol recovery and biodiesel purification steps to reach a low contamination level in the final product.[134]

Table 17. The American and European specifications for pure biodiesel (B100) prior to use or blending with diesel fuel.

Property	ASTM D 6751-08 limit	DIN EN 14214 limit	Unit
Acid Number	maximum 50	maximum 50	mgKOH/g
Calcium and magnesium	5	---	ppm
Carbon residue	maximum 0.050	maximum 0.3	wt%
Cetane number	minimum 47	minimum 51	No.
Cloud point	report	report	°C
Cold soak filterability	maximum 360	maximum 360	sec
Copper strip corrosion	maximum 3	Class 1	No./Rating
Density	---	860 - 900	Kg $m^{3\ -1}$
Distillation - Atmospheric equivalent temperature 90% recovery	maximum 360	---	°C
Flash point	minimum 130	minimum 101	°C
Glycerin – Free	maximum 0.020	maximum 0.02	wt%
Monoglyceride	---	maximum 0.80	wt%
Diglyceride	---	maximum 0.20	wt%
Triglyceride	---	maximum 0.20	wt%
Glycerin – Total	maximum 0.240	maximum 0.25	wt%
Iodine value	---	120	unit
Kinematic viscosity - 40°C	1.9 – 6.0	1.9 – 6.0	$mm^2\ sec^{-1}$
Linolenic acid methyl ester	---	12	wt%
Methanol content	maximum 0.20	maximum 0.20	wt%
Oxidation stability	minimum 3	minimum 6	hours
Phosphorus content	10	10	ppm
Polyunsaturated (>4 double bonds) methyl esters	---	maximum 1.00	wt%
Sodium and potassium	maximum 5	maximum 5	ppm
Sulfated ash	maximum 0.02	maximum 0.02	wt%
Sulfur (S15)	maximum 15.0	---	ppm
Sulfur (S500)	maximum 500	---	ppm
Total contamination	---	maximum 24.0	ppm
Viscosity 40°C	---	3.50 – 5.00	mm^2
Water content	---	maximum 500	ppm
Water and sediment	maximum 0.050	maximum 0.050	Vol.%

After transesterification, the separated glycerin phase is contaminated with alcohol, unused catalyst, soaps, free and partial glycerols.[135] In a commercial process the stream undergoes a subsequent neutralization step. (Figure 22) If a base is used as catalyst during the transesterification step, the separated glycerin phase is neutralized with an acid. After neutralization, commercial crude glycerin is produced by removing the water and alcohol in a subsequent distillation step.

For several industries, such as food, personal care, pharmaceutical and petrol, glycerol is utilized as a starting material or an additive, adding to the market value of this by-product and to the economical aspect of the transesterification process.[136] After the methanol recovery, the produced glycerol stream has an 80-88 wt% glycerin content and can be sold as a crude glycerin or can be further purified up to 98+ wt% to be sold as refined glycerol.[137] The refined glycerol has a higher market value and can be used directly. It also has the potential to be used as a starting material to convert it into other value added products, such as polyesters, nylons or valuable intermediates like propylene glycol or 1,3-propanediol by the chemical or the pharmaceutical industry.[138]

2.5 Integrating Biofuel and Pulp production

As outlined in the U.S.D.A.-D.O.E. 'Billion Ton' report, United States' agriculture and forestry reserves have the potential to address about a third of the current petroleum demand.[139] Shifting societal dependency from petroleum resources to renewable biomass resources have been proposed to have several positive ramifications, including enhanced national security, improved balance of trade, rural employment opportunities, and environmental performance parameters along with net reductions in

CO_2 emissions. Although the contribution of agro crops for biofuels production has been scrupulously examined, the potential for the forest products industry to contribute to this effort is frequently over-looked.[140]

Forest ecosystems constitute the world's largest accessible source of biomass that may be available for biofuel production in large scale.[1] The forest and agriculture industry can support renewable raw materials for the production of alternative biofuels. Lignocellulosic materials are the richest, yet one of the cheapest natural renewable resources in the world.[141] Table 18 summarizes the cost of some typical major lignocellulosic bioresources together with currently used and promising future energy corps suitable for biofuel production. [142,143,144]

Table 18. Cost of typical industrial bioresources and new generation lignocellulosic energy corps in the US, 2008.

Lignocellulosic bioresource	**Cost ($/ton)**
*Timber**	
Southern pine (SW)	40
Spruce and Douglas Fir (SW)	20
Oak (red, white, black) (HW)	37
Current agricultural energy corps	
Corn	281
Soybean	213
*New generation energy corps***	
Switch grass, Corn stover	35-45
Hybrid poplar, Eucalyptus	40-50

* Calculated as; standard cord is 1.4 SW or 1.6 HW short tons.
** Calculated farm-gate value for economical feasibility with existing technologies.

In 2002, North American pulp manufacturers produced approximately 62 million tons of paper and paperboard from 61 million tons of softwood pulpwood and 44 million tons of hardwood pulpwood.[145] The forest products industry is one of the few nationally based industries that have the necessary skill set and infrastructure available to collect sufficient biomass for the rapid development and commercialization of biofuel/biochemical technologies within the next 5-10 years.[146]

2.5.1 Current Pulp Manufacturing Technologies

Prior to any pulping operations, wood needs to be debarked and in most cases chipped. The bark and waste wood are burned in a furnace to capture its energy value, which generated 316 trillion BTU in the U.S. in 2002.[147] After debarking and chipping, wood samples are typically processed into pulp by one of two competing technologies.

In short, the wood can be defiberlated mechanically into mechanical pulp with 90+% yields which thereby utilize all three of the major wood biopolymers[148], or by chemical pulping which utilizes NaOH and NaSH (i.e., kraft pulping reagents) to delignifing wood. A typical U.S. kraft pulp mill will manufacture 350,000 tons of air-dried pulp/year which requires approximately 630,000 tons of wood. Typical kraft pulping conditions for bleach pulp grades are summarized in Table 19 and changes in wood fiber composition during kraft pulping are summarized in Table 20.[149]

Table 19. Softwood and hardwood kraft pulping conditions.[2,150,151]

	Softwood	Hardwood
Active alkali on dry wood	17 - 21 %	14 – 18 %
Liquor sulfidity (Na_2S)	25 %	25 %
Max. cooking temperature/ ^oC	170	170
Total cooking time/min	112 - 174	63 – 95
Kraft cook completed at lignin content	5 %	2 %
Yield	48 – 43	49 – 47

Table 20. Typical wood chemical distribution for wood before and after kraft pulping.[152]

Component	Wood Components		Kraft Pulp Components	
	Pine	Birch	Pine	Birch
	As a % of Original Wood			
Cellulose	38 – 40	40 – 41	35	34
Glucomannan	15 - 20	2 - 5	5	1
Xylan	7 - 10	25 – 30	5	16
Other carbohydrates	0 - 5	0 – 4	-	-
Lignin	27 - 29	20 – 22	2 – 5	1.5 – 3
Extraneous compounds	4 - 6	2 - 4	0.25	< 0.5

The delignification during the kraft cooking cycle proceeds in three distinct phases. Figure 23 depicts the three phases, the lignin content and reaction time in the case of a conventional SW kraft pulping.[152]

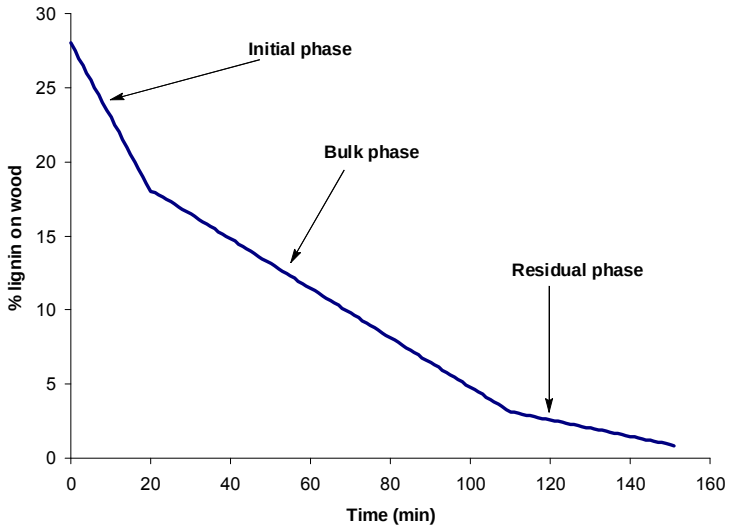

Figure 23. Lignin content (% on wood) vs. reaction time for conventional softwood kraft pulping.

The first phase of kraft pulping is commonly refereed to as the initial phase. In case of a conventional kraft pulping process, this occurs during the first 20-25 minutes of the cooking at temperatures of 150°C and under. The initial phase is mainly controlled by diffusion and the ~30% of the original lignin is removed from the chips during this time. The second phase of kraft pulping is called the bulk phase. In case of a conventional kraft pulping process, it stands for the cooking times between 25-100 minutes at temperatures 150-170°C. Most of the lignin is removed in this phase and it is controlled by chemical reactions rather than by diffusion. The last phase of kraft pulping is called the final or residual phase. In this phase the rate of delignification significantly decreases; begins when ~90% of the lignin has been removed and marks the end of the cooking.

During kraft pulping, lignin degradation reactions that are desirable lead to the liberation of lignin fragments and enhance their dissolution. The two main degradation reactions during kraft pulping involve the cleavage of α-aryl ether bonds and β-aryl ether

bonds. The reactivity of such linkages depends on its activation energy and the type of moiety present relative to the propane side chain.[153] At lower cooking temperatures during the initial phase, α-aryl ether linkages are cleaved by the conversion of the phenolate unit into the corresponding quinone methide (QM) intermediate. Initial phase lignin chemistry is depicted in Figure 24.

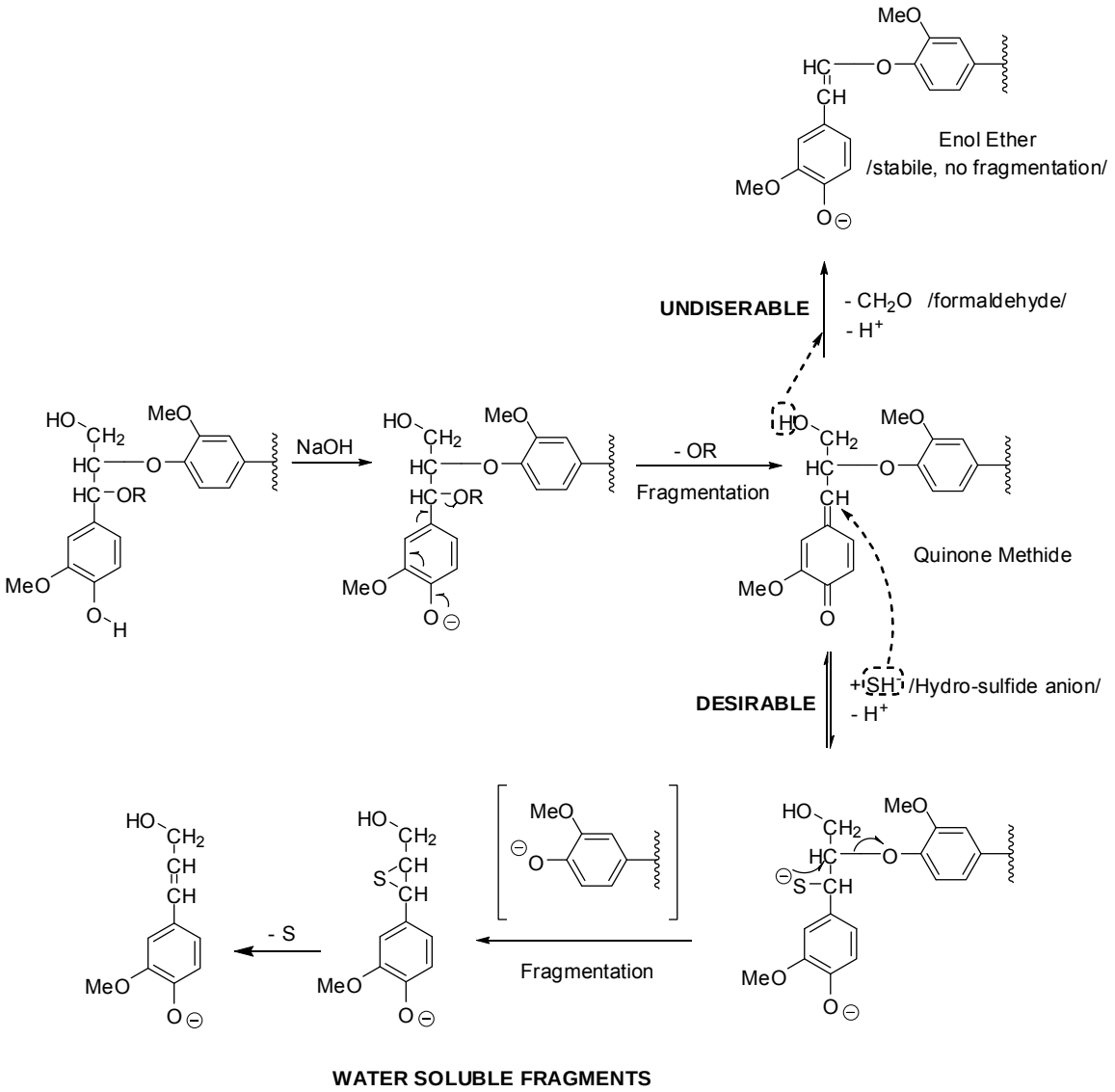

Figure 24. Kraft pulping; Initial phase lignin chemistry.

The first two steps involve an alkali assisted rearrangements, where the phenolate unit is converted into the QM intermediate if a suitable leaving group is present in the α-carbon. At optimal cooking conditions, the reaction proceeds by an addition of a hydrosulfide anion which yields a benzyl mercaptide structure. The mercaptide anion subsequently forms a thriirane intermediate by a nucleophilic attack on the β-carbon. The elimination of the β-aryloxy group leads to further fragmentation. Higher temperatures and increased alkali concentrations during the initial phase can lead to an undesired alternative chemical route. With the elimination of the terminal hydroxymethyl group as formaldehyde, the QM intermediate can be converted to alkali-stable enol ether and inhibit the polymer from further fragmentation.[154]

During the bulk phase, through a nucleophilic attack of an ionized hydroxyl group present on α or γ-carbon, will lead to the cleavage of β-aryl ether linkages in nonphenolic units. During fragmentation, the forming β-aryloxy fragment will convert into the corresponding QM intermediate regenerating initial phase molecules. Figure 25 summarizes the cleavage of a β-aryl ether linkage by an ionized hydroxyl from the α-carbon during bulk phase cooking conditions.

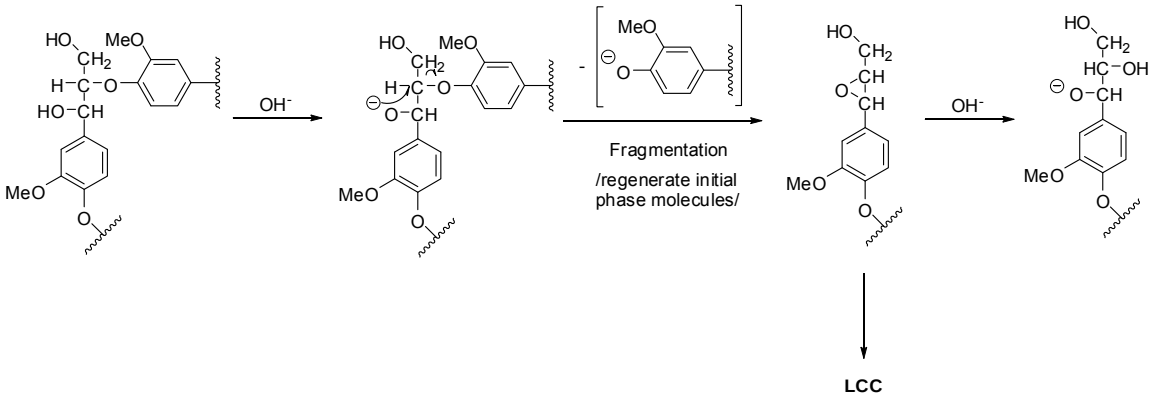

Figure 25. Kraft pulping; Bulk phase lignin chemistry. [155,156]

During chemical pulping, lignin is chemically degraded and extracted from wood in aqueous environment, removing 85-93% of the lignin and approximately 56-71% of the hemicelluloses. The dissolved lignin and carbohydrates are discarded in a form of a caustic side stream--black liquor. Currently, this material is burned in a low efficiency Thompson recovery furnace to recover energy and cooking chemicals. For further delignification to remove the residual lignin in the delignified pulp, it can undergo subsequent bleaching sequences to reach the desired lignin content for the production of pulp, paper and paperboard.[157]

2.5.2 Future Prospects for Pulp Manufacturing and Bioresources for Biorefinery

After the Kraft pulping cycle, the BL and the described valuable chemicals in it are burned in a low efficiency Thompson recovery furnace to recover energy and cooking chemicals. Although the recovery furnace has been refined through generations, it remains the single largest capital investment in a kraft pulp mill and is not amendable to incremental increases in production. Hence, for several pulp mills the capacity of the recovery furnace dedicates the pulp mill's production capacity. A continuing interest in this field is the desire to recover fractions of carbohydrates and/or lignin from the Kraft cooking liquors for biopower, biochemical and biomaterial utilization.

2.5.2.1 Carbohydrates

The loss of select wood polysaccharides during kraft pulping is a natural outcome of kraft pulping conditions. As summarized in Table 20, kraft pulping of softwood pulps leads to an extensive removal of glucomannans,[158] and for hardwoods a loss of xylans.[159] During kraft pulping, these extracted hemicelluloses are degraded into low-value isosaccharinic acids.[160,161] The sugars and lignin extracted during kraft pulping[162] are subsequently concentrated and incinerated in a recovery furnace. The heating values of several major components in BL are summarized in Table 21.[163]

Table 21. Heating values for some components in black liquor.

Component	Heating value [kJ/kg TDS*]
Softwood lignin	26.900
Hardwood lignin	25.100
Carbohydrates	13.600
Resins, fatty acids	37.700
Sodium sulphide	13.900
Sodium thiosulphate	5.800

* TDS: Total dissolved solids.

Table 21 shows that the heating value of kraft BL (i.e. the amount of heat released during combustion) varies on the wood species being pulped. If the heating values summarized in Table 21 are combined with the chemical composition of the BL, it can be calculated that the extracted hemicelluloses only provides ~25% of energy resources for a recovery furnace. Since the bulk of the energy is derived from the combustion of lignin, the carbohydrate fraction in the BL is an under-utilized renewable resource during the energy recovery.[164,165]

2.5.2.2 Lignin Structures Recovered After Kraft Cooking

After the kraft pulping, the lignin is separated into two fractions: the dissolved lignin that is discarded with the BL and the residual lignin that remains in the pulp. The lignin content of a typical conventionally-produced kraft pulp is in the range of 4-5%.[153] Pulping to lower lignin contents under these conditions causes a severe degradation to the carbohydrate fraction resulting in a pulp with poor papermaking qualities. The reasons for the poor selectivity of kraft pulping have been the subject of much debate. One reason given is that the structure of the residual lignin that remains in the fiber at the end of the cook has a low reactivity towards the pulping chemicals, making its fragmentation and dissolution difficult.[166,167,168] Alternatively, it has been proposed that dissolution is hindered by attachment of the residual lignin to carbohydrates forming lignin-carbohydrate complexes (LCC).[169,170]

After the chemical pulping, the chemically-degraded soluble lignin fraction is extracted from wood providing the dissolved lignin in the BL, while the insoluble and/or condensed lignin fraction in the pulp fraction provides the residual lignin. The molecular composition of the residual and dissolved lignin after kraft cooking are depicted in Table 22.[171]

Table 22. Number of functional groups per 100 carbon atoms in spruce mill wood lignin (MWL) and in the residual and dissolved lignin after a Kraft cook (kappa# 30.5).

Type of Carbon	MWL	Residual lignin	Dissolved lignin
Carbonyl	0.8	-	0.3
Carboxyl	-	2.1	1.5
Olefinic + Substituted Aromatic C	39	54	39
Aliphatic CH_X-OR	23.6	9.5	10.1
Methoxyl	11.2	9.1	8.9
Aliphatic CH_X	4.9	10.4	16.0

There are three categories of reactions that are believed to occur during kraft delignification: 1) degradation reactions that liberate lignin fragments and enhance solubility, 2) condensation reactions in which lignin fragments recombine to form alkali stable linkages, and 3) other reactions in which no net fragmentation occurs but alkali stable structures--like LCC, stilbenes and vinyl ethers--are formed, making additional fragmentation difficult.[172] The increased olefinic and substituted aromatic functional groups in the residual lignin compared to MWL in Table 22 are due to condensation reactions, while the decreased methoxyl content after kraft cooking is due to the nucleophilic attack and cleavage of the methoxyl moietes by hydroxyl anions.[171] These various reactions and their significance concerning the structural features of residual and dissolved lignins will be reviewed.

2.5.2.2.1 Degradation Reactions

The type of lignin reactions that occur during kraft pulping can be classified as degradation and condensation reactions. Degradation reactions are desirable, since they lead to lignin fragmentation and enhancement in solubility in aqueous media. The two main degradation mechanisms, the initial phase- and the bulk phase delignification mechanism, are depicted in section: 2.5.1 Current Pulp Manufacturing Technologies.

2.5.2.2.2 Condensation Reactions

In contrast to the degradation reactions, condensation reactions lead to the formation of alkali-stable linkages and are, therefore, less desirable during delignification. During the initial phase the hydrogen sulfide and sodium hydroxide anions have to compete with the lignin nucleophiles for QM intermediates. Figure 26 illustrates the proposed competitive addition of external nucleophile and an internal nucleophile with a C_5 resonance structure.[173]

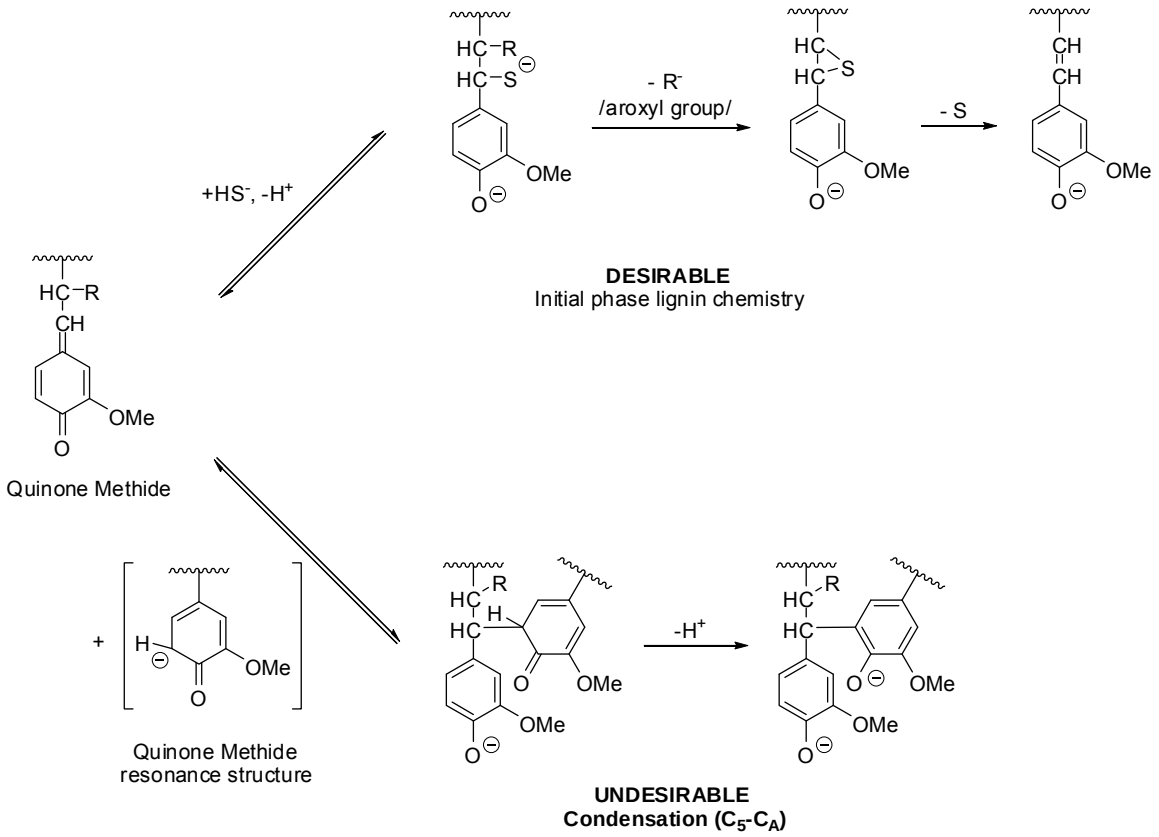

Figure 26. Competitive addition of external and internal nucleophiles to quinone methide intermediates.

Since the addition of the nucleophile to the QM is reversible, the competition is not only depending on the nucleophicity of the species, but also the product undergoing an irreversible reaction. In case of a good leaving group on the β-carbon (aryl ether) the cleavage of the β-aryl ether will predominate over condensation reactions.[174] During condensation reactions, the QM acts as an acceptor and the phenolate ion acts as the nucleophile. The addition of the nucleophile is followed by abstraction of a proton and rearomatization. The forming C-C bond in the condensation product is alkali stable, survives the cook and either ends up in the residual lignin or lowers the solubility of a dissolved lignin by increasing its aromatic character and DP.

Figure 26 depicts the competitive addition of an internal nucleophile with a C_5 (#5 carbon on the aromatic ring) resonance structure. An additional route for condensation reactions involving an internal nucleophile is the alkali-promoted condensation reaction. As shown in Figure 24, higher temperatures and increased alkali concentrations during the initial phase can lead to an undesired, alternative chemical route involving the formation of formaldehyde with the elimination of the terminal hydroxymethyl group. The forming formaldehyde with two QM intermediates can form alkali stable C-C bond in the condensation product that survives the cook and ends up in the residual lignin.[175] The condensation reaction involving two phenolic ions and formaldehyde has been drawn schematically in Figure 27.

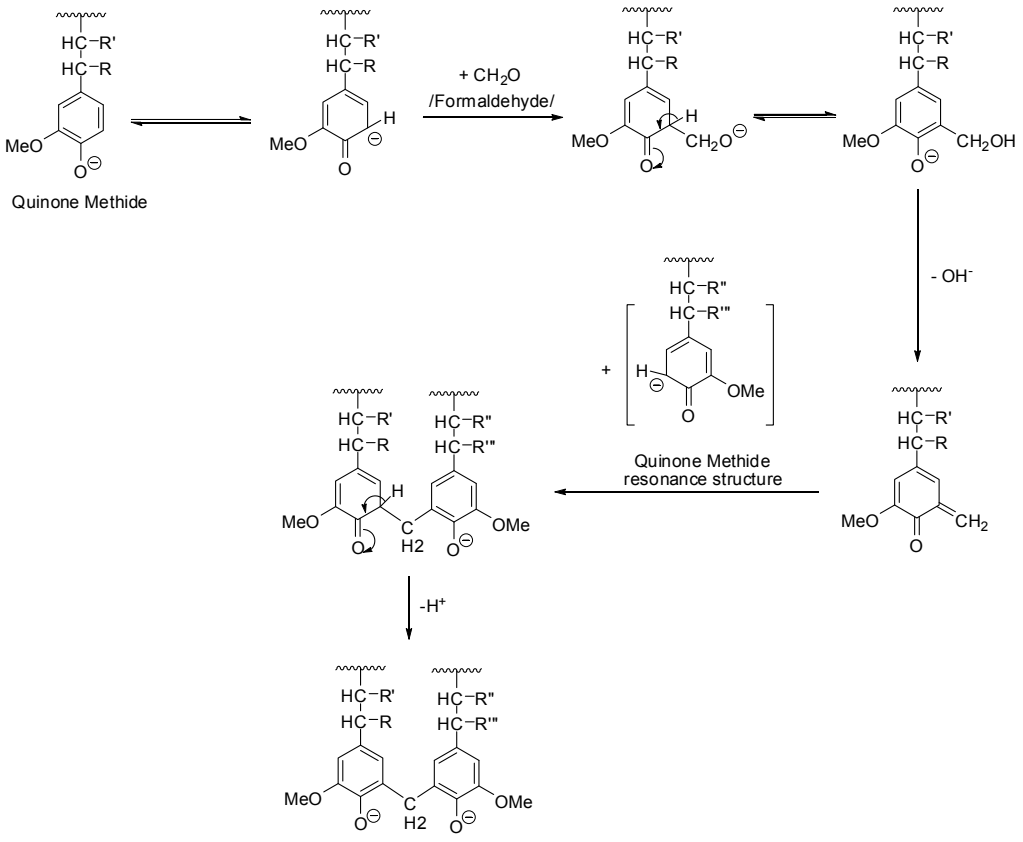

Figure 27. Alkali-promoted condensation reaction of phenolic units.
R: are H or aroxyl groups.

2.5.2.2.3 Lignin Carbohydrate Complexes

Both the residual lignin and the dissolved lignin contain LCC. While it believed to be present in the native wood, it mainly forms during the kraft cooking cycle.[176,177] There are several different linkage types between lignin and carbohydrate and they can be generalized as either being alkali sensitive or alkali stable.[178]

The alkali sensitive linkages are cleaved under the harsh alkali conditions of the kraft cook. The formation of an alkali sensitive phenolic LCC linkage is depicted in Figure 28.

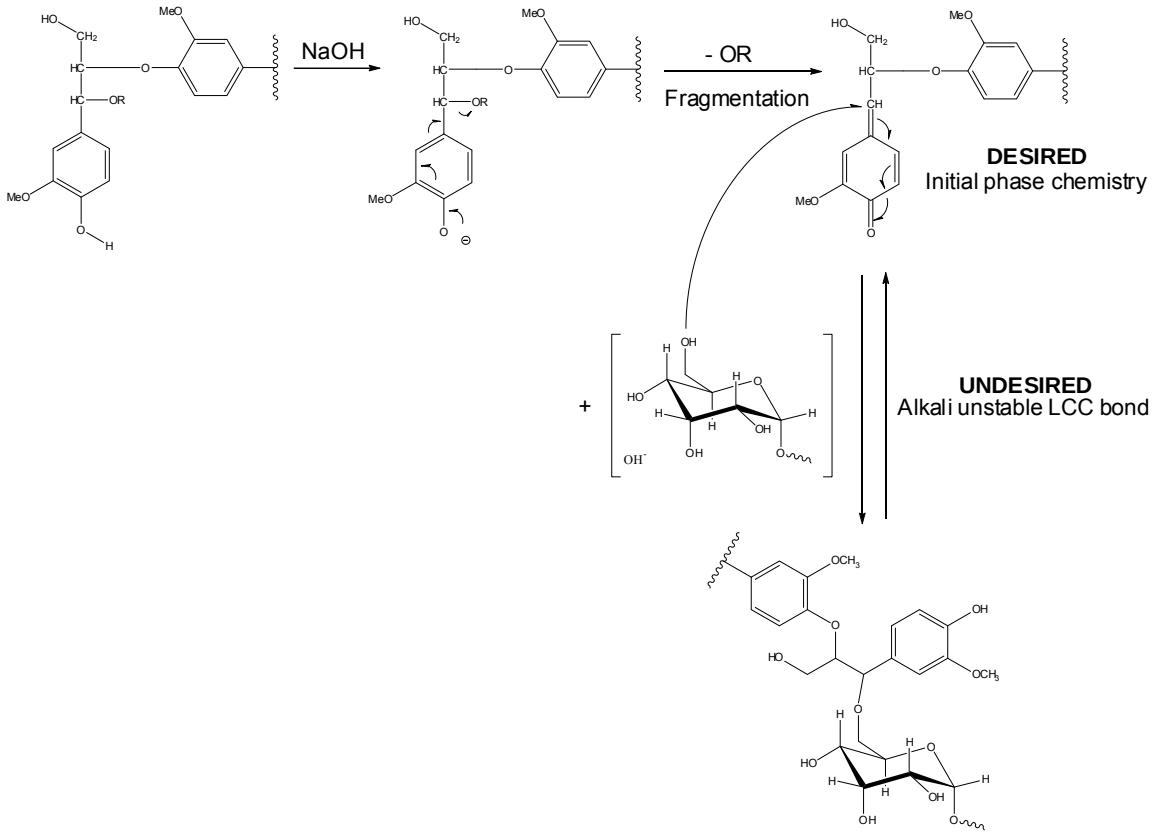

Figure 28. Formation of lignin carbohydrate complex (LCC) under Kraft pulping conditions. (phenolic)

Figure 28 shows the reaction between carbohydrate and a phenolic lignin fragment during the initial phase. Phenolic LCC formation can happen after the first two steps in the initial phase delignification, when, after the cleavage of the α -aryl ether and the rearrangements to the QM intermediate, instead of an addition of a hydrosulfide anion yielding a benzyl mercaptide structure, a carbohydrate hydroxyl attacks the α –carbon to form the LCC. Due to the free phenolic hydroxyl, the formed structure is alkali sensitive and not stable under kraft cooking conditions.

The alkali stable linkages that survive the kraft cook, have been suggested to be present in kraft pulps and have been proposed to contribute to the difficulty in removing lignin at the end of the kraft cook. [179] The formation of an alkali stable non-phenolic LCC linkage is depicted in Figure 29.

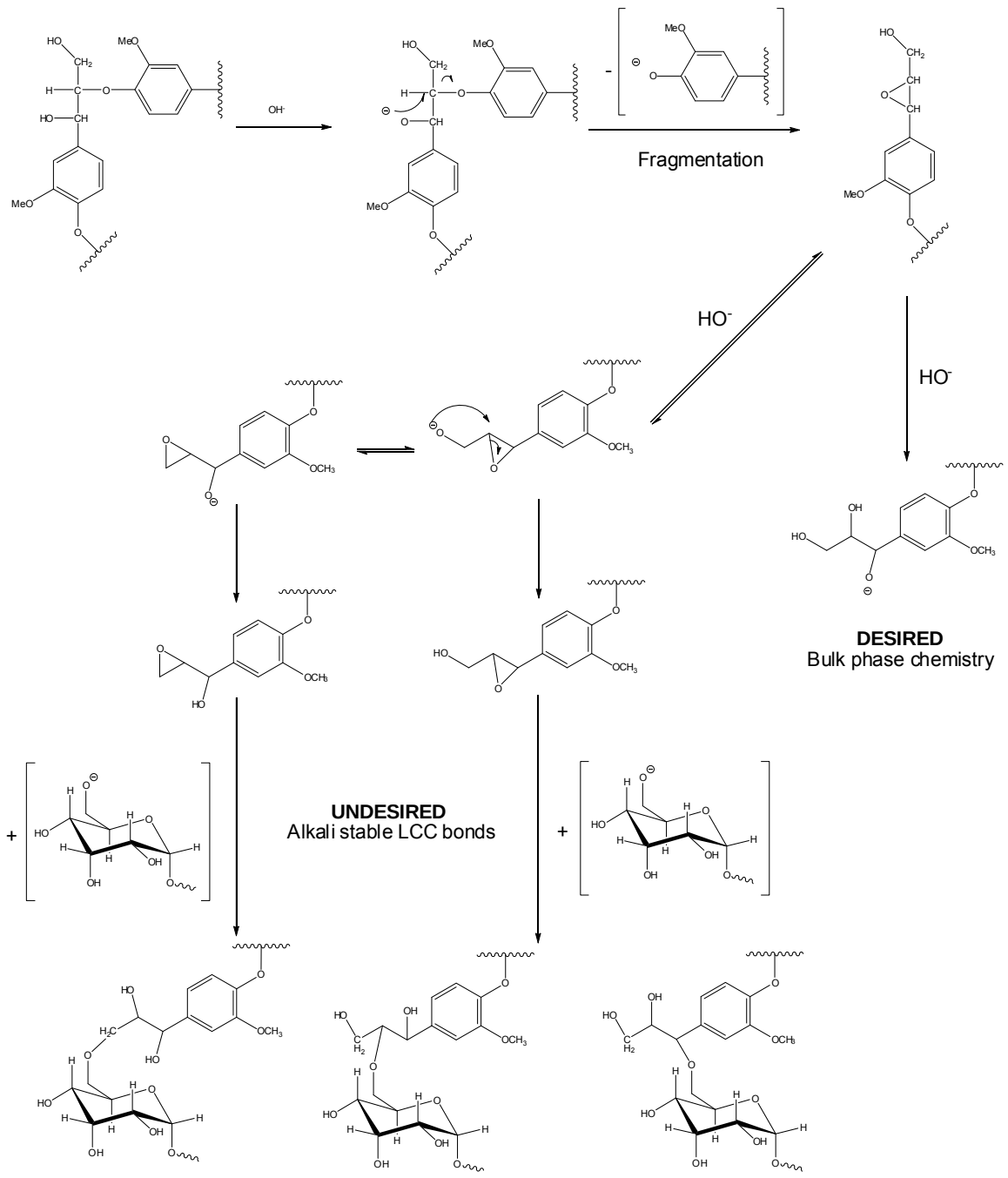

Figure 29. Formation of lignin carbohydrate complexes (LCC) under Kraft pulping conditions. (non-phenolic)

Figure 29 summarizes the reaction between a carbohydrate and a non-phenolic lignin fragment under the bulk phase. Non-phenolic LCC formation can happen after the second step in the bulk phase delignification, after the nucleophilic attack of an ionized hydroxyl group present on α or γ-carbon lead to the cleavage of β-aryl ether linkages. For LCC formation, instead of the addition of a hydroxyl anion depicted in bulk phase delignification, the other hydroxyl group becomes ionized also and forms an epoxy linkage either between the α-β or β-γ carbons. When the highly reactive epoxy linkage is attacked by a carbohydrate hydroxyl group, it ties the lignin fragment to cellulose or hemicellulose. The LCC formed with non-penolic lignin fragments are alkali stable and difficult to remove.

2.5.3 Promising Lignin Conversion Methods

The distinct difference between the chemical and physical properties of lignin and fossil fuels mainly result from their higher oxygen content and the difference in their carbon chain length.[180] Previous attempts to decrease the degree of polymerization and/or the oxygen content of lignin have involved various transformations, including hydrothermal decarboxylation[181], pyrolysis[182], carbonization[183], metal-catalyzed decarboxylation[184,185,186], metal-catalyzed hydrogenation[187], and hydrogenolysis.[188] Examples of these various reactions and their significance concerning the structural features of the lignin after conversion will be reviewed.

2.5.3.1 Lignin Hydrogenation and Hydrogenolyis

During hydrogenolysis, the hydrogen is utilized for the cleavage of C-O inter-lignin linkages. During hydrogenation, carbon-carbon or a carbon-oxygen double bonds is saturated by hydrogen: the H/C ratio is elevated, but depolymerization does not occur. Figure 30 depicts the differences between lignin hydrogenation and hydrogenolysis.

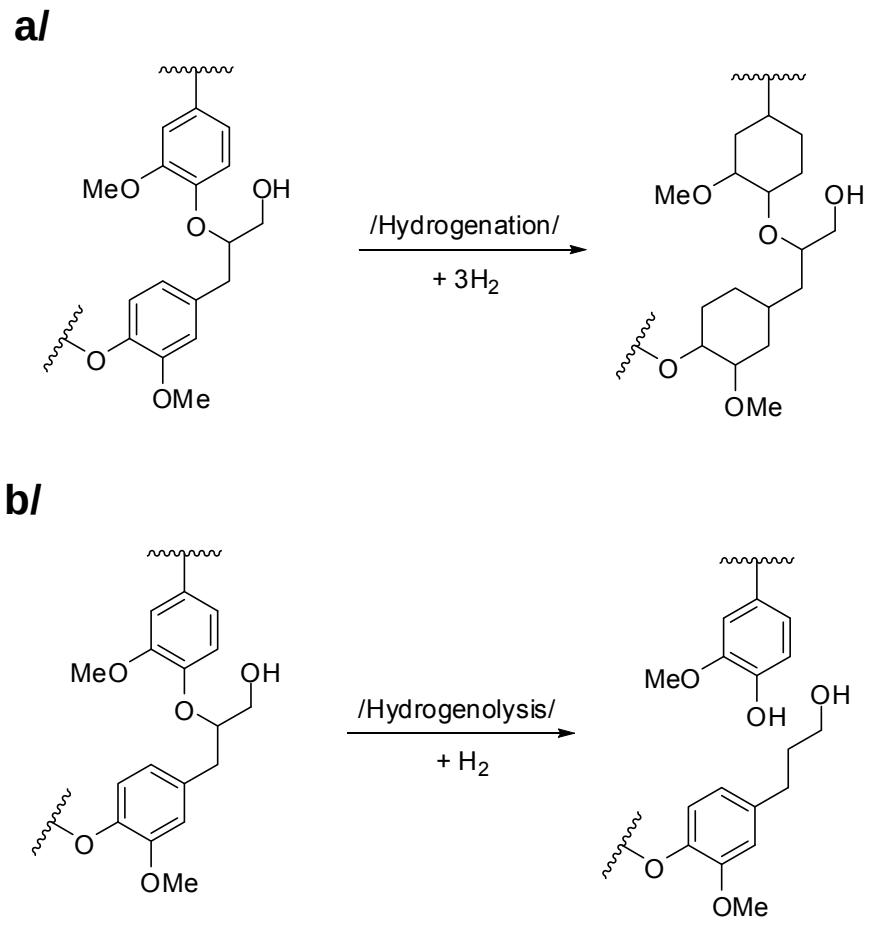

Figure 30. Example for hydrogenation (a) and hydrogenolysis (b) of a β-O-4 lignin dimer.

Previous lignin hydrogenation studies employed either high temperatures (> 200ºC) and/or high H_2 pressures (>7 MPa), or strong acidic or basic media. Depending on the reaction conditions, up to 60-80% conversion of the starting lignin to liquefied mixtures was obtained. These mixtures contained hydrogenated products such as *o*- and *p*-cresol, phenol and *p*-ethylphenol.[189,190,191] The knowledge concerning the chemical mechanisms involved in these harsh conditions, the reusability of the catalyst, and tailoring the selectivity of the hydrogenation towards specific lignin groups is improved.[192,193]

Recent hydrogenation studies with colloidal Ru or mono-, di- and tetra-nuclear Ru-Arene complexes as catalyst on milled wood lignin indicate that a 50% decrease in DP can be accomplished. However these catalyst systems are designed for the hydrogenation of the aromatic ring in the lignin polymer, the decrease in DP during the hydrogenation suggests that hydrogenolysis of the biopolymer also happened simultaneously.[194,195] Table 23 summarizes the extent of aromatic hydrogenation of several ruthenium containing catalyst systems on MWL.

Table 23. Extent of aromatic hydrogenation of a mill wood lignin catalyzed by various Ru systems.

Ru catalyst system*	Ru conc. [mM]	Time [h]	Conversion (%)
$RuCl_3.3H_2O$/3.5 TOA	3.0	24	56.4
$RuCl_3.3H_2O$/3.5 TOA	3.0	96	64.9
$RuCl_3.3H_2O$/7 TOA	1.5	24	33
$RuCl_3.3H_2O$/3.5 TOA/TPPMS	1.9	24	21
$RuCl_3.3H_2O$/3.5 TOA/TPPMS	1.9	72	48
$Ru_2Cl_4(C_6Me_6)$	2.2	24	5
$Ru_2Cl_4(C_6Me_6)$/3 Na_2CO_3	0.7	72	5

* 80 °C under 50 bar in 2:1:1 PrOH:H_2O:$CH_3OCH_2CH_2OH$.

Hydrogenation with phosphine ligand containing ruthenium complexes of carbon-carbon double bond and/or carbon-oxygen bond containing chemicals has provided additional insight on how to tailor the catalytic selectivity towards carbon-oxygen bond cleavage over carbon-carbon double bond hydrogenation.[196,197] The expectation is that selective hydrogenolysis of lignin leads to potential fuel precursors or other value added chemicals by oxygen decrement and hydrogen increment and to products with lower molecular weight by reductive cleavage of C-O-C bonds.[198] Despite the extensive research, lignin still has a low commercial value and only combusted as a low grade fuel.

2.5.3.2 Lignin Liquefaction

Lignin liquefaction is mainly conducted on high temperatures by flash pyrolysis.[182] While there are a variety of catalytic and non-catalytic pyrolysis techniques for biomass and lignin liquefaction, flash pyrolysis techniques are conducted primarily at relatively high temperatures: 300-500°C with a short resident time only ranging between 1-90 minutes.[199] Table 24 summarizes several liquefaction techniques on lignin or lignin containing feedstock and their bio-oil yields.[200]

Table 24. Bio-oil yields in case of different lignin and lignocellulosic liquefaction techniques with reaction conditions.

Staring material	Technique	T [°C]	Gas /pressure	Space time [min]	Bio-oil yield [%]
Pinus insignis,	Fast pyrolysis (Zeolite: HZSM-5)	400	N_2/ Atm.	5	64
Raw pyrolytic bio-oil (SW)	Fast pyrolysis (Zeolite: HZSM-5)	450	Atm.	30	86
Thio lignin*	High pressure catalytic hydrogenation	400-450	H_2/200 bar	30	80
Eucalyptus gummifera	Carbonization	400	Sealed	90	52

* Precipitated from BL with flue gas (CO_2) at pH 8.5.

During the catalytic liquefaction of lignin retrieved from BL, it is important that the catalyst not be deactivated by sulfur. Since the sulfur content in lignin obtained from BL can be as high as 5%, conventional commercial catalyst such as nickel, molybdenum and copper can not used.[153] Another requirement is that the activity of the catalyst should be high enough so that the reaction does not stop at tar formation, which is the first stage reaction, but advances to tar decomposition, which is the second stage during pyrolysis.[201] With recent advances in the control of feedstock, water content, temperature ramping and control of the space and time on stream, most of the problems created by coke formation can be avoided.[202,203]

Given that novel pyrolysis yields ranging between 60 and 80% and the produced biomass pyrolysis oil has heating values between 16-18 MJ kg^{-1} on dry basis, it is of great interest in the valorization of the bio-oils as a fuel or fuel substitutes. However the use of crude biomass pyrolysis oil as fuel for diesel engines has several limitations. The oils produced by the pyrolysis of biomass, due to the high levels of oxygen, may be highly viscous and corrosive, relatively unstable and may exhibit a poor heating value.[204] As a

low-cost solution that avoids the adaptation and technological modifications of diesel engines, these limitations can be partially solved by preparing bio-oil/diesel emulsions.

Despite the extensive research on this field, there are still serious limitations such as; pH in the range of 2.5-3.4, high corrosiveness and instability.[205] Thus, before pyrolytic oils can be used as a regular fuel, it is essential to upgrade the crude bio-oil to impart favourable fuel properties. There is a wide variety of reaction mechanisms published in the field of upgrading of pyrolytic oils and they are essentially involve the removal of oxygen. Promising methods for upgrading pyrolytic oils involves reactions, such as deoxygenation, decarboxylation and decarbonylation of the oil constituents, as well as cracking, oligomerisation, alkylation, isomerisation, cyclisation and aromatisation.[206,207]

2.5.3.3 LignoBoost

As mentioned in section 2.5.1 (Current Pulp Manufacturing Technologies), today's modern chemical pulp mills have the potential of producing excess heat and/or power. However, the recovery boiler is often the bottleneck in the process due to its high investment cost, thus preventing an increase in production. Recently, a green process referred to as "LignoBoost" provides a viable separation of lignin from kraft cooking liquors by employing carbon-dioxide to precipitate lignin from alkaline solutions.[208,209,210,211]

This process reduces the heat of combustion of the BL before it is burned in the recovery boiler by removing a fraction of the lignin in BL thus, the lignin can be exported from the process and used in other applications. The application of this process involves acidification of an alkaline cooking liquor with CO_2, precipitation, filtration and washing.[212,213,214] Figure 31 shows the schematic diagram of the lignin extraction process by LignoBoost.

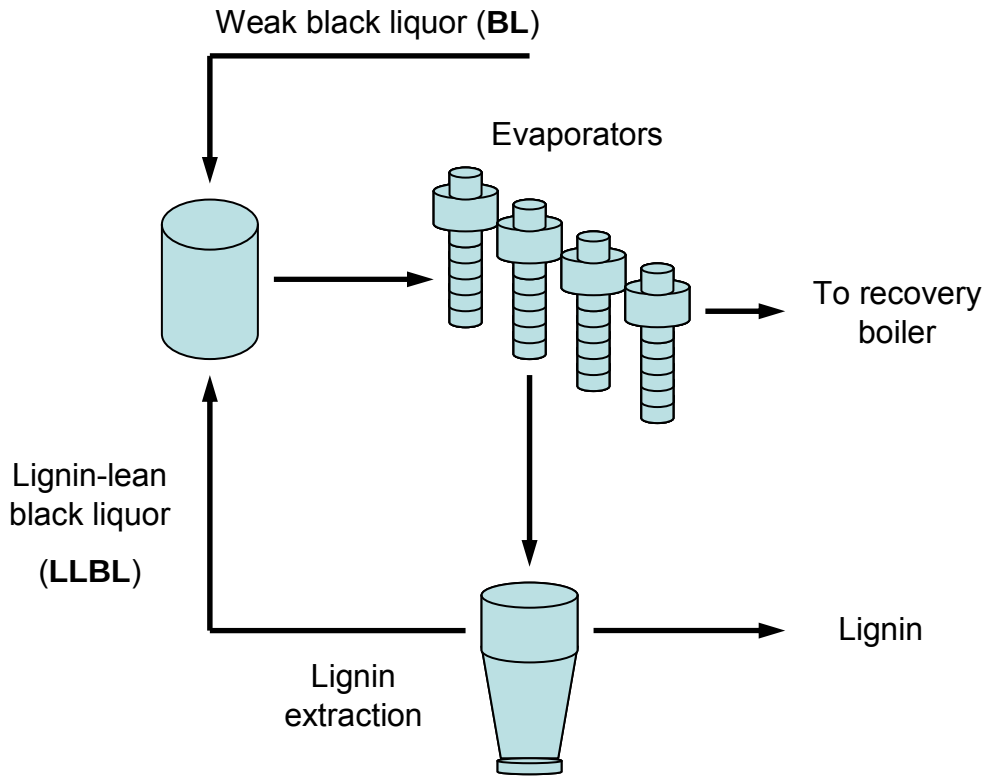

Figure 31. Schematic diagram of the lignin extraction section (LigniBoost) in the chemical recovery sytem.

BL contains both organic and inorganic components, with approximately 50% of the organic part being lignin.[215] The composition of BL obtained from SW is summarized in Table 25.[216]

Table 25. The chemical species in kraft black liquor obtained from North American softwood species.

Chemical component	Concentration [w/w-% dry basis]
Lignin	30-45
Hydroxy acids	25-30
Extractives	3-5
Acetic acid	5
Formic acid	3
Methanol	1
Suphur	3-5
Sodium	15-20

One obvious consequence of the extraction of a substantial fraction of lignin is that the properties of the BL will change; important properties include viscosity, boiling point elevation and heating value.[217] Viscosity has a significant influence on heat transfer during evaporation, on capacity of the pumps and on size of the droplets in the recovery boiler system; however, the reduction in viscosity is only pronounced when lignin-lean black liquor (LLBL) at dry contents is above 40%.[218] Furthermore, a change in the composition of BL affect the interaction of the ions and the water molecules when lignin is removed from the liquor; this, in turn, affect the boiling point elevation and, thus, the total available temperature difference at a given temperature of live steam and condensing water in the evaporators. Since the boiling point elevation of LLBL levels off approximately 40% dry contents and above, in contrast to the original BL, the process

problem is easily avoidable.[219] Table 26 summarizes the dry content before (BL) and after (LLBL) the LignoBoost delignification process at different final pHs in case of SW and HW BL samples.[220]

Table 26. Dry content of original black liquor (BL) and lignin-lean black liquor (LLBL) utilizing different softwood and hardwood kraft cooking processes for LignoBoost lignin precipitation.

Black liquor	Dry content of BL [%]	pH of BL	Dry content of LLBL [%]	pH of LLBL
Hardwood	29.7	13.4	25.7	9.2
Softwood	37.2	13.3	25.7	9.9
Softwood	31.5	13.1	28.0	9.0
Softwood	41.0	13.8	34.8	10.1
Mixed softwood and hardwood	42.3	13.7	35.9	10.0

Study on the precipitated lignin's polymer structure has shown that it is mainly the high molecular lignin that is precipitated from BL during the LignoBoost process.[221] Thus, not only does the liquor LLBL have a lower lignin concentration, but the lignin also has a lower molecular weight than that of the liquor BL. The lignin recovered by the LignoBoost process has been shown to be a valuable green resource for biopower production.[222] This method not just enables lignin to be exported in the form of a solid biofuel but also gives the opportunity to transform it into materials of higher value.[223,224,225]

2.5.4 The Integrated Biorefinery Concept

Sustainability is undoubtedly one of the most important cornerstones of energy independence, rendering it desirable to utilize all biomaterial in the most efficient manner possible. Society's challenge is not only to develop new green technologies and products, but also to help establish commercial practices to become green industrial practices.

The forest biorefinery is an evolving vision of wood utilization in an environmentally sustainable and economically viable manner to produce biopower, biofuels and biomaterials, including paper.[1] On an annual basis the U.S pulp and paper industry collects and processes 142 x 10^6 short tons of wood for the production of paper products.[98] That could be equally employed to produce 14-128 x 10^6 barrels of fuel oil.[226] As illustrated in Figure 32, a modern pulp and paper mill employs 70% of the technologies needed to contribute to a modern biorefinery, which provides a strong incentive for the development of innovative biorefinery technologies.[227] This existing infrastructure and capability suggest that once a practical/profitable wood-based biorefining technology is developed, the technology would be quickly implemented in the market place. Figure 32 provides an overview of a proposed biorefinery combining the currently used pulp mill operations depicted in section 2.5.1 (Current Pulp Manufacturing Technologies) with the proposed techniques described in section 2.5.2 (Future Prospects for Pulp Manufacturing and Bioresources for Biorefinery) and in section 2.5.3 (Promising Lignin Conversion Methods).

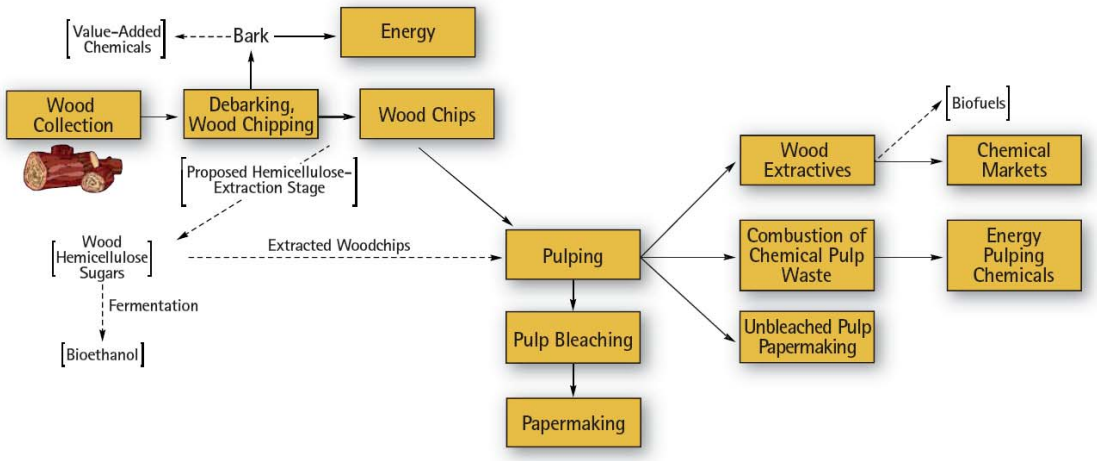

Figure 32 Overview of proposed biorefinery (broken lines) – pulp mill operations (solid lines).

CHAPTER 3

3. EXPERIMENTAL MATERIALS AND PROCEDURES

3.1 Materials

3.1.1 Chemicals

All chemicals were purchased from Sigma-Aldrich (St. Louis, MO, USA) and used as received. Solvents were purchased from VWR (West Chester, PA, USA). All gases were ultra high purity and purchased from Airgas (Radnor Township, PA, USA).

For hydrogenation catalysts syntheses, all chemicals used were high purity (>98%). All solvents were dry and saturated with ultra high purity (UHP) nitrogen. Dionized water (DW) was degassed with UHP nitrogen. Catalyst synthesis and preparation were all performed using Schlenk-techniques. Schlenk techniques other air sensitive chemical handling methods are depicted in section 3.2.2.1 (Storage and Handling of Air Sensitive Chemicals).

3.1.2 Wood samples

For studies on ethanol organosolv lignin (EOL), a single Loblolly pine (*Pinus taeda*) tree, visually free of disease and compression wood was obtained from the University of Georgia research plot in Baldwin County, GA, USA. The wood was manually debarked and chipped using a mechanical chipper.

3.1.3 Lignin Samples

LignoBoost lignin samples were separated from a commercial soft wood kraft pulping liquor and EOL from Loblolly pine (*Pinus taeda*) chips. Lignin samples are prone to degradation by oxidation or UV light. Hence, EOL, industrial black liquor and LignoBoost lignin samples are stored at -20ºC, while dried purified lignin samples are stored in a light protected desiccator until further use.

3.1.4 Biodiesel Samples

Due to the fact that industrial biodiesel samples are not sterile and they are mixtures of alcohols, fatty acids, glycerol, mono, and disubstituted glycerides, they are prone to biodegradation.[187] To acquire an accurate analytical data, it is essential that no change happens in the sample composition between the times of sampling till analysis. Thus, industrial biodiesel samples were stored in a light protected sample holder at -20ºC until analysis. Glycerol samples were obtained from the National Renewable Energy Laboratory and the United States Department of Agriculture (Washington, DC, USA), industrial process samples were obtained from Piedmont Biofuels (Pittsboro, NC, USA) and BDI-BioDiesel International AG (Graz, Austria).

3.2 Handling and Safety

3.2.1 LigniBoost Lignin Characterization Experiment

During industrial LignoBoost sample purification the pH of the initial sample is adjusted to a value of 6 with aqueous sulfuric acid (2 M) and stirred for 1 h. Depending on the industrial process sample, during the pH adjustment the sample is prone to substantial gas release. In case of kraft liquor samples, the forming gas mainly contains carbon dioxide and hydrogen sulfide. Since hydrogen sulfide is a highly toxic and flammable gas, this step has to be done in the fume hood.

As a last step of the purification, the extracted retentate was dissolved in dioxane:water (9:1) solution (1 g L^{-1}). Dioxane combine with atmospheric oxygen on standing to form peroxides, hence the used dioxane should be distilled over $NaBH_4$ before solvent preparation. Since distillation of p-dioxane concentrates these peroxides appropriate precautions should be taken due to the increasing danger. Dioxane distillation should be always performed in a fume hood using shield. The distillation should never go dry and the apparatus should never leave unattended. The remaining dioxane and $NaBH_4$ should be diluted with water (1:1, v/v) and treated as waste.

3.2.2 Ethanol Organosolv Lignin Hydrogenolysis Experiment

3.2.2.1 Storage and Handling of Air Sensitive Chemicals

Activated hydrogenation catalysts are extremely sensitive to oxidation hence they were stored in an anaerobic glove-box (Figure 33) to avoid any contact with air and humidity.

Figure 33. Glove-box set for air sensitive chemical storage.

The moisture and oxygen free atmosphere was produced with a HE-493 DRI TRAIN (VAC, Hawthorne, CA, USA). The unit replaces the air from the box with dry, inert gas that is later continuously cycled through a purifier which removes moisture and oxygen contamination. The system maintained an inert atmosphere with less than one ppm by volume moisture and oxygen in a hermetically sealed system. Inert atmosphere glove box was kept at a higher pressure than the surrounding air, so that any microscopic leaks are mostly leaking inert gas out of the box instead of letting air in.

Chemicals and equipments were moved in and out through a vacuum chamber attached to the box. Before moving them into the box, the oxygen and moisture should be removed from the atmosphere of the chamber by three vacuum cycles (15 min, 10 min and 5 min) pressurized from the box atmosphere between.

The recirculating gas continuously undergoes moisture and oxygen removal. Due to contamination from sources such as: diffusion through the rubber gloves in the glove box, insertion of contaminated parts into the glove box or use of make up gas which is not completely free of moisture (UHP Nitrogen under 800 psi) or oxygen, the catalyst inside the HE-493 DRI TRAIN system must be regenerated every 1-2 months.[228] (Figure 34)

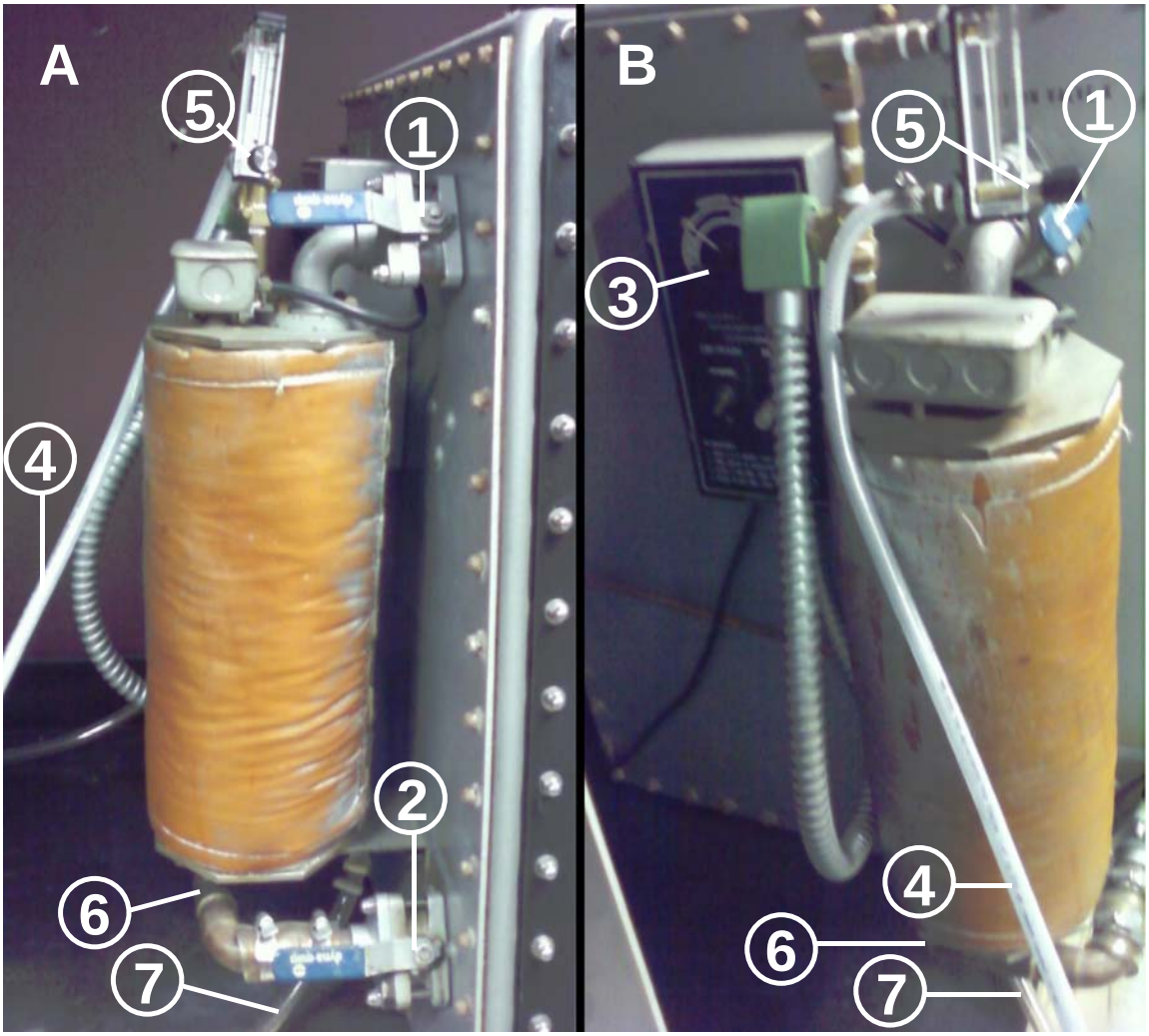

Figure 34. The side view (A) and the front view (B) of the HE-493 DRI TRAIN unit showing the circulation valves (1,2), the regeneration programmer (3), the forming gas line (4), the flow meter (5), release valve (6) and the tube for the condensate (7).

Regeneration is accomplished by isolating the purifier from the glove box by closing the circulation valve "1" and "2". The regeneration process is performed by activating the regeneration programmer which is an integral part of the unit "3", allowing an automatic regeneration of the purifier. The purification capability of the catalyst bed is regenerated using forming gas (~4% Hydrogen/Nitrogen) "4" at fixed flow rate of one-third cubic foot per minute "5". Both the absorbed oxygen and the water are leaving the

system in the form of steam. Due to the pressure release and to lead away the condensed water, the release valve (6) should be open and the exit hole should be connected with a tube (7). However the amount of the condensed water is depending on the amount of the absorbed oxygen and water by the catalyst bed, a collection basket is suggested to use. As total the regeneration cycle contains; 3 hours heating and purging followed by an overnight evacuation/vacuum period. The purifier is then refilled from the glove box by first closing the release valve and later opening the circulation outlet valves.[228]

For synthesis and preparation of air sensitive chemicals before hydrogenation runs a Schlenk-line was utilized with UHP nitrogen (Figure 35).

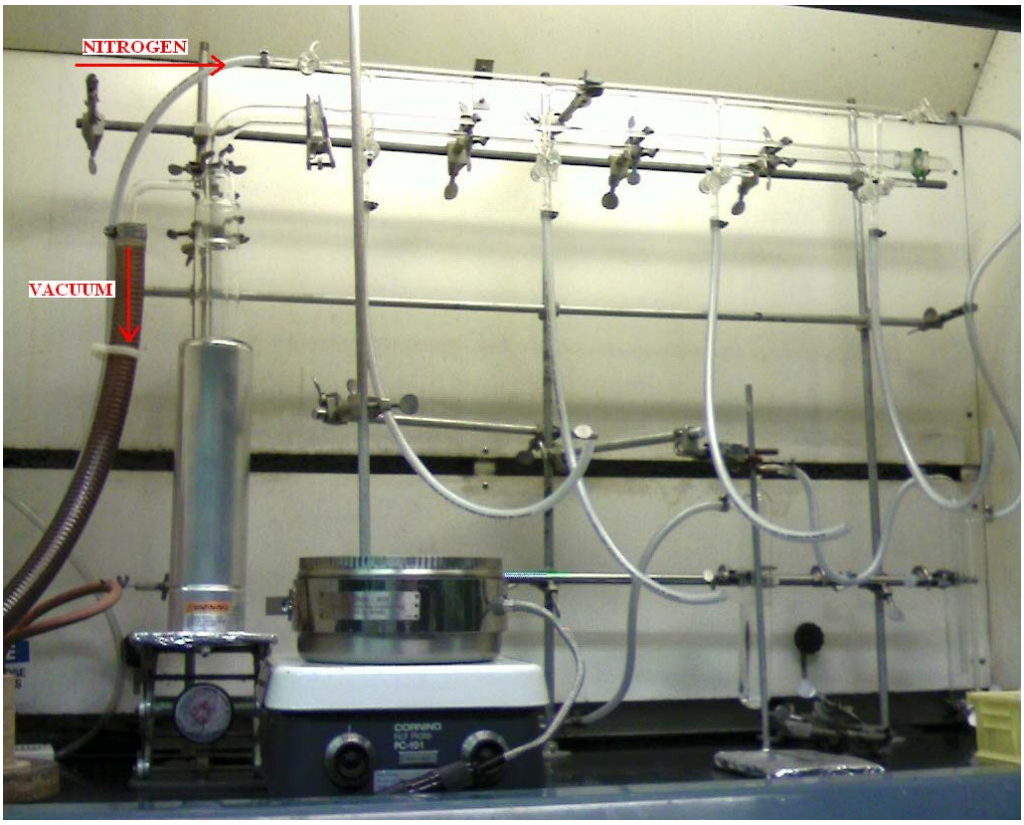

Figure 35. Schlenk-line set up for air sensitive catalyst preparation.

3.2.2.2 Pressure Vessels, Hydrogenation

Since hydrogenation studies were performed pressurized reactor using high temperatures (up to 250°C) and UHP hydrogen gas at pressures (5+ MPa) it is essential to use safety cautions.

Hydrogen poses a number of hazards to human safety, from potential detonations and fires when mixed with air to creating a severely deficient supply of oxygen to the body in its pure, oxygen-free form. Due to these safety concerns, hydrogenation experiments were performed in a fume hood using shield, on-line temperature control, cooling and safety gas shut-off valves. (see Figure 36 and Figure 37)

Figure 36. Parr 4560 reactor with a Parr 4842 set for hydrogenation.

Figure 37. Safety shut-off valve connected to a hydrogen (CGA-350) regulator.

3.2.3 Biodiesel Analysis Experiment

Since the exact composition of an industrial process sample is unknown, it is essential to use safety cautions such as; lab coat, chemical-resistant gloves and safety goggles when these samples are handled or prepared for analysis.

The used phosphitylating agents; 2-chloro-4,4,5,5-tetramethyl-1,3,2-dioxaphospholane (TMDP) and 2-chloro-1,3,2-dioxaphospholane (DOP) are highly corrosive, cause burns and reacts violently with water. These chemicals should be always used in a fume hood, close to a safety shower and an eye wash stations. Use caution and protective equipments such as; lab coat, chemical-resistant gloves, safety goggles and if necessary a face shield. When used, avoid breathing the dust and the white fume that forms after opening the vial and avoid any exposure. In case of a spill, cover it with dry lime or soda ash, pick up and keep it in a closed container, and hold for waste disposal. Ventilate the area and wash spill site after material pick up is complete.

3.3 Experimental Procedures

3.3.1 Experimental Procedures for LignoBoost Lignin Characterization and Pyrolysis

3.3.1.1 Lignin Separation by LignoBoost

Lignin separation from a commercial Scandinavian softwood Kraft pulping liquor was accomplished following published methods.[229,230] In brief, the kraft cooking liquor (BL) was precipitated (P) with pressurized carbon dioxide (CO_2) then filtered (F). Two different final pH conditions were used for precipitation: 10.5 and 9.5, the obtained fractions subsequently get lyophilized and provided unwashed crude samples. (Figure 38)

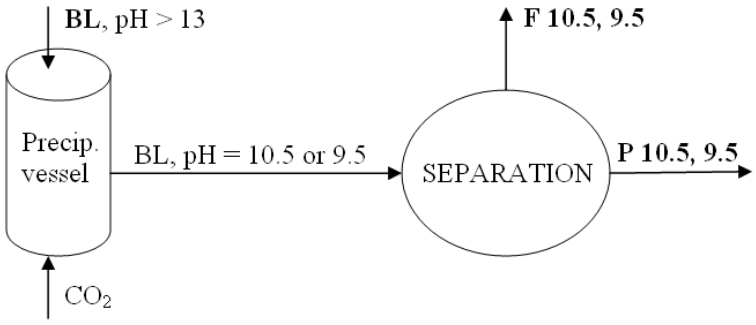

Figure 38. Precipitation of lignin from black liquor (BL) using LignoBoost technique at pH 9,5 and 10,5, and its separation to precipitate (P) and filtrate (F).

3.3.1.2 Lignin Purification

For detailed structural analysis of the unwashed lignin samples isolated in Section 3.3.1.1, additional purification was required. The initial LignoBoost samples were diluted in DW to 5 wt% solid content. Next EDTA-2Na^+ was added to the aqueous solution (5.00 g L^{-1}) to facilitate metal-ion removal and the pH was adjusted to a value of 6 with aqueous sulfuric acid (2 M) and stirred for 1 h at RT. Subsequently, the pH was further lowered to a value of 3 facilitating lignin precipitation.[231] The resulting samples were frozen (-20°C) over night, thawed and filtered through medium sintered glass funnel at 0°C. Retentates were mixed with pH 3 aqueous sulfuric acid solution up to 5 wt% and the filtration process was repeated three times for effective salt removal. All filtrates were collected, the solvent was removed under reduced pressure and the remaining solid provided the salt fraction. Retentates were air dried, Soxhlet extracted with pentane to remove free sulfur and dissolved in p-dioxane:water (9:1) solution (1 g L^{-1}). After filtration through a medium sintered glass funnel the solvent was removed under reduced pressure. The resulting solid provided purified lignin samples which were stored in a freeze dried form at -20°C until analysis. Figure 39 depicts the flow diagram of the lignin purification process used.

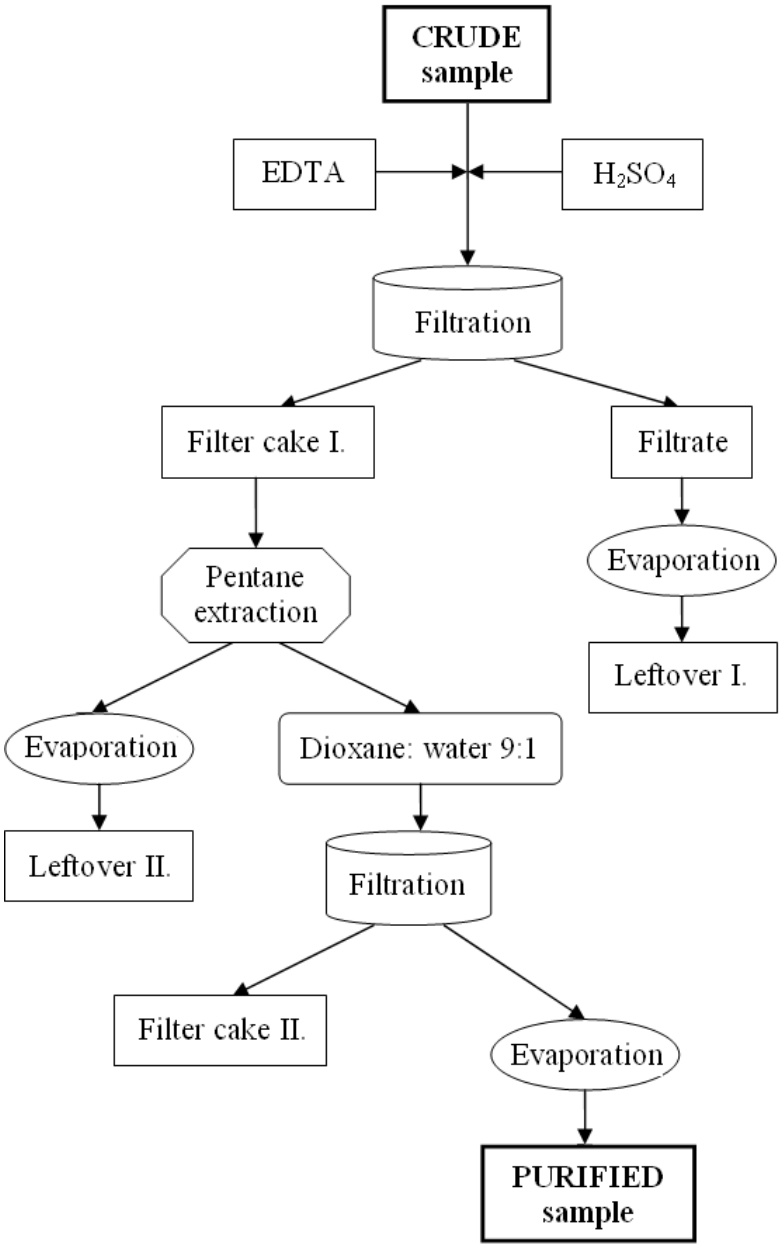

Figure 39 Lignin separation and purification from LignoBoost black liquor precipitate.

3.3.1.3 Purified LignoBoost Lignin Pyrolysis

The pyrolysis of the different biomass samples was accomplished using a micro-reactor designed for this study. The temperature for the pyrolysis was maintained at 400^{o}C, with the biomass residing on the heating element for 2 min. After 2 min, the char was removed from the top of the heating element by a sweeping arm fixed to the reactor, and another sample was dropped on to the plate. The biomass samples were dropped onto the heating plate in 50 mg increments up to 1.2 g. Helium was used as a purge gas and also as a means of maintaining an inert environment. The resulting gases were fed to a condenser immersed in liquid nitrogen. At the end of the experiment, the condenser was allowed to heat back up to room temperature, and the bio-oil samples were collected.

Figure 40. The experimental lignin pyrolysis setup used for bio-oil production.

3.3.2 Experimental Procedures for Ethanol Organosolv Lignin Hydrogenolysis

3.3.2.1 EOL Extraction

EOL was extracted from loblolly pine chips using a modified literature procedure of Pan et al.[232] In brief, chips were grounded using a Wiley mill with a 4-mesh screen. The passing fraction was collected and Soxhlet extracted with 2:1 (v/v) benzene/ethanol mixture for 24 h followed by a further extraction with ethanol for 24 h. (Figure 41)

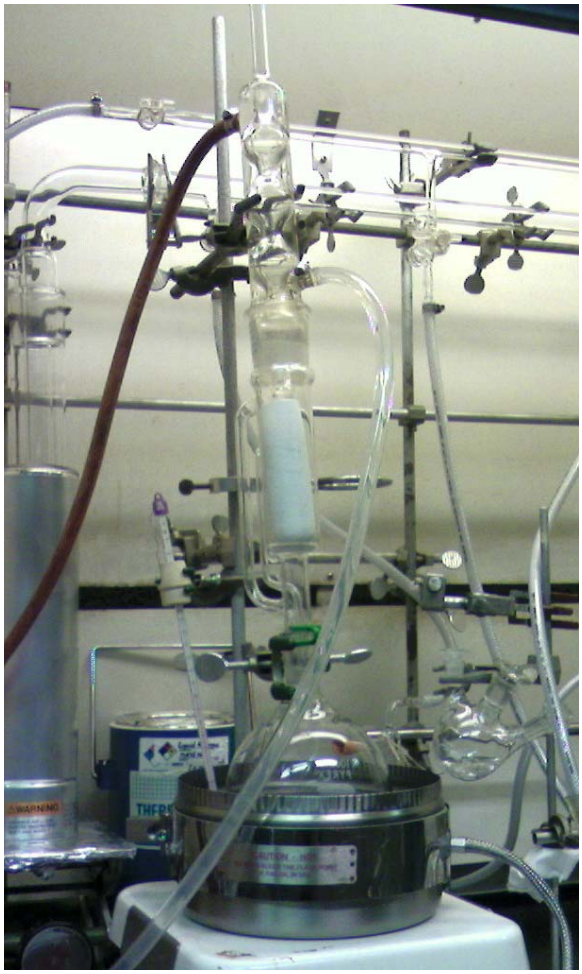

Figure 41. Soxhlet extractor used for ethanol organosolv lignin preparation.

The extractives free wood was air dried in a vacuum oven for (40ºC, 10-30 torr, 24 h) and stored at -20ºC. Wood chips (200 g) were mixed with 65% aqueous ethanol solution in a 1:7 (w/w) wood/liquid ratio in a 4 L stainless steel Parr reactor (Moline, IL, USA). Under stirring (150 r min^{-1}) concentrated (96%) H_2SO_4 was injected to the reaction mixture in a 1.1:100 (w/w) H_2SO_4/wood ratio. The mixture was heated (2-4ºC min^{-1}) up to 170ºC and cooked for 1 h. After the vessel had cooled to room temperature, the spent liquid phase was discarded and the chips were washed three times with hot 65% aqueous ethanol (300 mL). The ethanol washes were combined and the dissolved lignin was precipitated by adding three volumes of DW. The lignin precipitate was filtered and dried in a vacuum oven (40ºC, 10-30 torr, 24 h) and stored in a light protected desiccator at room temperature (RT) until further use. Using 200 g woodchip per extractions, on average the recovery yield was 16 g EOL. (Figure 42)

Figure 42. Picture of ethanol organosolv lignin from different resources.

3.3.2.2 Preparation of the Hydrogenation Catalysts

$Ru(Cl)_2(PPh_3)_3$ was synthesized as previously described by Armit et. al.[233] $RhCl(PPh_3)_3$ was synthesized as previously described by J. A. Osborn et. al.[234] Co/Mo was activated following published methods[235,236] from aluminum supported 3.5% CoO and 14% MoO_3. Ru-PVP was synthesized as previously described by Ning Yan et. al.[237] following the technique of W.Yu et. al[238]. The dry catalysts were stored in a glove-box under dry nitrogen pressure at RT until further use.

3.3.2.3 Hydrogenation

Hydrogenation studies were performed in a Parr 4560 reactor with a Parr 4842 temperature controller (Moline, IL, USA), charged with catalyst (50 mg) and EOL (500 mg). The closed reactor was purged with nitrogen several times. During the borane/iodine catalytic hydrogenation, the catalyst consisted 25 mg sodium borohydride (0.66 mmol) and 25 mg iodine (0.20 mmol).[239] Using a gas-tight syringe, degassed ethanol (50 mL) was introduced under nitrogen pressure and the closed reactor was then purged several times with hydrogen under stirring (200 r min^{-1}) at RT. The reaction mixture was then pressurized (5 MPa) with 100% hydrogen or with 5 ppm (v/v) hydrogen sulfide/hydrogen mixture when Co/Mo was used as a catalyst and heated to the desired temperature (2-4 ºC min^{-1}). After stirring for 20 h, the reactor was cooled to room temperature (RT) and hydrogen was slowly released in the fume hood. The reaction mixture was introduced into a Schlenk-flask under nitrogen pressure and stored at -20°C until further analysis.

3.3.3 Experimental Procedures for Biodiesel Analysis

3.3.3.1 Sample Preparation and Phosphitylation for Preliminary Experiments

The potential ability to characterize hydroxyl groups of glycerol-related compounds was assessed using DOP and TMDP as the phosphitylating agent. Initial studies were conducted primarily with analytical pure compounds to establish a data base of chemical shifts and later demonstrate the applicability on a commercial biodiesel and glycerol sample.

3.3.3.1.1 Reaction Mixture Preparation and Phosphitylation with DOP

A solvent mixture consisting of anhydrous pyridine:deuterated chloroform in 1.6:1 ratio with ~3.60 mg/mL chromium acetylacetonate as relaxation agent and ~4.00 mg/mL cyclohexanol as internal standard was prepared and stored at -20ºC until sample preparation. For phosphitylation, the biodiesel sample (150 μL) or the glycerol sample (10 μL) was mixed with the solvent mixture (500 μL), stirred for several minutes and then reacted with DOP (100 μL) at RT and stirred for 1-2 min. The reaction mixture was then transferred into an NMR tube and ^{31}P–NMR spectrum was recorded.

3.3.3.1.2 Reaction Mixture Preparation and Phosphitylation with TMDP

A solvent mixture consisting of anhydrous pyridine:deuterated chloroform:N,N-dimethylformide in 1:1.2:1 ratio with ~3.60 mg/mL chromium acetylacetonate as relaxation agent and ~4.00 mg/mL cyclohexanol as internal standard was prepared and stored at -20ºC until sample preparation. For phosphitylation, the biodiesel sample (150

μL) or the glycerol sample (10 μL) was mixed with the solvent mixture (500 μL), stirred for several minutes and then reacted with TMDP 100 (μL) at RT and stirred for 1-2 min. The reaction mixture was then transferred into an NMR tube and ^{31}P–NMR spectrum was recorded.

3.3.3.2 NMR Analysis on Industrial Biodiesel Process Samples

3.3.3.2.1 NMR Chemical Shift Assignment

After the preliminary experiments, to establish a database of ^{31}P-NMR chemical shift information on relevant biodiesel precursors, a series of representative samples on analytical pure compounds were acquired treated with TMDP and analyzed by ^{31}P-NMR. All chemical shifts reported are relative to the product of TMDP with cyclohexanol, which has been observed to give a sharp signal at 144.9 ppm.

3.3.3.2.2 Optimized TMDP/^{31}P–NMR Method for Industrial Biodiesel Samples

A solvent mixture consisting of anhydrous pyridine:deuterated chloroform:N,N-dimethylformamide in 1:1.2:1 ratio with ~3.60 mg/mL chromium acetylacetonate ($Cr(acac)_3$) as relaxation agent and ~4.00 mg/mL cyclohexanol as internal standard was prepared and stored at -20 ºC until sample preparation. For phosphitylation, the industrial biodiesel sample (150 μL), industrial glycerol sample (10 μL) or the biodiesel precursor (10 mg) was mixed with the solvent mixture (500 μL), stirred for several min and then reacted with TMDP (100 μL) at RT and stirred for 1-2 min. The reaction mixture was then transferred into an NMR tube and ^{31}P–NMR spectrum was recorded.

3.4 Analytical Analysis Procedures

3.4.1 NMR Spectroscopy for Lignin Studies

All NMR analysis on lignin samples were carried out using a 400 MHz DMX Bruker spectrometer (Billerica, MA, USA) at 25°C. For PPh_3-ligand containing catalysts, a 500 MHz Bruker system (Billerica, MA, USA) at 25°C was used.

3.4.1.1 Qualitative ^{1}H-NMR Characterization of Lignin

Qualitative ^{1}H–NMR spectra were acquired on dried lignin samples (15-20 mg) dissolved in deuterated dimethyl sulfoxide (DMSO–d_6) (450 μL). Qualitative ^{1}H-NMR spectra were recorded under the following conditions: 2.0 s pulse delay, 30° pulse angle, 15 ppm sweep width, 16 scans, a time domain of 32K, 16 acquisition transients and 0.3 Hz line broadening.

3.4.1.2 Qualitative ^{13}C-NMR Characterization of Lignin

Qualitative ^{1}H–NMR and ^{13}C–NMR spectra were acquired on dried lignin samples (80–120 mg) dissolved in DMSO–d_6 (450 μL). Qualitative ^{13}C-NMR spectra were recorded under the following conditions: 1.0 s pulse delay, 30° pulse angle, a time domain of 32K and a minimum of 10K acquisition transients.

3.4.1.3 Quantitative ^{1}H-NMR Characterization of Lignin

An anhydrous, internal standard solution was prepared by first adding 30 mL of DMSO-d_6 to pre-dried 4 Å molecular sieves for 24 hr using 99.9-100% DMSO-d_6. Extra precaution should be taken so as to remove almost all of the water present in the solvent. Pentafluorobenzaldehyde (PFB) was weighed out into a 25 mL volumetric flask (~20 mg), which was then filled with the anhydrous DMSO-d_6. The DMSO-d_6 transfer was halted halfway through to allow the PFB to dissolve completely before the flask was filled to the mark. The NMR sample was prepared by adding 0.45 mL of internal standard solution into a known weight of dry lignin (20 to 25 mg). The lignin was previously dried under vacuum (~20 mm Hg) for a minimum of 24 h. [240,241] Internal standard solution and NMR samples were prepared in a glove box under a moisture free atmosphere.

Quantitative ^{1}H-NMR spectra were recorded under the following conditions: 15.0 s pulse delay, 90° pulse angle, 15 ppm sweep width, 100 scans, a time domain of 32K, 32 acquisition transients and 0.3 Hz line broadening.

3.4.1.4 Quantitative ^{31}P-NMR Characterization of Lignin

Quantitative ^{31}P–NMR spectra were acquired on dry lignin samples (~25 mg) dissolved in a solvent mixture consisting of 1.6:1 (v/v) anhydrous pyridine/deuterated chloroform with chromium(III) acetylacetonate (~3.6 mg mL^{-1}) as relaxation agent and cyclohexanol (~4.0 mg mL^{-1}) as internal standard following published methods.[242,243] Quantitative ^{31}P–NMR analysis was acquired under the following conditions: 25.0 s pulse

delay, inverse–gated decoupling (Waltz–16), 90° pulse angle, a time domain of 32K with one degree of zero filling, 100 acquisition transients and 4.0 Hz line broadening.

3.4.1.5 Quantitative ^{31}P-NMR Characterization of PPh_3-ligand Containing catalysts

Quantitative ^{31}P–NMR spectra were acquired on dry PPh_3-ligand containing catalysts (~20 mg) by transferring into NMR tubes under nitrogen pressure and dissolving in degassed $CDCl_3$ (450 μL). After NMR sample preparation, the ^{31}P–NMR spectra were immediately recorded. Quantitative ^{31}P–NMR analysis was acquired under the following conditions: 2.5 s pulse delay, inverse–gated decoupling (Waltz–16), 90° pulse angle, a time domain of 32K with one degree of zero filling, 200 acquisition transients and 4.0 Hz line broadening.

3.4.2 NMR Spectroscopy for Biodiesel Studies

All NMR analysis on lignin samples were carried out using a Bruker Avance-400 spectrometer operating at frequencies of 161.951 MHz for ^{31}P at 25°C in a magnetic field of 9.4 Tesla.

3.4.2.1 Quantitative ^{31}P-NMR Characterization for Preliminary Experiments

During the preliminary experiments, quantitative ^{31}P-NMR spectra were recorded with a 25–second pulse delay, inverse–gated decoupling (Waltz–16), 8 μs (90° pulse), a time domain of 32K with one degree of zero filling, 100 acquisition transients and were processed using a line broadening of 4.0 Hz.

3.4.2.2 Spin-lattice Relaxation Time Measurement

The ^{31}P spin-lattice (T_1) relaxation times were measured using standard inversion recovery pulse sequence (recycle delay-180°-τ-90°-acquistion) with 8 μs (90° pulse), 16 μs (180° pulse), 20 s recycle delay and 8 scans. Standard software (TopSpin 2.1) supplied with the Bruker instrument and IGOR Pro 6 was used for fitting the recorded relaxation [$M(\tau)/M_o=1-C_o*\exp(-\tau/T_1)$] to obtain relaxation values.

3.4.2.3 Optimized Quantitative ^{31}P-NMR Characterization for Industrial Biodiesel Process Samples

The NMR pulse program optimized for biodiesel constituents for a 400 MHz Bruker system at 25 °C utilizes a 5 s pulse delay, inverse–gated decoupling (Waltz–16) to avoid NOE effects, 90° pulse angle, a time domain of 32 K with one degree of zero filling, 4.0 Hz line broadening and only 16 acquisition transients.

3.4.3 Solubility Measurement of Hydrogenated EOL

After hydrogenation, the lignin fraction from the ethanol phase provided a soluble hydrogenated EOL fraction. The soluble and insoluble phases were separated at RT by centrifugation (2500 r min^{-1}, 10 min) and concentrated under reduced pressure. The insoluble EOL fraction was dissolved in dimethyl sulfoxide (DMSO), metallic particles were separated by centrifugation (2500 r min^{-1}, 10 min) and product was recovered under reduced pressure at 50°C. Typically, the mass yield recovery of lignin was 97±1%.

3.4.4 Lignin MWD Analysis

Molecular weight distribution analysis was performed by GPC of acetylated lignin samples. Dry lignin (~20 mg) was acetylated by stirring with 1:1 (v/v) acetic anhydride/pyridine mixture (2 mL) at room temperature for 72 h. The solvent mixture was removed under reduced pressure at 50°C. The acetylated lignin was dissolved in chloroform (50 mL) and washed with water (20 mL). The chloroform phase was dried over anhydrous $MgSO_4$ and then concentrated under reduced pressure. The dry acetylated lignin was then dissolved in THF (~1 mg mL^{-1}) for GPC analysis. Instrument: HP 1090 HPLC equipped with a DAD-UV/VIS detector (New Castle, DE, USA) at 270 nm. Columns: 7.8 mm Ø 300 mm Waters styragel HR4, HR3, and HR1 (Milford, MA, USA). GPC data were calibrated based on polystyrene standards. Weight average (M_w) and number average molecular weight (M_n) were determined by following the calculation strategy of Baumberger et al. for whole curve integration.[244]

3.4.5 Lignin DSC Measurements

The T_g of the starting EOL were determined using a TA Instruments Q100 DSC (New Castle, DE, USA). Lignin samples (1 mg) were placed in aluminum pans, sealed and heated (10°C min^{-1}) up to 225°C under nitrogen purge (50 mL min^{-1}). The difference in the amount of heat required to increase the temperature of a sample is recorded and the T_g is determined by EXCEL.

3.4.6 Elemental Microanalysis

3.4.6.1 Elemental Microanalysis for LignoBoost Studies

Carbon and hydrogen analysis were performed by combustion, oxygen analysis was performed by pyrolysis and sulfur analysis was performed by flask combustion followed by ion chromatography by Atlantic Microlab Inc. (Norcross, GA, USA).

3.4.6.2 Elemental Microanalysis for EOL Hydrogenolysis Studies

Carbon and hydrogen analysis were performed by combustion, oxygen analysis was performed by pyrolysis and iodine analysis was performed by flask combustion followed by ion chromatography by Atlantic Microlab Inc. (Norcross, GA, USA).

3.4.7 Error Analysis

3.4.7.1 Error Analysis for EOL Hydrogenolysis Studies

The accuracy of all analytical techniques used during the EOL hydrogenation experimental series were determined by the comparison of the analytical data of three experimental runs performed under the same reaction conditions. The error margin was measured; ±1.5% for solubility, ±1.6% for GPC, ±1.6% for quantitative ^{1}H-NMR, ±2.0% for qualitative ^{31}P-NMR and ±0.7% for DSC. MWD curves were calibrated based on polystyrene standards and fitted with a second degree polynomial with a ±2^-13% deviation.

3.4.7.2 Error Analysis for Biodiesel Studies

The standard deviation, sensitivity and quantitative accuracy were determined from five separate measurements using a solvent mixture containing analytically pure 99+% biodiesel precursors and cyclohexanol as an internal standard. The sensitivity of the TMDP/^{31}P–NMR technique was calculated to have a 1.9 μmol/mL lower limit of detection. The error margin of the technique was measured to be ±1.1%.

CHAPTER 4

4. LIGNOBOOST LIGNIN CHARACTERIZATION[1] AND PYROLYSIS[2] FOR BIO-OIL PRODUCTION

4.1 Introduction

The forest biorefinery concept involves converting a pulp mill into a multi-propose biofuels, biomaterials, and biopower production facility. In which these products are made in an environmentally compatible and sustainable manner. A key challenge in this process is the recovery of lignin from process streams such that it can be utilized in a variety of innovative green chemistry processes. This study examines the fundamental chemical structure of lignin recovered from Kraft pulping streams using an acid precipitation/washing methodology. Functional group analysis and molecular weight profiles were determined by nuclear magnetic resonance (NMR) and size exclusion chromatography (SEC).

Sustainability is undoubtedly one of the most important cornerstones of energy independence rendering it desirable to utilize all biomaterial in the most efficient manner. Society's challenge is to not only develop new green technologies and products but also help established commerce practices become green industrial practices. The forest

[1] This manuscript was submitted for publication in Green Chemistry, 2009. It is entitled as "A Green Prospect for Paper Industry's Lignin Rich Solutions". The other authors are Arthur J. Ragauskas and Matyas Kosa from School of Chemistry and Biochemistry at the Georgia Institute of Technology and Hans Theliander from Forest Products and Chemical Engineering at the Chalmers University, Sweden.

[2] This manuscript was published and presented at the Abstracts of Papers, 237th ACS National Meeting, Salt Lake City, UT, United States, March 22-26, (2009), CELL-191. It is entitled "New energy: Fuel resources from kraft pulping". The other authors are Arthur J. Ragauskas and Matyas Kosa from School of Chemistry and Biochemistry at the Georgia Institute of Technology and Hans Theliander from Forest Products and Chemical Engineering at the Chalmers University, Sweden.

biorefinery is an evolving vision of wood utilization in an environmentally sustainable and economically viable manner to produce biopower, biofuels and biomaterials, including paper.[245]

During chemical pulping, lignin is chemically degraded and extracted from wood in aqueous environment in a pressure reactor at pH values of 13-14 and temperatures of 140-170°C.[246,247] These conditions remove 85-93% of the lignin and approximately 56-71% of the hemicelluloses.[246,247,248] The approach when NaSH is used in the cooking process along with caustic to delignify wood is referred to as Kraft pulping. In the United States alone the pulp and paper industry collects and processes ~108 million tones of pulpwood for the production of pulp, paper and paperboard annually.[246] In turn, the paper industry produces over 50 million tons of residual lignin per year worldwide in a form of a caustic side stream.[246] Currently, this material is burned in a low efficiency Thompson recovery furnace to recover energy and cooking chemicals. A continuing interest in this field is the desire to recover fractions of lignin from the Kraft cooking liquors for biopower, biochemical and biomaterial utilization. Recently, a green process referred to as "LignoBoost" provides a viable separation of lignin from these cooking liqours by employing carbon-dioxide to precipitate lignin from alkaline solutions.[248,249,250] (Equation 1-2)

$$L\text{-}OH + OH^- \leftrightarrow L\text{-}O^- + H_2O$$

Equation 1. Lignin precipitation by lowering the pH.

$$CO_2(g) \leftrightarrow CO_2(aq)$$

$$CO_2(aq) + 2OH^- \leftrightarrow CO_3^{2-} + H_2O$$

Equation 2. Lowering pH by carbon-dioxide gas injection.

The application of this process involves acidification of an alkaline cooking liquor with CO_2, precipitation, filtration and washing.[251] Process integration and mill trials have tested this process from an engineering and economic point of view.[252] The lignin recovered by the LignoBoost process has been shown to be valuable green resource for biopower production.[253] This method enables lignin to be exported in the form of a solid biofuel and also gives the opportunity to transform it into materials of higher value.[254]

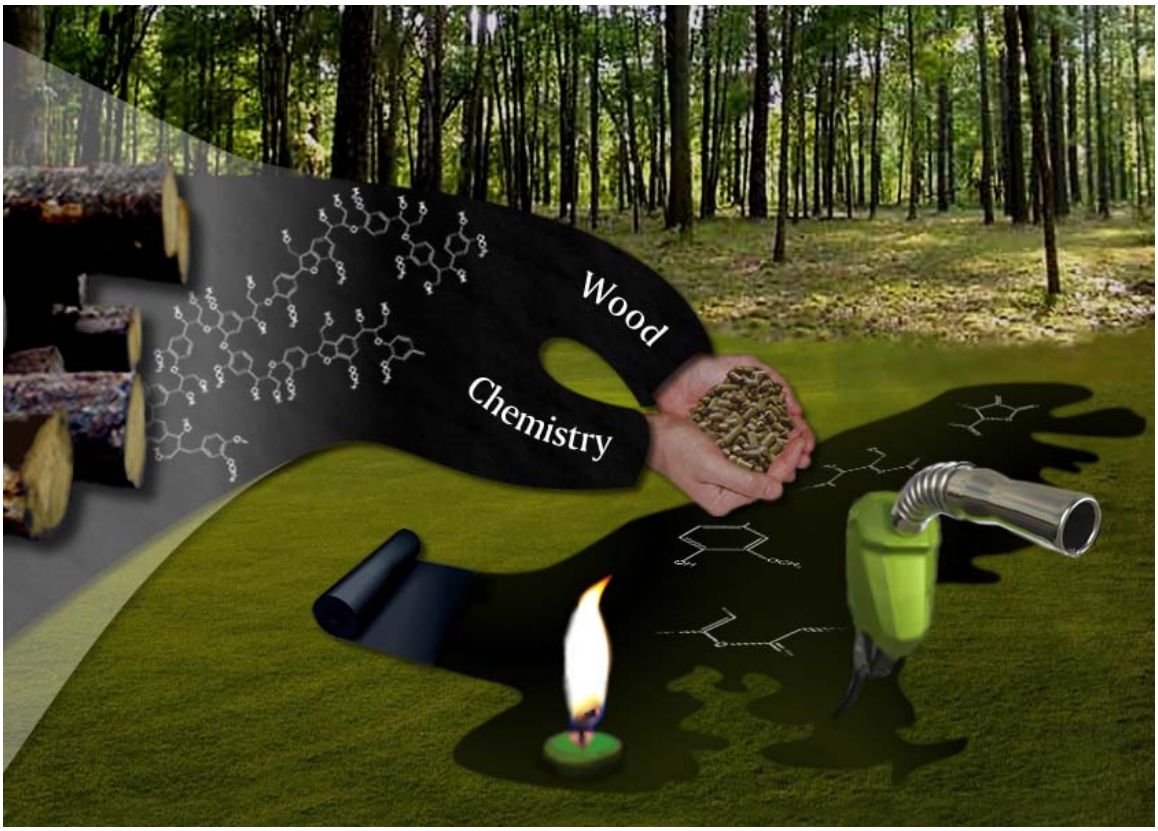

Figure 43. Lignin recovered by the LignoBoost process and its proposed value added commercial products after chemical conversion.

Recognizing the possibilities in recovering lignin from black liquor via CO_2 precipitation and washing, we became interested in the detailed chemical composition and structure of the lignin isolated anticipating that this data could facilitate future applications of this bioresource. These findings will provide valuable insight of the physical and its determining chemical properties of this currently under utilized renewable bioresource. A known chemical structure and composition can help to optimize a subsequent controlled high yield catalytic conversion by pyrolysis. Pyrolysis with a chemically characterized feedstock gives the opportunity for a controlled catalytic deoxygenation and liquefaction of the precipitated lignin fractions for high yield bio-oil production. Herein, we wish to report the characterization of LignoBoost derived lignin and its pyrolysis in terms of molecular weight profiles and functional group properties.

4.2 Experimental Section

4.2.1 Materials

Lignin separated from commercial Scandinavian soft wood Kraft pulping liquor, all reagents were purchased from Sigma-Aldrich (St. Louis, MO, USA) and used as received. Solvents were purchased from VWR (West Chester, PA, USA). All gases were ultra high purity and purchased from Airgas (Radnor Township, PA, USA).

4.2.2 LignoBoost Lignin Separation from Kraft Pulping Liquor

Lignin separation from Kraft pulping liquors using LignoBoost technique is described in Chapter 3. (3.3.1.1 Lignin Separation by LignoBoost)

4.2.3 LignoBoost Lignin Purification

Lignin separation and purification of LignoBoost lignin precipitated from Kraft pulping liquors is described in Chapter 3. (3.3.1.2 Lignin Purification)

4.2.4 NMR Measurements on Purified LignoBoost Lignin samples

Qualitative ^{1}H, qualitative ^{13}C, quantitative ^{1}H and quantitative ^{31}P NMR analysis procedures on purified lignin samples are described in Chapter 3. (3.4.1 NMR Spectroscopy for Lignin Studies)

4.2.5 SEC Measurements on Purified LignoBoost Lignin samples

Analysis procedure for SEC measurements on purified LignoBoost samples is described in Chapter 3. (3.4.4 Lignin MWD Analysis)

4.2.6 Pyrolysis of LignoBoost Lignin

Pyrolysis of characterized purified LigniBoost lignin is described in Chapter 3. (3.3.1.3 Purified LignoBoost Lignin Pyrolysis)

4.3 Results and Discussion

4.3.1 Mass Balance and Elemental Analysis Data

After purification of the unwashed samples, the lignin content of the initial LignoBoost samples could be determined. The mass balance data showed that the initial unpurified dry samples had varying amounts of lignin as the following (in wt%): 25.8% in BL, 73.3% in P 9.5, 71.3% in P 10.5, 11.1% in F 9.5 and 20.0% in F 10.5. Figure 44 shows the mass balances of the purification step normalized to 10.00 g crude samples. Mass values of H_2SO_4 and EDTA added through filtrations were subtracted from the figure for better transparency.

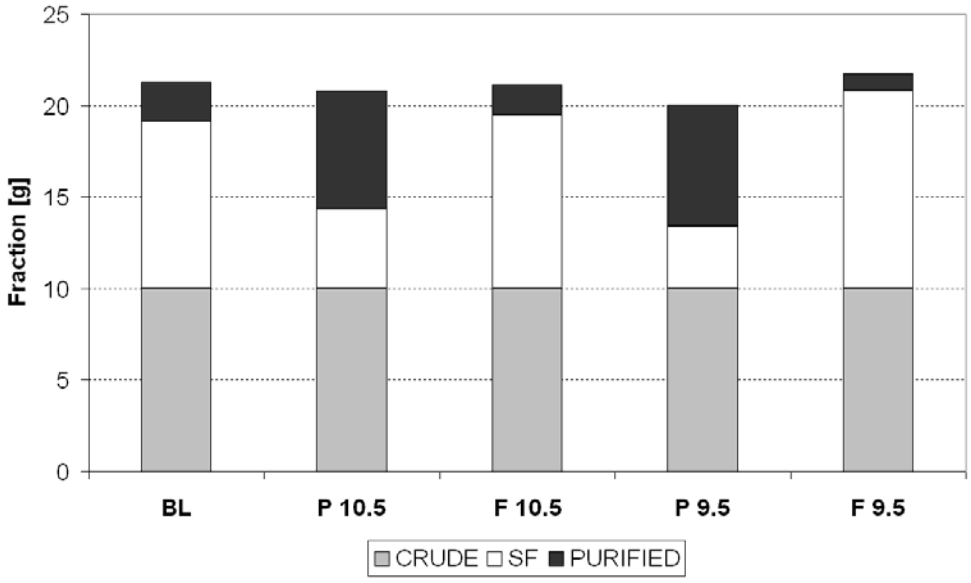

Figure 44. Mass balances of the purification process from black liquor (BL) precipitated lignin (P) at pH 9,5 and 10,5, and its filtrate (F).

This data clearly shows that treatment of the pulping liquor with CO_2 yields a lignin rich stream and a filtrate fraction that is enriched in salts. The pH 9.5 treatment

condition resulted in a better separation of lignin. Results of the elemental analysis are consistent with the mass balance data and shows that the purified lignin samples contain only organic elements up to 97.1 %. Results of the elemental analysis on the crude, salt and purified fractions are shown in Figure 45; C, H, O and S contents were measured and are depicted in weight percentage (wt. %). The non measured (NM) regions in all weight compositions come from alkali and alkali earth metals as well as silica, aluminium and BL trace elements.[255]

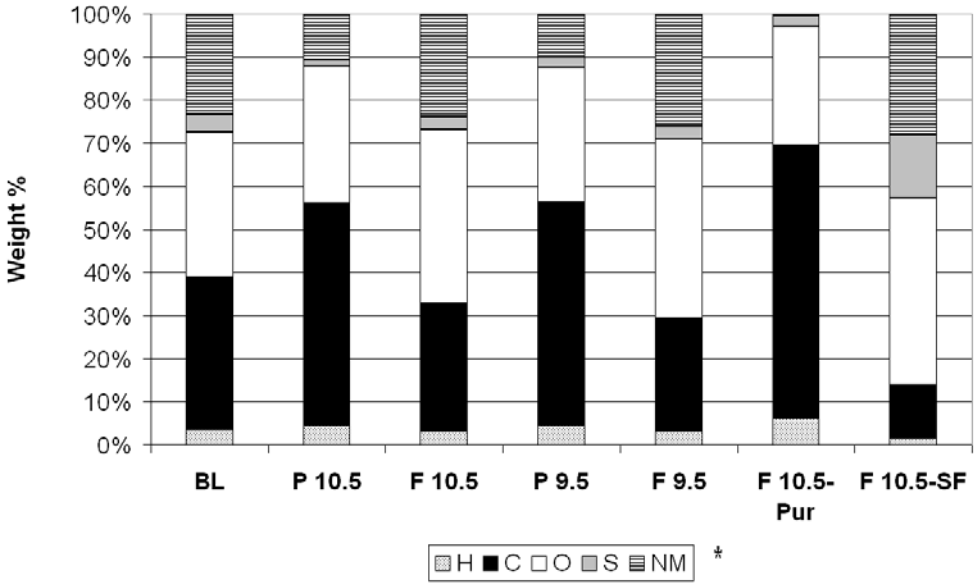

* H: Hydrogen, C: Carbon, O: Oxygen, S: Sulfur, NM: Not measured.

Figure 45. Elemental analysis of the LignoBoost crude samples and the purified (Pur) samples of black liquor (BL) precipitated lignin (P) and its filtrate (F) at pH 9,5 and 10,5, and the salt fraction (SF), prepared from commercial Scandinavian soft wood kraft pulping liquor.

Figure 45 shows that the precipitate is enriched in lignin while the filtrate fraction is enriched in salt. The data also shows that the separation is better at lower pH which findings are consistent with Figure 44. Results on the purified (F 10.5-Pur) and salt

fractions (F 10.5-SF) shows the high efficiency of the purification method. While the purified fraction enriched in organic elements up to 99.62 %, the SF is enriched inorganics. Simililar purifification yields were achieved in case of all crude samples.

4.3.2 NMR Data of the Purified LignoBoost Lignin Samples

To evaluate the primary components present in the initial LignoBoost fractions and in their purified samples, qualitative ^{1}H and ^{13}C NMR measurements were conducted (Figure 46) following literature methods.[256,257]

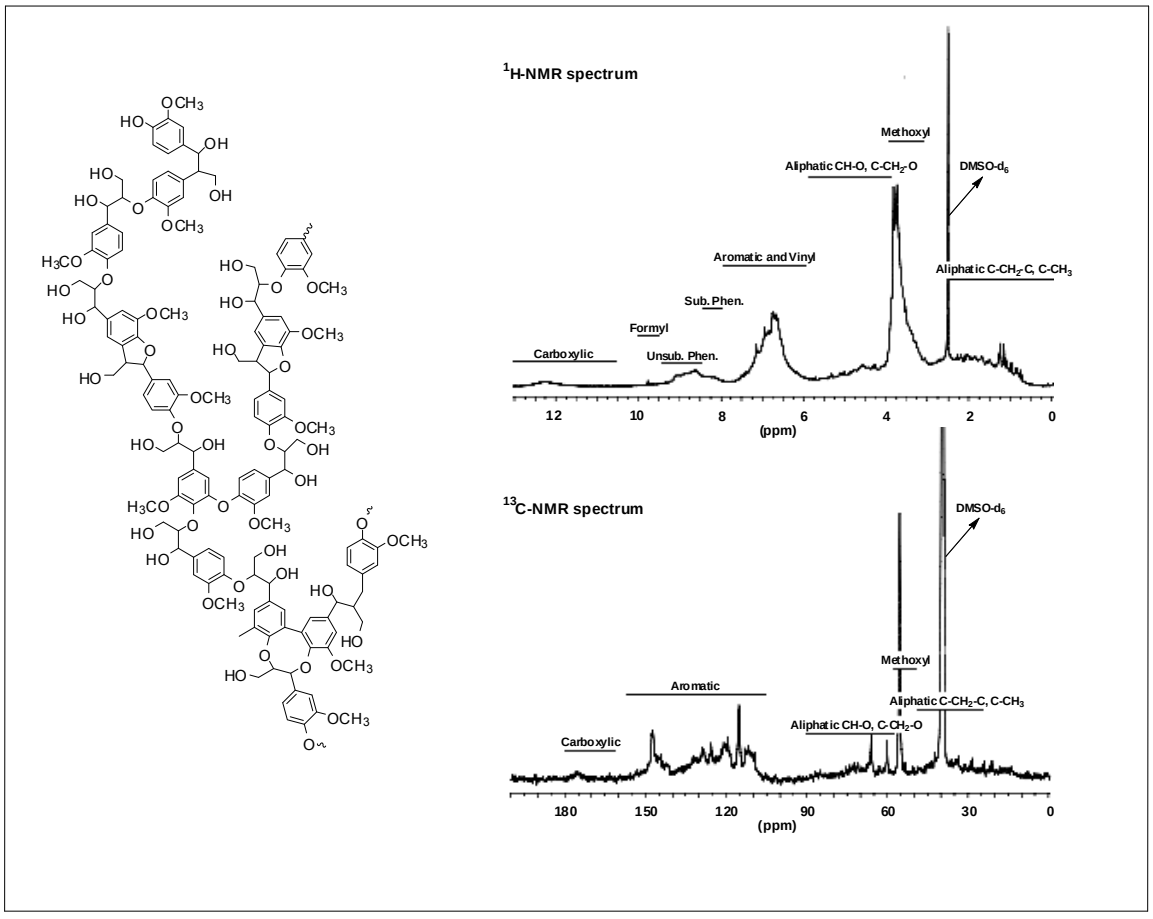

Figure 46. Example for structure of native lignin, and qualitative ^{1}H and ^{13}C-NMR spectrum of purified black liquor LignoBoost sample. (Solvent: DMSO-d_6).

Qualitative NMR data shows that during the purification step, sugars and fatty acids were removed with salts and salt-EDTA complexes from the initial LignoBoost samples and ended up in the SF. With the lignin purification method used in this study, the chemicals earlier used to bring lignin into solution can be separated from the crude samples. This allows the process chemicals to be returned to the main stream and reused, while it also produces lignin with 95-97% purity, resulting in a higher environmental and economic efficiency

To selectively follow the structural changes of the lignin biopolymer on the molecular level, quantitative ^{1}H-NMR measurements were conducted on the purified fractions. The differences between the process fractions and the changes in the distribution of selected lignin moieties at different final pHs are shown in Table 27.

Table 27. Partial hydrogen content [mol mol^{-1}] % of different lignin functional groups in the ratio of all H containing functional groups as determined by quantitative ^{1}H-NMR.

Sample name *	Hydrogen content of selected groups (mol mol^{-1} % relative to all H cont. groups)						
	Carboxylic acid	Formyl	Phenolic	Aromatic, Vinyl	Aliphatic	Methoxyl	Aliphatic
	(13.50-10.50) ppm -C(O)OH	(10.10-9.35) ppm -C(O)H	(9.35-8.00) ppm =HC-OH	(8.00-6.00) ppm CH=CH CH2=CH	(6.00-4.05) ppm CH-O C-CH2-O	(4.05-3.45) ppm -OCH3	(2.25-0.00) ppm C-CH2-C C-CH3
Black liquor	1.26	1.50	6.73	20.22	8.44	45.84	14.42
P 9.5	1.06	0.90	4.19	18.75	5.92	52.42	16.70
P 10.5	0.81	0.98	3.66	19.69	8.22	49.16	16.04
F 9.5	1.71	1.61	6.16	19.82	7.89	41.25	17.35
F 10.5	1.22	1.67	5.73	19.58	6.78	44.58	16.87

* BL: black liquor, P: precipitated lignin, F: filtrate at pH 9,5 and 10,5.

Quantitative ^{1}H-NMR shows that the F lignin has more carboxylic and phenolic groups while P is enriched in methoxyl moieties. The hydroxyl group content on the lignin polymer plays a crucial role on determining the solubility of the biopolymer.[256,257] Selective phosphitylation of the hydroxyl groups on the lignin polymer with 2-chloro-4,4,5,5-tetramethyl-1,3,2-dioxaphospholane (TMDP), followed by quantitative ^{31}P-NMR measurement provides a facile monitoring of the changes in the hydroxyl content of the lignin polymer throughout the process.[257]

Table 28. Hydroxyl content of different purified LignoBoost fractions as determined by quantitative ^{31}P-NMR after derivatized with 2-chloro-4,4,5,5-tetramethyl-1,3,2-dioxaphospholane, from commercial Scandinavian soft wood kraft pulping liquor.

Sample name	Total –OH content (μmol mg^{-1})	Hydroxyl content of selected groups (μmol mg^{-1})			
		Aliphatic hydroxyl	Condensed phenolic	Guaiacyl phenolic	Carboxylic hydroxyl
	(149.0-133.8) ppm[a]	(149.0-145.6) ppm[a]	(144.4-140.4) ppm[a]	(140.4-137.6) ppm[a]	(136.0-133.8) ppm[a]
Black liquor	6.37	1.49	1.73	2.46	0.69
P 9.5	4.30	1.11	1.14	1.47	0.59
P 10.5	3.18	0.91	0.85	1.03	0.39
F 9.5	6.74	1.27	1.80	2.55	1.11
F 10.5	5.76	1.22	1.57	2.20	0.78

* BL: black liquor, P: precipitated lignin, F: filtrate at pH 9,5 and 10,5.

Table 28 shows that the total hydroxyl content of F 9.5 and F 10.5 lignins are 56% and 45% higher respectively, than their analogous P fractions which is consistent with the results from ^{1}H-NMR analysis. In addition, pH 9.5 conditions resulted in 69% higher hydroxyl content in the F fraction and a 35% increase in the P fraction than when pH 10.5 was applied. The pKa values of phenolic lignin groups are between 9.4 and 10.85 hence at pH 9.5 and 10.5 these groups get protonated consequently affecting the solubility of the polymer by determining –lowering- its charge. A polymer with a higher total

hydroxyl and charge content has better solubility and remains in solution thereby enriching the F phase under our reaction conditions.

4.3.3 SEC Data of the Purified LignoBoost Lignin Samples

Changes in the polymer structure of the lignin were followed by molecular mass distribution analysis with size exclusion chromatography (SEC) on the purified fractions using acetylated lignin samples.[257] Polystyrene equivalent weight average molecular weight (Mw), number average molecular weight (Mn) and polydispersity (PD) were determined using calculation strategies from Baumberger for whole curve integration. [258] Mw/Mn gives PD that directly shows how accurate it is to evaluate a peak as one and not as a sum of multiple peaks. (Table 29)

Table 29. Size exclusion chromatography results for purified and acetylated LignoBoost lignin samples from commercial Scandinavian soft wood kraft pulping liquor.

Sample*	M_w**	M_n**	PD
BL	3601	812	4.44
P 10.5	2939	1694	1.73
F 10.5	2718	795	3.42
P 9.5	2979	1795	1.66
F 9.5	2101	735	2.86

* BL: black liquor, P: precipitated lignin, F: filtrate at pH 9,5 and 10,5.
** Polystyrene standards were used with Mw 1.200-195.000 g mol^{-1}

SEC data shows that P samples were enriched in the lower MW fraction in the 200-300 g mol^{-1} region which represents a lignin DP of 1-2 units.[259] Their peaks were recognizable and easy to separate from the main peak resulted from the higher Mw lignin fractions.[258]

While on the contrary in case of F and BL samples, no additional peaks were recognizable in the lower MW region and their SEC curves were integrated as one peak and as a result their respective PD's got 2-3 times larger than in case of the precipitates. These results are consistent with previous research data of Wallmo.[260] It is noteworthy that polydispersity of all separated lower MW peaks fell between 1.02 and 1.12 (data not shown) that confirms the validity of the calculation strategy used.

4.3.4 Pyrolysis Data on Purified LignoBoost Lignin Samples

With a known chemical composition in hand, a subsequent pyrolysis step could be optimized for a high yield bio-oil production. Yields have been compared in case of crude BL, crude P 9.5 and purified P 9.5 samples. The results on bio-oil yields are summarized in Table 30.

Table 30. Bio-oil yields from LignoBoost lignin feed stocks precipitated from commercial Scandinavian soft wood kraft pulping liquor at pH: 9.5. Pyrolysis conditions: 400°C with 2 min resident time.

LignoBoost sample	Pyrolysis oil yield [wt%]	Solid yield (Char) [wt%]	Unaccounted (Gas) [wt%]
Black liquor (crude)	33.16	64.14	2.71
P 9.5 (crude)	31.53	67.55	0.92
P 9.5 (extracted)	42.98	42.25	14.78

Table 30 clearly shows that the highest bio-oil yield is provided by the purified precipitate that had the highest lignin content in the feedstock. The elemental composition of the product fractions was followed by elemental analysis and the data is summarized in Table 31.

Table 31. Elemental analysis on bio-oils produced from LignoBoost lignin feed stocks precipitated from black liquor (BL) at pH: 9.5. Pyrolysis conditions: 400°C with 2 min resident time.

	Measured Element				
Sample name*	Hydrogen [wt%]	Carbon [wt%]	Oxygen [wt%]	Sulfur [wt%]	NM [wt%]
Black Liquor	3.63	35.14	33.80	4.13	23.30
BL Solid	2.36	36.06	30.24	1.53	29.81
BL Pyr. Oil	8.88	67.69	17.18	2.19	4.06
P 9.5 Crude	4.54	51.65	31.42	2.30	10.09
P 9.5 Crude Solid	4.14	58.53	20.82	1.28	15.23
P 9.5 Crude Pyr. Oil	7.69	64.02	23.30	2.94	2.05
P 9.5 Extracted	5.87	62.73	28.56	1.67	1.17
P 9.5 E. Solid	4.67	71.67	22.07	0.97	0.62
P 9.5 E. Pyr. Oil	7.22	64.67	23.22	3.19	1.70

* BL: black liquor, P: precipitated lignin at pH 9,5, E: extracted purified lignin, NM: not measured.

In Table 31 the NM regions in all weight compositions come from alkali and alkali earth metals as well as silica, aluminium and BL trace elements.[260] This data is consistent with Table 30 showing that the inorganic salt remained unreacted during our pyrolysis conditions. This finding combined with the fact that only the lignin fraction contributed to bio-oil production, resulted in an increased yield in case of the purified lignin feedstock observed in Table 31.

Since our project is aiming to convert biomass to fossil fuel substitutes, it is essential to understand the main chemical and physical properties of these chemicals. The distinct differences between the chemical and physical properties of lignin and fossil fuels mainly result from their different oxygen contents and the difference in their carbon chain length.[198] Lignin's O/C content is higher and its H/C molar ratio is lower than in gasoline or diesel. The carbon chain length of the lignin building unit is between the

gasoline and diesel range. Table 32 summarizes the main chemical and physical properties of the lignin feedstock and the final bio-oil compared with major fossil fuels.

Table 32. The main chemical and physical properties of fossil fuels, LignoBoost lignin precipitated from black liquor at pH: 9.5 (P9.5) and the final pyrolysis oil. Pyrolysis conditions: 400°C with 2 min resident time.

	Gasoline	Gasoil /diesel	LignoBoost lignin (P9.5)	LignoBoost lignin (P9.5) Pyr. Oil
Carbon chain length	5-10	12-20	[9-10]n	---
O/C molar ratio	0	0	0.34	0.26
H/C molar ratio	1-2	~2	1.12	1.34
Phase behavior (ambient T)	liquid	liquid	solid	liquid
Polarity	a-polar	a-polar	a-polar	a-polar
Preferred structure	branched/ aromatic /cyclic/ unsaturated	linear/ saturated	Branched (3D)	---

Table 32 shows that the O/C ratio of the bio-oil is decreased by 24% and its H/C ratio increased by 20% compared to the purified LignoBoost lignin feedstock. Increased hydrogen content with decreased oxygen content suggests that during pyrolysis the oxygen leaves by either deoxygenation or decarboxylation. Unfortunately the chemical composition of the final products does not provide sufficient insight into the fundamental chemistry. During the pyrolysis of the purified P 9.5 phase 14.78% of the feedstock left by the gas phase. With the composition of the gas phase in hand, the fundamental chemistry during pyrolysis could be solved.

4.4 Conclusions

In conclusion, the entering BL separates into phase P which is enriched in lignin and into phase F which is enriched in salts, together with sugars and short chain acids from the original BL. Lower final pH resulted in a better lignin separation. The LignoBoost sample purification method used in this study is efficient and the SEC data obtained on the purified P phase showed that the fraction is enriched in the 200-300 g mol^{-1} region, making it a viable staring feedstock for a future biofuel or biomaterial production step. Quantitative NMR data showed that phase F is enriched in carboxylic and phenolic groups while phase P in methoxyl moieties. Under our reaction conditions the total hydroxyl content of phase F at pH 9.5 was 56% higher, while at pH 10.5 it was 45% higher than phase P that led to the higher solubility of the lignin biopolymer. A lower final pH resulted in a 69% enrichment of the total hydroxyl content in the F fraction while only a 35% increase in the P fraction, which resulted in a better lignin separation when lower pH was employed. These findings gave valuable insight of the physical and its determining chemical properties of this currently under utilized renewable bioresource. A known chemical structure and composition can help to optimize a future controlled high yield catalytic conversion. With our pyrolysis setup, we reached bio-oil yields up to 43%, and the highest yield of the purified lignin feedstock was 36% higher than in case of an unpurified lignin feedstock. Compared to the starting purified lignin, the bio-oil's O/C decreased by 24% and the H/C ratio increased by 20%. However this change in molecular composition led to improved physical-chemical properties –liquerification- toward fossil fuels, its fundamental deoxigenation/decarboxilation chemistry is unsolved.

CHAPTER 5

5. CATALYTIC HYDROGENOLYSIS OF ETHANOL ORGANOSOLV LIGNIN [3]

5.1 Introduction

The production of ethanol based on lignocellulosic materials will bring about the coproduction of significant amounts of under-utilized lignin. This study examines the potential of conventional heterogeneous and novel homogeneous catalysts for the selective cleavage of the aryl-O-aryl and aryl-O-aliphatic linkages of ethanol organosolv lignin to convert it from a low grade fuel to potential fuel precursors or other value added chemicals. The development of hydrogenolysis conditions that effectively increase the solubility of lignin were initially examined with $Ru(Cl)_2(PPh_3)_3$ and demonstrated the ability to decrease the molecular weight and enhance the solubility of the lignin polymer. Later studies examined several heterogeneous and homogeneous hydrogenation catalysts at optimized reaction conditions resulting; 96.4% solubility with $Ru(Cl)_2(PPh_3)_3$, increase in H/C ratio with Raney-Ni, Pt/C and extensive monomer formation with $NaBH_4/I_2$. The changes in molecular structure of lignin were followed by size exclusion chromatography, qualitative and quantitative NMR spectroscopy and elemental analysis. These studies demonstrated that aryl-O-aryl and aryl-O-aliphatic linkages could be

[3] This manuscript was published in [Holzforschung (DOI: 10.1515/HF.2009.097)] Reproduced by the permission of Walter de Gruyter GmbH & Co. KG with K. G. Saur Verlag and Max Niemeyer Verlag. It is entitled as "Organosolv lignin hydrogenolysis to value added chemicals". The other authors are Arthur J. Ragauskas and Kasi David from School of Chemistry and Biochemistry at the Georgia Institute of Technology and George J. P. Britovsek from the Department of Chemistry at the Imperial College of London, United Kingdom.

cleaved and the hydrogenated lignin had a decrease in oxygen functionality and the formation of products with lower oxygen content.

Global energy demand has increased by 120% over the last four decades and projected economic growth is anticipated to increase by +50% in 2025.[25] Accompanying these energy requirements and the dwindling supply of geological reserves has been renewed interest in renewable bioresources. Currently, biomass based resources contribute ~3% of the world's primary energy supplies.[34] Biomass is an abundant resource with an annual global production rate of $17x10^{10}$ metric tons which consists of approximately 75% carbohydrates, 20% lignin and 5% other products.[261,262] The biosphere is estimated to have $3x10^{11}$ metric tons of lignin with an annual biosynthesis rate of $2x10^{10}$ metric tons.[263] The O/C and H/C molar ratios in lignin are lower than in carbohydrates and the carbon chain length of the basic building unit is between the gasoline and diesel range.[264,265,266]

Table 33. The main chemical and physical properties of fossil fuels and major biopolymers.

	Gasoline	Gas oil/diesel	Carbohydrate	Lignin
Carbon chain length	5-10	12-20	$[5\text{-}6]_n$	$[9]_n$
O/C molar ratio	0	0	1	0.3-0.4
H/C molar ratio	1-2	~2	2	0.7-1.1
Phase behavior (ambient T)	liquid	liquid	solid	liquid-solid
Polarity	a-polar	a-polar	polar	a-polar
Preferred structure	branched/aromatic /cyclic/unsaturated	linear/saturated	linear/cyclic	branched

The distinct differences between the chemical and physical properties of the listed biomaterials and fossil fuels mainly result from their higher oxygen contents and the difference in their carbon chain length.[187] Previous attempts to decrease the degree of polymerization and/or the oxygen content of biomass has involved various transformations, including hydrothermal decarboxylation,[181] pyrolysis,[182] carbonization,[183] acid-catalyzed dehydration,[267,268] metal-catalyzed decarboxylation,[184,185,186] metal-catalyzed hydrogenation,[187] and hydrogenolysis.[188] Despite the extensive research, lignin still has a low commercial value and mainly just simply combusted as a low grade fuel.

In focus of the present study is a recently optimized ethanol organosolv process providing a high yield recovery of carbohydrate and lignin.[269] The aim is to examine a series of hydrogenation conditions to identify catalytic hydrogenolysis conditions for the selective cleavage of the aryl-O-aryl and aryl-O-aliphatic linkages of the lignin polymer.

Previous lignin hydrogenation studies employed either high temperatures (> 200ºC) and/or high H_2 pressures (>7 MPa), or strong acidic or basic media. Depending on the reaction conditions, up to 60-80% conversion of the starting lignin to liquefied mixtures was obtained. These mixtures contained hydrogenated products such as; *o*- and *p*-cresol, phenol and *p*-ethylphenol.[270,271,272] The knowledge is improved concerning the chemical mechanisms involved in these harsh conditions, the reusability of the catalyst, and tailoring the selectivity of the hydrogenation towards specific lignin groups.[273,274]

Recent hydrogenation studies with colloidal Ru or mono-, di- and tetra-nuclear Ru-Arene complexes as catalyst on milled wood lignin indicate that a 50% decrease in the degree of polymerization (DP) can be accomplished.[275,276] Hydrogenation with phosphine ligand containing ruthenium complexes of carbon-carbon double bond and/or carbon-oxygen bond containing chemicals has provided additional insight on how to tailor the catalytic selectivity towards carbon-oxygen bond cleavage over carbon-carbon double bond hydrogenation.[277,278]

During hydrogenolysis, the hydrogen is utilized under harsh conditions for the cleavage of C-O inter-lignin linkages. During hydrogenation, carbon-carbon or a carbon-oxygen double bonds are saturated by hydrogen: the H/C ratio is elevated but depolymerization does not occur. The expectation is that selective hydrogenolysis of lignin leads to potential fuel precursors or other value added chemicals by oxygen decrement and hydrogen increment and to products with lower molecular weight by reductive cleavage of C-O-C bonds.[187]

The aim of the present work was to investigate the performance and fundamental chemistry of several heterogeneous catalysts (Co/Mo, Raney-Ni, Pd/C, Pt/C) and homogeneous catalysts ($NaBH_4/I_2$, $RhCl(PPh_3)_3$, $Ru(Cl)_2(PPh_3)_3$, $Ru(H)(Cl)(PPh_3)_3$, Ruthenium-polyvinylpyrrolidone nanoparticle (Ru-(PVP)) on a hydrogenolysis/ hydrogenation on organosolv lignin. The structure of the synthesized catalysts were examined by NMR and fundamental chemistry of the hydrogenation reactions was examined by differential differential scanning calorimetry (DSC), elemental analysis, molecular weight distribution (MWD) analysis, ^{1}H-NMR and ^{31}P-NMR spectroscopy.

5.2 Experimental Section

5.2.1 Materials

A single Loblolly pine (*Pinus taeda*) tree, visually free of disease and compression wood, was obtained from the University of Georgia research plot in Baldwin County, GA, USA. The wood was manually debarked and chipped using a mechanical chipper. From the hydrogenation catalysts, $Ru(Cl)_2(PPh_3)_3$, $RhCl(PPh_3)_3$ and Ru(PVP)-nanoparticle were synthesized, all other were purchased from Sigma-Aldrich (St. Louis, MO, USA) and used as received. Solvents were purchased from VWR (West Chester, PA, USA). All gases were ultra high purity and purchased from Airgas (Radnor Township, PA, USA).

5.2.2 Preparation of SW EOL

Softwood (SW) ethanol organosolv lignin (EOL) preparation from Loblolly pine chips are described in Chapter 3. (3.3.2.1 EOL Extraction).

5.2.3 Catalyst Synthesis

$Ru(Cl)_2(PPh_3)_3$, $RhCl(PPh_3)_3$ and Ru(PVP)-nanoparticle sythesis, and Co/Mo activation are described in Chapter 3. (3.3.2.2 Preparation of the Hydrogenation Catalysts).

5.2.4 Catalytic Hydrogenation

Catalytic hydrogenation is described in Chapter 3. (3.3.2.3 Hydrogenation).

5.3 Results and Discussion

5.3.1 Determining the Structure of $Ru(Cl)_2(PPh_3)_3$ and $RhCl(PPh_3)_3$ in Solution

It is shown that even small alternations of the structure of a catalyst can have a big effect on conversion yields and selectivity.[277,278] The dissociation of the tri-phenylphosphine (PPh_3) ligand is a known phenomenon.[279] Thus it is essential to understand how the structure of $Ru(Cl)_2(PPh_3)_3$ and $RhCl(PPh_3)_3$ will be altered after dissolution.

5.3.1.1 $RuCl_2(PPh_3)_3$

$RuCl_2(PPh_3)_3$; ^{31}P NMR ($CDCl_3$): δ -5,48 (s), 39,55 (d), 40,85 (d), 38-44 (m), 47,29 (d), 51,08 (d). (see: Appendix A.2.2)

However in solution the extensive dissociation of the (PPh_3)-ligand from the $RuCl_2(PPh_3)_3$ complex is a known phenomena, its nature highly temperature dependent and still not fully understood.[233] The dissociation is clearly shown by the singlet at (δ – 5,48 ppm), which stands for the free (PPh_3)-ligand. The broad peak around (δ 41,1 ppm) and the two doublet at (δ 47,29 ppm) and (δ 51,08 ppm) are consistent with the previous results measured at 25°C, and stands for the highly fluctuating trigonal-bipiramid (I) in $RuCl_2(PPh_3)_3$ and for the cis-dimer (II) in $[RuCl_2(PPh_3)]_2$.[233] The two dimers at (δ 39,55 ppm) and (δ 40,85 ppm) are connected and their coupling frequency is 183 Hz, thus we suggest that these two peaks stand for the proposed distorted trans-dimer (IV) in $[RuCl_2(PPh_3)]_2$. These structures are depicted in Equation 3.

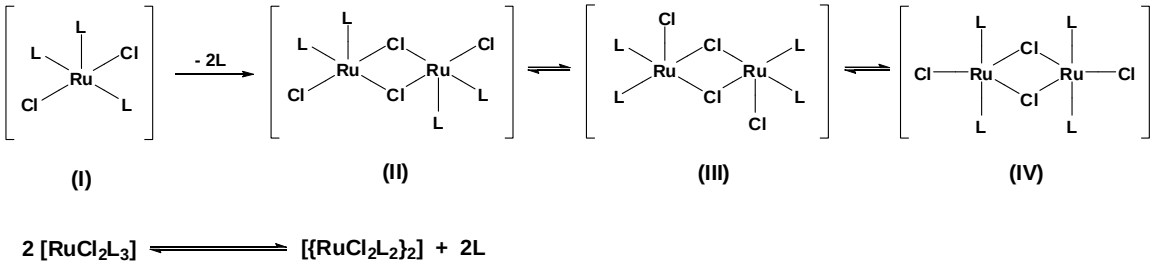

Equation 3. The proposed dissociation pathway of $RuCl_2(PPh_3)_3$ and the formation of cis/trans-dimers of $[RuCl_2(PPh_3)]_2$.

5.3.1.2 $RhCl(PPh_3)_3$

$RhCl(PPh_3)_3$; ^{31}P NMR ($CDCl_3$): δ -5,50 (s), 30,08 (d), 30,97 (d), 46,81 (t), 47,99 (t), 50,99 (s), 52,21 (s). (see: Appendix A.2.1)

The two doublets at (δ 30,08 ppm) and (δ 30,97 ppm) stand for the two symmetrically situated phosphine ligand. The two triplets at (δ 46,81 ppm) and (δ 47,99 ppm) stand for the third ligand as coupling with the two symmetrical ligands and the ruthenium. The dissociation of the phosphine ligand is shown by the singlet at (δ –5,50 ppm), which stands for the free (PPh_3)-ligand and the two singlet at (δ 50,99 ppm) and (δ 52,21 ppm) which stand for the symmetrical dimer coupled with ruthenium. We suggest that unlike $RuCl_2(PPh_3)_3$, it is a monomer-monomer not a monomer-dimer equilibrium. These structures are depicted in Equation 4.

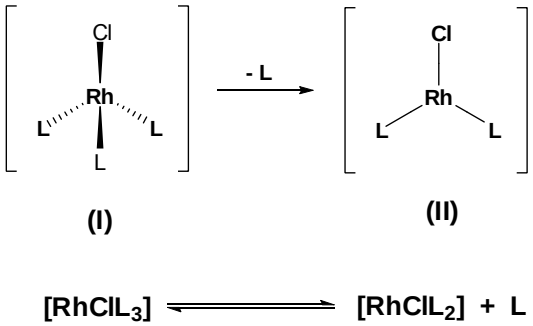

Equation 4. The proposed dissociation pathway of $RhCl(PPh_3)_3$ and the formation of $RhCl(PPh_3)_2$.

5.3.2 The Effect of Temperature on SW EOL Hydrogenation

Based on the experimental results quoted in the introduction (Section 5.1), our initial studies examined $RuCl_2(PPh_3)_3$ as catalyst for SW EOL hydrogenolysis. Hydrogenation runs were performed from 50 to 200°C. The changes of the ethanol solubility and the average molar mass data of the hydrogenated SW EOL are summarized in Table 34.

Table 34. Solubility in ethanol and average molar mass data (M_w, M_n) of the untreated softwood ethanol organosolv lignin (EOL), blank runs and when $RuCl_2(PPh_3)_3$ used as a catalyst at different temperatures for 20 hours.

Reaction conditions	Soluble fraction			Insoluble fraction		
	(% dry wt.)	M_w (g mol^{-1})	M_n (g mol^{-1})	(% dry wt.)	M_w (g mol^{-1})	M_n (g mol^{-1})
EOL	52.1	2440	1191	47.9	219790	79025
Blank						
50°C	50.1	2205	1090	49.9	258650	77000
200°C	40.0	1781	712	11.0	211580	72415
				49.0 (charred)	---	---
$RuCl_2(PPh_3)_3$						
50°C	59.1	2317	1100	40.9	258460	63918
100°C	72.0	2405	1094	28.0	320480	90490
150°C	73.0	2416	1091	27.0	348030	119520
175°C	96.4	2142	893	3.6	330580	103490
200°C	80.7	2221	980	19.3	265700	73229

DSC analysis indicated that the glass transition temperature (T_g) of the starting EOL was 147.8 ±1°C. Ethanol solubility of the hydrogenated lignin significantly increased if treated above T_g of the starting EOL (Table 34). The M_w of the soluble phase of hydrogenated EOL decreased by ~10% to 2100-2200 g mol^{-1} which represents a lignin DP of 10-11 units.[101] The weight average of the insoluble lignin fraction after hydrogenation increased by 50% at reaction temperatures of >100°C due to condensation reactions of the lignin polymer.[280,281] When no catalyst was added at 200°C, 49.0% of all EOL was charred. However, under the same reaction conditions with $RuCl_2(PPh_3)_3$ the EOL solubility increased by 40.7% and no charring was observed.

When the hydrogenation reaction temperature was higher than the EOL T_g, the solubility of the treated EOL increased from 73.0% at 150°C to 96.4% at 175°C and 80.7% at 200°C. The decrease in the formation of the lower molecular weight fraction at 200°C is attributed to the thermal instability of the catalyst.[222] Based on these results, the optimal reaction temperature for the catalyst screening on SW EOL was chosen to be 175°C.

5.3.3 Catalyst screening for SW EOL hydrogenation

In previous works, it has been demonstrated that carbon-oxygen bond cleavage can be catalyzed by several conventional heterogeneous hydrogenation catalysts such as: platinum, palladium and nickel,[282,283,284] and homogeneous catalysts such as: ruthenium, rhodium, and borane with iodine.[285,286,287,288,289] These results provided valuable insight into the design of selective hydrogenolysis conditions for the cleavage of aryl-O-aryl and

aryl-O-aliphatic linkages in lignin. The catalytic efficiency of several conventional and novel catalysts (Table 35) for SW EOL hydrogenation was evaluated at 175°C.

Table 35. Selected hydrogenation catalysts for ethanol organosolv lignin hydrogenolysis.

Homogeneous catalysts	
Borane/Iodine	$NaBH_4/I_2$, 1/1 w/w
Rhodium	$RhCl(PPh_3)_3$
Ruthenium	$Ru(Cl)_2(PPh3)_3$ $Ru(H)(Cl)(PPh3)_3$ Ru-PVP nanoparticle
Heterogeneous catalysts	
Cobalt/Molybdenum (Co/Mo)	3.5% CoO, 14% MoO_3 (Aluminum-supported)
Nickel	Raney-Ni
Palladium	10% Carbon-supported (Pd/C)
Platinum	5% Carbon-supported (Pt/C)

Under our standard reaction conditions, homogeneous catalysts in general increased the solubility of treated SW EOL to a greater extent when compared to the heterogeneous catalysts. When $RuCl_2(PPh_3)_3$ was used, the solubility of the hydrogenated lignin in ethanol increased to 96.4%, resulting a nearly complete solubilization and a 12.2% decrease in M_w. Compared to the untreated SW EOL, the solubility decreased in case of Co/Mo or Ru-PVP as catalysts, the M_w of the soluble phase decreased by 15.4% and 20.2%, respectively (Table 36).

Table 36. Solubility in ethanol, average molar mass data (M_w, M_n) and polydispersity (M_w/M_n) of the soluble phase for the untreated ethanol organosolv lignin (EOL), the blank run and after hydrogenation with different catalysts at175°C for 20 hours.

Reaction conditions	Solubility in ethanol (% dry wt.)	M_w (g mol^{-1})	M_n (g mol^{-1})	M_w/M_n
EOL	52.1	2440	1191	2.0
Blank	65.0	2030	1026	2.0
Heterogeneous catalysts				
Co/Mo	54.3	1717	1075	1.6
Raney-Ni	71.8	2225	1148	1.9
Pd/C	69.8	2050	995	2.1
Pt/C	76.5	2069	953	2.2
Homogeneous catalysts				
$NaBH_4/I_2$	72.4	1079	404	2.7
$RhCl(PPh_3)_3$	76.3	1878	787	2.4
$Ru(Cl)_2(PPh_3)_3$	96.4	2142	893	2.4
$Ru(H)(Cl)(PPh_3)_3$	77.2	1974	837	2.4
Ru-(PVP)	58.1	1620	902	1.8

While ethanol solubility significantly increased in most cases, the M_w of the soluble phase only decreased by ~20% to 1900-2100 g mol^{-1}, which represents a lignin DP of 9-10 units. However, when the MWD are examined (Figure 47), an increase of the lower MW fraction can be observed in the 200-300 g mol^{-1} region (DP = 1-2 units) when compared to the blank run. This finding was most pronounced with $NaBH_4/I_2$ as catalyst.

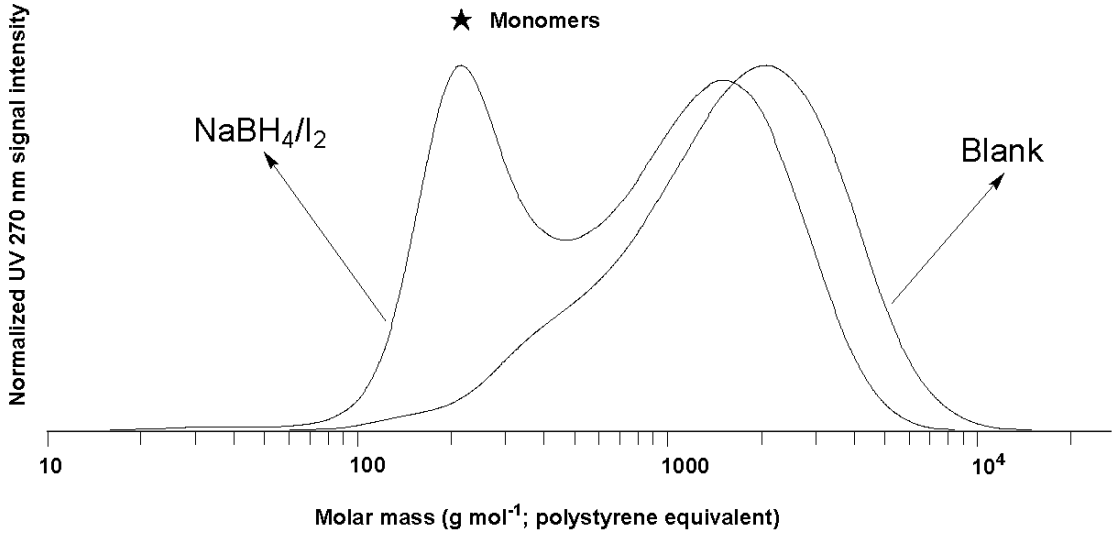

Figure 47. Apparent molar distributions (polystyrene standard equivalent) of the soluble fraction of the blank run and when $NaBH_4/I_2$ was used as catalyst for softwood ethanol organosolv lignin hydrogenation at 175°C for 20 hours.

5.3.4 Investigation of the Reaction Mechanism: Hydrogenation vs. Hydrogenolysis

Both hydrogenolysis and hydrogenation of lignin results in the enrichment of the saturated aliphatic region in the ^{1}H-NMR spectra.[290] Quantitative ^{1}H-NMR measurements provided a reliable means of monitoring the enrichment of the hydrogen containing groups (Figure 48).

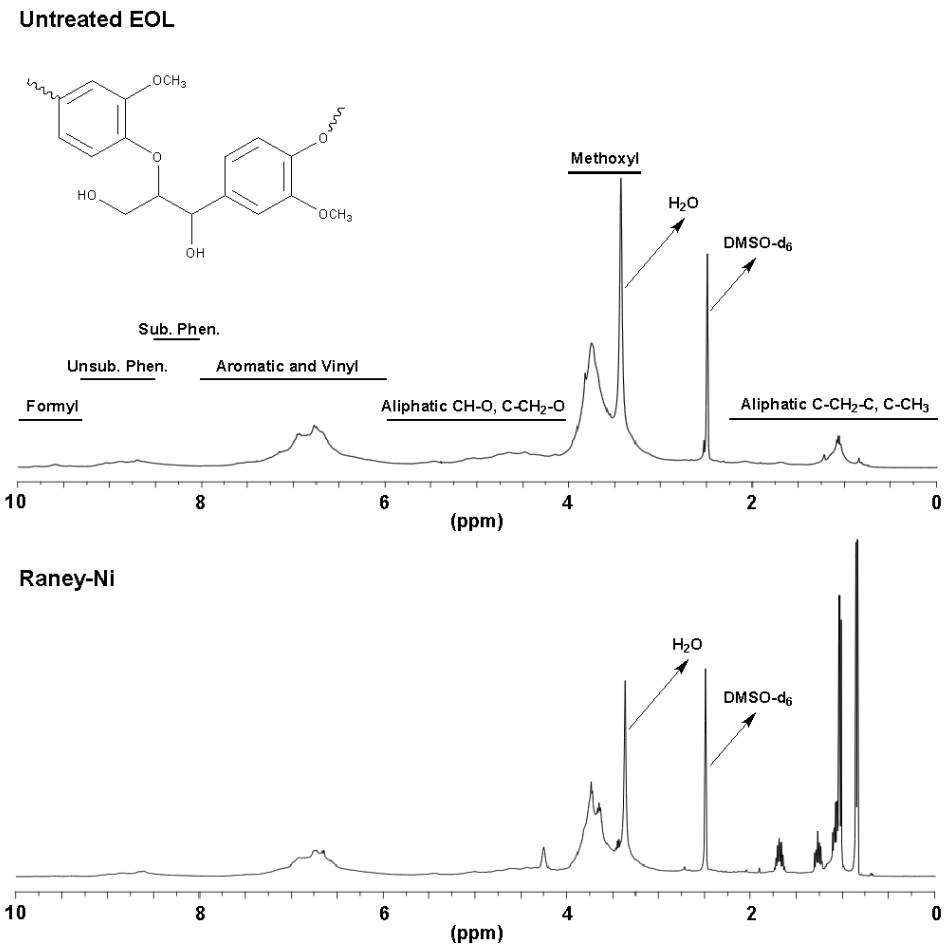

Figure 48. Qualitative ^{1}H-NMR of the softwood EOL soluble fraction in case of the untreated ethanol organosolv lignin(EOL) and when Raney-Ni was used as catalyst at 175°C for 20 hours. (solvent: DMSO-d_6).

The solubility, and the data of gel permeation chromatography (GPC) and NMR spectra indicate that the EOL undergoes condensation reactions above 100°C. Accordingly, the DP of the insoluble fraction is increased from ~1000 up to ~1700 units. Lower MW fractions were formed during hydrogenation when smaller fragments of the EOL polymer underwent hydrogenolytic cleavage. When the DP of the insoluble polymer decreases to 10-12 monomeric units, the hydrogenated lignin fragments become soluble in ethanol.

Highest yields were achieved when Raney-Ni, Pt/C, $NaBH_4/I_2$ or $RuCl_2(PPh_3)_3$ were used as catalyst. In case of $RuCl_2(PPh_3)_3$, the free PPh_3 ligands, which dissociated from the $RuCl_2(PPh_3)_3$ complex, contaminate the soluble fraction.[233] Thus, quantitative elemental analysis was performed on soluble fractions of the SW EOL for experiments with Raney-Ni, Pt/C, or $NaBH_4/I_2$ as catalyst.

Haenel et al. reported in the context of hydrogenation studies with borane and iodine catalysts for coal liquefaction about high catalytic activity towards aromatic compounds, increasing the original coal's aliphatic carbon content from 11% up to 60%.[288] Previous hydrogenation studies with Raney-Ni or Pt/C both have shown catalytic activity towards carbon-carbon double bond hydrogenation and also carbon-oxygen bond cleavage.[290]

The aim of the present study is to identify catalytic hydrogenolysis conditions for the selective cleavage of the aryl-O-aryl and aryl-O-aliphatic linkages of the lignin polymer. The fundamental hydrogenation chemistry of SW EOL was monitored by elemental analysis (Table 37), ^{1}H and ^{31}P-NMR.

Table 37. Elemental analysis and H/C molar ratio data of the soluble fraction of the untreated softwood ethanol organosolv lignin (EOL), the blank run and after hydrogenation with different catalysts at 175°C for 20 hours.

Used catalyst	Measured element (w/w)			H/C
	H	C	O	(mol/mol)
EOL	5.85	65.33	27.81	1.07
Blank	6.55	67.19	26.25	1.16
Raney-Ni	6.69	67.65	24.65	1.18
Pt/C	6.59	67.45	25.51	1.17
$NaBH_4/I_2$	9.66	63.23	27.06	1.83

The elemental analysis shows an increase in the H/C ratio in all cases. The enrichment of the hydrogen containing groups in the soluble phase was followed by quantitative ^{1}H-NMR (Table 38).

Table 38. Hydrogen content of the soluble fraction of the untreated softwood ethanol organosolv lignin (EOL), the blank run and after hydrogenation with different catalysts at 175°C for 20 hours as determined by quantitative ^{1}H-NMR.

Used catalyst	Total H content (μmol mg^{-1})	Hydrogen content of selected groups (μmol mg^{-1})					
		Carboxylic acid	Formyl	Phenolic	Aromatic, Vinyl	Aliphatic	Aliphatic
	(13.50-0.00) ppm*	(13.50-10.50) ppm* -C(O)OH	(10.10-9.35) ppm* -C(O)H	(9.35-8.00) ppm* =HC-OH	(8.00-6.00) ppm* CH=CH CH2=CH	(6.00-4.05) ppm* CH-O C-CH2-O	(2.25-0.00) ppm* C-CH2-C C-CH3
EOL	50.91	---	0.00	1.20	12.53	5.26	3.28
Blank	64.58	---	0.00	2.11	15.60	5.42	8.85
Raney-Ni	73.34	---	0.04	1.96	14.13	6.42	20.75
Pt/C	74.04	---	0.13	3.05	16.12	5.57	15.71
$NaBH_4/I_2$	143.29	0.83	1.43	2.29	23.91	10.16	55.03

* Li and Lundquist 1994; Ragauskas et al. 1997; Moe and Ragauskas 1999; Runge and Ragauskas 1999.

Based on the increment of the lower MW fraction it is obvious that hydrogenolysis has taken place, and the decrease in the aromatic content is a clear indication of simultaneous hydrogenation of the aromatic ring. The increase in hydrogen content both in regions of phenolic groups and oxygen containing aliphatic groups is an indication of a hydrogenolytic cleavage of aryl-O-aryl and aryl-O-aliphatic linkages, but this effect is pronounced only in the case of Pt/C as catalyst. The enrichment in the non-oxygen containing aliphatic group content is an indication of the simultaneous

hydrogenation by saturation of the carbon-carbon double bonds of the aryl and aliphatic groups.

The analytical data provided by the GPC and NMR measurements showed that each catalyst provided different final product after SW EOL hydrogenation. Based on previous literature and the analytical data provided by quantitative NMR, we propose three distinct reaction mechanism that could lead either hydrogenation or hydrogenolysis of the starting biopolymer.

5.3.4.1 Proposed Reaction Mechanism Using Heterogeneous Metal Catalysts

During heterogeneous hydrogenation on metal surfaces such as; Raney-Ni, carbon supported platinum and carbon supported palladium, the reaction is proposed to take place on the surface of the metal catalyst.[283] Based on our quantitative ^{1}H-NMR data combined with previous literature data, our proposed reaction mechanism is depicted in Equation 5.

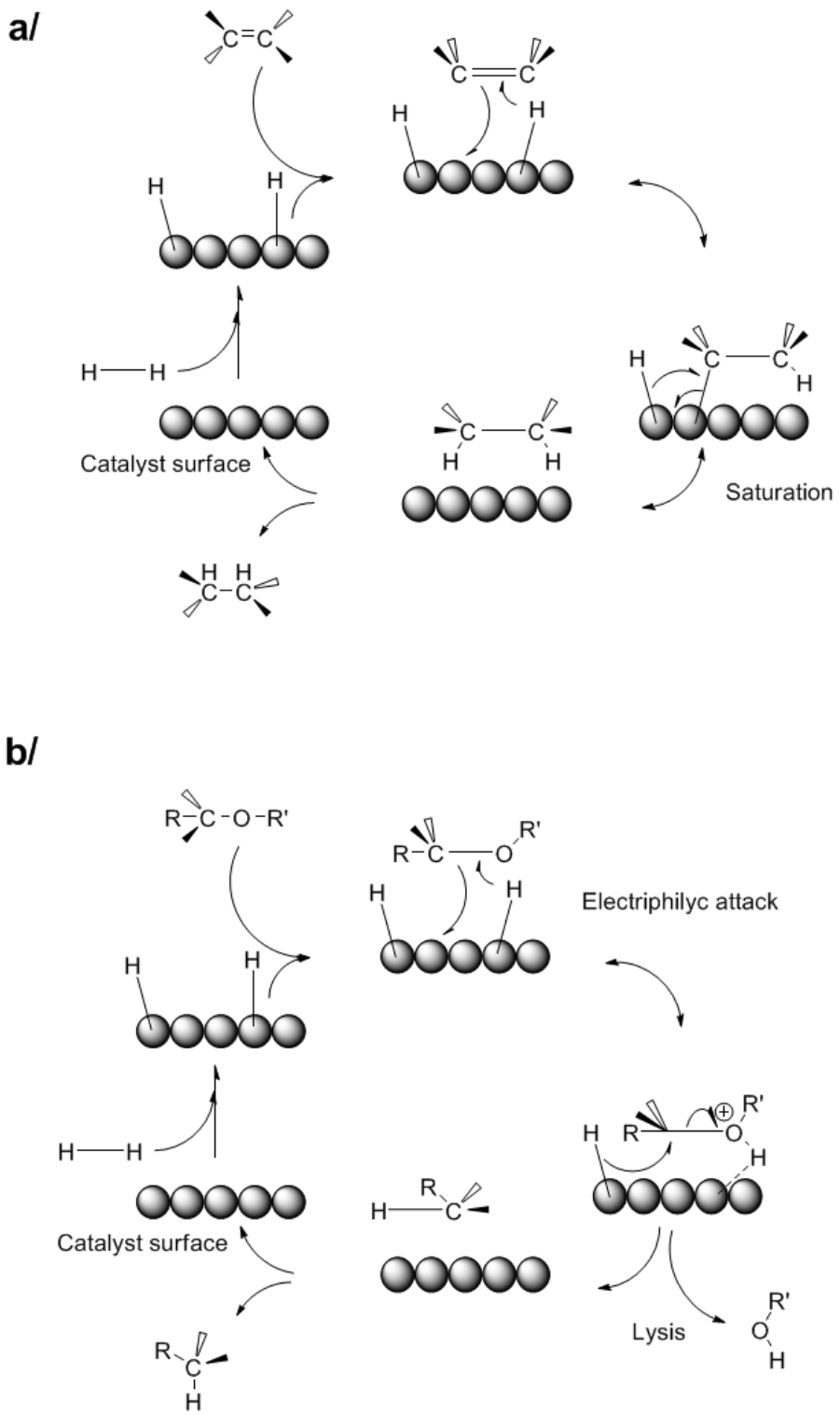

Equation 5. The proposed reaction mechanism for heterogeneous hydrogenation (a) and hydrogenolysis (b) on catalyst surface with metal-hydride.

As the first step, the hydrogen molecules react with the metal atoms at the catalyst surface while their σ-bond is broken and replaced with weaker metal-hydride bonds. During the second step, the π-bond in case of the C-C double bond or the σ-bond in case a C-O bond interacts with the metal catalyst weakening it metal-hydrate bond. As a result a hydrogen atom is transferred from the catalyst surface to one of the carbons (C=C) or oxygen (C-O). As the third step; during hydrogenation the π-bond (C=C) of the alkene interacts with the metal catalyst weakening its bond while a second hydrogen atom is transferred from the catalyst surface forming the alkane. During hydrogenolysis (C-O) when the second hydrogen atom is transferred from the catalyst surface to the carbon, the weakened σ-bond get cut and the hydrogenolysis happened. At the last step the products are released from the catalyst's surface, allowing it to accept additional hydrogen molecules for a subsequent catalytic cycle.

5.3.4.2 Proposed Reaction Mechanism Using Homogeneous Metal Catalysts

During homogeneous hydrogenation has been performed using $RhCl(PPh_3)_3$, $RuCl_2(PPh_3)_3$ and $Ru(H)(Cl)(PPh_3)_3$ as catalysts. Our P^{31}-NMR data described in section 5.3.1 (Determining the Structure of $Ru(Cl)_2(PPh_3)_3$ and $RhCl(PPh_3)_3$ in Solution) provided valuable information on the structural behavior of these Wilkinson catalysts. Combining this acquired analytic data with literature from previous experiments using the same Ru and Rh catalyst systems gave valuable data on the reaction mechanism during our hydrogenation reactions.[277,278] The proposed reaction mechanism for $RhCl(PPh_3)_3$ is depicted in Equation 6.

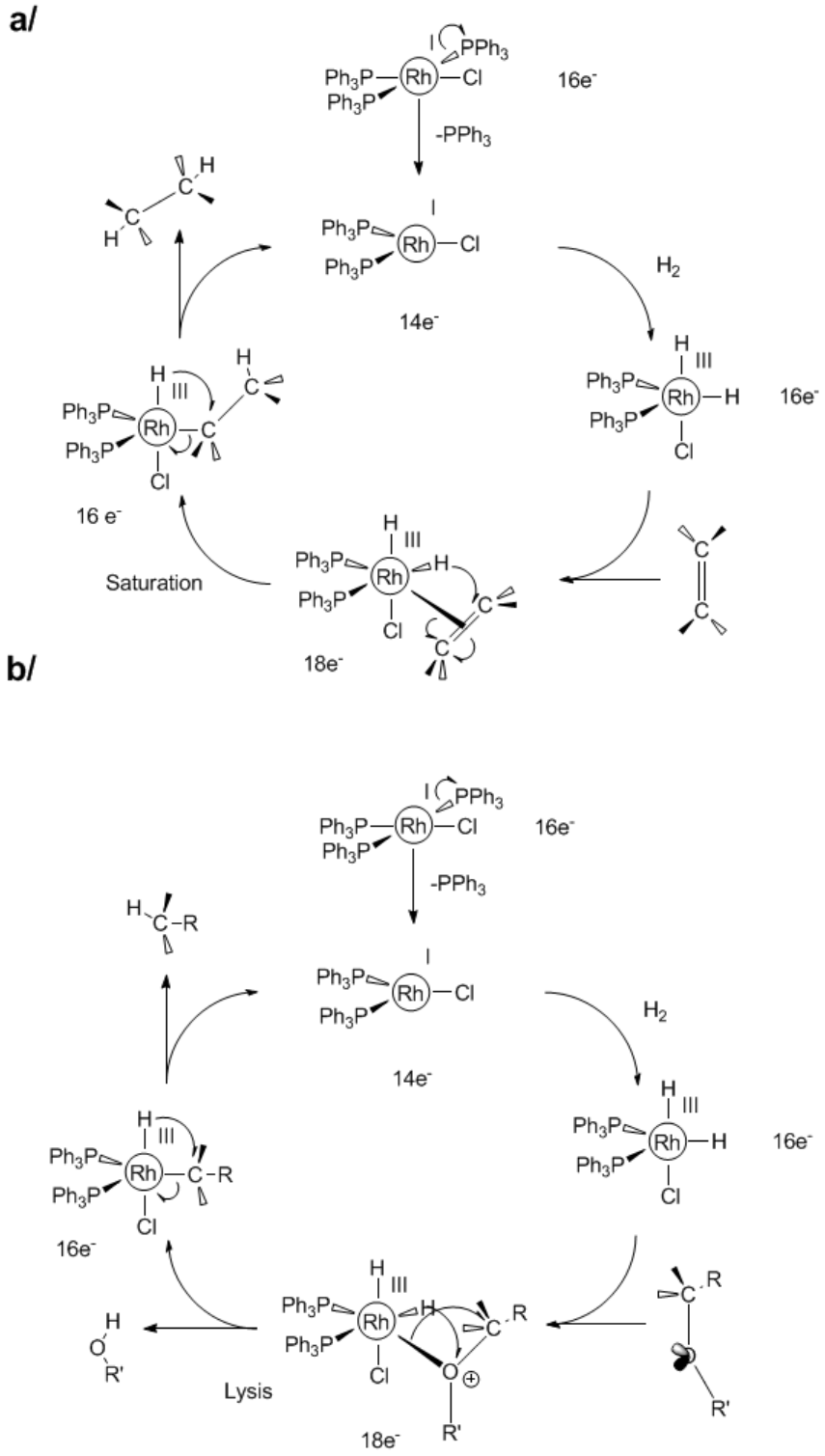

Equation 6. The proposed mechanism for hydrogenation (a) and hydrogenolysis (b) with $RhCl(PPh_3)_3$ catalyst.

As the first step, it is proposed that the PPh_3 is readily lost due to steric crowding. This step is consistent with our data where the dissociation of the phosphine ligand has been clearly shown by the singlet at (δ –5,50 ppm) in the P^{31}-NMR spectrum, which stands for the free (PPh_3)-ligand and the two singlet at (δ 50,99 ppm) and (δ 52,21 ppm) that stand for the symmetrical dimer coupled with ruthenium.

Previous literature shown that the Rh-PPh_3 hydrogenation catalyst system is compatible with a variety of functional groups (ketones, esters, carboxylic acids, nitriles, nitro groups, and ethers) and indicates that the metal hydride intermediate is primarily covalent in character.[278,287] Due to these findings, we propose that in case of a reaction of a π-electron system (Equation 6/a) as the next step, the catalyst forms a metal-hydride intermediate, that coordinative bonds to the unsaturated C-C bond leading to the saturation of the double bond. In case of an oxygen containing C-O σ-electron system (Equation 6/b), the cationic metal center due to it's electrophillic character, coordinates to the oxygen rather to the carbon leading to a hydrogenolysis by the formation first of the hydroxyl product and later the hydrogenated carbon group.

When $RuCl_2(PPh_3)_3$ and Ru(H)(Cl)(PPh3)3 were used as catalysts, literature suggests that Ru has a strong tendency to perform a heterolytic activation of H_2 instead of oxidative addition to make a metal dihydride. This can occur either via hydrogenolysis or heterolytic cleavage mechanisms.[257] Complexation of the dihydrogen to the metal leads to a decrease in H-H σ-bond character. This decrease in bonding leaves it with a partial positive charge hence making it more acidic, or easier to deprotonate with a 'base'. Based on these findings combined with our P^{31}-NMR data and proposed catalyst structures

depicted in section 5.3.1.1 ($RuCl_2(PPh_3)_3$), the proposed $RuCl_2(PPh_3)_3$ activation step is depicted in Equation 7.

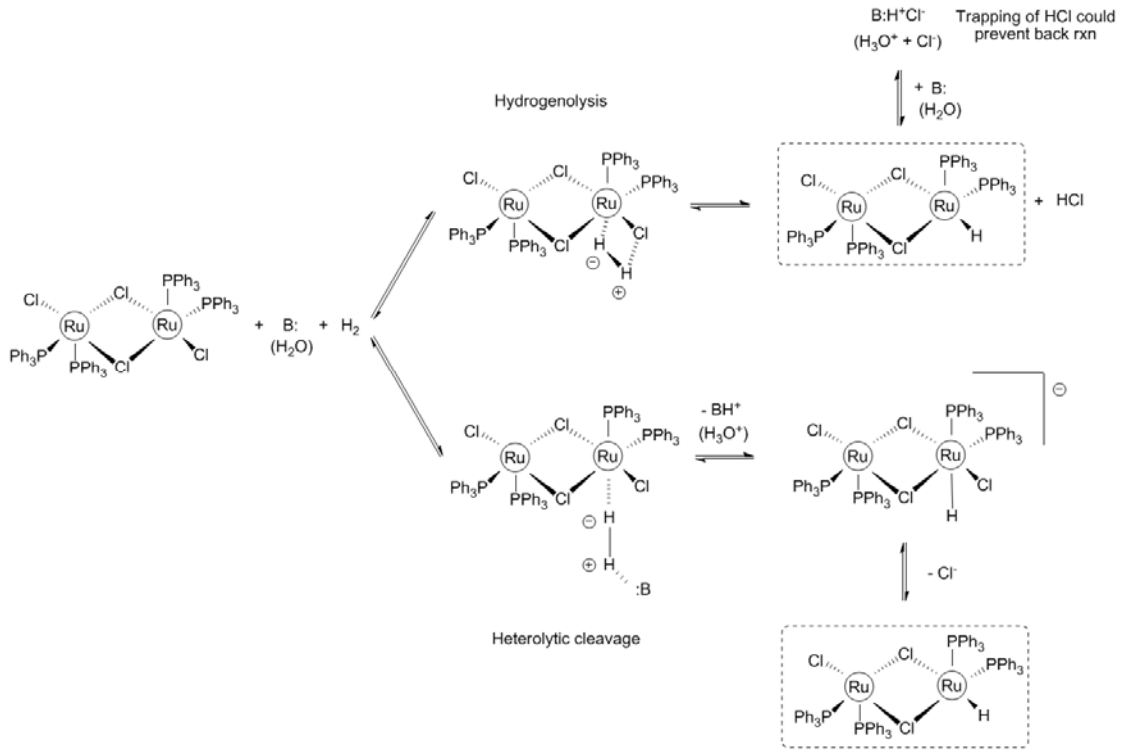

Equation 7. The proposed mechanism for heterolytic activation of $[RuCl_2(PPh_3)]_2$ catalyst by σ-bond metathesis and heterolytic cleavage.

As it is shown in Equation 7, both hydrogenolysis (σ-bond metathesis) and heterolytic cleavage mechanism give the same net result. The proposed catalytic cycle for activated $[RuCl_2(PPh_3)]_2$ is depicted in Equation 8.[257]

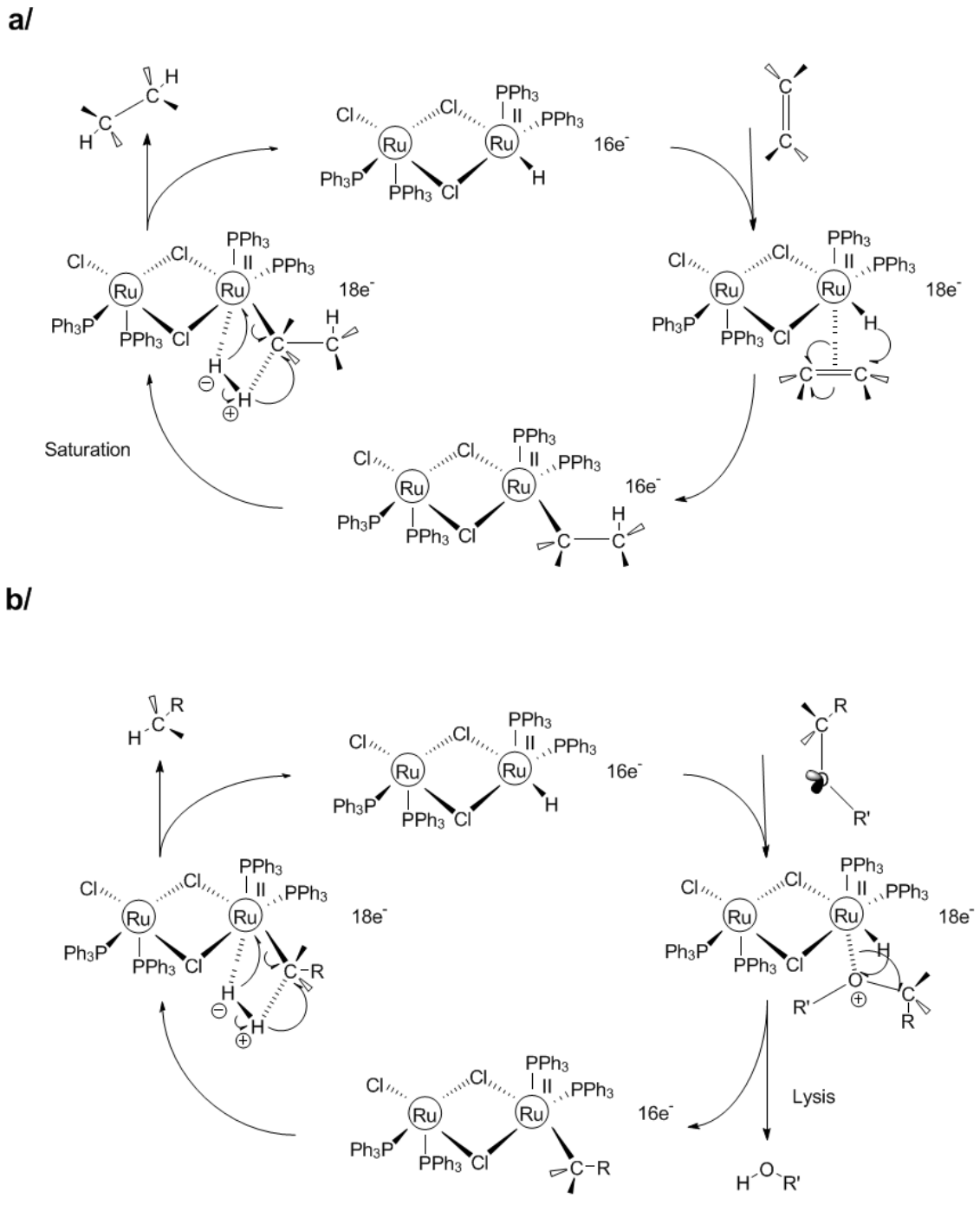

Equation 8. The proposed mechanism for hydrogenation (a) and hydrogenolysis (b) with activated $[RuCl_2(PPh_3)]_2$ catalyst.

Beside the activation step, the obvious difference between the proposed catalytic cycle between Rh and Ru is that while the oxidation state of the Rh during the cycle is changing between (+3) and (+1), there is no change in oxidation state of the Ru (+2). With all utilized Wilkinson catalysts, our quantitative H^1-NMR measurements shown an increase in hydrogen content both in regions of phenolic groups and oxygen containing aliphatic groups which is an indication of a hydrogenolytic cleavage of aryl-O-aryl and aryl-O-aliphatic linkages. The enrichment in the non-oxygen containing aliphatic group content is an indication of the simultaneous hydrogenation by saturation of the carbon-carbon double bonds of the aryl and aliphatic groups. This is an indication that both reaction proposed in (Equation 6,8/a&b) has happened under our reaction conditions.

Since the coordination of the metal hydride to the substrate is the rate determining step, we propose that the ratio of hydrogenation and hydrogenolysis is determined by the electrophillic character of cationic metal center and its favor towards nucleophillic attack on oxygen containing σ-electron system over a carbon-carbon π-electron system by alkene coordination.

5.3.4.3 Proposed Reaction Mechanism for I_2/BH_4 System

It is well known that $NaBH_4$ decomposes in protic solvents (like alcohols).[291] It is proposed that the extent of this undesired side reaction being a function of the alcohol and experimental conditions used such as: concentration and temperature (T). Equation 9 represents the decomposition reaction in ethanol, which is the solvent of choice in our experimental setup.

$$4\ EtOH + NaBH_4 \rightarrow (EtO)_4B^-Na^+ + 4H_2$$

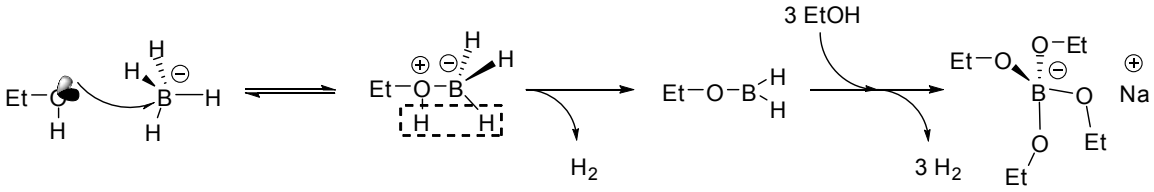

Equation 9. The decomposition reaction of $NaBH_4$ in ethanol.

After the hydrogenation experiments, the iodine is separated from the reaction media as a solid dark-purple pastille under our reaction conditions. Due to this observation, our proposed reaction mechanisms will avoid NaI formation. Based on our product distribution and previous literature data, thee main pathways were postulated for the hydrogenation and hydrogenolysis of SW EOL. Regioselective reduction and ether cleavage is depicted in Equation 10.

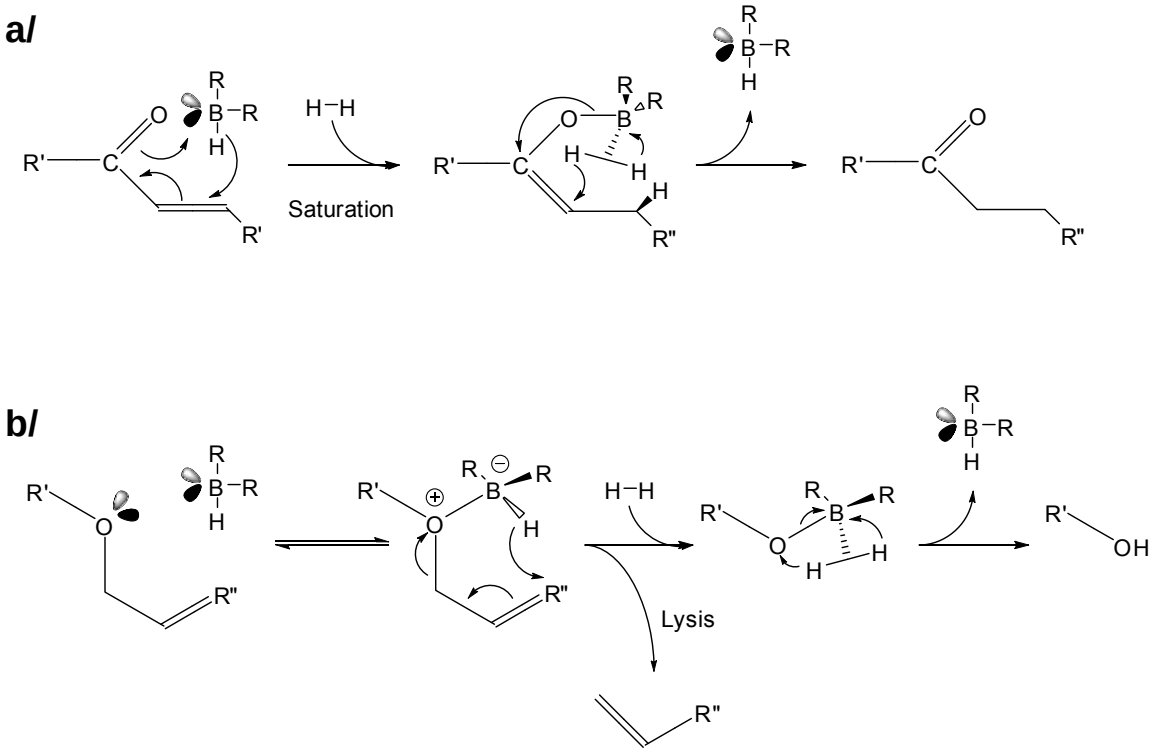

Equation 10. The proposed mechanism for hydrogenation (a) and hydrogenolysis (b) with $NaBH_4/I_2$ catalyst system. (R: H or OEt; R', R": Aliphatic or aryl group)

Equation 10 shows that both the hydrogenation and the hydrogenolysis assume a six member cyclic model.[292] Both reaction mechanism starts with the initial coordination of the borane with the carbonyl (a) or etherial (b) oxygen.[293] In both cases the second step is the hydride addition to the allyl system forming the boro ether, that followed by a subsequent complexation of the dihydrogen to the borane. The proposed reaction mechanism will lead to increased oxygen containing aliphatic and vinyl group formation in the final product, which is consistent with our quantitative H^1-NMR measurements. It worth mentioning that the proposed reaction pathways involve a hydride addition, thus the coordinating borane has to have a free hydrogen and as a conclusion this reaction can not work with $(EtO)_3B$.

The third proposed pathway is postulated for the reduction of carbonyl species with $NaBH_4$ involving the protic solvent. Figure 49 shows the transition state of the reduction of carbonyl specie with borohydrate anion assisted by ethanol as the protic solvent.[294]

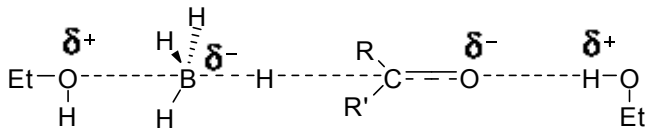

Figure 49. Postulated transition state for reduction of carbonyl specie with $NaBH_4$ in ethanol.

In the light of the above consideration combined with previous research data, two initial step could be considered during carbonyl hydrogenation.[294] The first step could involve both linear and six-member cyclic mechanisms leading to interchangable intermediates depicted in Equation 11. Since the coordinating borane specie has to have a free hydrogen to form the proposed transition state involved in the initial step, a borohydrate anion can enter four times into the proposed reaction cycle before forming the unreactive $(EtO)_4B^-$.

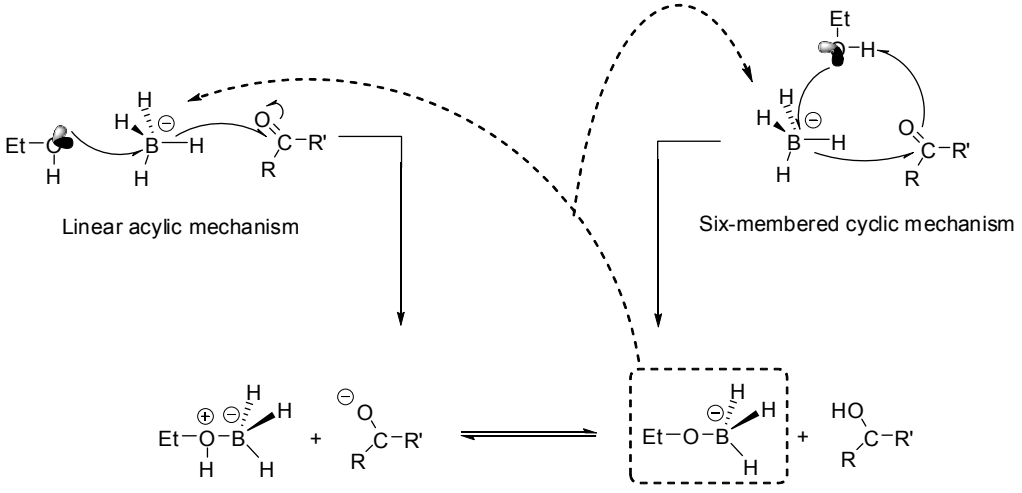

Equation 11. Postulated reaction pathways for the reduction of carbonyl specie with $NaBH_4$ in ethanol. (R, R': Aliphatic or aryl group)

The enrichment in the oxygen containing aliphatic group content is an indication that the reaction proposed in Equation 10 and/or Equation 11 has happened under our reaction conditions. It is worth mentioning that while in the first two proposed reactions the borane specie is a catalyst, in the third reaction mechanism it is a reactant, and the initial borohydrate anion is not regenerated.

The fourth proposed pathway is based on the common mechanism via hydroboration of aromatic π-bonds at high temperatures leading to C_{aryl}-C_{alkyl} bond hydrogenolysis and partial hydrogenation.[295] Equation 12 shows that reversible hydroboration can occur on the alkylated π-bond at C_1 or at C_2 positions. As the second step, rearomatization is possible by hydrogenolysis or hydrogenation. Hydrogenolysis can happen by the elimination of the aliphatic fraction (dehydroboration) or the aromatic group (deorganoboration) leading to cleavage. As an alternative route, hydrogenation can occur by reversible hydroboration of aromatic π-bonds followed by B-C hydrogenolysis. It is noteworthy that while during hydrogenolysis the borane specie is a reactant, during hydrogenation it is a catalyst. It could lead to an increased hydrogenation ratio over hydrogenolysis which can result in an increased aliphatic group formation in the final product. This finding is consistent with our quantitative H^1-NMR measurements.

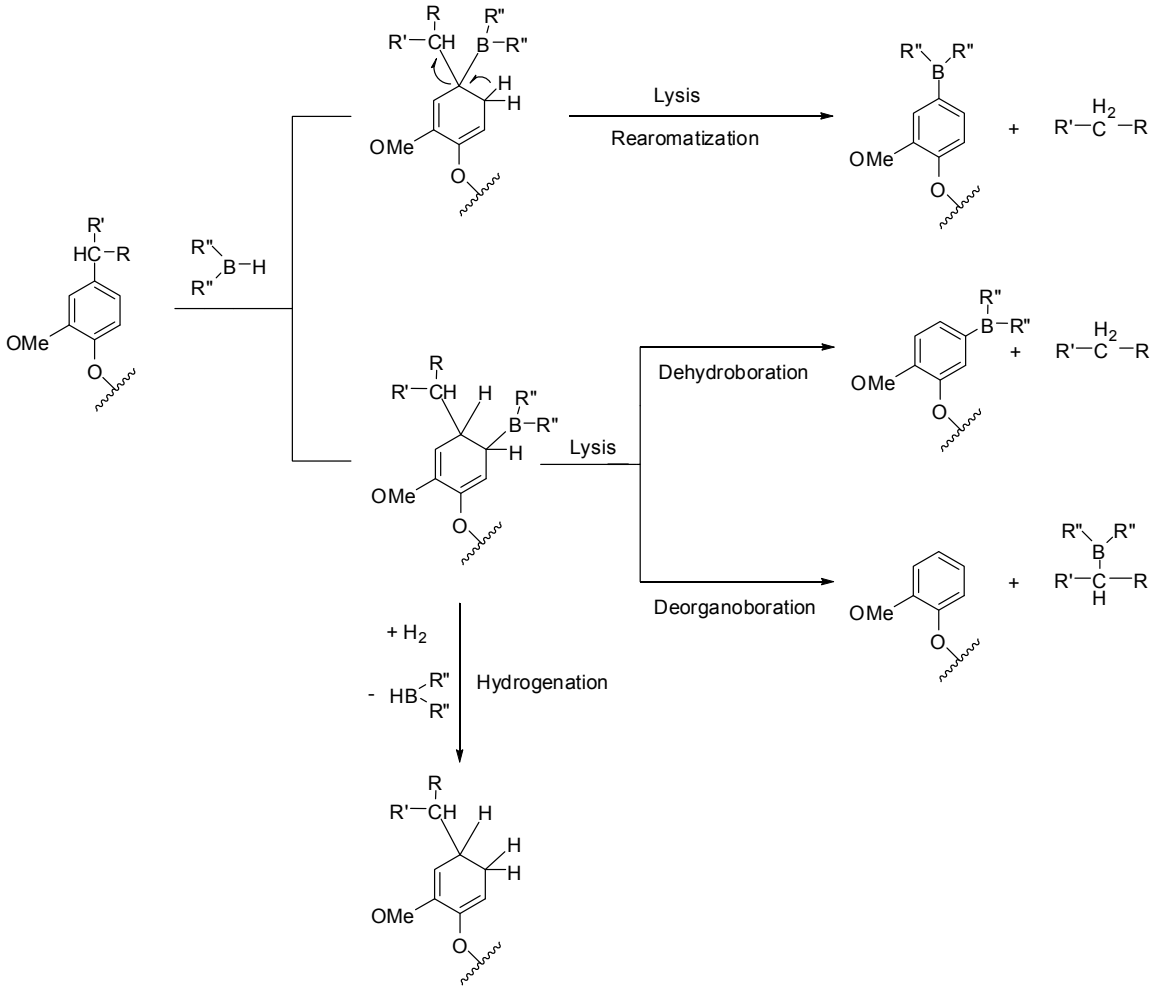

Equation 12. The proposed mechanism for softwood ethanol organosolv lignin hydrogenation and hydrogenolysis catalyzed by organoboranes.
(R, R': Aliphatic or aryl group, R": H or OEt)

5.3.5 Quantitative Analytical Tool to Follow Hydrogenation and Hydrogenolysis

The hydrogenolytic cleavage of an interlinking aryl-O-aryl and aryl-O-aliphatic linkage increases the hydroxyl group content of the final product. The hydrogenation of the aromatic ring decreases the phenol concentration and elevates the concentration of aliphatic hydroxyl groups. Selective phosphitylation of the hydroxyl groups on the lignin polymer with TMDP, followed by quantitative ^{31}P-NMR measurements provided a reliable means of monitoring these changes (Equation 13, Figure 50, Table 39).[231]

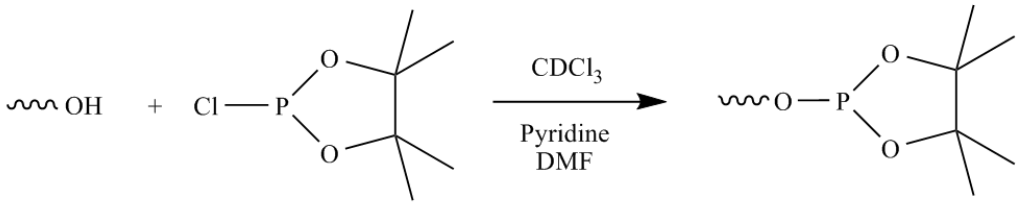

Equation 13. Phosphitylation of a free hydroxyl group on the lignin polymer with 2-chloro-4,4,5,5-tetramethyl-1,3,2-dioxaphospholane.

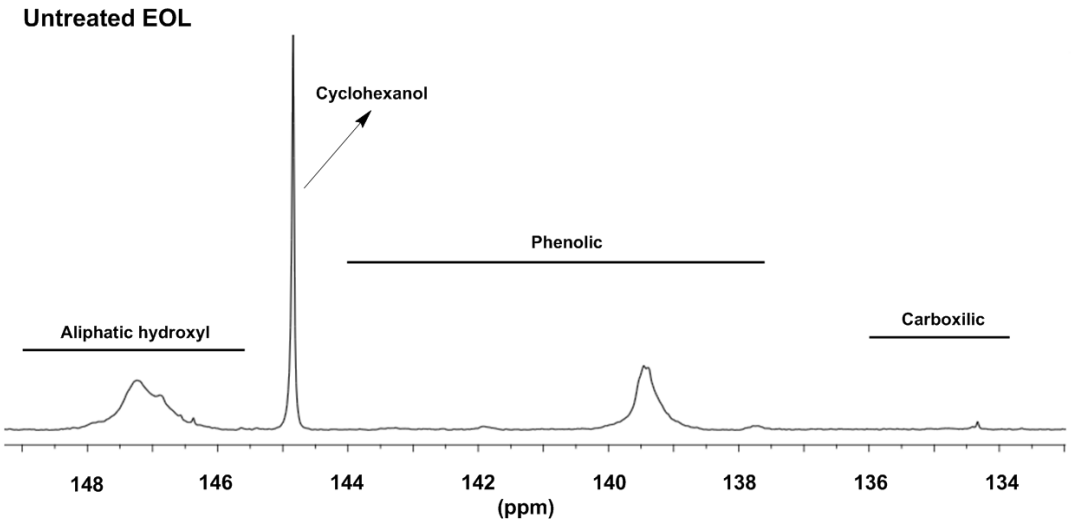

Figure 50. Qualitative ^{31}P-NMR of the soluble fraction of the untreated softwood ethanol organosolv lignin (EOL) after derivatized with 2-chloro-4,4,5,5-tetramethyl-1,3,2-dioxaphospholane.

Table 39. Hydroxyl content of the soluble fraction of the untreated softwood ethanol organosolv lignin (EOL), the blank run and after hydrogenation with different catalysts at 175°C for 20 hours as determined by quantitative ^{31}P-NMR after derivatized with 2-chloro-4,4,5,5-tetramethyl-1,3,2-dioxaphospholane.

Used catalyst	Total –OH content (μmol mg^{-1})	Hydroxyl content of selected groups		
		Aliphatic hydroxyl	Total phenolic	Carboxylic hydroxyl
	(149.0-133.8) ppm[a]	(149.0-145.6) ppm[a]	(144.4-137.6) ppm[a]	(136.0-133.8) ppm[a]
EOL	4.80	1.00[b]	1.05	0.00
Blank	4.66	0.87	1.12	0.00
Raney-Ni	5.14	1.21	1.12	0.00
Pt/C	5.05	1.01	1.14	0.00
$NaBH_4/I_2$	5.33	1.08	0.81	0.38

[a] Granata and Argyropoulos. [Ref. 231]
[b] EOL aliphatic hydroxyl value is used as reference for hydroxyl content of selected groups.

The results of ^{31}P-NMR analysis of the starting and treated SW EOL indicated that the hydrogenolysis was accompanied by a 5-11% increase in total hydroxyl group content for the treated SW EOL. Furthermore, the greatest increase in hydroxyl group content was observed to be due aliphatic hydroxyl groups except when $NaBH_4/I_2$ was employed, where carboxylic acid hydroxyl groups were detected in agreement with the results of ^{1}H-NMR. However, the increase of the aliphatic hydroxyl group content could be the result of either a cleavage of an aryl-O-aliphatic group, or the hydrogenation of a phenolic ring. While both hydrogenation and hydrogenolysis can affect the absolute value of the aliphatic hydroxyl content, the observed increase in the overall hydroxyl content on the treated SW EOL is a clear indication of hydrogenolysis. Thus, based on the elevated concentration of the total phenolic and aliphatic hydroxyl groups, we suggest that hydrogenolytic cleavage of the aryl-O-aryl and aryl-O-aliphatic linkages occurred.

5.4 Conclusion

Selective hydrogenolysis could provide an economically feasible route to convert lignin from a low grade fuel to potential fuel precursors or other value added chemicals by decreasing the carbon chain length, while increasing the H/C ratio and lowering the O/C ratio. We propose that the lower temperature limit for a high yield hydrogenation is determined by the chosen lignin's glass transition temperature. The upper temperature limit is determined by the stability of the catalyst and the charring of the biopolymer at higher temperatures. In general, homogeneous catalysts provided higher yields, but they were difficult to separate from the final products and have stability problems at elevated temperatures. The opposite is true for heterogenous catalysts. The highest hydrogenation yields were obtained with $NaBH_4/I_2$, Raney-Ni, $RuCl_2(PPh_3)_3$ or Pt/C. Our data shows that each catalyst has different hydrogenative selectivity towards aryl-O-aryl and aryl-O-aliphatic linkages over carbon-carbon double bonds, and hydrogenation simultaneously happened with hydrogenolysis.

CHAPTER 6

6. QUANTITATIVE ANALYSIS OF PARTIALLY SUBSTITUTED BIODIESEL GLYCEROLS [4]

6.1 Introduction

The interest and development of biofuels has grown exponentially over the last few years in response to the need to develop sustainable energy resources and address climate change.[296,297] Currently, bioethanol and biodiesel are the most successful fossil fuel supplements. The absolute annual biodiesel potential of the US is estimated to be 3.2 billion gallons.[298] The current biodiesel production capacity in the US is 400 million gallons which is projected to double within the next two years.[299,300] Although this is less than the current bioethanol production, recent research efforts in algae-oil production could significantly change this outlook.[301] Biodiesel production involves the transesterification of triglycerides from vegetable and algae oils or animal fats yielding glycerol and the corresponding alkyl fatty ester as summarized in Figure 51.

[4] This manuscript was published in [Journal of Biobased Material and Bioenergy, 2009, 3(1), 108-111] Reproduced by the permission of Dr. H.S. Nalwa, JBMBE. It is entitled as "Quantitative NMR analysis of partially substituted biodiesel glycerols". The other authors are Arthur J. Ragauskas from School of Chemistry and Biochemistry at the Georgia Institute of Technology, Thomas Dyer from the Institute of Paper Science and Technology at the Georgia Institute of Technology and Teresa L. Alleman from the National Renewable Energy Laboratory, CO, USA.

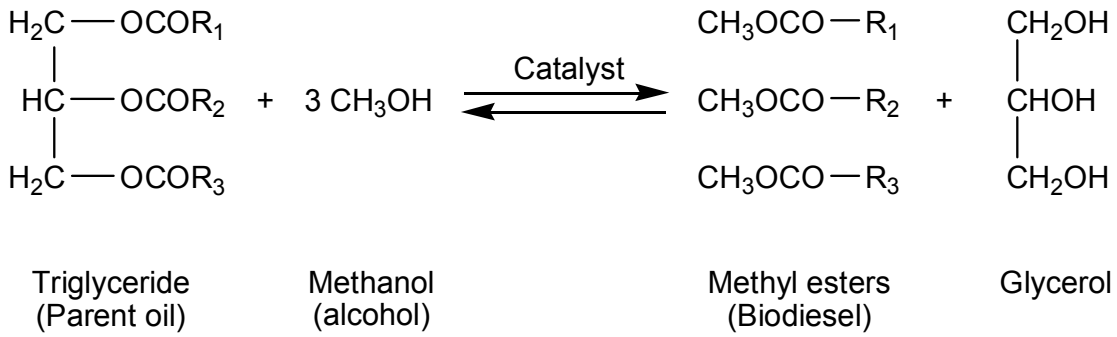

Figure 51. Transesterification reaction for biodiesel production, $R_{1\text{-}3}$ are hydrocarbon groups.

The transesterified ester typically has excellent diesel-like properties and research efforts are ongoing to develop new chemical applications for glycerol as the conventional applications have been unable to fully utilize the world growth in glycerol.[302,303] Although a wide variety of alcohols can be used for the transesterification reaction to influence the properties of the final biodiesel product, the most frequently employed alcohol is methanol.[304]

About 90% of the biodiesel produced in the US is based on soybean oil as the raw material.[305] The efficiency of the production steps and the quality of the product is monitored by measuring the concentration of free, mono and disubstituted glycerols, methanol and free fatty acids. For these constituents the currently used analytical methods are primarily chromatographic; high pressure liquid chromatography (HPLC), [306] gas chromatography (GC),[307] spectroscopic; mass spectroscopy (MS), [308] near infrared spectroscopy (NIRS),[309] and wet chemical techniques (potentiometric, iodometric titration)[310] which are often time consuming typically due to sample preparation, extended analysis time and/or complicated data analysis. Because of these limitations

there is a clear need for a rapid and accurate quantitative analysis technique for biodiesel constituents.

The yield of the transesterification step and the quality of the final product can be determined by measuring the free hydroxyl groups in the reaction mixture. In lignin chemistry, phosphytilation of hydroxyl groups with 2-chloro-4,4,5,5-tetramethyl-1,3,2-dioxaphospholane (TMDP) followed by ^{31}P-NMR analysis has become a powerful technique to characterize the chemical nature of carboxylates, phenoxy and aliphatic hydroxyl groups.[311,312,313,314] Employing this technique, partially substituted glycerol samples (i.e., see Figure 52) and biodiesel samples were phosphitylated with TMDP and analyzed.

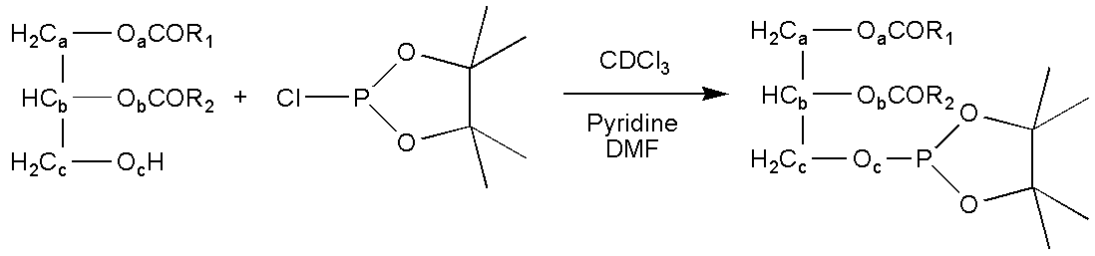

Figure 52. Phosphitylation of 1,2-diacylglycerol with 2-chloro-4,4,5,5-tetramethyl-1,3,2-dioxaphospholane at c-position. $R_{1,2}$ are hydrocarbon groups.

6.2 Experimental Section

6.2.1 Materials

Commercial biodiesel samples received from the National Renewable Energy Laboratory (Golden, CO, USA), all precursors and reagents were purchased from Sigma-Aldrich (St. Louis, MO, USA) and used as received.

6.2.2 Sample Preparation and Phosphitylation

Sample preparation and phosphitylation is described in Chapter 3. (3.3.3.1.2 Reaction Mixture Preparation and Phosphitylation with TMDP)

6.2.3 NMR Measurements on Biodiesel Precursors and Commercial Samples

The NMR pulse program used for chemical shift assignment and for commercial biodiesel samples is depicted in Chapter 3. (3.4.2.1 Quantitative ^{31}P-NMR Characterization for Preliminary Experiments) The method for chemical shift assignment is depicted in Chapter 3. (3.3.3.2.1 NMR Chemical Shift Assignment)

6.3 Results and Discussion

6.3.1 Initial ^{31}P-NMR Chemical Shift Database of Biodiesel Precursors

To establish a database of ^{31}P-NMR chemical shift information on relevant biodiesel precursors, a series of representative pure samples were acquired treated with TMDP and analyzed by ^{31}P-NMR. The results of this analysis are summarized in Table 40.

Table 40. Chemical shift assignments for ^{31}P-NMR spectrum of biodiesel standards after phosphitylation of free hydroxyl groups with 2-chloro-4,4,5,5-tetramethyl-1,3,2-dioxaphospholane.

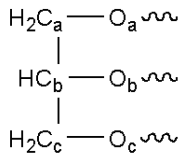	δ ^{31}P-NMR (ppm)*	Designated phosphitylated position
Glycerol derivatives		
Mono-substituted		
1-Monopalmitoleoyl-rac-glycerol**	146.2	O-b
	147.6	O-c
1-Octanoyl-rac-glycerol	146.2	O-b
	147.4	O-c
2-Oleoylglycerol	147.8	O-a & O-c
Di-substituted		
1,2- Dioleoylglycerol	147.7	O-c
1,3- Dioleoylglycerol	146.4	O-b
Tri-substituted/ transesterified		
Glyceryl trioleate	-----	-----
Fatty acids		
Saturated		
Hexanoic acid**	134.3	O-a
Palmitic acid	134.4	O-a
Stearic acid	134.4	O-a
Unsaturated		
Oleic acid	134.4	O-a
Linoleic acid	134.3	O-a
Linolenic acid	134.3	O-a
Biodiesel production by-products		
Free Glycerol**	147.1	O-a & O-c
	146.1	O-b
Methanol	147.9	O-a

* All samples were referenced to an internal standard of cyclohexanol at δ 144.9 ppm.
** Quantitative accuracy measured.

When the spectrum was recorded on the fully substituted glyceryl trioleate which has no free hydroxyl group no signal has been detected. This result ensures that the TMDP reagent only reacts with free hydroxyl groups and no side reaction occurs under our reaction conditions.

Di-substituted glycerol derivatives have only one free hydroxyl group which yields only one ^{31}P-NMR signal after phosphitylation. A phosphitylated terminal glyceride hydroxyl group; O_c yields a signal at δ 147.8 whereas a secondary; O_b hydroxyl derivative provides ^{31}P-NMR absorption at δ 146.4.

In the case of the mono-substituted glycerol derivatives and free glycerol, phosphitylation can occur on two or three hydroxyl groups depending on the degree of substitution. By integrating the spectra recorded on the symmetrical compound; free glycerol, the difference in the chemical shift of terminal hydroxyl groups and the secondary hydroxyl group could be measured. With the chemical shift differences in hand, the signals for phosphitylated primary and secondary hydroxyl groups in case of the mono-substituted glycerol derivatives were assigned.

Typically, a terminal hydroxyl group treated with TMDP yielded a signal from δ 147.0-147.8 whereas a secondary hydroxyl group yielded a signal from δ 146.1-146.4 in the ^{31}P-NMR spectrum.

Another key component to industrial sources of biodiesel is the presence of free fatty acids. As summarized in Table 40, several fatty acids were derivatized and analyzed by ^{31}P-NMR. These results suggest that for the fatty acids studied the length of the hydrocarbon chain or the degree of unsaturation has little or no effect on the chemical shifts.

A common biodiesel production line utilizes a downstream alcohol recovery and biodiesel purification step.[315] However those processes are not 100% efficient thus the final product always has contamination from the alcohol used for the catalytic transesterification of the parent oil. Soybean oil is a mixture of C16 and C18 fatty-acid substituted glycerols. The phosphitylated fatty acids and mono-substituted standards in Table 40 shows, that differences between chain lengths of the substituting fatty acid had little or no effect on the chemical shift measured in case of the substituted compounds studied. Thus the method can be used to selectively measure the differences between different substitution levels.

6.3.2 Quantitative TMDP/ ^{31}P–NMR Analysis of Commercial Biodiesel Samples

With cyclohexanol used as an internal standard, the quantitative accuracy of the TMDP/ ^{31}P–NMR technique was calculated in case of mono-phosphitylated carboxylic-acid group, di- and tri-phosphitylated hydroxyl groups. The accuracy of all quantitative measurements were within 95+%.

The main step during biodiesel production is the catalytic transesterification of triglycerides. By selectively measuring the amount of glycerol with different substitution levels, the yield of this step and the quality of the final biodeiesel can be determined.

The phosphitylation/NMR analysis method has been tested on original biodiesel samples processed from soybean oil (Figure 53). The quantitative data have been compared with conventional analytical methods as summarized in Table 41.

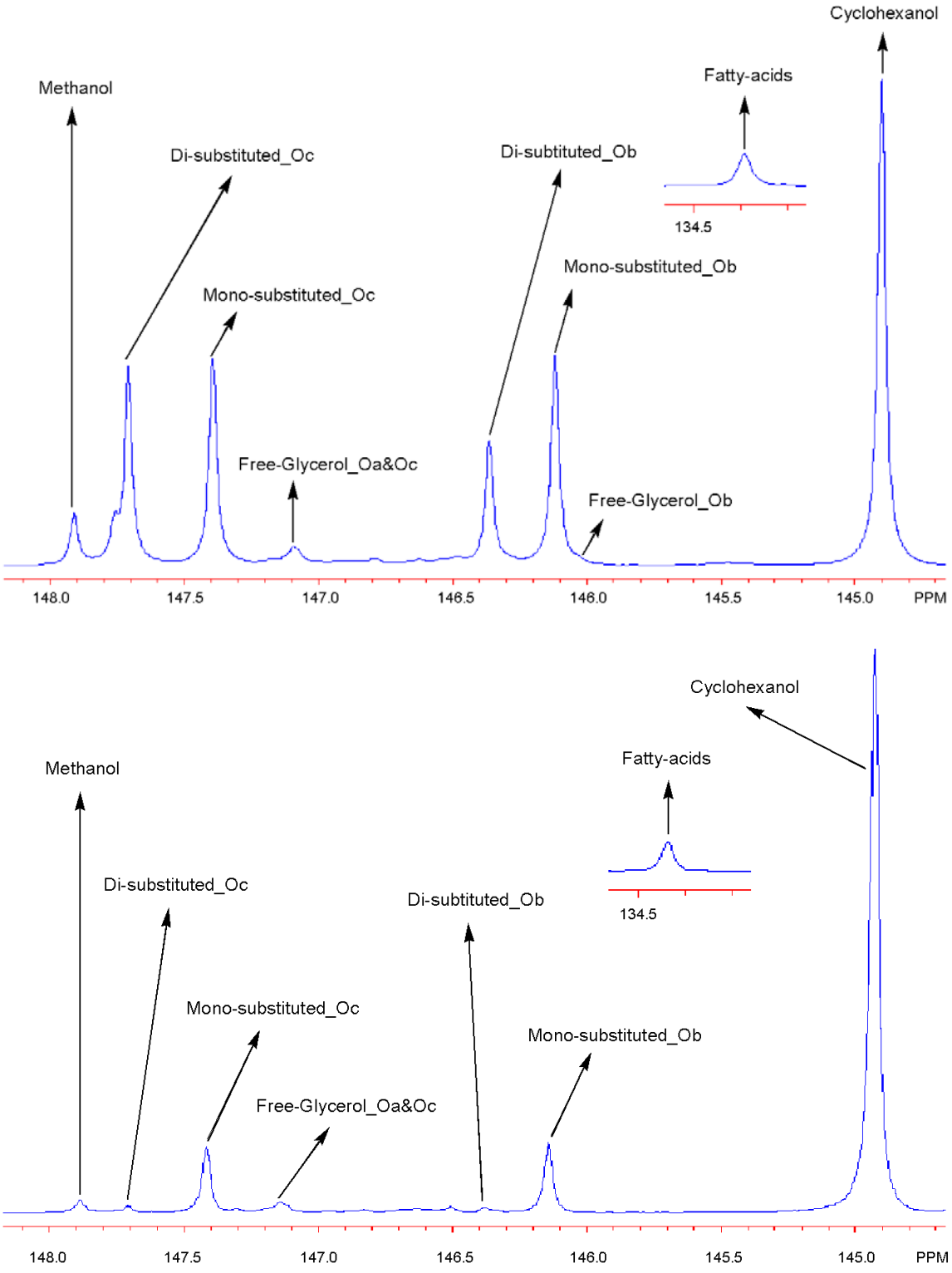

Figure 53. Quantitative ^{31}P-NMR spectra of two commercial biodiesel sample produced from soybean oil with cyclohexanol as an internal standard, derivatized with 2-chloro-4,4,5,5-tetramethyl-1,3,2-dioxaphospholane.

With cyclohexanol used as an internal standard, the concentration of various biodiesel constituents can be readily calculated and the results of this analysis are summarized in Table 41.

Table 41. Measured data of various biodiesel constituents with conventional techniques and with phosphitylation with subsequent ^{31}P-NMR for biodiesel sample.

Component	Conventional technique used	Data Measured	Phosphitylation with ^{31}P-NMR
Free Glycerol	Chromatographic (LC/GC)* (weight %)	0.01	0.03
Mono Glycerol	Chromatographic (LC/GC)* (weight %)	1.4	1.8
Di Glycerol	Chromatographic (LC/GC)* (weight %)	1.7	1.9
Tri Glycerol	Chromatographic (LC/GC)* (weight %)	0.3	---
Fatty acids	Potentiometric titration (mgKOH/g)**	0.3	0.3
Methanol	Chromatographic (LC/GC) (weight %)*	---	0.04

* Following analytical method: Ref. 4.
** Following analytical method: Ref: 5.

The TMDP/ ^{31}P–NMR technique has the capability to become a qualitative method for biodiesel analysis of partially hydrolyzed triglycerides yielding valuable data which currently can require up to three different methods at this moment.

6.4 Conclusions

Within the conventional techniques used, chromatographic methods usually are preferred over wet chemical methods which are often time consuming as they can require complex sample preparation. While many individual compounds can be separated with chromatographic techniques, even with one of the most up to date silyl-derivatized GC method reported, often some overlap in elution time occurs in complex mixtures.[4]

On the other hand the TMDP/ ^{31}P–NMR technique provides a rapid and accurate quantitative method. Since the spectroscopic information is related to the structure of the compound and the phosphitylating agent employed, it provides a spectra with good separation even in case of a complex sample, becoming a novel research tool for the characterization of biodiesel and its processing components.

CHAPTER 7

7. QUANTITATIVE ^{31}P-NMR ANALYSIS OF COMMERCIAL BIODIESEL GLYCEROL[5]

7.1 Introduction

The challenges of energy sustainability and climate change have to begun to impact scientific research, social policy and business practices. Although bioethanol represents the predominant first generation biofuel, biodiesel continues to garner regional support and in the U.S. it represents approximately 6.5% of the biofuels market. [316] Despite this limited market share, biodiesel has several strong attributes which suggests that its usage will continue to grow in the future. Attractive properties of biodiesel include ease of incorporation into existing fuels distribution systems, ready utilization in modern diesel combustion engines, growing demand and favourable exhaust emission profiles.[85] Of course, these positive attributes need to be balanced against the limited global production of plant oils and animal renderings needed to propel growth in this industry. One of the most promising next generation of technologies that may address current production limitations is the development of algae energy farms for the efficient production triglycerides for biodiesel. [317] Regardless of source, the conversion of triglycerides to biodiesel involves a transesterification step as shown in Figure 54.

[5] This manuscript was published in [FUEL, 2009, 88(9), 1793-1797] Reproduced by the admission of the Copyright Clearance Center's Rightslink. It is entitled as "Phosphitylation and Quantitative ^{31}P-NMR Analysis of Partially Substituted Biodiesel Glycerols". The other authors are Arthur J. Ragauskas from School of Chemistry and Biochemistry at the Georgia Institute of Technology, and Cherie J. Ziemer and Brial J. Kerr from the ARS-USDA.

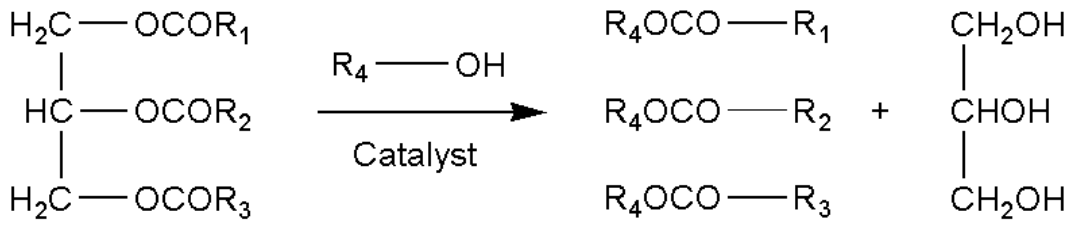

Figure 54. Transesterification reaction for biodiesel production $R_{1\text{-}4}$ are hydrocarbon groups.

The transesterification step is required to impart favourable fuels properties as direct use of plant oils with conventional diesel engines has been reported to result in coking and trumpet formation on the fuel injectors, carbon deposits, gelling of lubricating engine oil and incomplete combustion. [318] Transesterification of triglycerides, as shown in Figure 54, has been shown to mitigate these problems yielding a valuable renewable biofuel resource. Many alcohols have been used in this reaction and influence final biodiesel properties the most common employed commercially used alcohol is methanol. [319,320] Although commonly manufactured from natural gas, in the future gasification of biomass could yield a bio-based source of methanol. [321] A host of catalysts and conditions have been used to accomplish this reaction including assorted acids, bases, enzymes and physical treatments. [322,323] Along with these chemical and biochemical developments a constant need exists for new and improved analytical techniques to monitor the quality of incoming feedstocks and their respective conversion products. Current analytical methods include HPLC [324], GC [325], spectroscopic (i.e., MS [326], NIR [327]) and wet chemical techniques (i.e., potentiometric, iodometric titration) [328] which are often time consuming typically due to sample preparation, extended analysis time and/or complicated data analysis.

Chapter 6 describes, a novel approach to characterizing mixtures of multi-substituted glycerol's which involves an initial phosphitylation of hydroxyl groups of substituted glycerol with 2-chloro-4,4,5,5-tetramethyl-1,3,2-dioxaphospholane (TMDP) followed by ^{31}P-NMR analysis. [329] These initial studies were conducted primarily with analytical pure compounds to establish a data base of chemical shifts and demonstration of the applicability to a commercial biodiesel sample. This study examines the application of this methodology to a broad spectrum of glycerol samples from commercial operations and to evaluate the applicability of alternative phospitylation agent 2-chloro-1,3,2-dioxaphospholane (DOP).

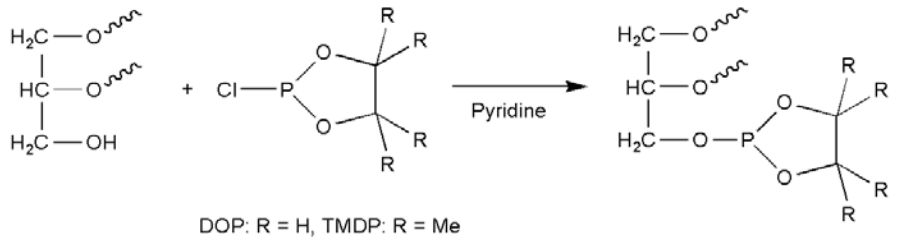

Figure 55. Phosphitylation of partially substituted glycerols with 2-chloro-1,3,2-dioxaphospholane (DOP) or with 2-chloro-4,4,5,5-tetramethyl-1,3,2-dioxaphospholane (TMDP).

7.2 Experimental Section

7.2.1 Materials

Commercial glycerol and biodiesel samples received from the Agricultural Research Service, United States Department of Agriculture (Ames, IA, USA), all precursors and reagents were purchased from Sigma-Aldrich (St. Louis, MO, USA) and used as received.

7.2.2 Sample Preparation and Phosphitylation

Sample preparation and phosphitylation with DOP is described in Chapter 3. (3.3.3.1.1 Reaction Mixture Preparation and Phosphitylation with DOP) Sample preparation and phosphitylation with TMDP is described in Chapter 3. (3.3.3.1.2 Reaction Mixture Preparation and Phosphitylation with TMDP)

7.2.3 NMR Measurements on Biodiesel Precursors and Commercial Glycerol and Biodiesel Samples

The NMR pulse program used for chemical shift assignment and for commercial glycerol samples is depicted in Chapter 3. (3.4.2.1 Quantitative ^{31}P-NMR Characterization for Preliminary Experiments) The method for chemical shift assignment is depicted in Chapter 3. (3.3.3.2.1 NMR Chemical Shift Assignment)

7.3 Results and Discussion

7.3.1 DOP vs TMDP

The efficient conversion of trigylcerides to glycerol and alkyl esters is predicated on complete conversion and separation of biodiesel for glycerol. The optimization of this reaction requires analysis of the amounts of glycerol, alcohol, mono and disubstituted glycerols present in the product mixture. The potential ability to characterize hydroxyl groups of glycerol-related compounds was assessed using DOP and TMDP as the phosphitylating agent.

a/

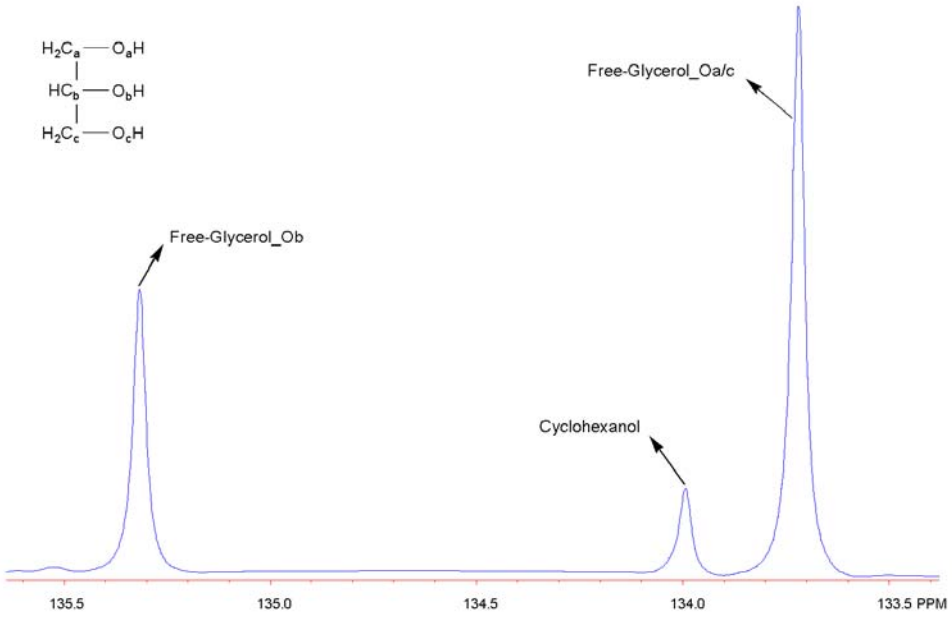

b/

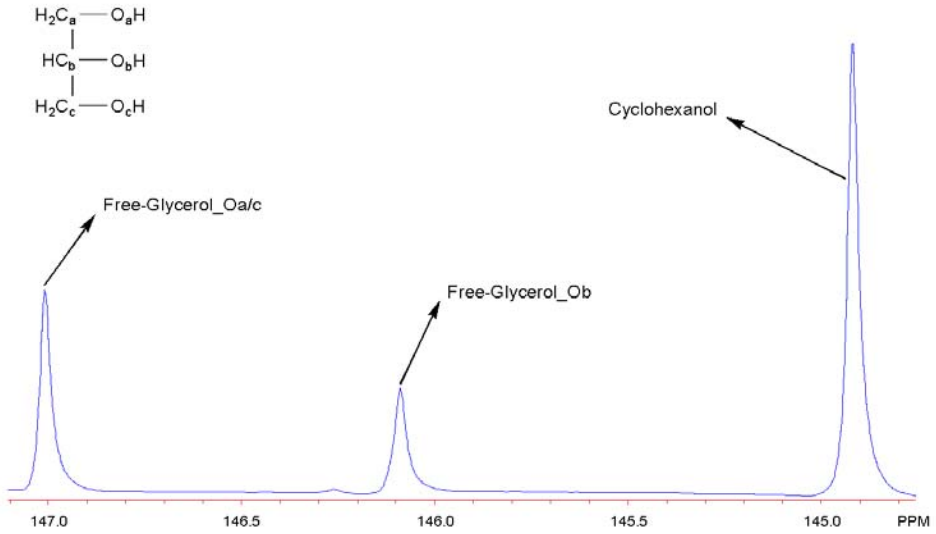

Figure 56. ^{31}P-NMR of glycerol derivatized with (a) 2-chloro-1,3,2-dioxaphospholane and with (b) 2-chloro-4,4,5,5-tetramethyl-1,3,2-dioxaphospholane.

a/

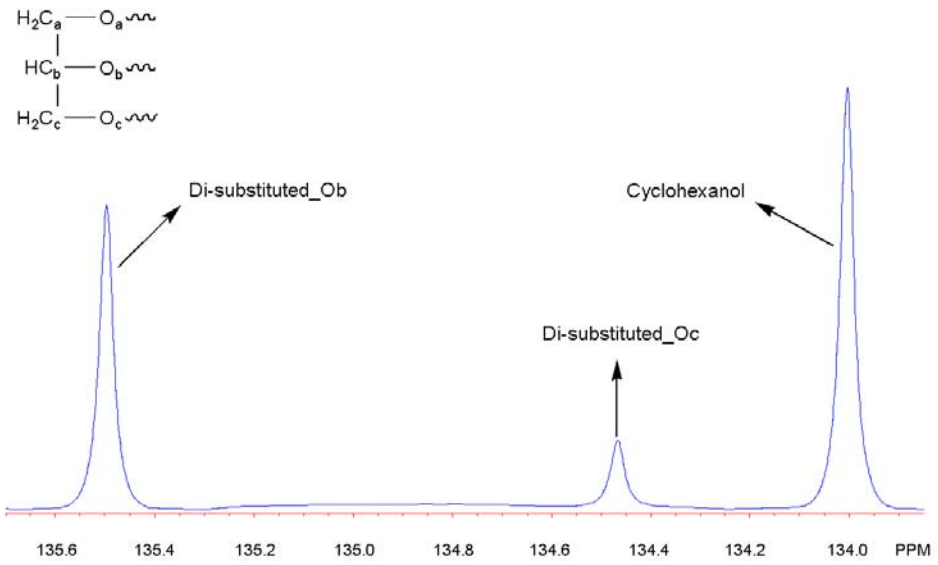

b/

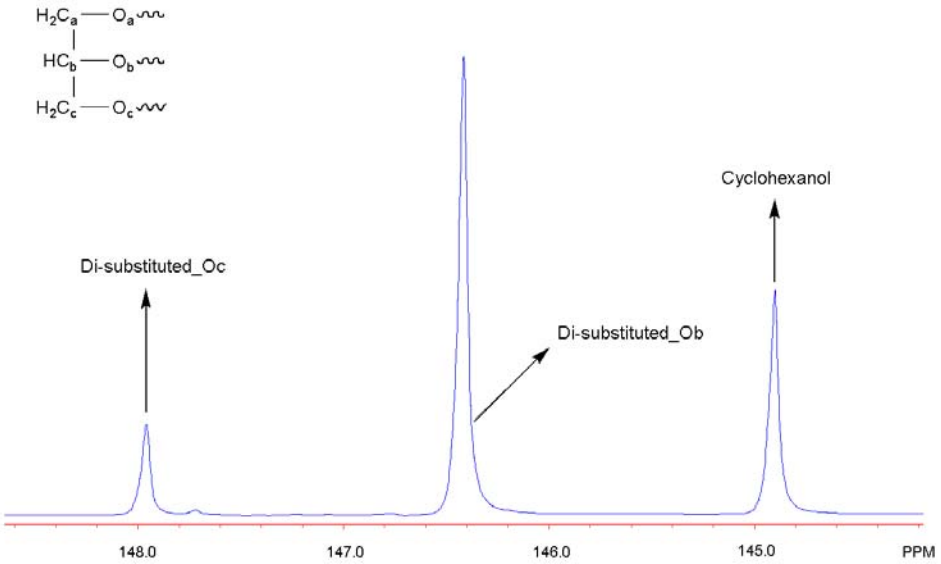

Figure 57. ^{31}P-NMR of ~85% 1,3-Dioleoylglycerol and ~15% 1,2-Dioleoylglycerol mixture derivatized with (a) 2-chloro-1,3,2-dioxaphospholane and with (b) 2-chloro-4,4,5,5-tetramethyl-1,3,2-dioxaphospholane.

Figure 56 and Figure 57 summarizes the ^{31}P-NMR spectra for derivatized glycerol and for a mixture of ~85% 1,3-dioleoylglycerol and ~15% 1,2-dioleoylglycerol. These results suggest that TMDP provides greater spectral resolution of the individual hydroxyl groups of glycerol-derivatives and hence is the reagent of interest for additional studies.

7.3.2 Extended ^{31}P-NMR Chemical Shift Database of Biodiesel Precursors

Table 42. ^{31}P-NMR chemical shifts for partially substituted glycerols, fatty acids, alcohols and glycerol after phosphitylated with 2-chloro-4,4,5,5-tetramethyl-1,3,2-dioxaphospholane.

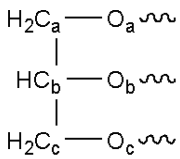	δ ^{31}P-NMR (ppm)*	Designated phosphitylated position
Glycerol derivatives		
Mono-substituted		
1-Mono-substituted C_{16}-C_{18} **	146.2-146.3	O-b
	147.6-147.8	O-c
2- Mono-substituted C_{16}-C_{18}	147.8-147.9	O-a/c
Di-substituted		
1,2- Dioleoylglycerol **	147.7	O-c
1,3- Dioleoylglycerol **	146.4	O-b
Tri-substituted/ transesterified		
Glyceryl trioleate	-----	-----
Fatty acids		
Saturated		
C_6-C_{18} **	134.3-134.4	
Mono- and Di-unsaturated		
C_{18}	134.3-134.4	
Biodiesel production by-products		
Free glycerol **	147.1	O-a/c
	146.1	O-b
Methanol **	147.9	
Ethanol	146.3	
Isopropanol	146.4	

* All samples were referenced to an internal standard of cyclohexanol at δ 144.9 ppm.
** Quantitative accuracy measured

As summarized in Table 42, ^{31}P-NMR analysis of glycerol, mono and disubstituted glycerols treated with TMDP provides characteristic chemical shifts that can be readily assigned to specific substitution patterns. The standard deviation, sensitivity and quantitative accuracy were determined from five separate measurements using a solvent mixture containing analytically pure 99+% biodiesel precursors and cyclohexanol as an internal standard. The sensitivity of the TMDP/^{31}P–NMR technique was calculated to be 2.1 nmol/ml with a 1.9 μmol/ml lower limit of detection. The error margin of the technique was measured to be ±1.1%.

TMDP procedure only reacts with free hydroxyl groups and no side reaction occurs under the reaction conditions employed.[328] The spectroscopic information is related to the structure of the compound and the phosphitylating agent employed.[330] If the amount of the sample is known, by integrating the spectra and using an internal standard the amount of the biodiesel processing components can be calculated.[331] Figure 58 demonstrates the characterization of a mixture of common constituents during biodiesel production, utilizing cyclohexanol as an internal standard to facilitate quantification.

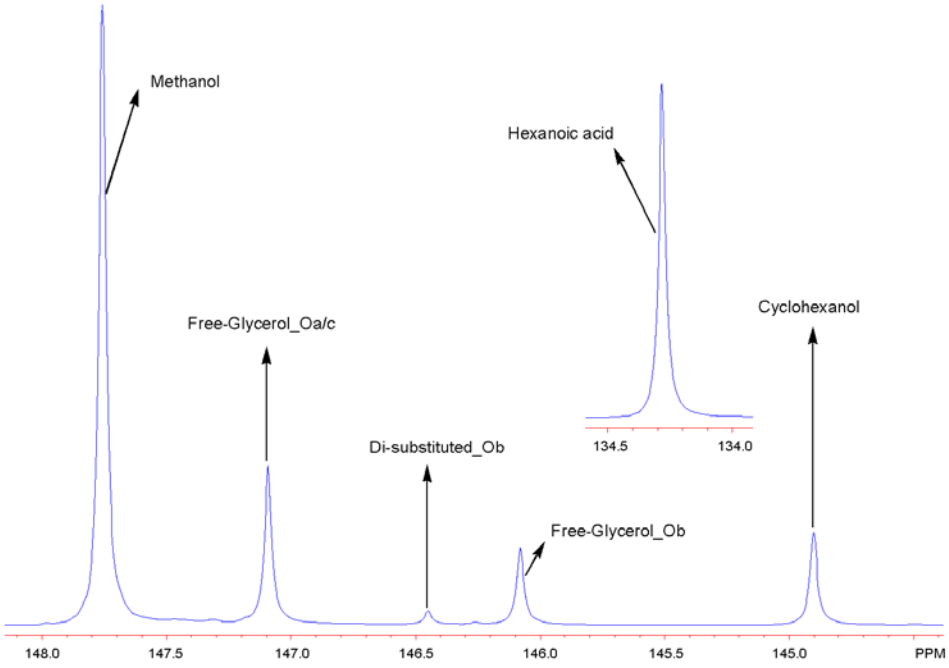

Figure 58. Analysis of solvent mixture consisting of methanol:glycerol:1,3-dioleoylglycerol:hexanoic-acid in 3:1:1:5 ratio, phosphylited with 2-chloro-4,4,5,5-tetramethyl-1,3,2-dioxaphospholane using cyclohexanol as internal standard.

7.3.2 Quantitative TMDP/ ^{31}P–NMR Analysis of Commercial Glycerol Samples

Following this same procedure a series of commercial glycerol samples acquired from biodiesel operations using different feedstock were phosphitylated and analyzed by ^{31}P-NMR. The qualitative results of this analysis are summarized in Figure 59. The quantitative data have been compared with conventional analytical methods on commercial glycerol sample produced from tallow and summarized in Table 43.

a/

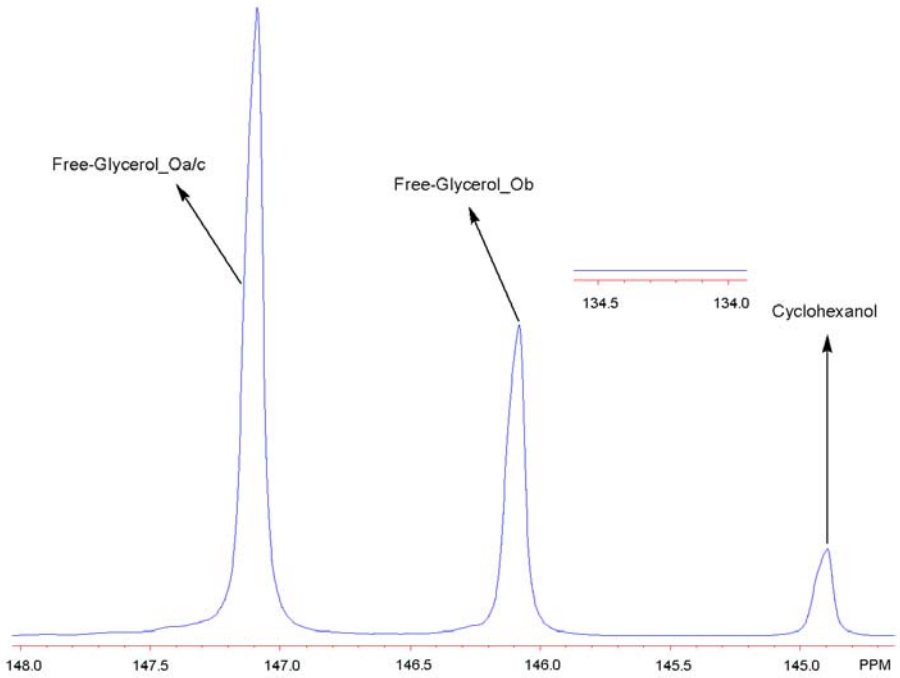

b/

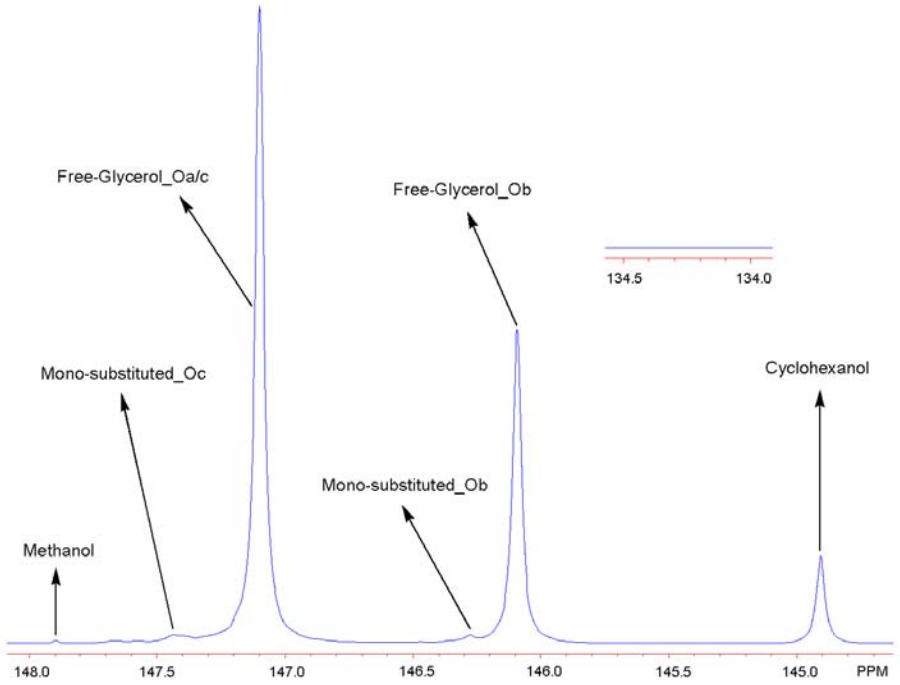

Figure 59. Quantitative ^{31}P-NMR spectra of glycerol samples from commercial biodiesel operations phosphylited with 2-chloro-4,4,5,5-tetramethyl-1,3,2-dioxaphospholane using cyclohexanol as internal standard based on (a) soy oil, (b) tallow, (c) restaurant grease and (d) poultry fat.

c/

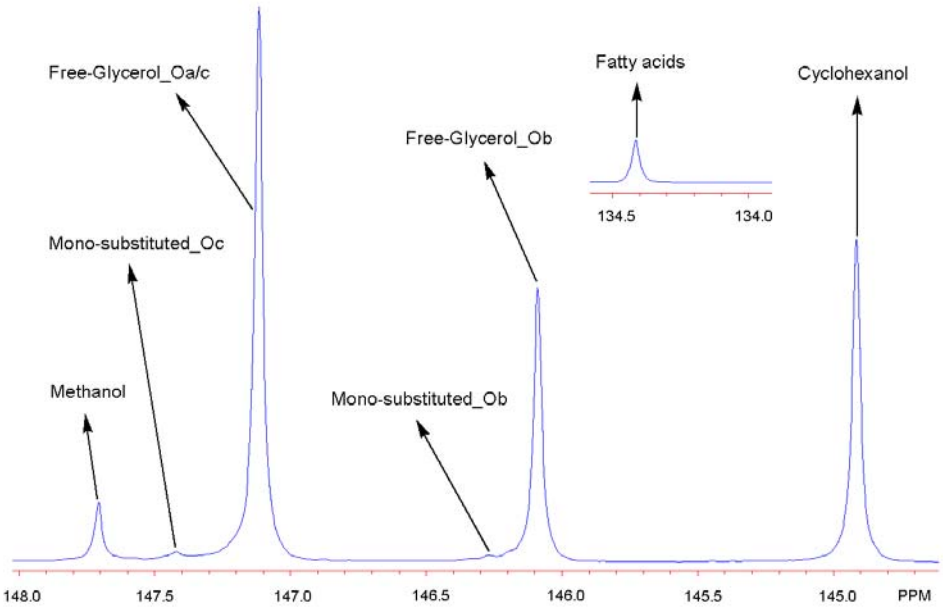

d/

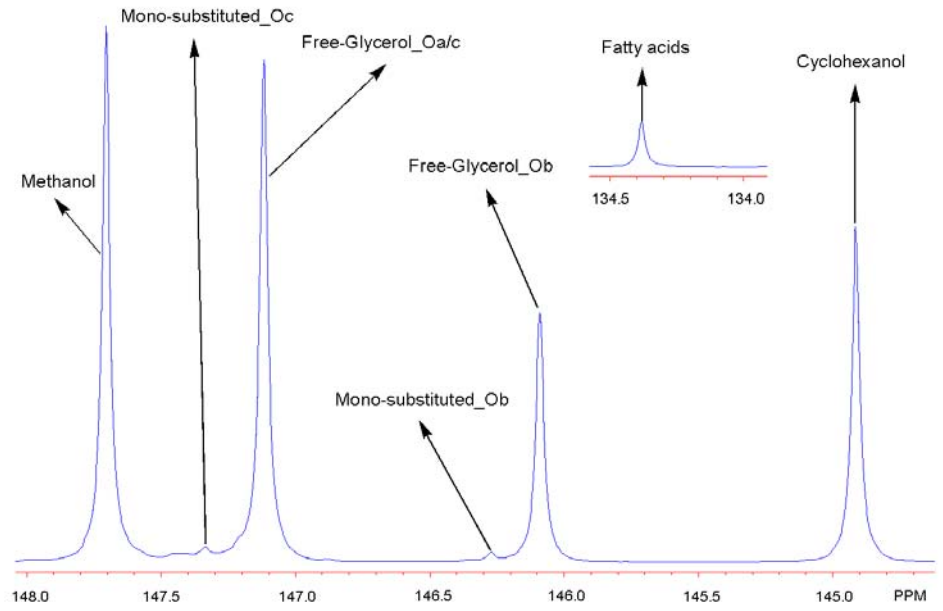

Figure 59. Quantitative ^{31}P-NMR spectra of glycerol samples from commercial biodiesel operations phosphylited with 2-chloro-4,4,5,5-tetramethyl-1,3,2-dioxaphospholane using cyclohexanol as internal standard based on (a) soy oil, (b) tallow, (c) restaurant grease and (d) poultry fat.

Table 43. Measured data of various constituents with conventional technique [332] and with phosphitylation with 2-chloro-4,4,5,5-tetramethyl-1,3,2-dioxaphospholane using cyclohexanol as internal standard and subsequent ^{31}P-NMR on commercial glycerol sample produced from tallow.

Component	Technique used	
	Conventional (weight %)	TMDP / ^{31}P-NMR (weight %)
Free glycerol	---	75.9
Mono substituted glycerol	---	7.7
Total glycerol	81.9	83.6
Fatty acids	0.0	0.0
Methanol	0.1	0.1

In addition, the fatty acid ester product must meet specifications to carry the designation "biodiesel fuel" set by the latest American (ASTM D 6751-08) and European (DIN EN 14214) standards.[333] Elevated glycerin values in the biodiesel are indicators of incomplete esterification reactions and predictors of excessive carbon deposits in the engine, while elevated acid number can lead to corrosion and may be a symptom of water in the fuel. [334] In America the limit for total glycerin concentration is 0.24 wt%, for acid number 0.80 mg KOH/g. In Europe the limit for total glycerin concentration is 0.25 wt%, for acid number 0.50 mg KOH/g. Following our procedure, commercial biodiesel samples can be rapidly analyzed for alcohol, free fatty acids and the presence of glycerol derivates containments as shown in Figure 60.

a/

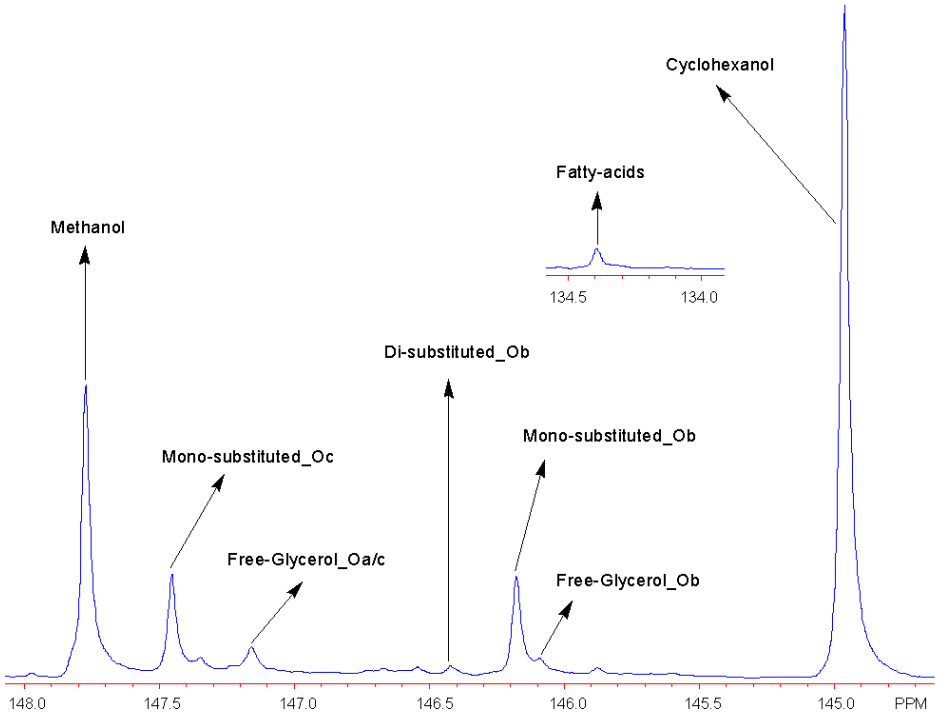

b/

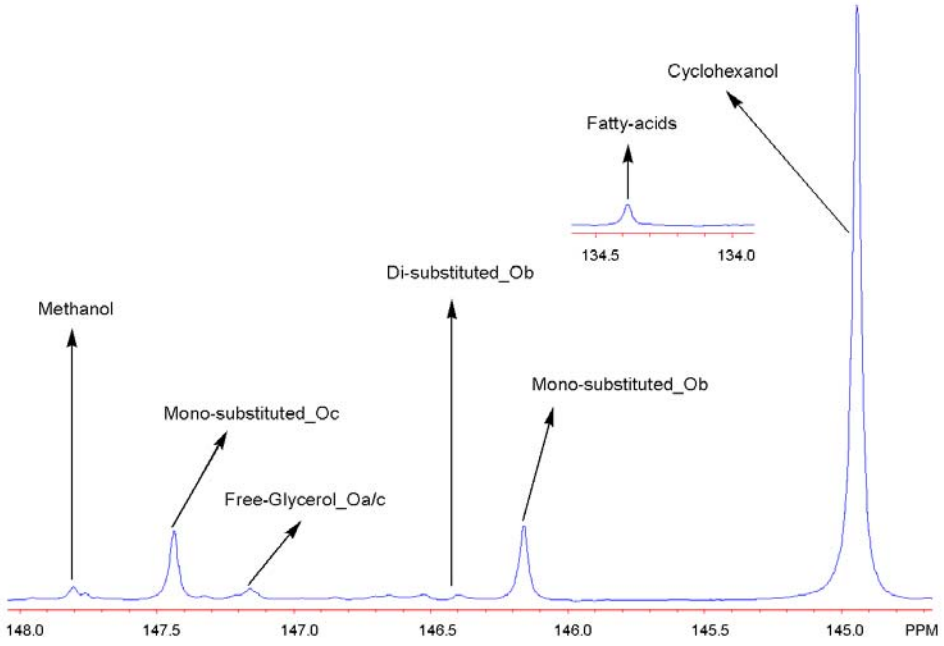

Figure 60. Quantitative ^{31}P-NMR spectra of two commercial biodiesel samples produced from soybean oil, using cyclohexanol as an internal standard, derivatized with with 2-chloro-4,4,5,5-tetramethyl-1,3,2-dioxaphospholane.

7.4 Conclusions

TMPD is shown to be a better phosphitylating agent than DOP for the characterization of biodiesel and its processing components. It provides a spectrum with a good separation and high quantitative accuracy even in case of a complex sample. The yield of the transesterification step and the quality of the final product can be determined by measuring the free hydroxyl groups in the reaction mixture. The TMDP/^{31}P–NMR technique provides a rapid and accurate quantitative method, becoming a novel research tool for the biodiesel industry. The novel solvent mixture used in this study is capable of handling samples with high hydroxyl content e.g. pure glycerol sample, therefore the technique can be used for samples throughout the whole production line, from the parent oil up to the biodiesel and glycerol streams. The above mentioned study, where the novel TMDP/^{31}P–NMR method is tested on samples throughout the whole production line in a rapid manner is described in Chapter 8.

CHAPTER 8

8. OPTIMIZATION AND INDUSTRIAL TRIAL OF THE NOVEL TMDP/^{31}P-NMR METHOD [6]

8.1 Introduction

The method widely used to produce biodiesel is transterification which involves triglycerides from vegetable oils or animal fats and an alcohol in the presence of a catalyst. The reaction yields mono-alkyl esters of the fatty acids with excellent diesel like properties and glycerol as a by-product.[335] However a common biodiesel production line utilizes a down-stream alcohol recovery and biodiesel purification step, the final product can be contaminated with partially substituted glycerols, glycerol, free fatty acids, residual alcohol and catalyst.[336] These by-products of the biodiesel production are considered contaminants and they alter the physical-chemical properties of the final product and can create engine problems such as engine deposits, corrosion and failure.[337]

The efficiency of the process steps utilized during the biodiesel production and the quality of the final products can be monitored by measuring the concentration of these contaminants. Currently, primary analytical methods involve chromatography (HPLC, GC),[338,339] spectroscopy (MS, NIR)[340,341] and wet chemical techniques (potentiometric, iodometric titration)[342] which are often time consuming due to sample preparation, extended analysis time and/or complicated data analysis. Because of these limitations

[6] This manuscript was accepted for publication in the Journal of Physical Chemistry A It is entitled as "A Rapid Quantitative Analytical Tool for Characterizing the Preparation of Biodiesel". The other authors are Arthur J. Ragauskas and Marcus Foston from School of Chemistry and Biochemistry at the Georgia Institute of Technology.

there is a clear need for a rapid and accurate quantitative analysis technique for biodiesel constituents.

Nucleic magnetic resonance (NMR) analysis when applied to phosphitylated hydroxyl groups has been shown to be a rapid quantitative analytical tool to characterize alcohols, phenols and carboxylic acid groups. Accordingly, our laboratory has been focused on developing ^{31}P-NMR methods for the quantitative characterization of biodiesel process samples using 2-chloro-4,4,5,5-tetramethyl-1,3,2-dioxaphospholane (TMDP) as a phosphitylating agent. (Figure 61) Since the spectroscopic information is related to the structure of the compound and the phosphitylating agent employed, it provides a spectra with good separation and high accuracy even in case of complex mixtures.[343] This work has been described in Chapter 6 and Chapter 7, while the TMDP/^{31}P–NMR technique has been tested for quantifying biodiesel processing components such as; alcohols, partially substituted glycerols and free fatty acids from final biodiesel and later from final glycerol samples.[344]

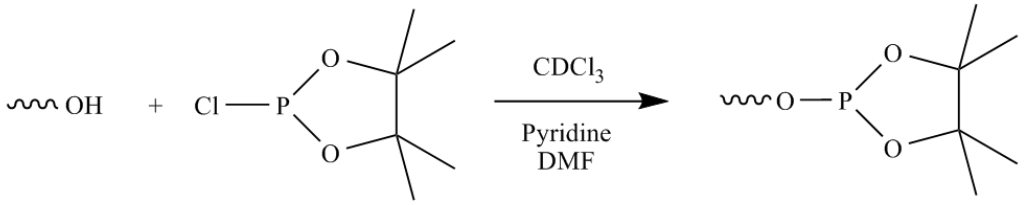

Figure 61. Phosphitylation of a free hydroxyl group with 2-chloro-4,4,5,5-tetramethyl-1,3,2-dioxaphospholane.

The present work describes our effort to fully develop this method to be able to provide quantitative information through the whole production line in a rapid manner, regardless of feedstock or process step employed. A comprehensive database of ^{31}P-NMR chemical shift information of relevant biodiesel precursors has been established with analytical pure compounds and the NMR pulse sequence has been optimized for industrial samples. The application of the optimized TMDP/^{31}P–NMR method was demonstrated on two series of industrial process samples utilizing first pure vegetable oil and later waste vegetable oil as feedstock.

8.2 Experimental Section

8.2.1 Materials

Commercial glycerol and biodiesel samples received from Piedmont Biofuels (Pittsboro, NC, USA) and BioDiesel International AG (Graz, Austria), all precursors and reagents were purchased from Sigma-Aldrich (St. Louis, MO, USA) and used as received.

8.2.2 Sample Preparation and Phosphitylation

Sample preparation and phosphitylation with TMDP is described in Chapter 3. (3.3.3.1.2 Reaction Mixture Preparation and Phosphitylation with TMDP)

8.2.3 NMR Method Optimization

The method for chemical shift assignment is depicted in Chapter 3. (3.3.3.2.1 NMR Chemical Shift Assignment) The protocol to determine the spin-lattice relaxation times is depicted in Chapter 3. (3.4.2.2 Spin-lattice Relaxation Time Measurement)

8.2.4 Optimized NMR Measurements on Biodiesel Precursors and Commercial Glycerol and Biodiesel Samples

The optimized method used for industrial biodiesel process samples is depicted in Chapter 3. (3.3.3.2.2 Optimized TMDP/^{31}P–NMR Method for Industrial Biodiesel Samples). The optimized NMR pulse program is depicted in Chapter 3. (3.4.2.3 Optimized Quantitative ^{31}P-NMR Characterization for Industrial Biodiesel Process Samples)

8.3 Results and Discussion

8.3.1 NMR Pulse Program Optimization

Phosphytilation of hydroxyl groups with TMDP followed by ^{31}P-NMR analysis has become a powerful technique in lignin chemistry to characterize the chemical nature of carboxylates, phenoxy and aliphatic hydroxyl groups.[345,346,347] During our initial studies in Chapter 6 and Chapter 7, the pulse delay and the number of acquisition acquired was selected based on our past experiences with lignocellulosics samples and not for biodiesel constituents.[348,349]

To develop a novel rapid analytical method it is essential to tailor the pulse program for biodiesel constituents and reduce the analysis time to a minimum. Using a paramagnetic relaxational agent such as ($Cr(acac)_3$) provides a reliable means to significantly reduce the pulse delay time when acquiring quantitative ^{31}P-NMR spectra of organic compounds.[328] To establish a database of phosphorous-31 spin lattice relaxation times on relevant biodiesel precursors, a series of representative pure samples were acquired treated with TMDP and analyzed by ^{31}P-NMR in the presence and in the absence of a relaxation agent. The results of this analysis are summarized in Table 44.

Table 44. Spin-lattice relaxation time of biodiesel precursors after phosphitylation of free hydroxyl groups with 2-chloro-4,4,5,5-tetramethyl-1,3,2-dioxaphospholane (TMDP) in the presence and in the absence of a relaxation agent.

Compound name	Relaxation time (ms)* With ($Cr(acac)_3$)	Relaxation time (ms)* Without ($Cr(acac)_3$)
Glycerol derivates C_{16}-C_{18} 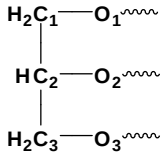		
1-Monosubstituted	701	1241
1,2-Disubstituted	617	1183
1,3-Disubstituted	584	1146
Fatty acids		
Saturated C_{16}	785	1298
Unsaturated C_{18}	797	1365
Biodiesel production by-products		
Free glycerol	629	1156
Methanol	912	1391
Analysis by-products		
Cyclohexanol (internal standard)	855	1347
TMDP	947	1422
TMDP hydrolyzate	745	1254

* Typical error average is determined from three consecutive measurements: ± 15 ms.

The maximum spin-lattice relaxation time (T_1) relaxation time belongs to unreacted TMDP, and in the presence of the relaxation agent its T_1 relaxation is approximately half that in the absence of ($Cr(acac)_3$). Our measured data on the effect of $Cr(acac)_3$ as a relaxation agent on spin-lattice relaxation times are consistent with previous data published by Argyropoulos.[350] Measurement shows that the biodiesel precursor with the longest relaxation time is methanol with T_1 of 912 ms. A quantitative NMR method has to obtain accurate signal areas after Fourier transform thus, a sufficiently long recycle delay or time between excitation pulses should be used to allow full relaxation of all the nuclei in the sample. Therefore, a T_1 of 912 ms requires a recycle delay time of at least 5 s allowing 99.3% of ^{31}P nuclei in the sample to fully relax, and satisfying conditions to obtain a quantitative spectra.[349] The NMR pulse program optimized for biodiesel constituents for a 400 MHz Bruker system at 25°C utilizes depicted in Chapter 3. (3.4.2.3 Optimized Quantitative ^{31}P-NMR Characterization for Industrial Biodiesel Process Samples)

The standard deviation, sensitivity and quantitative accuracy were determined from five separate measurements using a solvent mixture containing analytically pure 99+% biodiesel precursors and cyclohexanol as an internal standard. The results of this analysis are summarized in Table 45. The sensitivity of the TMDP/^{31}P–NMR technique remained at 1.9 μmol/mL lower limit of detection with an error margin of ±1.1%.[2] Due to the optimization of the acquisition program, compared to our initial studies the analysis time reduced from 50 min to 80 s.[84,328] All spectra acquired on the industrial samples in this article were recorded using the optimized NMR program parameters.

Table 45. Measured quantitative data of an analytically pure solvent mixture of various biodiesel constituents with phosphitylation using 2-chloro-4,4,5,5-tetramethyl-1,3,2-dioxaphospholane and cyclohexanol as internal standard, followed by ^{31}P-NMR using the optimized pulse program.

	Concentration (mmol/mL)	
Compound name	Solvent mixture	Detected*
Cyclohexanol	0.056	(internal standard)
1,2-Dioleoylglycerol	0.012	0.012±1
1,3- Dioleoylglycerol	0.002	0.002±1
Free glycerol	0.137	0.136±2
Hexanoic acid	0.399	0.395±4
Methanol	0.740	0.734±7

* Error averages are determined from five consecutive measurements.

8.3.2 Finalized ^{31}P-NMR Chemical Shift Database of Biodiesel Precursors

During transesterification the entering triglyceride reacts with an alcohol in the presence of an acid or base catalyst to yield the corresponding alkyl esters and glycerol. Currently the most widely used feed stocks for biodiesel production are pure vegetable oils, waste vegetable oils and animal fats. The composition and the fatty acid chain length in the entering parent oil and on the partially substituted glycerols and unreacted triacylglycerols after the transesterification step is dependent on the feedstock used.[351,352,353] To be able to develop an analytical method that can be applied through the whole production line for differing feedstock it is essential to establish a database of ^{31}P-NMR chemical shift information on relevant biodiesel intermediates, alcohol and by-products. A series of representative pure samples were acquired, treated with TMDP and analyzed by ^{31}P-NMR. The results of this analysis are summarized in Table 46.

Table 46. ^{31}P-NMR chemical shifts for partially substituted glycerols, fatty acids (a), and alcohols, glycerol, analysis by-products (b) after phosphitylated with 2-chloro-4,4,5,5-tetramethyl-1,3,2-dioxaphospholane (TMDP).

a 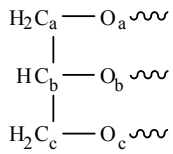	Glycerol derivatives					Fatty acid
	Mono-substituted		**Di-substituted**		**Tri-substituted**	
	a		**a,b**	**a,c**	**a,b,c**	
Phosphitylated hydroxyl	**O-b**	**O-c**	**O-c**	**O-b**	**N/A**	
Lipid chain						
Lauric	146.2	147.5	---	146.5	No signal	134.5
Myristic	146.2	147.5	---	146.4	No signal	134.5
Palmitic	146.2*	147.6*	147.9	146.4	No signal	134.4*
Stearic	146.2	147.4	147.9	146.4	No signal	134.4*
Oleic	146.1	147.4	147.7*	146.4*	No signal	134.4*
Linoleic	146.2	147.4	147.7	146.4	No signal	134.3*
Linolenic	---	---	---	---	---	134.3*
δ ^{31}P Signal (ppm) **	**146.1-146.2**	**147.4-147.6**	**147.7-147.9**	**146.4-146.5**	**No signal**	**134.3-134.5**

* Chemical shift data from [83,330].

** All samples were referenced to an internal standard of cyclohexanol at δ 144.9 ppm.

b	**δ ^{31}P Signal (ppm)**	**Phosphitylated hydroxyl**
Biodiesel production by-products		
Free glycerol	147.1*	O-a/c
	146.1*	O-b
Methanol	147.8	
Ethanol	146.3*	
Isopropanol	146.4*	
Analysis production by-products		
TMDP	174.7	
TMDP hydrolyzate	132.0	
Cyclohexanol (internal standard)	144.9*	

* Chemical shift data from [83,330].

When the spectrum was recorded on the fully substituted glyceryl trioleate which has no free hydroxyl group no signal has been detected. As anticipated, the phosphitylation reaction conditions used in this study reacts only with free hydroxyl groups and no side reaction occurs under the conditions employed. Di-substituted glycerol derivatives have only one free hydroxyl group which yields only one ^{31}P-NMR signal after phosphitylation. The phosphitylated terminal glyceride hydroxyl group O_c (see Table 46) yields a signal at δ 147.7-147.9 whereas a secondary O_b hydroxyl derivative provides a ^{31}P-NMR absorption at δ 146.4-146.5. Signals for primary and secondary hydroxyl groups in case of the 1-mono-substituted glycerol derivatives are found at δ 147.4-147.6 and δ 146.1-146.2 respectively.

Another key component in industrial sources of biodiesel is the presence of free fatty acids. The ^{31}P NMR analysis of several phosphitylated fatty acids are summarized in Table 46. These results indicate that the length of the hydrocarbon chain or the degree of unsaturation has little or no effect on the chemical shift, yielding a signal at δ 134.3-134.5. All chemical shifts recorded on relevant biodiesel precursors were consistent with data from our preliminary studies.[84,328]

8.3.3 Analysis of Industrial Process Samples

With a comprehensive database of ^{31}P-NMR chemical shift information in hand on relevant biodiesel precursors, the technique can be applied on process samples such as; parent oil (PO), after transesterification (AT), biodiesel before wash (BW), biodiesel after one wash (A1W), final biodiesel (FB), separated glycerol before neutralization (SG) and final demethylated glycerol (DG). The commercial sampling points to acquire the test samples are shown in Figure 62.

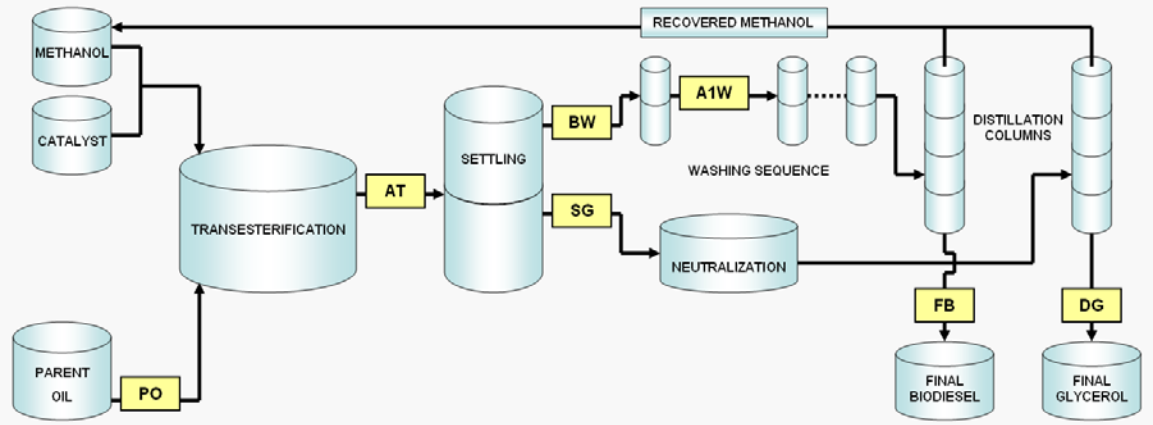

Note: Sampling points as; PO: parent oil, AT: after transesterification, BW: biodiesel before wash, A1W: biodiesel after one wash, FB: final biodiesel, SG: separated glycerol before neutralization, DG: final demethylated glycerol.

Figure 62. Sampling points used through the biodiesel production line.

Regardless of the feedstock, the conversion of triglycerides to biodiesel involves a transesterification step. Transesterification of the parent oil is the main step during biodiesel production and is required to impart favourable fuel properties. Direct use of plant oils with conventional diesel engines will result in coking and trumpet formation on the fuel injectors, gelling of lubricating engine oil, incomplete combustion and carbon deposits.[354] To be able to achieve a high conversion yield and a low contaminant level, it

is essential to have accurate information on the incoming feedstock and on the leaving product. High levels of by-product formation during the catalytic step will lead not just an underutilized feedstock due to the low conversion yields, but also to a highly contaminated stream entering the washing sequence. Figure 63 demonstrates the TMDP/^{31}P–NMR method on a series of commercial feedstock samples acquired from biodiesel operations.

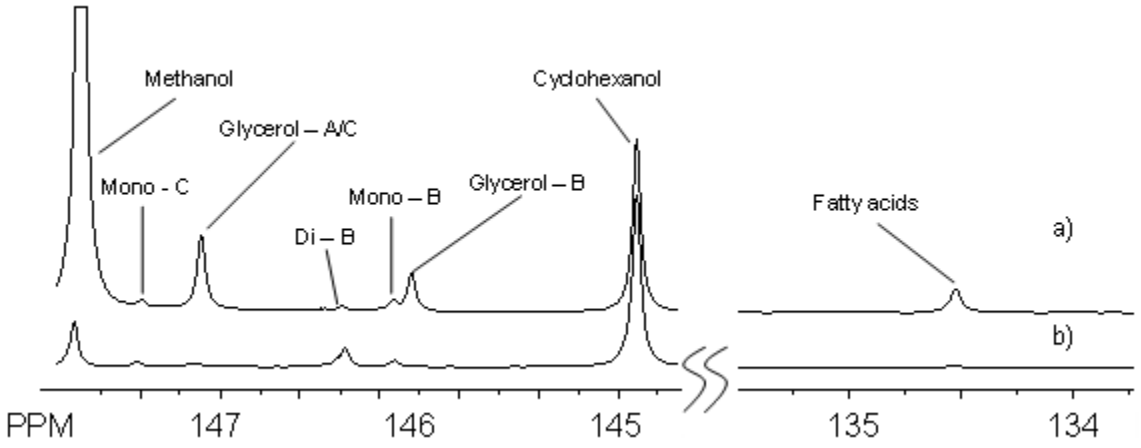

Figure 63. Quantitative ^{31}P-NMR spectra of parent oil samples of waste vegetable oil (a) and soybean oil (b) with cyclohexanol as an internal standard, derivatized with 2-chloro-4,4,5,5-tetramethyl-1,3,2-dioxaphospholane.

The yield of the transesterification step and the quality of the final product can be determined by measuring the free hydroxyl groups in the reaction mixture. The TMDP/^{31}P–NMR method can selectively follow the concentration of alcohol, free glycerol, partially hydrolyzed triglycerides and free fatty acids in a rapid manner from the entering feedstock to the leaving product, becoming a novel research tool for process optimization of the catalytic transesterification step. Results of utilizing different transesterification conditions on the same feedstock are shown in Figure 64.

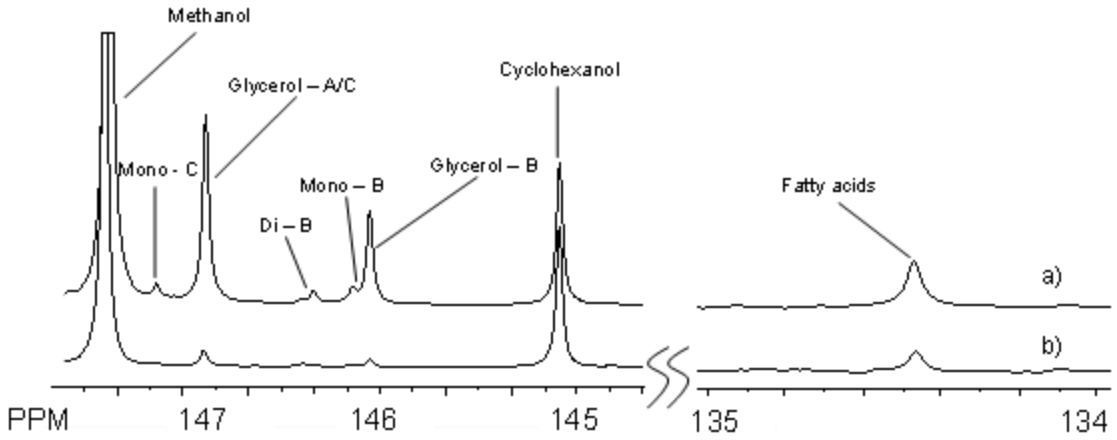

Figure 64. Quantitative ^{31}P-NMR spectra of samples taken after the transesterification step utilizing different process conditions using soybean oil as feedstock with cyclohexanol as an internal standard, derivatized with2-chloro-4,4,5,5-tetramethyl-1,3,2-dioxaphospholane.

Mono-alkyl esters and glycerin are the main products of the catalytic transesterification step. Glycerin is denser than the mono-alkyl esters and can be gravity-separated with the use of a settling vessel. After the glycerin is separated, the supernatant is washed with water to remove contaminants. The wash water is heavier than the mono-alkyl esters and during the washing sequence it absorbs contaminants such as: excess methanol, catalyst, soap, free and partial glycerols.[132] A common biodiesel production sequence utilizes several washing cycles to lower the concentration of process containments before the methanol recovery. By being able to selectively follow the level of contamination after each washing cycle, the washing efficiency can be calculated and the sequence can be optimized. Figure 65 demonstrates the TMDP/^{31}P–NMR method on samples taken entering the washing sequence and after one washing cycle.

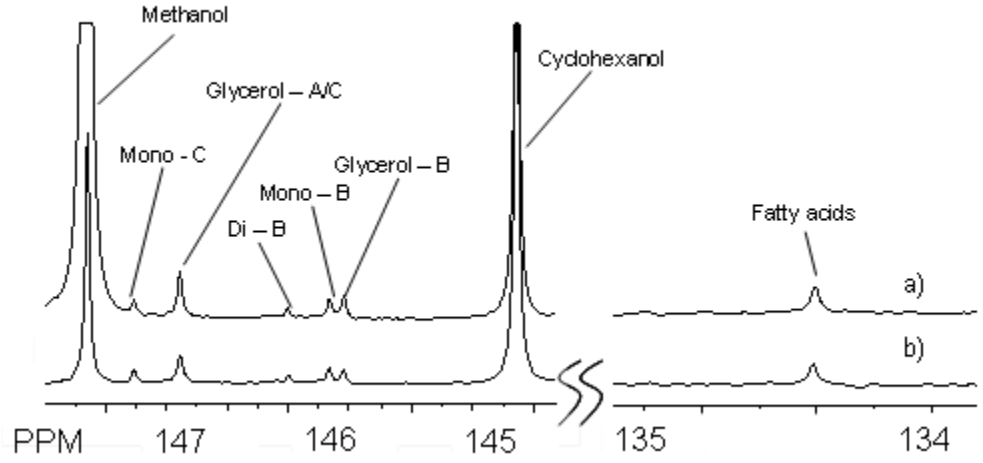

Figure 65. Quantitative ^{31}P-NMR spectra shows the washing efficiency of a soybean oil based commercial process on samples taken before wash (a) and after the first washing cycle (b) with cyclohexanol as an internal standard, derivatized with 2-chloro-4,4,5,5-tetramethyl-1,3,2-dioxaphospholane.

After the washing sequence, the mono-alkyl ester stream enters into a subsequent alcohol recovery stage, where the excess alcohol remaining is removed through distillation and recycled for reuse. After the washing sequence and the alcohol recovery, the purified product is the desired biodiesel. Quantitative ^{31}P-NMR spectra on commercial finished biodiesel samples utilizing different feed stocks are shown in Figure 66.

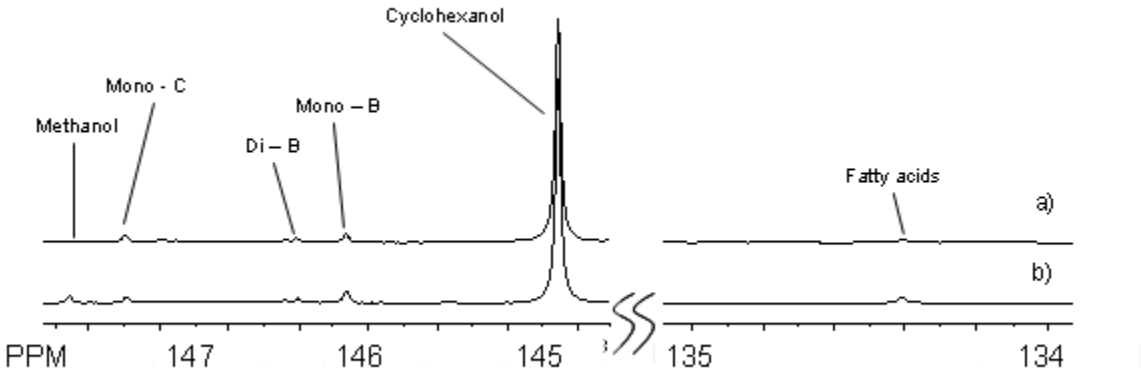

Figure 66. Quantitative ^{31}P-NMR spectra of final biodiesel samples from soybean oil (a) and waste vegetable oil (b) with cyclohexanol as an internal standard, derivatized with 2-chloro-4,4,5,5-tetramethyl-1,3,2-dioxaphospholane.

Quantitative ^{31}P-NMR spectra of final biodiesel samples show that different feedstock resulted in final biodiesel products with different compositions. To carry the designation "biodiesel fuel" the final purified fatty acid ester product must meet specifications set by the latest American (ASTM D 6751-08) and European (DIN EN 14214) standards.[355,356] To meet these standards, a common biodiesel production line utilizes downstream alcohol recovery and biodiesel purification steps to reach a low contamination level in the final product.[357] The optimized TMDP/^{31}P–NMR method has a 1.9 μmol/mL lower limit of detection that allows following the level of contamination through all purification steps. By selectively measuring the amount of alcohol, fatty acids and glycerols at different substitution levels, the yield of these process steps and the quality of the final biodiesel can be determined in a rapid manner.

After transesterification, the separated glycerin phase is contaminated with alcohol, unused catalyst, soaps, free and partial glycerols.[133] In a commercial process, the stream undergoes a subsequent neutralization step. If a base is used as catalyst during the transesterification step, the separated glycerin phase is neutralized with an acid. After neutralization, commercial crude glycerin is produced by removing the water and alcohol in a subsequent distillation step. The yield of each step can be followed by analyzing the composition of the entering and the product steams. Quantitative ^{31}P-NMR spectra on glycerol samples leaving the settling vessel before neutralization and after the distillation stage are shown in Figure 67.

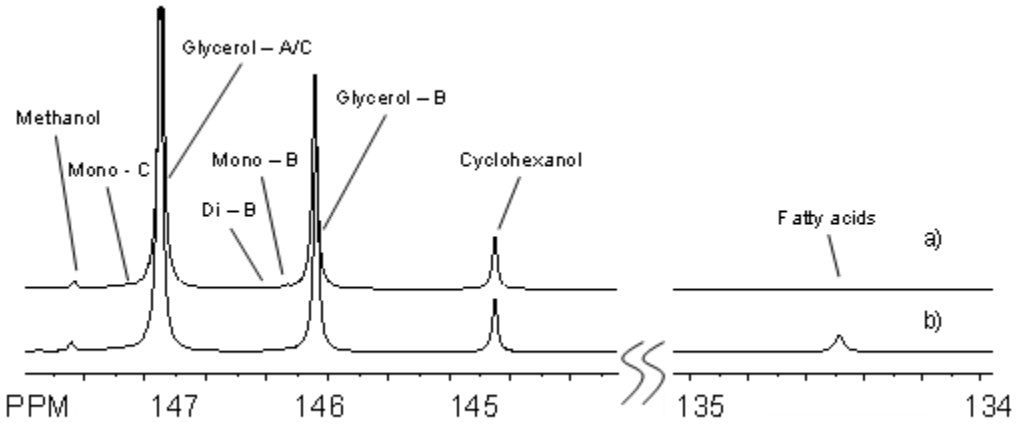

Figure 67. Quantitative ^{31}P-NMR spectra on glycerol samples from soybean oil based commercial process of the separated glycerol before neutralization (a) and of the final demethylated glycerol (b) with cyclohexanol as an internal standard, derivatized with 2-chloro-4,4,5,5-tetramethyl-1,3,2-dioxaphospholane.

For several industries such as; food, personal care, pharmaceutical and petrol, glycerol is utilized as a starting material or an additive, adding to the market value of this by-product and the economic of the transesterification process.[358] After the methanol recovery, the produced glycerol stream has a 80-88 wt% glycerin content and can be sold as a crude glycerin or can be further purified up to 98+ wt% to be sold as refined glycerol.[5] The refined glycerol has a higher market value and can be used directly or has a potential to be used as a starting material to convert it into other value added products such as; polyesters, nylons or valuable intermediates like propylene glycol or 1,3-propanediol by the chemical or the pharmaceutical industry.[26] To be able to sell and use the glycerol by-product as an additive or a starting material in a subsequent industrial process, it is essential to determine the composition and contamination levels during the purification steps and in the final glycerol product. Figure 67 shows that beside samples from the biodiesel streams, the solvent mixture used in this study is also capable handling samples from the glycerol streams, and the optimized TMDP/^{31}P–NMR method provides spectra with good separation regardless of the process step used.

8.4 Conclusions

A novel qualitative method has been developed for the determination of the various types of hydroxyl groups present in biodiesel production streams. The use of 2-chloro-4,4,5,5-tetramethyl-1,3,2-dioxaphospholane as a phosphitylation reagent for quantitative ^{31}P NMR analysis of the hydroxyl groups in biodiesel process samples has been fully developed. This experimental protocol allows for rapid analysis of biodiesel mixtures of alcohols, fatty acids, glycerol, mono, and disubstituted glycerides. Characteristic chemical shifts ranges were developed with model compounds and used to fully characterize the conversion triglyceride samples to biodiesel for two commercial production processes.

We have demonstrated that the TMDP/^{31}P–NMR technique has the capability to become a promising research tool for the biodiesel industry. This methodology provides quantitative data on the concentration of alcohol, free glycerol, partially hydrolyzed triglycerides and free fatty acids in a rapid manner, which currently can require up to three different methods.

Since the spectroscopic information acquired by the TMDP/^{31}P–NMR technique is related to the structure of the compound and the phosphitylating agent employed, it provides a spectra with good separation even in case of a complex sample, becoming a rapid and accurate quantitative method. Due to optimized sample preparation and signal acquisition used in this study, our TMDP/^{31}P–NMR method can handle samples through the whole production line regardless of process step or feedstock used, becoming a novel research tool for process step optimization and for the characterization of biodiesel and its processing components.

CHAPTER 9

9. OVERALL CONCLUSIONS

The original idea to develop new green technologies and products from future possible industrial lignin rich solutions while helping currently used commerce practices become green industrial practices were met at the first part of this thesis. First in Chapter 4 when LignoBoost technique was used in case of a commercial softwood kraft pulping liquor, it enabled lignin to be exported in the form of a solid biofuel and also gave the opportunity to transform it into materials of higher value. A novel high yield purification method has been developed yielding purified samples up to 97% lignin content, and later all products fractions were characterized. The chemical structure analysis of lignin in all process streams was determined. Under our reaction conditions the total hydroxyl content of phase F at pH 9.5 was 56% higher, while at pH 10.5 it was 45% higher than phase P that led to the higher solubility of the lignin biopolymer. A lower final pH resulted in a 69% enrichment of the total hydroxyl content in the F fraction while only a 35% increase in the P fraction, which resulted in a better lignin separation when lower pH was employed. These findings gave valuable insight on the fundamental chemistry during LignoBoost lignin precipitation from BL, while its known chemical structure and composition can help to optimize a subsequent controlled high yield pyrolysis for biooil production. Preliminary studies achieved pyrolysis oil yields up to 42.98 wt% with 24% decrease in the O/C ratio and 20% increase in the H/C ratio when compared to the purified LignoBoost lignin feedstock.

As a second step, it was shown in Chapter 5 that a selective hydrogenolysis could provide an economically feasible route to convert lignin from a low grade fuel to potential fuel precursors or other value added chemicals by decreasing the carbon chain length, while increasing the H/C ratio and lowering the O/C ratio. The development of hydrogenolysis conditions that effectively increase the solubility of lignin were initially examined with $Ru(Cl)_2(PPh_3)_3$ and demonstrated the ability to decrease the molecular weight and enhance the solubility of the lignin polymer. Later studies examined several heterogeneous and homogeneous hydrogenation catalysts at optimized reaction conditions resulting; 96.4% solubility with $Ru(Cl)_2(PPh_3)_3$, increase in H/C ratio with Raney-Ni, Pt/C and extensive monomer formation with $NaBH_4/I_2$. We proposed that the lower temperature limit for a high yield hydrogenation is determined by the chosen lignin's glass transition temperature, while the upper temperature limit is determined by the stability of the catalyst and the charring of the biopolymer at higher temperatures. In general, homogeneous catalysts provided higher yields, but they were difficult to separate from the final products and have stability problems at elevated temperatures. The opposite was true for heterogeneous catalysts. The highest hydrogenation yields were obtained with $NaBH_4/I_2$, Raney-Ni, $RuCl_2(PPh_3)_3$ or Pt/C. Our data showed that each catalyst has different hydrogenative selectivity towards aryl-O-aryl and aryl-O-aliphatic linkages over carbon-carbon double bonds, and hydrogenation simultaneously happened with hydrogenolysis.

In the second part of this thesis, the original idea to develop a novel analytical method that will provide quantitative information on biodiesel constituents through the whole biodiesel production line in a rapid manner, regardless of feedstock or process step

employed were met. In Chapter 6, it was demonstrated that the TMDP/^{31}P–NMR technique has the capability to become a promising research tool for the biodiesel industry. This methodology provides quantitative data on the concentration of alcohol, free glycerol, partially hydrolyzed triglycerides and free fatty acids in a rapid manner, which currently can require up to three different methods.

In Chapter 7, it was shown that since the spectroscopic information acquired by the TMDP/^{31}P–NMR technique is related to the structure of the compound and the phosphitylating agent employed, it provides a spectra with good separation even in case of a complex sample, becoming a rapid and accurate quantitative method. In Chapter 8, it was demonstrated that due to optimized sample preparation and signal acquisition, the TMDP/^{31}P–NMR method can handle samples through the whole commercial production line regardless of process step or feedstock used, becoming a novel research tool for process step optimization and for the characterization of biodiesel and its processing components.

CHAPTER 10

10. RECOMMENDATIONS FOR FUTURE WORK

10.1 Recommendations for the LigniBoost Project

With a known chemical structure and composition in hand, a subsequent controlled high yield catalytic conversion by pyrolysis could be optimized. In our preliminary studies, we utilized a rapid pyrolysis (2 min, 400 °C) and achieved bio-oil yields up to 43% while decreasing its O/C ratio by 24%. Some particularly attractive options to optimize reaction conditions for increased bio-oil yields are follows:

- Utilizing different heating profiles and resident times.
- Selectively sample light and heavy pyrolysis oils and determine their product distribution.
- A known product distribution and chemical structure could provide information on the fundamental chemistry, which could be utilized for optimization of the pyrolysis parameters.
- The chemistry during pyrolysis could be modified by the addition of selected metal catalysts for the production of additional value added final products.

10.2 Recommendations for the EOL Hydrogenolysis Project

Our data shows that each catalyst has different hydrogenative selectivity towards aryl-O-aryl and aryl-O-aliphatic linkages over carbon-carbon double bonds, and hydrogenation simultaneously happened with hydrogenolysis. Our approach was sufficient for an initial screening experimental series to search for possible candidates to convert lignin from a low grade fuel to potential fuel precursors or other value added chemicals. However to gain insight into the fundamental chemistry of selected catalyst systems, and being able to optimize the reaction conditions for a high hydrogenative selectivity towards aryl-O-aryl and aryl-O-aliphatic linkages over carbon-carbon double bonds, a new approach is needed. Such an approach and research data from preliminary test runs are depicted in Sections 10.2.1 – 10.2.3.

10.2.1 Designing the suitable model compound for softwood lignin

The lack of success to convert lignin into valuable fine chemicals relies on its highly complex structure and difficult separation of its native form. Lignin in its native state (protolignin) is a three dimensional amorphous polymer, which exact structure remains virtually unknown. Fortunately, through extensive research many of the main structural features of lignin have been worked out and the dominant linkages have been determined and are summarized in Table 47.[185]

Table 47. Proportions of different types of linkages connecting the phenylpropane units in softwood lignin.

Linkage type	Dimer structure	Approximate percentage
β-O-4	Phenylpropane β-aryl ether	45-50
α-O-4	Phenylpropane α -aryl ether	6-8
β-5	Phenylcoumaran	9-12
5-5	Bipheny; and Dibenzodioxocin	18-25
4-O-5	Diaryl ether	4-8
β-1	1,2-Diaryl propane	7-10
β-β	β-β-Linked structures	3

The β-Aryl ether structure is the dominant linkage in the native lignin structure. However during conventional kraft pulping the principal pathway of lignin depolymerization happens by the fragmentation of α and β-O-Aryl linkages, the (β-O-4) is still one of the dominant linkage in the residual black liquor (BL).[359] Since the β–Aryl-ether structure is the main interlinking unit both at the native state of lignin and in the BL, it was an obvious pick to design a model compound based on its structure for our hydrogenation studies.

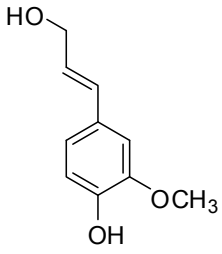

Conyferyl alcohol, the main building block of lignin in softwood

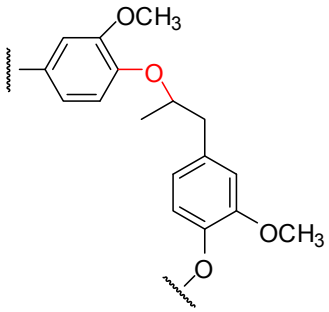

(β–O–4) linkage in lignin and BL

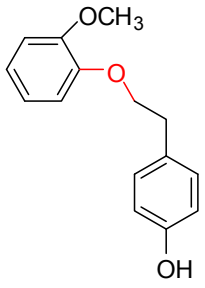

Model compound

Figure 68. The model compound *Phenol, 4-[2-(2-methoxyphenoxy)ethyl]*, designed to mimic the (β-*O*-4) linkage in the native lignin and in the black liquor.

10.2.2 Preparation and characterization of Phenol, 4-[2-(2-methoxyphenoxy)ethyl] "the model compound"

Our first attempt based on the conventional Williamson ether synthesis using 2-(4-hydroxyphenyl)ethyl-chloride and guaiacol-sodium salt. However despite the use of different protection groups and various solvents, the selectivity and yields were remained low (<10%). Phenol, 4-[2-(2-methoxyphenoxy)ethyl] was successfully synthesized with a different approach in three steps.

10.2.2.1 Preparation of 1-Tosyloxy-2-(4-tosyloxyphenyl)ethane

First step is the protection of the *2-(4-Hydroxyphenyl)ethanol* forming the protected tosylate ester *1-Tosyloxy-2-(4-tosyloxyphenyl)ethane*.

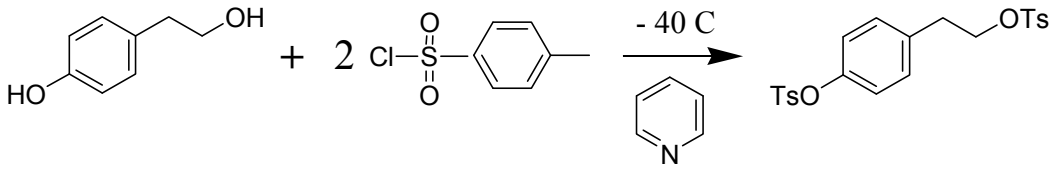

Equation 14. Protection by tosylation of the 2-(4-Hydroxyphenyl)ethanol forming the protected tosylate ester 1-Tosyloxy-2-(4-tosyloxyphenyl)ethane.

5,0 g of 2-(4-Hydroxyphenyl)ethanol (36,2 mmol) dissolved in 50 ml of pyridine and cooled to -40°C. 15,2 g p-toluenesulfonyl-chloride (79,6 mmol) in 100 ml of pyridine was added drop wise for the solution, under vigorous stirring. The vigorous stirring was maintained at -40°C for 2 h. The resultant mixture was placed in a freezer overnight and then poured into ice-water 400 ml. The tosylate was extracted with ether (3 X 250 ml).

The combined organic fraction was washed with ice-cold aqueous hydrochloric acid (50% by volume, 3 X 300 ml) and then with water (2 X 250 ml), dried over anhydrous magnesium sulphate, and finally the solvent removed by rotary evaporator. The residue was recrystallized from 10:3:2 ligroin (30-60):ether:dichloromethane. 1-Tosyloxy-2-(4-tosyloxyphenyl)ethane obtained in ~42% yield as white needle shape crystals.

^{1}H NMR ($CDCl_3$) δ 2,44 (s, 3H), 2,45 (s, 3H), 2,91 (t, 2H), 4,16 (t, 2H), 6,87 (d, 2H) 7,01 (d, 2H), 7,30 (m, 4H), 7,68 (m, 4H).

10.2.2.2 Preparation of 1-Tosyloxyphenyl-4-[2-(2-methoxyphenoxy)ethyl]

Second step is the synthesis of *1-Tosyloxyphenyl-4-[2-(2-methoxyphenoxy)ethyl]* from the protected tosylate ester with guaiacol.

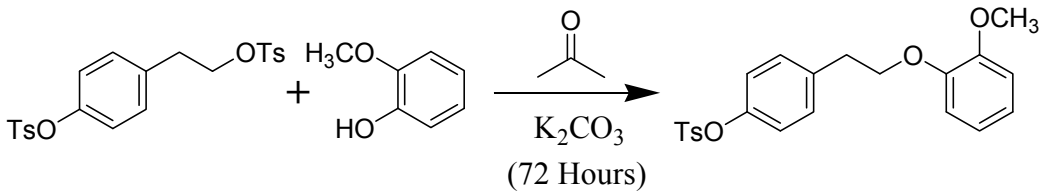

Equation 15. Synthesis of 1-Tosyloxyphenyl-4-[2-(2-methoxyphenoxy)ethyl] from the protected tosylate ester with guaiacol.

1,65 g 1-Tosyloxy-2-(4-tosyloxyphenyl)ethane (3,7 mmol), 0,45 g guaiacol (3,6 mmol) and 0,76 g oven dried potassium carbonate (5,5 mmol) dissolved in acetone 20 ml and refluxed for 72 h under vigorous stirring. After the filtering and solvent removal, the resulting light brown oil dissolved in dichloromethane (20 ml) and washed with aqueous HCl (3M, 10 ml). The organic layer was washed with water (2 X 20 ml) and the original

aqueous layer was extracted with dichloromethane (30 ml). The combined dichloromethane extracts were dried over anhydrous magnesium sulphate, and the solvent removed by rotary evaporator. The ^{1}H NMR analysis indicated that the crude mixture contained; ~80% product, ~5% unreacted starting material contaminated with ~15% 4-tosyloxystyrene as the elimination by-product of the reaction.

10.2.2.3 Preparation of Phenol, 4-[2-(2-methoxyphenoxy)ethyl]

Third step is the cleavage of the remaining protecting group from the (β-*O*-4)-ether with methanol, resulting in Phenol, 4-[2-(2-methoxyphenoxy)ethyl].

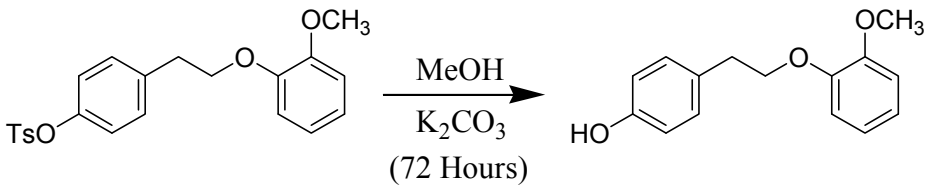

Equation 16. Cleavage of the tosyl protecting group from 1-Tosyloxyphenyl-4-[2-(2-methoxyphenoxy)ethyl] to form the (β-*O*-4)-model compound: Phenol, 4-[2-(2-methoxyphenoxy)ethyl].

The crude reaction mixture from step two with 3,8 g oven dried potassium carbonate (27 mmol) dissolved in methanol (50 ml) and refluxed for 72 h under vigorous stirring. The reaction mixture was mixed with dichloromethane (50 ml) filtered and washed with aqueous HCl (3M, 10 ml). The organic layer was washed with water (2 X 30 ml), dried over anhydrous magnesium sulphate, and the solvent removed by rotary evaporator. The residue was recrystallized from 33%ethyl acetate in hexane.

Phenol, 4-[2-(2-methoxyphenoxy)ethyl] obtained in ~75% yield as white fluffy crystals. Which resulting a 32% overall yield on 2-(4-Hydroxyphenyl)ethanol after three steps.

^{1}H NMR ($CDCl_3$) δ 3,09 (t, 2H), 3,87 (s, 3H), 4,17 (t, 2H), 4,65 (s, 1H), 6,77 (d, 2H) 6,91 (m, 4H), 7,15 (d, 2H); (see: Appendix A.1.1)

^{13}C NMR ($CDCl_3$) δ 34,75, 55,92, 69,94, 111,96, 113,02, 115,32, 120,95, 121,13, 129,86, 130,11, 148,16, 149,26, 154,28; (see: Appendix A.1.2)

MS-EI m/z (relative intensity) 244 (14), 152 (9), 137 (5), 124 (11), 125 (12), 121 (100), 107 (5), 103 (7), 93 (13), 92 (8), 91 (11), 84 (9), 77 (14), 65 (7), 49 (7), 43 (12); (see: Appendix A.1.3)

10.2.3 The Test Hydrogenation of 4-[2-(2-methoxyphenoxy)ethyl] with Raney-Ni

With the model compound in hand, the hydrogenation runs can be performed on analytically pure model compound with selected catalysts. Since beside the solvent and the catalyst, 4-[2-(2-methoxyphenoxy)ethyl] is the only compound in the starting reaction mixture, by carefully analyzing the product mixture the fundamental chemistry could be determined. Since the model compound has two aromatic rings and two aryl-O-aliphatic linkages, the hydrogenative selectivity could be calculated. Due to the simplicity of the model compound compared to the native lignin structure, by following the product distribution in the final mixture, it provides a reliable means to gain insight into the fundamental chemistry and optimize the reaction conditions for the production of desired value added chemicals.

After the reaction, the Raney-Ni catalyst is separated by centrifugation and the solvent removed under reduced pressure. The residue is dissolved in $CDCl_3$ and NMR spectra are recorded. (Appendix A.3.1) shows the H^1-NMR spectra recorded before and after the hydrogenation run on the blank run (no catalyst) and using Raney-Ni as catalyst.

The change in the H^1-NMR spectra is a clear indication of the hydrogenative activity of the selected catalyst towards aryl-O-aliphatic and/or carbon-carbon double bonds. By separating the products by chromatography, and analyzing their structure by Gas chromatography-mass spectroscopy (GC-MS) the yield and hydrogeative selectivity can be determined. (Appendix A.3.2) shows the LC-MS spectra recorded on the products of the model compound hydrogenation using Raney-Ni as catalyst.

This approach utilizing a model compound provides an easy new method to determine the fundamental chemistry and hydrogenative selectivity of the selected catalysts during hydrogenation. Due to the nature of the model compound and the low number of possible products, the compounds in the final mixture are easily separable, thus the yields can be determined providing a reliable means for reaction condition optimization for selected catalysts systems.

APPENDIX A

NMR AND MASS SPECTRA OF NEW COMPOUNDS

A.1 NMR and ESI-MS Spectra of the Model Compound

Phenol, 4-[2-(2-methoxyphenoxy)ethyl]

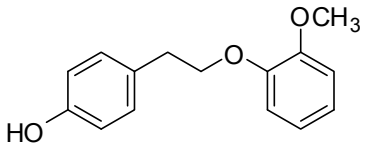

…

A.1.1 ^{1}H-NMR Spectrum of Compound Phenol, 4-[2-(2-methoxyphenoxy)ethyl] in $CDCl_3$

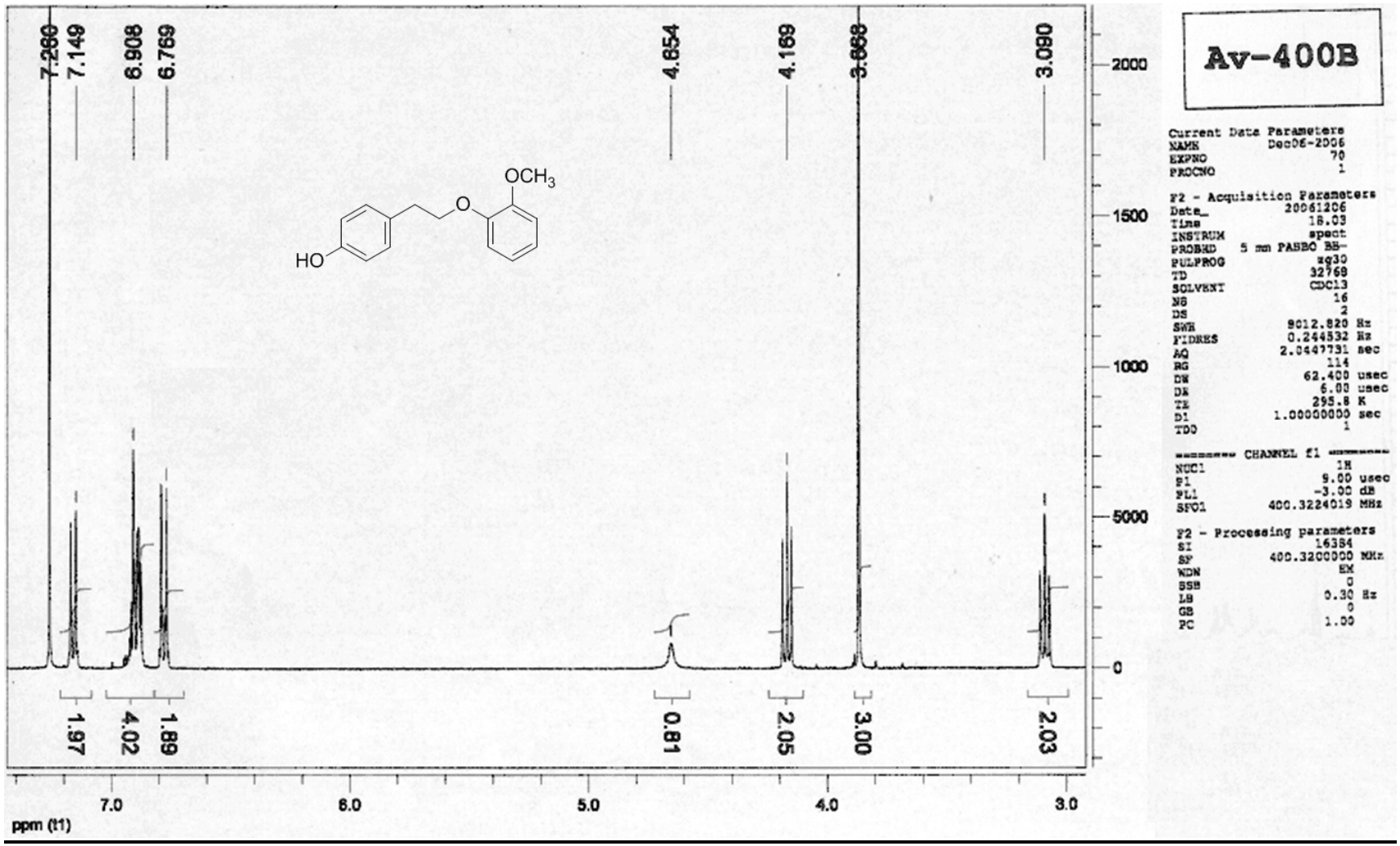

A.1.2 ^{13}C-NMR Spectrum of Compound Phenol, 4-[2-(2-methoxyphenoxy)ethyl] in $CDCl_3$

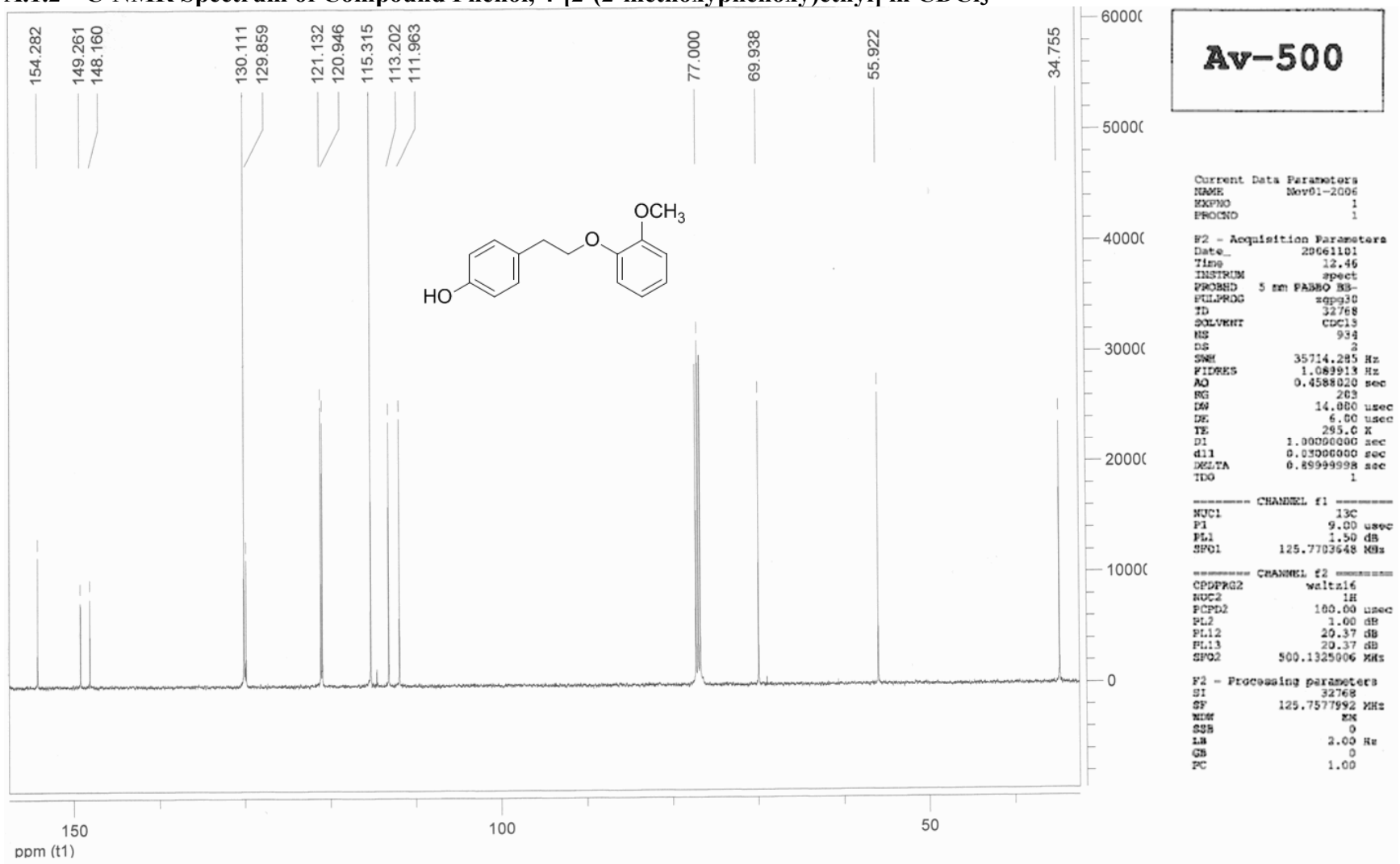

A.1.3 ESI-MS Spectrum of Compound Phenol, 4-[2-(2-methoxyphenoxy)ethyl] in $CDCl_3$

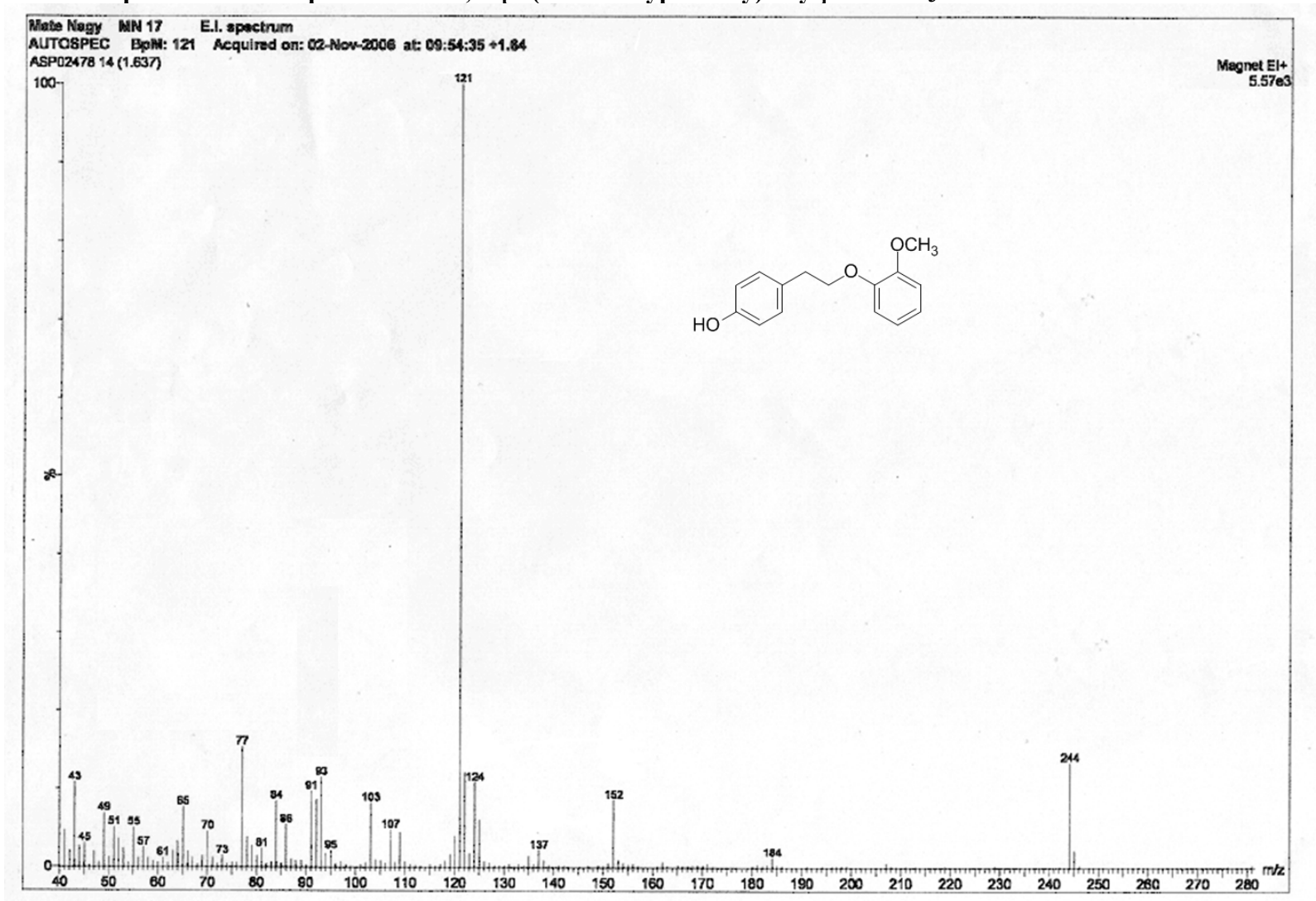

A.2 ^{31}P-NMR Spectra of Synthesized Catalysts

$RhCl(PPh_3)_3$,

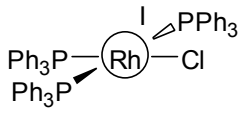

$RuCl_2(PPh_3)_3$

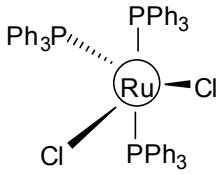

A.2.1 ^{31}P-NMR Spectrum of Compound $RhCl(PPh_3)_3$ in $CDCl_3$

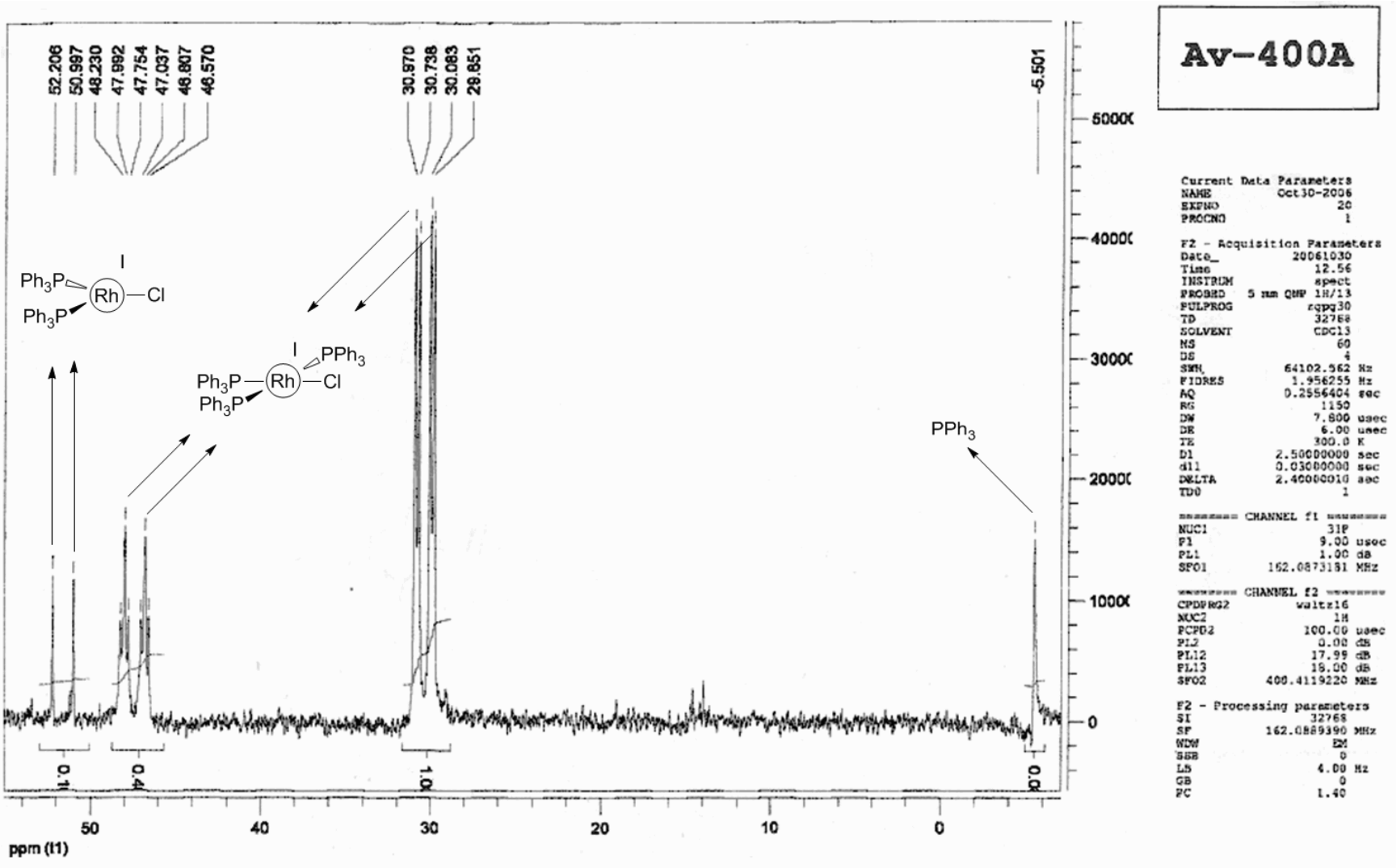

A.2.2 ^{31}P-NMR Spectrum of Compound $RuCl_2(PPh_3)_3$ in $CDCl_3$

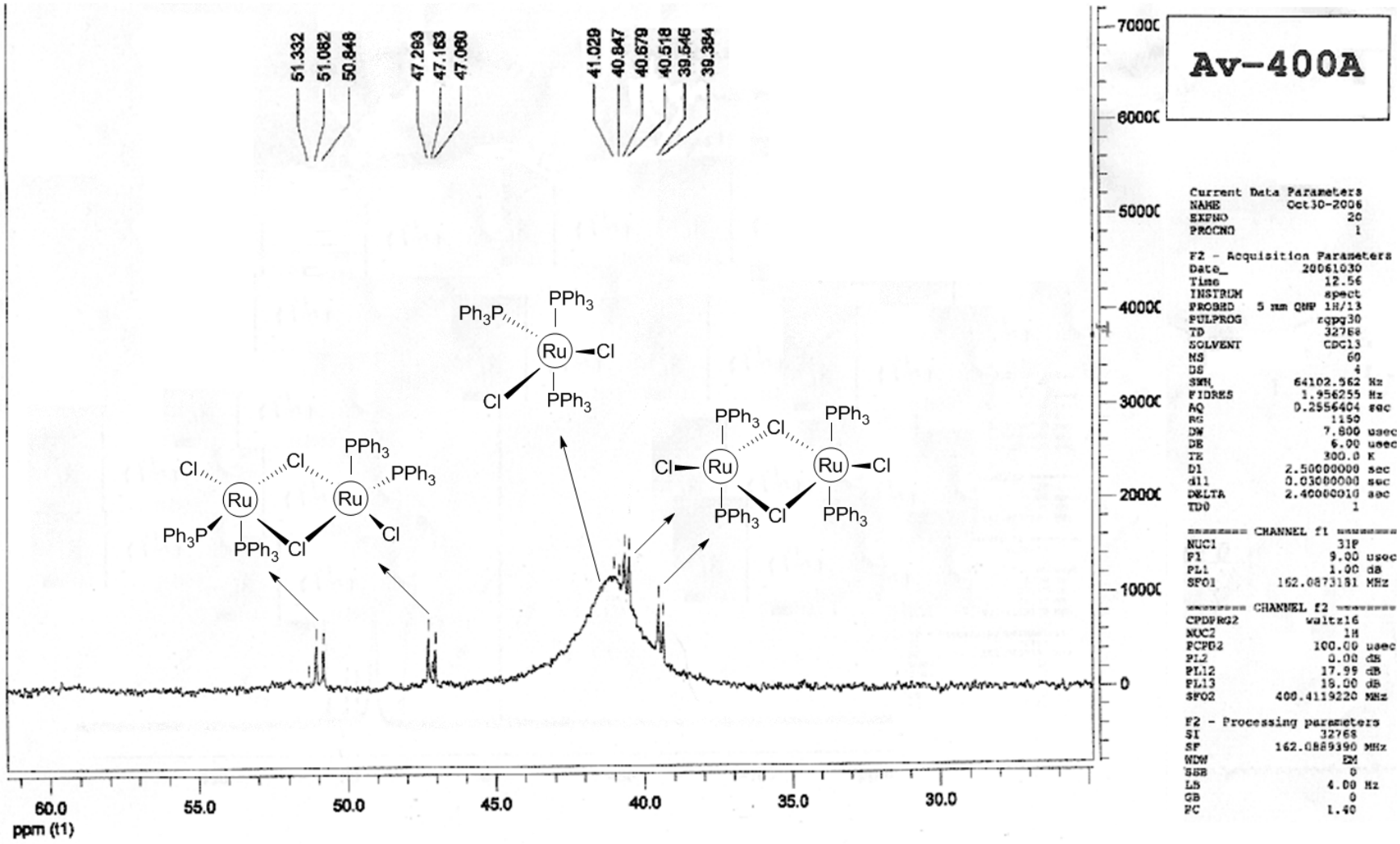

A.3 H-NMR and LC-MS Spectra of the Model Compound Phenol, 4-[2-(2-methoxyphenoxy)ethyl] Hydrogenated with Raney-Ni.

Phenol, 4-[2-(2-methoxyphenoxy)ethyl]

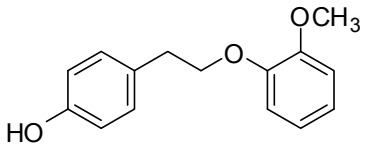

A.3.1 ^{1}H-NMR Spectrum of Phenol, 4-[2-(2-methoxyphenoxy)ethyl] Hydrogenated in Ethanol with Raney-Ni in $CDCl_3$. (50 bar H_2, 150°C, 20 hours)

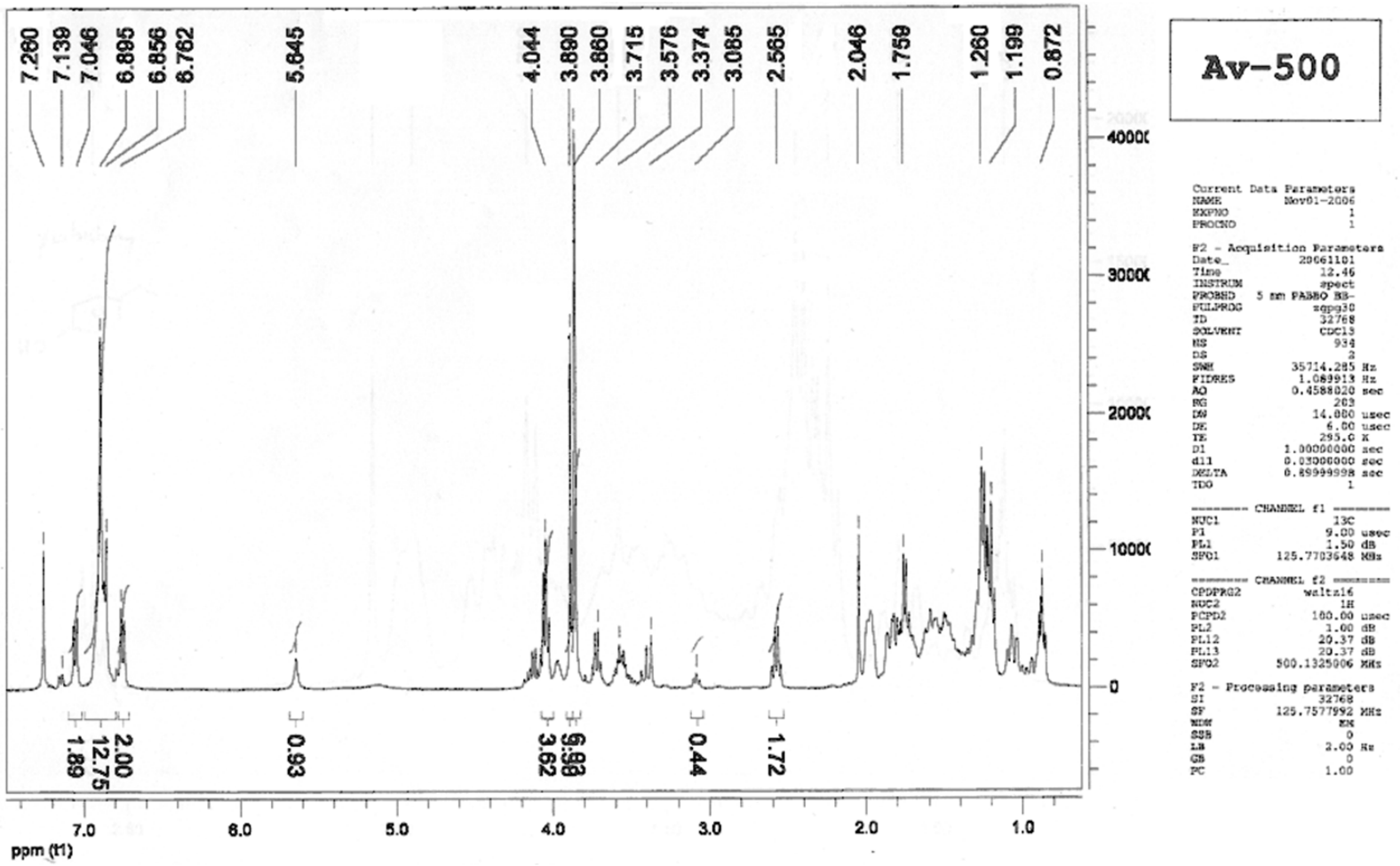

A.3.1 LC-MS Spectrum of Phenol, 4-[2-(2-methoxyphenoxy)ethyl] Hydrogenated in Ethanol with Raney-Ni in $CDCl_3$. (50 bar H_2, 150°C, 20 hours)

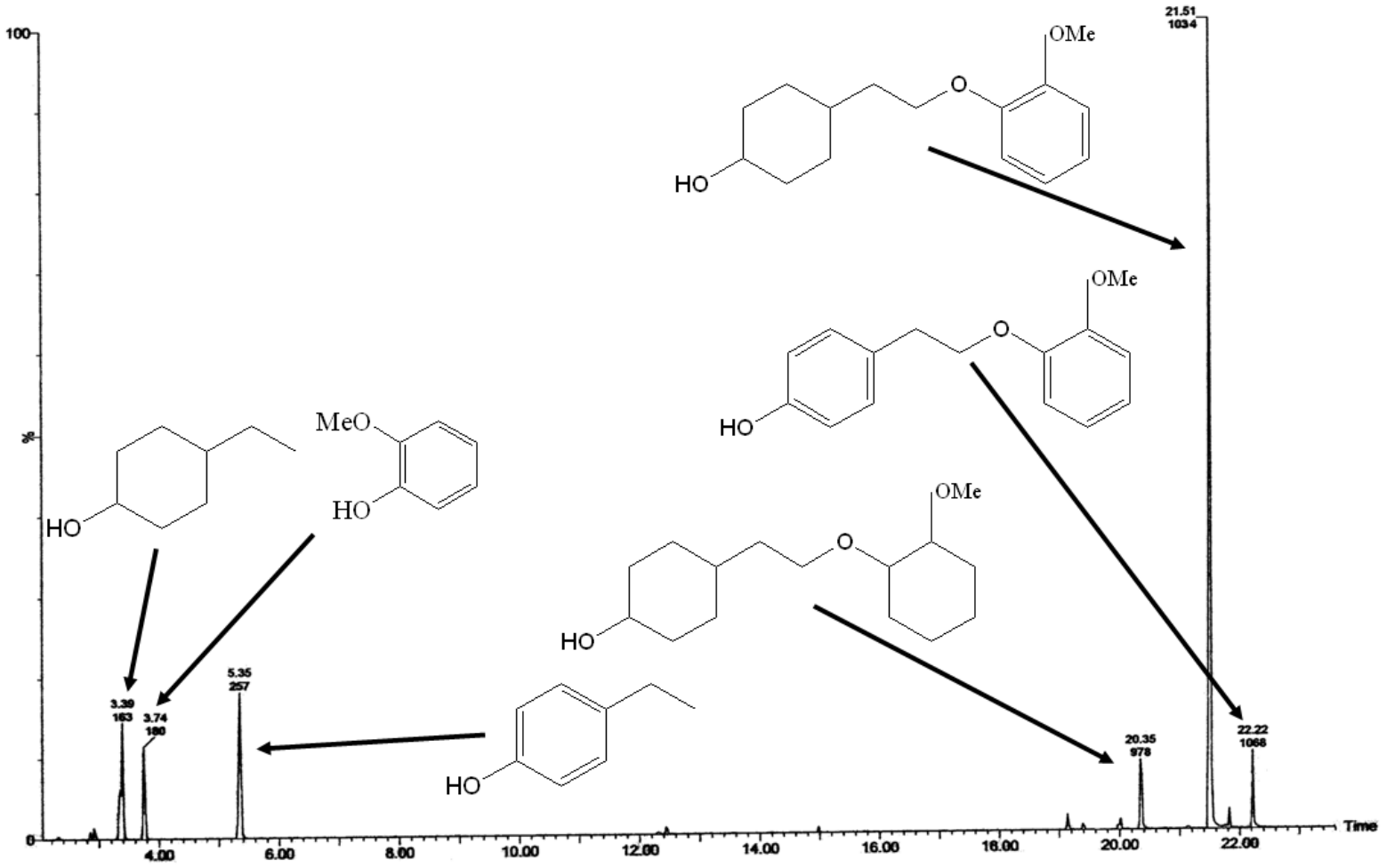

APPENDIX B

COPYRIGHT PERMISSIONS

B.1 Permission from Industrial Biotechnology

Dear Dr. Nagy:
Copyright permission is granted for this request.
Kind regards,
Karen Ballen
Manager, Reprints and Permissions

-----Original Message-----
From: Mate Nagy [mailto:Mate.Nagy@ipst.gatech.edu]
Sent: Thursday, July 16, 2009 6:26 PM
To: Ballen, Karen
Subject: Copyright Permission - Mate Nagy_ GaTech, Atlanta, GA

Dear permission office,

I am preparing my Ph. D. dissertation for publication at the Georgia Institute of Technology, Atlanta, GA.
I would very much appreciate your permission to use the following material:

- Ragauskas, Arthur J.; Nagy, Máté; Kim, Dong Ho; Eckert, Charles A.; Hallett, Jason P. and Liotta, Charles L. *From wood to fuels: Integrating biofuels and pulp production*, Industrial Biotechnology, (2006), 2(1), 55-65.

Thank you very much for your help!

Kind regards:

Mate Nagy
Ph.D. Candidate

School of Chemistry and Biochemistry
Institute of Paper Science and Technology at Georgia Institute of Technology
500 10th St., NW
Atlanta, GA, 30332-0620
404-894-6652 (O)
404-894-4778 (F)

B.2 Permission from ASP (JBMBE)

Hi Mate:

ASP allows to use materials in your PhD thesis.

H. S. Nalwa

From: Mate Nagy [mailto:Mate.Nagy@ipst.gatech.edu]
Sent: Friday, July 17, 2009 3:48 PM
To: nalwa@mindspring.com
Subject: Copyright Permission - Mate Nagy_ GaTech, Atlanta, GA

Dear Dr. H. S. Nalwa,

I am preparing my Ph. D. dissertation for publication at the Georgia Institute of Technology, Atlanta, GA.
I would very much appreciate your permission to use the following material:

- Nagy, Máté; Alleman, Teresa L.; Dyer, Thomas and Ragauskas, Arthur J. *Quantitative NMR analysis of partially substituted biodiesel glycerols*, Journal of Biobased Material and Bioenergy, (2009), 3(1), 108-111.

Thank you very much for your help!

Kind regards:

Mate Nagy
Ph.D. Candidate

School of Chemistry and Biochemistry
Institute of Paper Science and Technology at Georgia Institute of Technology
500 10th St., NW
Atlanta, GA, 30332-0620
404-894-6652 (O)
404-894-4778 (F)

B.3 Permission from Elsevier (Fuel)

ELSEVIER LICENSE
TERMS AND CONDITIONS

Sep 28, 2009

This is a License Agreement between Mate Nagy ("You") and Elsevier ("Elsevier") provided by Copyright Clearance Center ("CCC"). The license consists of your order details, the terms and conditions provided by Elsevier, and the payment terms and conditions.

Supplier	Elsevier Limited The Boulevard,Langford Lane Kidlington,Oxford,OX5 1GB,UK
Registered Company Number	1982084
Customer name	Mate Nagy
Customer address	500 10th Street, NW Atlanta, GA 30332
License Number	2235510980600
License date	Jul 24, 2009
Licensed content publisher	Elsevier
Licensed content publication	Fuel
Licensed content title	Phosphitylation and quantitative ^{31}P NMR analysis of partially substituted biodiesel glycerols
Licensed content author	Máté Nagy, Brian J. Kerr, Cherie J. Ziemer and Arthur J. Ragauskas
Licensed content date	September 2009
Type of Use	Thesis / Dissertation
Portion	Full article
Format	Both print and electronic
You are an author of the Elsevier article	Yes
Are you translating?	No
Elsevier VAT number	GB 494 6272 12

GENERAL TERMS

2. Elsevier hereby grants you permission to reproduce the aforementioned material subject to the terms and conditions indicated.

3. Acknowledgement: If any part of the material to be used (for example, figures) has appeared in our publication with credit or acknowledgement to another source, permission must also be sought from that source. If such permission is not obtained then that material may not be included in your publication/copies. Suitable acknowledgement to the source must be made, either as a footnote or in a reference list at the end of your publication, as follows:

"Reprinted from Publication title, Vol /edition number, Author(s), Title of article / title of chapter, Pages No., Copyright (Year), with permission from Elsevier [OR APPLICABLE SOCIETY COPYRIGHT OWNER]." Also Lancet special credit - "Reprinted from The Lancet, Vol. number, Author(s), Title of article, Pages No., Copyright (Year), with permission from Elsevier."

4. Reproduction of this material is confined to the purpose and/or media for which permission is hereby given.

5. Altering/Modifying Material: Not Permitted. However figures and illustrations may be altered/adapted minimally to serve your work. Any other abbreviations, additions, deletions and/or any other alterations shall be made only with prior written authorization of Elsevier Ltd. (Please contact Elsevier at permissions@elsevier.com)

6. If the permission fee for the requested use of our material is waived in this instance, please be advised that your future requests for Elsevier materials may attract a fee.

7. Reservation of Rights: Publisher reserves all rights not specifically granted in the combination of (i) the license details provided by you and accepted in the course of this licensing transaction, (ii) these terms and conditions and (iii) CCC's Billing and Payment terms and conditions.

8. License Contingent Upon Payment: While you may exercise the rights licensed immediately upon issuance of the license at the end of the licensing process for the transaction, provided that you have disclosed complete and accurate details of your proposed use, no license is finally effective unless and until full payment is received from you (either by publisher or by CCC) as provided in CCC's Billing and Payment terms and conditions. If full payment is not received on a timely basis, then any license preliminarily granted shall be deemed automatically revoked and shall be void as if never granted. Further, in the event that you breach any of these terms and conditions or any of CCC's Billing and Payment terms and conditions, the license is automatically revoked and shall be void as if never granted. Use of materials as described in a revoked license, as well as any use of the materials beyond the scope of an unrevoked license, may constitute copyright infringement and publisher reserves the right to take any and all action to protect its copyright in the materials.

9. Warranties: Publisher makes no representations or warranties with respect to the licensed material.

10. Indemnity: You hereby indemnify and agree to hold harmless publisher and CCC, and their respective officers, directors, employees and agents, from and against any and all claims arising out of your use of the licensed material other than as specifically authorized pursuant to this license.

11. No Transfer of License: This license is personal to you and may not be sublicensed, assigned, or transferred by you to any other person without publisher's written permission.

12. No Amendment Except in Writing: This license may not be amended except in a writing signed by both parties (or, in the case of publisher, by CCC on publisher's behalf).

13. Objection to Contrary Terms: Publisher hereby objects to any terms contained in any purchase order, acknowledgment, check endorsement or other writing prepared by you, which terms are inconsistent with these terms and conditions or CCC's Billing and Payment terms and conditions. These terms and conditions, together with CCC's Billing and Payment terms and conditions (which are incorporated herein), comprise the entire agreement between you and publisher (and CCC) concerning this licensing transaction. In the event of any conflict between your obligations established by these terms and conditions and those established by CCC's Billing and Payment terms and conditions, these terms and conditions shall control.

14. Revocation: Elsevier or Copyright Clearance Center may deny the permissions described in this License at their sole discretion, for any reason or no reason, with a full refund payable to you. Notice of such denial will be made using the contact information provided by you. Failure to receive such notice will not alter or invalidate the denial. In no event will Elsevier or Copyright Clearance Center be responsible or liable for any costs, expenses or damage incurred by you as a result of a denial of your permission request, other than a refund of the amount(s) paid by you to Elsevier and/or Copyright Clearance Center for denied permissions.

LIMITED LICENSE

The following terms and conditions apply to specific license types:

15. **Translation**: This permission is granted for non-exclusive world **English** rights only unless your license was granted for translation rights. If you licensed translation rights you may only translate this content into the languages you requested. A professional translator must perform all translations and reproduce the content word for word preserving the integrity of the article. If this license is to re-use 1 or 2 figures then permission is granted for non-exclusive world rights in all languages.

16. **Website**: The following terms and conditions apply to electronic reserve and author websites:
Electronic reserve: If licensed material is to be posted to website, the web site is to be password-protected and made available only to bona fide students registered on a relevant course if:
This license was made in connection with a course,

This permission is granted for 1 year only. You may obtain a license for future website posting,
All content posted to the web site must maintain the copyright information line on the bottom of each image,
A hyper-text must be included to the Homepage of the journal from which you are licensing at http://www.sciencedirect.com/science/journal/xxxxx or, for books, to the Elsevier homepage at http://www.elsevier.com,
Central Storage: This license does not include permission for a scanned version of the material to be stored in a central repository such as that provided by Heron/XanEdu.

17. **Author website** for journals with the following additional clauses:

All content posted to the web site must maintain the copyright information line on the bottom of each image, and
The permission granted is limited to the personal version of your paper. You are not allowed to download and post the published electronic version of your article (whether PDF or HTML, proof or final version), nor may you scan the printed edition to create an electronic version,
A hyper-text must be included to the Homepage of the journal from which you are licensing at http://www.sciencedirect.com/science/journal/xxxxx,
Central Storage: This license does not include permission for a scanned version of the material to be stored in a central repository such as that provided by Heron/XanEdu.

18. **Author website** for books with the following additional clauses:
Authors are permitted to place a brief summary of their work online only.
A hyper-text must be included to the Elsevier homepage at http://www.elsevier.com.
All content posted to the web site must maintain the copyright information line on the bottom of each image
You are not allowed to download and post the published electronic version of your chapter, nor may you scan the printed edition to create an electronic version.
Central Storage: This license does not include permission for a scanned version of the material to be stored in a central repository such as that provided by Heron/XanEdu.

19. **Website** (regular and for author): A hyper-text must be included to the Homepage of the journal from which you are licensing at http://www.sciencedirect.com/science/journal/xxxxx or, for books, to the Elsevier homepage at http://www.elsevier.com.

20. **Thesis/Dissertation**: If your license is for use in a thesis/dissertation your thesis may be submitted to your institution in either print or electronic form. Should your thesis be published commercially, please reapply for permission. These requirements include permission for the Library and Archives of Canada to supply single copies, on demand, of the complete thesis and include permission for UMI to supply single copies, on demand, of the complete thesis. Should your thesis be published commercially, please reapply for permission.

21. **Other conditions:** None

v1.5

B.4 Permission from Walter de Gruyter GmbH & Co (Holzforschung)

Dear Mate Nagy,

Thank your very much for your message and your request concerning the below mentioned material.

As you are one of the authors and as you are using it for your Ph. D. dissertation, we do not have objections against your intended re-use of the article.

This permission is of course subject to full acknowledgement of the source of material used and provides that full credit is given to the original publication.
Please notice that permission is granted for the mentioned use only.

We wish you all the best for your dissertation!
If you should have any further questions, please do not hesitate to contact us again.

Best regards,
Andrea Troidl

Andrea Troidl
Rights & Licenses

Walter de Gruyter GmbH & Co. KG with
K. G. Saur Verlag and
Max Niemeyer Verlag
Mies-van-der-Rohe-Str. 1
80807 München
Germany

Tel. 089/ 7 69 02 -257
Fax 089/ 7 69 02 -350
Andrea.Troidl@degruyter.com
www.degruyter.com
www.reference-global.com

- Nagy, Máté; David, Kasi; Britovsek, George J. P.; Ragauskas, Arthur J. O*rganosolv lignin hydrogenolysis to value added chemicals*, Holzforschung (DOI: 10.1515/HF.2009.097)

B.7 Permission from BAFF for Figure 1 and Figure 17. (Chapter 2)

Dear Mate,
Now I see that I have missed to answer this email and I hope that It not had delayed your publication.
You can use our picture if you give the source (BAFF) on it.
God Luck
/Karin Sandström
BAFF

Från: Mate Nagy [mailto:Mate.Nagy@ipst.gatech.edu]
Skickat: den 24 september 2009 21:18
Till: Karin Sandström
Ämne: Copyright Permission - Mate Nagy_ GaTech, Atlanta, GA

Dear Permission Office (BAFF),

My name is Mate Nagy and I am a PhD candidate at the Department of Chemistry at the Georgia Institute of Technology. During my MSc studies in 2001 at the Chalmers University, I came across two pictures that now I would like to use in my dissertation.
To avoid any copyright issues in the future, last month I contacted with Ilona Sarvari Horvath my supervisor at the Chalmers University at the time, and she told me to contact you since the pictures are provided by BAFF for scientific conference posters and presentations.
Now I am preparing my Ph. D. dissertation for publication at the Georgia Institute of Technology, Atlanta, GA, and I would very much appreciate your permission to use the following pictures attached to this mail.
Thank you very much for your help!
I am looking forward to your reply.

Kind regards,

Mate Nagy
Ph.D. Candidate

School of Chemistry and Biochemistry
Institute of Paper Science and Technology at Georgia Institute of Technology
500 10th St., NW
Atlanta, GA, 30332-0620
404-894-6652 (O)
404-894-4778 (F)

REFERENCES

[1] Ragauskas AJ, Williams CK, Davison BH, Britovsek G, Cairney J, Eckert CA, Frederick W Jr, Hallett JP, Leak DJ, Liotta CL, Mielenz JR, Murphy R, Templer R, Tschaplinski T. The Path Forward for Biofuels and Biomaterials. Science 2006;311(5760):484-9.

[2] Gullichsen J, Fogelholm CJ. Chemical Pulping. Atlanta: TAPPI Press, 1999.

[3] Chakar FS, Ragauskas AJ. Review of current and futures of wood kraft lignin process chemistry. Ind Crops Prod 2004;20:131–41.

[4] Demirbas A. Biodiesel: A Realistic Fuel Alternative for Diesel Engines. London: Springer - Verlag London Ltd, 2008.

[5] Holcapek M, Jandera P, Fischer J, Prokes B. Analytical monitoring of the production of biodiesel by high-performance liquid chromatography with various detection methods. J Chromatogr A 1999; 858(1):13-31.

[6] Plank C, Lorbeer E. Simultaneous determination of glycerol, and mono-, di- and triglycerides in vegetable oil methyl esters by capillary gas chromatography. J Chromatogr A 1995; 697(1+2):461-8.

[7] ASTM. ASTM D 6584-07. In: ASTM, editors. Annual Book of ASTM Standards, West Conshohocken: ASTM International; 2007.

[8] Knothe, G. Monitoring a progressing transesterification reaction by fiber-optic near infrared spectroscopy with correlation to 1H nuclear magnetic resonance spectroscopy. J Am Oil Chem Soc 2000; 77(5):489-93.

[9] Knothe G. Analyzing biodiesel: standards and other methods. J Am Oil Chem Soc 2006; 83(10):823-33.

[10] DOE. Carbon Cycling and Biosequestration, Integration Biology and Climate Through Systems Science DOE/SC-108; DOE Office of Science: Washington, 2008 see also: http://genomicsgtl.energy.gov/carboncycle/ (July, 2009)

[11] Boden, TA., Marland G, Andres RJ. Global, Regional, and National Fossil-Fuel CO_2 Emissions. Carbon Dioxide Information Analysis Center., Oak Ridge: ORNL, USDE, 2009.

[12] DOE. Bioethanol; Moving into the marketplace DOE/GO-102000-1109; DOE Office of Science: Washington, 2000.

[13] EERE (2005). U.S. Department of Energy/Energy Efficiency and Renewable Energy http://www.eere.energy.gov/biomass/biomass_benefits.html (October, 2009)

[14] IEA (International Energy Association). Annual report 2000 - Bioenergy. Washington: IEA, 2000.

[15] EIA (Energy Information Administration): http://www.eia.doe.gov/emeu/international/petroleu.html#IntlConsumption (Jan. 29, 2005)

[16] Hirsch RL, Bezdek R, Wendling R. Peaking of world oil production and its mitigation. AIChE Journal 2006;52(1):2-8.

[17] Pacala S, Socolow R. Stabilization wedges: Solving the climate problem for the next 50 years with current technologies. Science 2004;305(5686):968-72.

[18] CADIA (Carbon Dioxide Information Analysis Center) data base: http://cadiac.ornl.gov (October, 2009)

[19] Thoning KW, Tans PP, Komhyr WD. Atmospheric carbon dioxide at Mauna Loa Observatory 2. Analysis of the NOAA GMCC data, 1974-1985. J. Geophys. Research 1989;94:8549-65.

[20] USDC (United States Department of Commerce), NOAA (National Oceanic & Atmospheric Administration) research database http://www.esrl.noaa.gov/ (October, 2009)

[21] Hoffert MI, Caldeira K, Benford G, Criswell DR, Green C, Herzog H, Jain AK, Kheshgi HS, Lackner KS, Lewis JS, Lightfoot HD, Manheimer W, Mankins JC, Mauel ME, Perkins LJ, Schlesinger ME, Volk T, Wigley TML. Advanced technology paths to global climate stability: Energy for a greenhouse planet. Science 2002;298(5595):981-87.

[22] Pacala S, Socolow, R. Stabilization wedges: Solving the climate problem for the next 50 years with current technologies. Science 2004;305(5686):968-72.

[23] The Arlington Institute. A Strategy: Moving America Away from Oil. Arlington: AI, 2002.

[24] EIA (Energy Information Administration). Annual Energy Outlook 2007: with projections to 2030. Washington: Bernan PR, 2007.

[25] EIA. (Energy Information Administration). Annual Energy Outlook 2003: with projections to 2025. Washington: Diane Publishing, 2003.

[26] UCSB (United States Census Bureau). Foreign Trade Statistics 2005.-International trade in goods and services- Washington: USCB 2005. see also: http://www.census.gov/foreign-trade/Press-Release/current_press_release/#compressed (October, 2009)

[27] RFA (Renewable Fuel Association).Homegrown for the homeland. Washington: RFA, 2005. see also: http://www.ethanolrfa.org/outlook2005.pdf

[28] Kamm B, Kamm M. Principles of biorefineries. Appl Microbiol Biotechnol 2004;64:137–45.

[29] Kim SB, Jin WC. Pretreatment for enzymatic hydrolysis of used newspaper. In: ACS Symposium Series 889 (Lignocellulose Biodegradation) p 36-48. Washington: ACS, 2004.

[30] Wen Z, Liao W, Chen S. Hydrolysis of animal manure lignocellulosics for reducing sugar production. Biores Technol 2003;91(1):31-9.

[31] Palmarola AB, Choteborska P, Galbe M, Zacchi G. Ethanol production from non-starch carbohydrates of wheat bran. Biores Technol 2005;96(7):843-50.

[32] Stamatelatou K, Dravillas K, Lyberatos G. A two-stage process for the anaerobic digestion of sludge generated during the production of bioethanol from sweet sorghum: Wastewater sludge as a resource. In: Proceedings of the International Water Association - Specialist Conference p. 547-52. London: IWA, 2003.

[33] Saha BC, Iten LB, Cotta MA, Wu YV. Fuel ethanol production from rice hull. In: 227th ACS National Meeting, Anaheim p. BIOT-101. Washington: ACS, 2004.

[34] Schell DJ, Riley CJ, Dowe N, Farmer J, Ibsen KN, Ruth MF, Toon ST, Lumpkin RE. A bioethanol process development unit: initial operating experiences and results with a corn fiber feedstock. Biores Technol 2003;91(2):179-88.

[35] Mtui G, Nakamura Y. Bioconversion of lignocellulosic waste from selected dumping sites in Dar es Salaam, Tanzania. Biodeg 2005;16(6):493-9.

[36] Perlack RD, Wright LL, Turhollow AF, Graham RL, Stokes BJ, Erbach DC, Biomass as Feedstock for A Bioenergy and Bioproducts Industry: The Technical Feasibility of a Billion-Ton Annual Supply. Washington: USDOE, 2005.

[37] Baeza J, Parra C, Berrocal A, Perez S, Rodriguez J, Freer J. Prediction of bioethanol production from soft- and hardwood. In: 229th ACS National Meeting p. CELL-126. Washington: ACS, 2005.

[38] Timell TE. Recent progress in the chemistry of wood hemicelluloses. Wood Sci Technol 1967;1(1):45-70.

[39] Jones PD, Schimleck LR, Peter GF, Daniels RF, Clark A. Nondestructive estimation of wood chemical composition of sections of radial wood strips by diffuse reflectance near infrared spectroscopy. Wood Sci Technol 2006;40(8):709-20.

[40] Ona T, Sonoda T, Ohshima J, Yokota S, Yoshizawa N. A rapid quantitative method to assess eucalyptus wood properties for kraft pulp production by ft–raman spectroscopy. J Pulp Pap Sci 2003;29(1):6-10.

[41] Frédérique B, Bjarne H. Chemical composition of earlywood and latewood in Norway spruce heartwood, sapwood and transition zone wood. Wood Sci Technol 2004;38(4):245-56.

[42] Lawoko M, Henriksson G, Gellerstedt G. Structural Differences between the Lignin-Carbohydrate Complexes Present in Wood and in Chemical Pulps. Biomacromol 2005;6(6):3467-73.

[43] Aimi H, Matsumoto Y, Meshitsuka G. Structure of small lignin fragments retained in water-soluble polysaccharides extracted from birch MWL isolation residue. J Wood Sci 2005;51(3):303-8.

[44] Fry SC. Primary cell wall metabolism: Tracking the careers of wall polymers in living plant cells. New Phytol 2004;161(3):641-75.

[45] Fratzl P. Cellulose and collagen: from fibers to tissues. Curr Op Coll Interf Sci 2003;8(1):32-9.

[46] Reiter WD. Biosynthesis and properties of the plant cell wall. Curr Op Plant Biol 2002;5(6):536-42.

[47] Kumar R, Mago G, Balan V, Wyman CE. Physical and chemical characterizations of corn stover and poplar solids resulting from leading pretreatment technologies. Biores Technol 2009;100(17):3948-62.

[48] Pala H, Mota M, Gama FM. Enzymatic depolymerisation of cellulose. Carbohyd Poly 2007;68(1):101-8.

[49] Klimentov AS, Petropavlovskii GA, Kotel'nikova NE, Skvortsov SV, Volkova LA. Radiation-induced degradation of wood cellulose. Cellulose Chem Technol 1984;18(6):619-23.

[50] Holt C, Mackie W, Sellen DB. Degree of polymerization and polydis-persity of native cellulose. J Poly Sci 2007;42(3):1505-12.

[51] Vinod PP. Effect of crystallinity and degree of polymerization of cellulose on enzymatic saccharification. Biotechnol Bioeng 2004;26(10):1219-22.

[52] Thygesen A, Oddershede J, Lilholt H, Thomsen AB, Stahl K. On the determination of crystallinity and cellulose content in plant fibres. Cellulose 2005;12(6):563-76.

[53] Newman RH. Homogeneity in cellulose crystallinity between samples of *Pinus radiata* wood. Holzforschung 2004;58(1):91-6.

[54] Brown RM. Cellulose structure and biosynthesis: what is in store for the 21st century? J Poly Sci A 2004;42(3):487-95.

[55] Kadla JF, Gilbert RD. Cellulose structure: a review. Cellulose Chem Technol 2001;34(3-4):197-216.

[56] Gullichsen J, Fogelholm CJ. Papermaking Science and Technology, Book 6A: Chemical Pulping. Helsinki: Fapet Oy, 1999.

[57] Atalla RH, VanderHart DL. Native cellulose: a composite of two distinct crystalline forms. Science 1984;223(4633):283-5.

[58] Horii F, Hirai A, Kitamaru R. CP/MAS carbon-13 NMR spectra of the crystalline components of native celluloses. Macromol 1987;20(9):2117-20.

[59] Nishiyama Y, Langan P, Chanzy H. Crystal structure and hydrogen-bonding system in cellulose Iα from synchrotron x-ray and neutron fiber diffraction. J Am Chem Soc 2002;124(31):9074-82.

[60] Nishiyama, Y, Sugiyama J, Chanzy H, Langan P. Crystal Structure and Hydrogen Bonding System in Cellulose Iβ from Synchrotron X-ray and Neutron Fiber Diffraction. J Am Chem Soc 2003;125(47):14300-6.

[61] Wickholm K, Larsson PT, Iversen T. Assignment of non-crystalline forms in cellulose I by CP/MAS carbon-13 NMR spectroscopy. Carbohyd Res 1998;312(3):123-9.

[62] Wickholm K, Hult EL, Larsson PT, Iversen T, Lennholm H. Quantification of cellulose forms in complex cellulose materials: a chemometric model. Cellulose 2001;8(2):139-48.

[63] Chang M, Tsao GT. The effect of structure on hydrolysis of cellulose. Cellulose Chem Technol 1981;15(4):383-95.

[64] Zhao H, Kwak JH, Wang Y, Franz JA, White J, Holladay JE. Effects of Crystallinity on Dilute Acid Hydrolysis of Cellulose by Cellulose Ball-Milling Study. En Fuels 2006;20(2):807-11.

[65] Wickholm K, Hult EL, Larsson PT, Iversen T, Lennholm H. Quantification of cellulose forms in complex cellulose materials: a chemometric model. Cellulose 2001 ;8(2):139-48.

[66] Alen R. Structure and Chemical Composition of wood. In: Papermaking Science and Technology. Stenius P (ed.), 3, p. 11-57. Helsinki: Fapet Oy, 2000.

[67] Willfoer S, Sundberg A, Hemming J, Holmbom B. Polysaccharides in some industrially important softwood species. Wood Sci Technol 2005;39(4):245-57.

[68] Willfoer S, Sundberg A, Pranovich A, Holmbom B. Polysaccharides in some industrially important hardwood species. Wood Sci Technol 2005;39(8):601-17.

[69] Salmen L, Olsson AM. Interaction between hemicelluloses, lignin and cellulose: structure-property relationships. J Pulp Pap Sci 1998;24(3):99-103.

[70] Ebringerova A, Hromadkova Z, Heinze T. Hemicellulose. Adv Poly Sci 2005;186:1-67.

[71] Brunow G, Lundquist K, Gellerstedt G. Lignin; Analytical Methods in Wood Chemistry. In: Pulping, and Papermaking. Sjostrom E (ed.), p. 77-124. Berlin: Springer, 1999.

[72] Halpin C. Re-designing lignin for industry and agriculture. Biotechnol Genet Eng Rev 2004;21:229-45.

[73]Pirkko K, Petteri R, Jussi S, Gosta B. The formation of dibenzoxidioxicin structures by oxidative coupling. A model reaction for lignin biosynthesis. Tetrahedron letters 1995;36(25):4501-4.

[74] Ralph J, Lundquist K, Brunow G, Lu F, Kim H, Schatz P.F, Marita J.M, Hatfield, R.D, Ralph S.A, Christensen J.H, Boerjan W. Lignins: Natural polymers from oxidative coupling of 4-hydroxyphenyl- propanoids. Phytochem Rev 2004;3(1-2):29-60.

[75] Gang DR, Costa MA, Fujita M, Dinkova-Kostova AT, Wang HB, Burlat V, Martin W, Sarkanen S, Davin LB, Lewis NG. Regiochemical control of monolignol radical coupling: A new paradigm for lignin and lignan biosynthesis. Chem Biol 1999;6(3):143-51.

[76] John R, Knut L, Gosta B, Fachuang L, Hoon K, Paul FS, Jane MM, Ronald DH, Sally AR, Jorgen HC, Wout B. Lignins: Natural polymers from oxidative coupling of 4-hydroxyphenyl-propanoids. Phytochem Rev 2004;3(1-2):29-60.

[77] Laurence BD, Michael J, Ann MP, Kye-Won K, Daniel GV, Norman GL. Dissection of lignin macromolecular configuration and assembly: Comparison to related biochemical processes in allyl/propenyl phenol and lignan biosynthesis. Nat Prod Rep 2008;25:1015-90.

[78] Wout B, John R, Marie B. Lignin biosynthesis. Annu Rev Plant Biol 2003;54:519-46.

[79] Sjostrom E. Wood Chemistry: Fundamentals and Applications. Orlando: Academic Press, 1981.

[80] Guerra A, Xavier A, Hai A, Filpponen I, Lucia L, Argyropoulos D. Comparative Evaluation of Three Lignin Isolation Protocols for Various Wood Species. J Agric Food Chem 2006;54:9696-705.

[81] Evtuguin DV, Domingues P, Amado FL, Neto CP, Correia AJF. Electrospray Ionization Mass Spectrometry as a Tool for Lignins Molecular Weight and Structural Characterization. Holzforschung 1999;53:525-8.

[82] Evtuguin DV, Amando FL. Application of Electrospray Ionization Mass Spectrometry to the Elucidation of the Primary Structure of Lignin. Macromol Biosci 2003;3(7):339-43.

[83] Brosse N, Sannigrahi P, Ragauskas AJ. Pretreatment of Miscanthus x giganteus Using the Ethanol Organosolv Process for Ethanol Production. Ind Eng Chem Res 2009;48(18):8328–34.

[84] Nagy M, Kerr BJ, Ziemer CJ, Ragauskas AJ. Phosphitylation and quantitative ^{31}P NMR analysis of partially substituted biodiesel glycerols. Fuel 2009;88(9):1973-7.

[85] Estill L. Biodiesel power. Gabriola Island: New Society Publishers, 2005.

[86] Nagy M, Foston M, Ragauskas AJ. A Rapid Quantitative Analytical Tool for Characterizing the Preparation of Biodiesel. J Phy Chem A. 2009;(DOI: 10.1021/jp906543g)

[87] Gerpen JV, Shanks B, Pruszko R, Clements D, Knothe G. Biodiesel analytical methods. NREL/SR-510-36240. Colorado: NREL, 2004.

[88] Chisti Y. Biodiesel from microalgae. Biotechnol Adv 2007;25(3):294-306.

[89] NBB (National Biodiesel Board). Achieving 1 Billion Gallons of Biodiesel While Protecting Valuable Feedstocks. Jefferson City: NBB, 2009. Available at: http://www.biodiesel.org/ (October, 2009)

[90] Tat ME, Van Gerpen JH. Fuel Property Effects on Biodiesel In: American Society of Agricultural Engineering Annual Meeting p. paper 036034. Washington: ASAE, 2003.

[91] Ford H. Ford Predicts Fuel from Vegetation. New York Times 1925;Sept.20:24.

[92] Nitske WR. Rudolph Diesel Pioneer of the Age of Power. Oklahoma: University of Oklahoma Press, 1974.

[93] ORNL (Oak Ridge National Laboratory): http://www.ornl.gov/ (October, 2009)

[94] Sissine F. Energy Independence and Security Act of 2007: A Summary of Major Provisions. Washington: Congressional Research Service, 2007.

[95] Horváth IS, Franzén CJ, Taherzadeh MJ, Niklasson C, Lidén G. Effects of Furfural on the Respiratory Metabolism of *Saccharomyces cerevisiae* in Glucose-Limited Chemostats. App Env Microbiol 2003;69(7)4076-86.

[96] Grohmann K, Himmel M. Enzymes for fuels and chemical feedstock. Washington: ACS, 1991.

[97] USDOE (United Stated Department of Energy). Breaking the biological barriers to cellulosic ethanol: a joint research agenda. Washington: USDOE, 2006.

[98] Bothast RJ, Schlicher MA. Biotechnological Processes for Conversion of Corn into Ethanol, Appl Microbiol Biotechnol 2005;67:19–25.

[99] Ragauskas A.J, Nagy M, Kim DH, Eckert CA, Hallett JP, Liotta CL. From wood to fuels: Integrating biofuels and pulp production. Ind Biotechnol 2006;2:55-65.

[100] Wayman CE. Ethanol from lignocellulosic biomass: Technology economics, and opportunities. Bioreseur Technol 1994;50:3-16.

[101] Clark T, Mackie K. Fermentation inhibitors in wood hydrolyzates derived from the softwood Pinus radiate. J Chem Tech Biot 1984;34B:101-10.

[102] Palmqvist E, Almeida JS, Hahn HB. Fermentation of lignocellulosic hydrolyzates. II: inhibitiotors and mechanism of inhibition. Bioresource Technol 2000;74:25-33.

[103] Tacherzadeh MJ. Physiological effects of 5-hydroxymethylfurfural on *Saccharomyces cerevisiae*. Appl Microbiol Biotechnol 2000;53:701-703.

[104] Larsson S, Palmqvist E, Hahn HB, Tengborg C, Kerstin S, Guido Z, Nievebrant NO. The generation of fermentation inhibitors during dilute acid hydrolysis of softwood. Enzyme Microbial Techn 1999;24:151-9.

[105] Larsson S, Reimann A, Nilvebrant NO, Leif JJ. Comparison of different methods for the detoxification of lignocellulose hydrolyzates of spurce. Appl Biochem Biotechnol 1999;77-79:91-103.

[106] Horvath IS, Sjoede A, Nilvebrant NO, Zagorodni A, Leif JJ. Selection of anion exchangers for detoxification of dilute-acid hydrolyzates from spruce. Appl Biochem Biotechnol 2004;113-116:525-38.

[107] Larsson S, Cassland P, Leif JJ. Development of a Saccharomyces cerevisiae strain with enhanced resistance to phenolic fermentation inhibitors in lignocellulose hydrolyzates by heterologous expression of laccase. Applied Environ Microbiol 2001;67(3):1163-70.

[108] Linden T, Peetre J, Hahn HB. Isolation and characterization of acetic acid-tolerant galactose-fermenting strains of Saccharomyces cerevisiae from spent sulfite liquor fermentation plant. Appl Environ Microbiol 1192;58:1661-9.

[109] Taherzadeh MJ, Niklasson C, Gunnar L. Conversion of dillute-acid hydrolyzates of spruce and birch to ethanol by feb-batch fermentation. Biores Technol 1999;69:59-66.

[110] Sonderegger M, Jeppsson M, Larsson C, Gorwa GMF, Boles E, Olsson L, Spencer MI, Hahn HB, Sauer U. Fermentation performance of engineered and evolved xylose-fermenting Saccharomyces cerevisiae strains. Biotechnol Bioeng 2004;87(1):90-8.

[111] Ingram LO, Conway T, Alterthum F. Ethanol production by Escherichia coli strains co-expressing Zymomonas mobilis PDC and ADH genes. U.S. Patent No. 5,000,000, 1991.

[112] Olson L, Hahn HB. Fermentation of lignocellulosic hydrolyzates for ethanol production. Enzyme Microb Tech 1996;18:312-31.

[113] Sommer P, Georgieva T, Ahring BK. Potential for using thermophilic anaerobic bacteria for bioethanol production from hemicellulose. Biochem Soc Trans 2004;32(2):283-9.

[114] Panda D, Mallick J. Comparative study of ethanol production. Chem Eng World 2006;41(1):49-50, 53.

[115] Kroumov AD, Modenes AN, Tait MC. Development of new unstructured model for simultaneous saccharification and fermentation of starch to ethanol by recombinant strain. Biochem Eng J 2006;28(3):243-55.

[116] Ehnstroem L, Frisenfelt J, Danielsson M, Chematur AB, Karlskoga S. The BIOSTIL process. Bioproc Technol 1991;11:303-21.

[117] Lee J. Biological conversion of lignocellulosic biomass to ethanol. J Biotechnol 1997;56(1):1-24.

[118] Farrell AE, Plevin RJ, Turner BT, Jones AD, O'Hare M, Kammen DM. Ethanol Can Contribute to Energy and Environmental Goals. Science 2006;311(5760):506–8.

[119] Hammerschlag R. Ethanol's Energy Return on Investment: A Survey of the Literature 1999–Present. Environ Sci Technol 2006;40:1744–50.

[120] Brinkman N, Wang M, Weber T, Darlington T. Well-to-Wheels Analysis of Advanced Fuel/Vehicle Systems—A North American Study of Energy Use, Greenhouse Gas Emissions, and Criteria Pollutant Emissions. Detroit: GM, ANL, 2005. see also: www.transportation.anl.gov/pdfs/TA/339.pdf (October, 2009)

[121] RFA (Renewable Fuels Association): http://www.ethanolrfa.org (October, 2009)

[122] NREL (National Renewable Energy Laboratory). Urban Waste Grease Resource Assessment; NREL/SR-570-2614.1. Golden: NREL, 1998.

[123] Lovins AB, Datta EK, Bustnes OE, Koomey JG, Glasgow NJ. Winning the oil endgame. Snowmass: Rocky Mountain Institute, 2005.

[124] Chisti Y. Biodiesel from microalgae. Biotechnol Adv 2007;25(3):294-306.

[125] Demirbas A. Biodiesel: A Realistic Fuel Alternative for Diesel Engines. London: Springer - Verlag London Ltd, 2008.

[126] Ma F, Hanna MA. Biodiesel production: a review. Bioresour Technol 1999;70(1):1-15.

[127] Van Gerpen J. Biodiesel processing and production. Fuel Process Technol 2005;86(10):1097-1107.

[128] Kumabe K, Fujimoto S, Yanagida T, Ogata M, Fukuda T, Yabe A, Minowa T. Environmental and economic analysis of methanol production process via biomass gasification. Fuel 2008;87(7):1422-7.

[129] Al-Zuhair S. Production of biodiesel: possibilities and challenges. Biofuels Bioprod Bioref 2007;1(1):57-66.

[130] National Biodiesel Board: http://www.biodiesel.org, (October, 2009)

[131] Ma, F.; Hanna, A. M. Biodiesel production: a review. Biores Technol 1999;70:1-15.

[132] AOCS (American Oil Chemists' Society). Official Methods and Recommended Practices of the AOCS. 5th ed. Urbana: AOCS Press, 2000.

[133] Veljkovic VB, Lakicevic SH, Stamenkovic OS, Todorovic ZB, Lazic ML. Biodiesel production from tobacco (*Nicotiana tabacum L.*) seed oil with a high content of free fatty acids. Fuel 2006;85(17-18):2671-5.

[134] Al-Zuhair S. Production of biodiesel: Possibilities and challenges. Biofuels Bioprod Bioref 2007;1(1):57-66.

[135] Ma F, Hanna AM. Biodiesel production: a rewiew. Biores Technol 1999;70:1-15.

[136] NREL (National Renewable Energy Laboratory), PNNL (Pacific Northwest National Laboratory). Top value added chemicals from biomass Volume I – Results of screening for potential candidates from sugars and synthesis gas. Washington: U.S. Department of Commerce, 2004.

[137] Nagy M, Kerr BJ, Ziemer CJ, Ragauskas AJ. Phosphitylation and quantitative ^{31}P NMR analysis of partially substituted biodiesel glycerols. Fuel 2009;88:1793-7.

[138] NREL (National Renewable Energy Laboratory), PNNL (Pacific Northwest National Laboratory). Top value added chemicals from biomass Volume I – Results of screening for potential candidates from sugars and synthesis gas; Washington: U.S. Department of Commerce, 2004.

[139] Perlack RD, Wright LL, Turhollow AF, Graham RL, Stokes BJ, Erbach DC. Biomass as Feedstock for a Bioenergy and Bioproducts Industry: The Technical Feasibility of a Billion-Ton Annual Supply. Washington: USDE, 2005. available at: http://www.osti.gov/bridge (January, 2005)

[140] Bothast RJ, Saha C. Ethanol production from agricultural biomass substrates. Adv Appl Microbiol 1997;44:261-88.

[141] Zhu S, Wu Y, Yu Z, Gao M. Progress in production of fuel ethanol from lignocellulosic materials. Huaxue Yu Shengwu Gongcheng 2003;20(5):8-11. *General review written in Chinese*

[142] James LH. U.S. Timber production, trade, consumption and price statistics 1962-2002. Wisconsin, USDA Forest Service. Forest Product Laboratory, 2003.

[143] USDA-ERS (United States Department of Agriculture, Economic Research Service): http://www.ers.usda.gov (October, 2009)

[144] ORNL (Oak Ridge National Laboratory): http://www.ornl.gov/ (October, 2009)

[145] Rudder G. Pulp & Paper North American Fact Book 2002. San Francisco: Paperloop, 2002.

[146] EERE (Office of Energy Efficiency and Renewable Energy). Forest products industry of the future, annual report 2004. Washington: USDOE, 2004. Available electronically at: http://www.eere.energy.gov/industry/about/pdfs/forest_fy2004.pdf (October, 2009)

[147] EIA (Energy Information Administration). Selected Byproducts in Fuel Consumption in 2002. Available electronically: http://www.eia.doe.gov/emeu/mecs/mecs2002/data02/excel/table3.5_02.xls (October, 2009)

[148] Salmen L, Lucander M, Harkonen E, Sundholm J. Fundamentals of mechanical pulping. In: Papermaking Science and Technology. Gullichsen J (ed.), 5, p. 34-65. Helsinki: Fapet Oy, 1999.

[149] Pu Y, Lucia L, Ragauskas AJ, Naithani V, Jameel H. High-selectivity oxygen delignification of SW and HW kraft pulps with tailored bleachability properties. In: TAPPI Fall Technical Conference: Engineering, Pulping & PCE&I. p. 540-9. Norcross: TAPPI Press, 2003.

[150] Yang R, Lucia L, Ragauskas A, Jameel H. Oxygen degradation and spectroscopic characterization of hardwood kraft lignin. Ind Eng Chem Res 2002;41(24):5941-8.

[151] Carlton DW, Douglas RW. Pulp Bleaching, Principles and practice. Atlanta: TAPPI Press, 1996.

[152] Gullichsen J. Chemical Pulping. In: Papermaking Science and Technology, Book 6A. Fogelholm CJ (ed.), Helsinki: Fapet Oy, 1999.

[153] Gierer J. The chemistry of delignification. Holzforschung 1982;36:43-51.

[154] Gullichsen J, Fogelholm CJ. Chemical Pulping. Atlanta: TAPPI Press, 1999.

[155] Gellerstedt G, Lindfors E. Structural changes in lignin during Kraft pulping – Part 4: Phenolyc hydroxyl groups in wood and kraft pulps. Svensk Papperstidning 1984;15:115-7.

[156] Lai YZ, Mun S, Chen H. Variation of phenolic hydroxyl contents in unbleached Kraft pulps. Holzforschung 1995;49:319-22.

[157] Carlton DW, Douglas RW. Pulp Bleaching, Principles and practice. Atlanta: TAPPI Press, 1996.

[158] Suckling ID, Allison RW, Campion SH, McGrouther KG, McDonald AG. Monitoring cellulose degradation during conventional and modified kraft pulping. J Pulp Pap Sci 2001;27(10):336-41.

[159] Kim DH, Allison L, Carter B, Hou Q, Courchene C, Ragauskas AJ, Sealey J. Profiling the wood and pulping properties of southern pine thinning resources. Tappi J 2005;4(1)21-5.

[160] Casebier RL, Hamilton JK. Alkaline degradation of glucomannans and galactoglucomannans. Tappi J 1965;48(11):664-9.

[161] Gustavsson CAS, Al-Dajani WW. The influence of cooking conditions on the degradation of hexenuronic acid, xylan, glucomannan, and cellulose during kraft pulping of softwood. Nord Pulp Pap Res 2000;15(2)160-7.

[162] Chakar FS, Ragauskas AJ. Review of current and future softwood kraft lignin process chemistry. Ind Crop Prod 2004;20(2):131-41.

[163] Adams TN, Frederick WJ, Grace TM, Hupa M, Lisa K, Jones AK, Tran H. Kraft Recovery Boilers. Atlanta: TAPPI Press, 1997.

[164] Monzie-Giullemet D, Raoux H, Monzie P. Fractionation and determination of the organic constituents of black liquors. Chim Biochim Lignine In: Cellulose Hemicelluloses, p. 191-211. Grenoble, Actes Symp. Intern, 1964.

[165] Masura V. Combustion heat of black liquor components during kraft pulping. Vyskumne Prace z Odboru Papiera a Celulozy 1988;43(2-24):7-12.

[166] Gellerstedt G, Lindfors E. Structural Changes in Lignin During Kraft Pulping. Holzforschung 1984;38(3):151-8.

[167] Gellerstedt G, Lindfors, E. On the Formation of Enol Ether Structures in Lignin During Kraft Cooking. Nord Pulp Pap Res J 1987;2:71-5.

[168] Gellerstedt G, Lindfors E. On the Structure and Reactivity of Residual Lignin in Kraft Pulp Fibers. In: International Pulp Bleaching Conference Proceedings Vol. 1:73-88, Stockholm: SPCI, 1991.

[169] Iversen T, Wannstrom S. Lignin-Carbohydrate Bonds in a Residual Lignin Isolated from Pine Kraft Pulp. Holzforschung 1986;40(1):19-22.

[170] Gierer J, Wannstrom S. Formation of Ether Bonds between Lignins and Carbohydrates during Alkaline Pulping Processes. Holzforschung 1984;40(6):347-52.

[171] Froass PM, Ragauskas AJ, Jiang J. Chemical structure of residual lignin from Kraft pulp. J Wood Chem Technol 1996;16(4):347-65.

[172] Gierer J. Chemical Aspects of Kraft Pulping. Wood Sci Technol 1980;14:241-66.

[173] Froass PM, Ragauskas AJ, Jiang JE. NMR Studies. Part 3: Analysis of Lignins from Modern Kraft Pulping Technologies. Holzforschung 1998;52:385-90.

[174] Chakar FS, Ragauskas AJ. Review of current and future softwood kraft lignin process chemistry. Ind Corps Prod 2004;20:131-41.

[175] Gierer J. Chemistry of Delignification. Part 1. General Concept and Reactions during Pulping. Wood Sci Technol 1985;19:289-312.

[176] Minor JL. Chemical Linkage of Pine Polysaccharides to Lignin. J Wood Chem Technol 1982;2(1):1-16.

[177] Iverson T. Lignin-Carbohydrate Bonds in a Lignin-Carbohydrate Complex Isolated from Spruce. Wood Sci Technol 1985;19:243-51.

[178] Gierer J, Wannstrom S. Formation of Ether Bonds between Lignins and Carbohydrates during Alkaline Pulping Processes. Holzforschung 1984;40(6):347-52.

[179] Yamasaki T, Hosoya S, Chen CL, Gratzl JS, Chang HM. Characterization of Residual Lignin in Kraft Pulp. In: International Symposium on Wood and Pulping Chemistry Proceedings Vol.2:34-42, Stockholm: Eckman, 1981.

[180] Schlaf M. Selective deoxygenation of sugar polyols to α,ω-diols and other oxygen content reduced materials – a new challenge to homogeneous ionic hydrogenation and hydrogenolysis catalysis. Dalton Trans 2006:4645-53.

[181] Luijkx GCA, Rantwijk F, Bekkum H, Antal MJ. The role of deoxyhexonic acids in the hydrothermal decarboxylation of carbohydrates. Carbohydr Res 1995;272:191-202.

[182] Atutxa A, Aguado R, Gayubo AG, Olazar M, Bilbao J. Kinetic description of the catalytic pyrolysis of biomass in a conical spouted bed reactor. Energ Fuels 2005;19:765-74.

[183] Ercin D, Yurum Y. Carbonisation of fir (*Abies bornmuelleriana*) wood in an open pyrolysis system at 50° - 300°. J Anal Appl Pyrol 2003;67:11-22.

[184] Ohyama S, Popp KE, Kung MC, Kung HH. Effect of vanadia on the performance of NiO in vapor-phase oxidative decarboxylation of benzoic acid to phenol. Catal Comm 2002;3:357-62.

[185] Favier I, Dunach E, Hebrault D, Desmurs JR. $CoCl_2$ catalyzed decarboxylation-oxidation of mandelic acids by molecular oxygen. New J Chem 2004;28:62-6.

[186] Masende ZPG, Kuster BFM, Ptasinski KJ, Janssen FJJG, Katima JHY, Schouten JC. Support and dispersion effects on activity of platinum catalysts during wet oxidation of organic wastes. Top Catal 2005;33:87-99.

[187] Hu TQ, James BR, Rettig SJ, Lee CL. Stereoselective hydrogenation of lignin degradation model compounds. Can J Chem 1997;75:1234-39.

[188] Furimsky E. Catalytic hydrodeoxygenation. Appl Catal Gen 2000;199:147-90.

[189] Schweers W. Hydrogenolysis of lignin. III. Comparative hydration of 4-alkylphenols and 4-alkylguiacols. Holzforschung 1969;23:120-7.

[190] Hastbacka K, Bredenberg JBS. Hydrocracking of lignin tar and lignin model compounds. Pap Puu 1973;55:129-34.

[191] Stray G, Cassidy PJ, Jackson WR, Larkins FP, Sutton JF. Studies related to the structure and reactivity of coals. 11. The hydrogenation of lignin. Fuel 1986;65:1524-30.

[192] Schweers W, Beinhoff O. Hydrogenolysis of lignin. V. Comparative hydrogenation of 4-alkylsyringoles. Holzforschung 1974;28:20-4.

[193] Eachus SW, Dence CW. Hydrogenation of lignin model compounds in the presence of a homogeneous catalyst. Holzforschung 1975;29:41-8.

[194] Wong TYH, Pratt R, Leonog CG, James BR, Hu TQ. Catalytic hydrogenation of lignin aromatics using Ru-arene complexes. Chem Ind 2001;82:255-66.

[195] Hu TQ, James BR. Catalytic modification and photostabilization of lignin functional groups. In: Chemical modification, properties, and usage of lignin. Ed. Hu TQ, p. 247-65, New York: Kluwer Academic/Plenum Publishers, 2002.

[196] Hernandez M, Kalck P. Water-soluble ruthenium complexes containing tris(m-sulfonatophenyl)phosphine (TPPTS). Preparation of a series of $[Ru(H)(\eta^6\text{-arene})(TPPTS)_2]Cl$ complexes, $[Ru(H)_2(CO)(TPPTS)_3]$ and revisited procedures for previously described ruthenium-TPPTS compounds. J Mol Catal Chem 1997;116:117-30.

[197] Hernandez M, Kalck P. Study of the hydrogenation of α,β -unsaturated carbonyl compounds catalyzed by water-soluble ruthenium-TPPTS complexes. J Mol Catal Chem 1997;116:131-46.

[198] Schlaf M. Selective deoxygenation of sugar polyols to α,ω-diols and other oxygen content reduced materials – a new challenge to homogeneous ionic hydrogenation and hydrogenolysis catalysis. Dalton Trans 2006;4645-53.

[199] Luijkx GCA, Rantwijk F, Bekkum H, Antal MJ. The role of deoxyhexonic acids in the hydrothermal decarboxylation of carbohydrates. Carbohyd Res 1995;272:191-202.

[200] Atutxa A, Aguado R, Gayubo AG, Olazar M, Bilbao J. Kinetic Description of the Catalytic Pyrolysis of Biomass in a Conical Spouted Bed Reactor. Energ Fuels 2005;19:765-74.

[201] Motoyoshi O, Kan K. Liquefaction of lignin: Production of raw materials for organic synthesis by high pressure hydrogenation of lignin. In; Annual report of the Noguchi Institute. Ed. 9, Tokyo: The Noguchi Institute, 1960.

[202] Gayubo AG, Aguayo AT, Atutxa A, Aguado R, Bilbao J. Transformation of Oxygenate Components of Biomass Pyrolysis Oil on a HZSM-5 Zeolite. I. Alcohols and Phenols. Ind Eng Chem Res 2004;43:2610-8.

[203]Gayubo AG, Aguayo AT, Atutxa A, Aguado R, Bilbao J. Transformation of Oxygenate Components of Biomass Pyrolysis Oil on a HZSM-5 Zeolite. II. Aldehydes, Ketones, and Acids. Ind Eng Chem Res 2004;43:2619-26.

[204] Vitolo S, Bresci B, Seggiani M, GalloMG. Catalytic upgrading of pyrolytic oils over HZSM-5 zeolite: behaviour of the catalyst when used in repeated upgrading-regenerating cycles. Fuel 2001;80:17-26.

[205] Ercin D, Yurum Y. Carbonisation of Fir (*Abies bornmulleriana*) wood in an open pyrolysis system at 50–300 °C. J Anal App Pyr 2003;67:11–22.

[206] Gayubo AG, Aguayo AT, Atutxa A, Aguado R, Bilbao J. Transformation of Oxygenate Components of Biomass Pyrolysis Oil on a HZSM-5 Zeolite. I. Alcohols and Phenols. Ind Eng Chem Res 2004;43:2610-8.

[207] Gayubo AG, Aguayo AT, Atutxa A, Aguado R, Bilbao J. Transformation of Oxygenate Components of Biomass Pyrolysis Oil on a HZSM-5 Zeolite. II. Aldehydes, Ketones, and Acids. Ind Eng Chem Res 2004;43:2619-26

[208] Wallmo H, Richards T, Theliander H. Lignin precipitation from kraft black liquors: kinetics and carbon dioxide absorption. Paperi ja Puu 2007:89:436-42.

[209] Ohman F, Wallmo H Theliander H. Precipitation and filtration of lignin from black liquor of different origin. Nord Pulp Pap Res J 2007;22(2):188-193.

[210] Moosavifar A, Sedin P Theliander H. Viscosity and boiling point elevation of black liquor: Consequences when lignin is extracted from the black liquor. Nord Pulp Pap Res J 2006:21(2):180-7.

[211] Moosavifar A, Sedin P, Brelid H, Theliander H. Modification of precipitated kraft lignin through the addition of calcium - reduction of SO_2 emission. Nord Pulp Pap Res J 2006;21(4):493-5.

[212] Luotfi H, Blackwell B, Uloth V. Lignin recovery from kraft black liquor: preliminary process design. TAPPI J 1991:74(1):203-10.

[213] Ohman F, Theliander H, Tomani P, Axegard P, Patent WO 2006/031175 A1, 2006.

[214] Alen R, Sjostrom E, Vaskikari P. Carbon dioxide precipitation of lignin from alkaline pulping liquors. Cellulose Chem Technol 1985;19(5):537-41.

[215] Zaman AA, Fricke AL. Correlations for viscosity of kraft black liquors at low solids concentrations. AIChE J 1994;40(1):187-92.

[216] Adams TN, Frederick WJ, Grace TM, Hupa M, Lisa K, Jones AK, Tran H. Kraft Recovery Boilers. Atlanta: TAPPI Press, 1997.

[217] Moosavifar A, Sedin P, Theliander H. Viscosity and boiling point elevation of black liquor: consequences when lignin is extracted from the black liquor. Nord Pulp Pap Res J 2006;21(2):180-7.

[218] Wintoko J, Theliander H, Richards T. Experimental Investigation of black liquor pyrolysis using single droplet TGA. TAPPI J 2007;6(5):9-15.

[219] Öhman F, Theliander H. Washing lignin precipitated from kraft black liquor Paperi ja Puu 2006;88(5):287-92.

[220] Öhman F, Wallmo H, Theliander H. An improved method for washing lignin precipitated from kraft black liquor - the key to a new biofuel. Filtration 2007;7(4):309-15.

[221] Wallmo H, Theliander H, Richards T. Lignin precipitation from kraft black liquors: kinetics and carbon dioxide absorption. Paperi ja Puu 2007;89(7-8):436-42.

[222] Wisisng U, Algehed J, Berntsson T, Delin L. Consequences of lignin precipitation in the pulp and paper industry. Tappi J 2006;5(1):3-8.

[223] Ohman F, Theliander H. Washing lignin precipitated from kraft black liquor Paperi ja Puu 2006;88(5):287-92.

[224] Laaksometsa C, Axelsson E, Berntsson T, Lundstrom A. Energy savings combined with lignin extraction for production increase: case study at a eucalyptus mill in Portugal. Clean Techn Envinron Policy 2009:11(1):77-82.

[225] Olsson M, Axelsson E, Berntsson T. Heat integration opportunities in average Scandinavian kraft pulp mills: Pinch analyses of model mills. Nord Pulp Pap Res J 2006;21(4):466-75.

[226] Thorpe B. Industry/government partnership targets new energy strategies, Solutions! 2003;86(9):35-36.

[227] Kamm B, Kamm M. Principles of biorefineries. Appl Microbiol Biotechnol 2004;64(2):137-45.

[228] VAC (Vacuum/Atmospheres Company). DRI-TRAIN Technical Manual: Model HE-493. HE-493-7/80, Hawthorne: VAC, 1992.

[229] Öhman F, Theliander H, Tomani P Axegard P, Patent WO 2006/031175 A1, 2006.

[230] Öhman F, Wallmo H, Theliander H. An improved method for washing lignin precipitated from kraft black liquor - the key to a new biofuel. Filtration 2007;7(4):309-15.

[231] Froass P, Ragauskas AJ, Jiang JE. NMR Studies Part 3: Analysis of Lignins from Modern Kraft Pulping Technologies. Holzforschung 1998;52(4):385-90.

[232] Pan X, Xie D, Yu WR, Lam D, Saddler NJ. Pretreatment of logepole pine killed by mountain pine beetle using the ethanol organosolv process: Fractionation and process optimization. Ind Eng Chem Res 2007;46:2609-17.

[233] Armit PW, Boyd ASF, Stephenson TA. Synthesis and rearrangement reactions of dihalogenotris- and dihalogenotetrakis-(tertiary phosphine)ruthenium(II) compounds. Dalton Trans 1975:1663-72.

[234] Osborn JA, Wilkinson G. Tris(triphenylphosphine)halorhodium. Inorg Synth 1967;10:67-71.

[235] Senol OI, Viljava TR, Krause AOI. Effect of sulphiding agents on the hydrodeoxygenation of aliphatic esters on sulphided catalysts. Appl Catal Gen 2007;326:236-44.

[236] Yoosuk B, Kim JH, Song C, Ngamcharussrivichai C, Prasassarakich P. Highly active MoS_2, $CoMoS_2$ and $NiMoS_2$ unsupported catalysts prepared by hydrothermal synthesis for hydrodesulfurization of 4,6-dimethyldibenzothiophene. Catal Today 2008;130:14-23.

[237] Yan N, Zhao C, Luo C, Dyson PJ, Liu H, Kou Y. One-step conversion of cellobiose to C_6-alcohols using Ruthenium nanocluster catalyst. J Am Chem Soc. 2006;128(27):8714-5.

[238] Weiyong Y, Manhog L, Hanfan L, Xiaoming M, Zhijie L, J Coll Interface Sci 1998;208:439-44.

[239] Haenel WM, Narangerel J, Richter UB, Rufinska A. The first liquefaction of high-rank bituminous coals by preceding hydrogenation with homogeneous borane and iodine catalysts. Angew Chem Int Ed 2006;45:1061-66.

[240] Moe ST, Ragauskas AJ. Oxygen delignification of high-yield kraft pulp Part 1. Structural properties of residual lignins. Holzforschung 1999;53:416-22.

[241] Runge TM, Ragauskas AJ. NMR analysis of alkaline extraction stage lignins. Holzforschung 1999;53:623-31.

[242] Granata A, Argyropoulos DS. 2-Chloro-4,4,5,5-tetramethyl-1,3,2-dioxaphospholane, a reagent for the accurate determination of the uncondensed and condensed phenolic moieties in lignins. J Agric Food Chem 1995;43:1538-44.

[243] Pu Y, Ragauskas AJ. Structural analysis of acetylated hardwood lignins and their photoyellowing properties. Can J Chem 2005;83:2132-39.

[244] Baumberger S, Abaecherli A, Fasching M, Gellerstedt G, Gosselink R, Hortling B, Li J, Shaake B, Jong ED. Molar mass determination of lignins by size-exclusion chromatography: towards standardization of the method. Holzforschung 2007;61:459-68.

[245] Ragauskas A.J, Nagy M, Kim DH, Eckert CA, Hallett JP, Liotta CL. From wood to fuels: Integrating biofuels and pulp production. Ind Biotechnol 2006;2:55-65.

[246] Gullichsen J, Fogelholm CJ. Chemical Pulping. Atlanta: TAPPI Press, 1999.

[247] Carlton DW, Douglas RW. Pulp Bleaching, Principles and practice. Atlanta: TAPPI Press, 1996.

[248] Wallmo H, Theliander H, Richards T. Lignin precipitation from kraft black liquors: kinetics and carbon dioxide absorption. Paperi ja Puu 2007;89(7-8):436-42.

[249] Öhman F, Wallmo H Theliander H. Precipitation and filtration of lignin from black liquor of different origin. Nord Pulp Pap Res J 2007;22(2):188-193.

[250] Moosavifar A, Sedin P, Theliander H. Viscosity and boiling point elevation of black liquor: consequences when lignin is extracted from the black liquor. Nord Pulp Pap Res J 2006;21(2):180-7.

[251] Luotfi H, Blackwell B, Uloth V. Lignin recovery from kraft black liquor: preliminary process design. TAPPI J 1991:74(1):203-10.

[252] Olsson M, Axelsson E, Berntsson T. Heat integration opportunities in average Scandinavian kraft pulp mills: Pinch analyses of model mills. Nord Pulp Pap Res J 2006;21(4):466-75.

[253] Wisisng U, Algehed J, Berntsson T, Delin L. Consequences of lignin precipitation in the pulp and paper industry. Tappi J 2006;5(1):3-8.

[254] Laaksometsa C, Axelsson E, Berntsson T, Lundstrom A. Energy savings combined with lignin extraction for production increase: case study at a eucalyptus mill in Portugal. Clean Techn Envinron Policy 2009:11(1):77-82.

[255] Öhman F, Wallmo H, Theliander H. An improved method for washing lignin precipitated from kraft black liquor - the key to a new biofuel. Filtration 2007;7(4):309-15.

[256] Chakar FS, Ragauskas AJ. Review of current and future softwood kraft lignin process chemistry. Ind Corps Prod 2004;20:131-41.

[257] Nagy M, Kasi D, Britovsek GJP, Ragauskas AJ. Organosolv lignin hydrogenolysis to value added chemicals, Holzforschung 2009;63:513-20.

[258] Baumberger S, Abaecherli A, Fasching M, Gellerstedt G, Gosselink R, Hortling B, Li J, Saake B, and Jong E, Molar mass determination of lignins by size-exclusion chromatography: towards standardisation of the method. Holzforschung 2007;61(4):459-68.

[259] Davin LB, Lewis NG. Lignin primary structures and dirigent sites. Curr Opin Biotechnol 2005;16(4):407-15.

[260] Wallmo H, Richards T, Theliander H. Lignin precipitation from kraft black liquors: kinetics and carbon dioxide absorption. Paperi ja Puu 2007:89:436-42.

[261] Kamm B, Kamm M. Principles of biorefineries. Appl Microbiol Biotechnol 2004;64:137–45.

[262] Chiellini E. Environmentally degradable biobased polymeric blends and composites. In: Abstracts of Papers, 227th ACS National Meeting. Washington: ACS, 2004.

[263] Hu TQ, James BR, Rettig SJ, Lee CL. Stereoselective hydrogenation of lignin degradation model compounds. Can J Chem 1997;75:1234-9.

[264] Rodgers R, Blumer EN, Freitas MA, Marshall AG. Complete compositional monitoring of the weathering of transportation fuels based on elemental compositions from fourier transform ion cyclotron resonance mass spectrometry. Environ Sci Technol 200;34:1671-8.

[265] Briker Y, Ring Z, Iacchelli A, McLean N, Rahimi PM, Fairbridge C, Malhotra R, Coggiola MA, Young SE. Diesel fuel analysis by GC-FIMS: Aromatics, n-paraffins, and isoparaffins. Energ Fuels 2001;15:23-37.

[266] Pu Y, Zhang D, Singh PM, Ragauskas AJ. The new forestry biofuels sector. Biofuels Bioprod Bioref 2008;2:58-73.

[267] Vasilakos NP, Barreiros MT. Homogeneous catalytic hydrogenolysis of biomass. Ind. Chem. Process. Dev. 1984;23:755-63.

[268] Gayubo AG, Aguayo AT, Atutxa A, Aguado R, Olazar M, Bilbao J. Transformation of oxygenate components of biomass pyrolysis oil on a HZSM-5 zeolite. II: aldehydes, ketones, and acids. Ind. Eng. Chem. Res. 2004;43:2619-26.

[269] Pan X, Xie D, Yu WR, Lam D, Saddler NJ. Pretreatment of logepole pine killed by mountain pine beetle using the ethanol organosolv process: Fractionation and process optimization. Ind Eng Chem Res 2007;46:2609-17.

[270] Schweers W. Hydrogenolysis of lignin. III. Comparative hydration of 4-alkylphenols and 4-alkylguiacols. Holzforschung 1969;23:120-7.

[271] Hastbacka K, Bredenberg JBS. Hydrocracking of lignin tar and lignin model compounds. Pap. Puu 1973;55:129-34.

[272] Stray G, Cassidy PJ, Jackson WR, Larkins FP, Sutton JF. Studies related to the structure and reactivity of coals. 11. The hydrogenation of lignin. Fuel 1986;65:1524-30.

[273] Schweers W, Beinhoff O. Hydrogenolysis of lignin. V. Comparative hydrogenation of 4-alkylsyringoles. Holzforschung 1974;28:20-4.

[274] Eachus SW, Dence CW. Hydrogenation of lignin model compounds in the presence of a homogeneous catalyst. Holzforschung 1975;29:41-8.

[275] Wong TYH, Pratt R, Leonog CG, James BR, Hu TQ. Catalytic hydrogenation of lignin aromatics using Ru-arene complexes. Chem Ind 2001;82:255-66.

[276] Hu TQ, James BR. Catalytic modification and photostabilization of lignin functional groups. In: Chemical modification, properties, and usage of lignin. p. 247-56. New York: Kluwer Academic/Plenum Publishers, 2002.

[277] Hernandez M, Kalck P. Water-soluble ruthenium complexes containing tris(m-sulfonatophenyl)phosphine (TPPTS). Preparation of a series of $[Ru(H)(\eta^6\text{-arene})(TPPTS)_2]Cl$ complexes, $[Ru(H)_2(CO)(TPPTS)_3]$ and revisited procedures for previously described ruthenium-TPPTS compounds. J Mol Catal Chem 1997;116:117-30.

[278] Hernandez M, Kalck P. Study of the hydrogenation of α,β -unsaturated carbonyl compounds catalyzed by water-soluble ruthenium-TPPTS complexes. J Mol Catal Chem 1997;116:131-46.

[279] Armit PW, Boyd ASF, Stephenson TA. Synthesis and rearrangement reactions of dihalogenotris- and dihalogenotetrakis-(tertiary phosphine)ruthenium(II) compounds. Dalton Trans 1975:1663-72.

[280] Liitia T, Maunu SL, Sipila J, Hortling B. Application of solid-state ^{13}C NMR spectroscopy and dipolar dephasing technique to determine the extent of condensation in technical lignins. Solid State Nucl Magn Reson 2002;21:171-86.

[281] Gellerstedt G, Majtnerova A, Zhang L. Towards a new concept of lignin condensation in kraft pulping. C R Biol 2004;327:817-26.

[282] Palfray L, Gauthier B. Hydrogenation of some phenolic ethers with Raney nickel. Bull Soc Chim Fr 1947;676-9. *Manuscript is written in French*.

[283] Tundo P, Perosa A, Zinovyev S. Modifier effects on Pt/C, Pd/C, and Raney-Ni catalysts in multiphase catalytic hydrogenation systems. Appl Catal Gen 2003;204-5:747-54.

[284] Evdokimova G, Zinovyev S, Perose A, Tundo P. Selectivity issues in the catalytic multiphase reduction of functionalized halogenated aromatics over Pd/C, Pt/C, and Raney-Ni. Appl Catal Gen 2004;271:129-36.

[285] Hu TQ, James BR, Rettig SJ, Lee CL. Stereoselective hydrogenation of lignin degradation model compounds. Can J Chem 1997;75:1234-39.

[286] James BR, Wang Y, Alexander CS, Hu TQ. Catalytic hydrogenation of aromatic rings in lignin. Chem Ind 1998;75:233-42.

[287] Wong TYH, Pratt R, Leonog CG, James BR, Hu TQ. Catalytic hydrogenation of lignin aromatics using Ru-arene complexes. Chem Ind 2001;82:255-66.

[288] Haenel WM, Narangerel J, Richter UB, Rufinska A. The first liquefaction of high-rank bituminous coals by preceding hydrogenation with homogeneous borane and iodine catalysts. Angew Chem Int Ed 2006;45:1061-66.

[289] Yan N, Zhao C, Dyson PJ, Wang C, Liu LT, Kou Y. Selective degradation of wood lignin over noble-metal catalysts in a two-step process. ChemSusChem 2008;1:626-9.

[290] Thakar N, Polder NF, Djanashvili K, Bekkum H, Kapteijn F, Moulijn JA. Deuteration study to elucidate hydrogenolysis of benzylic alcohols over supported palladium catalysts. J Catal 2007;246:344-50.

[291] Brown HC, Mead EJ, Subba Rao BC. A Study of Solvents for Sodium Borohydride and the Effect of Solvent and the Metal Ion on Borohydride Reductions. J Am Chem Soc 1995;77(23):6209-13.

[292] Thomas RM, Mohan GH, Iyengar DS. A Novel, mild and facile reductive cleavage of allyl ethers by $NaBH_4/I_2$ sytem. Tetrahedron Lett 1998;39:677-8.

[293] Biswanath DA, Kashinatham P. Madhusudhan, Regioselective reduction of the α,β – double bond of some naturally occurring dienamides using $NaBH_4/I_2$ system. *Tetrahedron Lett, 1997;*38(26):4721-4.

[294] Russo A, Tonelli C. Unexpected effect of alkoxides on the reactivity of sodium borohydrid in the reduction of perfluoropolyether carboxylic esters. J F Chem 2004;125:181-8.

[295] Haenel MW, Narangerel J, Richter UB, Rufinska A. The first liquefaction of high-rank bituminous coals by preceding hydrogenation with homogeneous borane or iodine catalysts. Angew Chem Int Ed 2006;45:1061-66. (Supporting Information)

[296] Ragauskas AJ, Williams CK, Davison BH, Britovsek G, Cairney J, Eckert CA, Frederick W Jr, Hallett JP, Leak DJ, Liotta CL, Mielenz JR, Murphy R, Templer R, Tschaplinski T. The Path Forward for Biofuels and Biomaterials. Science 2006;311(5760):484-9.

[297] Pacala S, Socolow R. Stabilization Wedges: Solving the Climate Problem for the Next 50 Years with Current Technologies. Science 2004;305(5686):968-72.

[298] M. Johnston and T. Holloway, A Global Comparison of National Biodiesel Production Potentials. Environ Sci Technol 2007;41(23):7967-73.

[299] NBB (National Biodiesel Board): http://www.biodiesel.org (October, 2009)

[300] Demirbas A. Biodiesel: A Realistic Fuel Alternative for Diesel Engines London: Springer - Verlag London Ltd., 2008.

[301] Chisti Y. Biodiesel from microalgae. Biotechnol Adv 2007;25(3):294-306.

[302] Ito T, Nakashimada Y, Senba K, Matsui T, Nishio N. Hydrogen and ethanol production from glycerol-containing wastes discharged after biodiesel manufacturing process. J Biosci Bioeng 2005;100(3):260-5.

[303] Imandi SB, Bandaru VVR, Somalanka SR, Garapati HR. Optimization of medium constituents for the production of citric acid from byproduct glycerol using Doehlert experimental design. Enzyme Microbial Technol 2007;40(5):1367-72.

[304] Marchetti JM, Miguel VU, Errazu AF. Possible methods for biodiesel production. Renew Sustain En Rev 2007:11(6):1300-11.

[305] Gibbs HK, Johnston M, Foley JA, Holloway T, Monfreda C, Ramankutty N, Zaks D. Carbon payback times for crop-based biofuel expansion in the tropics: the effects of changing yield and technology. Environ Res Let 2008;3(3): doi:10.1088/1748-9326/3/3/034001

[306] Holcapek M, Jandera P, Fischer J, Prokes B. Analytical monitoring of the production of biodiesel by high-performance liquid chromatography with various detection methods. J Chromatogr A 1999; 858(1):13-31.

[307] Plank C, Lorbeer E. Simultaneous determination of glycerol, and mono-, di- and triglycerides in vegetable oil methyl esters by capillary gas chromatography. J Chromatogr A 1995; 697(1+2):461-8.

[308] ASTM. ASTM D 6584-07. In: ASTM, editors. Annual Book of ASTM Standards, West Conshohocken: ASTM International; 2007.

[309] Knothe, G. Monitoring a progressing transesterification reaction by fiber-optic near infrared spectroscopy with correlation to 1H nuclear magnetic resonance spectroscopy. J Am Oil Chem Soc 2000; 77(5):489-93.

[310] Knothe G. Analyzing biodiesel: standards and other methods. J Am Oil Chem Soc 2006; 83(10):823-33.

[311] Granata A, Argyropoulos DS. 2-Chloro-4,4,5,5-tetramethyl-1,3,2-dioxaphospholane, a reagent for the accurate determination of the uncondensed and condensed phenolic moieties in lignins. J Agric Food Chem 1995;43:1538-44.

[312] Zawadzki M, Ragauskas AJ. N-Hydroxy Compounds as New Internal Standards for the ^{31}P-NMR Determination of Lignin Hydroxy Functional Groups. Holzforschung 2001;55:283-5.

[313] Chakar FS, Ragauskas AJ. Review of current and futures of wood kraft lignin process chemistry. Ind Crops Prod 2004;20:131–41.

[314] Pu Y, Ragauskas AJ. Structural analysis of acetylated hardwood lignins and their photoyellowing properties. Can J Chem 2005;83:2132-39.

[315] Al-Zuhair S. Production of biodiesel: possibilities and challenges. Biofuels Bioprod Bioref 2007;1(1):57-66.

[316] RFA (Renewable Fuels Association): http://www.ethanolrfa.org, (October, 2009)

[317] Chisti Y. Biodiesel from microalgae. Biotechnol Adv 2007;25(3):294-306.

[318] Demirbas A. Biodiesel: A Realistic Fuel Alternative for Diesel Engines. London: Springer - Verlag London Ltd; 2008.

[319] Ma F, Hanna MA. Biodiesel production: a review. Bioresour Technol 1999;70(1):1-15.

[320] Van Gerpen J. Biodiesel processing and production. Fuel Process Technol 2005;86(10):1097-107.

[321] Kumabe K, Fujimoto S, Yanagida T, Ogata M, Fukuda T, Yabe A, Minowa T. Environmental and economic analysis of methanol production process via biomass gasification. Fuel 2008;87(7):1422-7.

[322] Al-Zuhair S. Production of biodiesel: possibilities and challenges. Biofuels Bioprod Bioref 2007; 1(1):57-66.

[323] NBB (National Biodiesel Board): http://www.biodiesel.org (October, 2009)

[324] Holcapek M, Jandera P, Fischer J, Prokes B. Analytical monitoring of the production of biodiesel by high-performance liquid chromatography with various detection methods. J Chromatogr A 1999; 858(1):13-31.

[325] Plank C, Lorbeer E. Simultaneous determination of glycerol, and mono-, di- and triglycerides in vegetable oil methyl esters by capillary gas chromatography. J Chromatogr A 1995; 697(1+2):461-8.

[326] ASTM. ASTM D 6584-07. In: ASTM, editors. Annual Book of ASTM Standards, West Conshohocken: ASTM International; 2007.

[327] Knothe, G. Monitoring a progressing transesterification reaction by fiber-optic near infrared spectroscopy with correlation to ^{1}H nuclear magnetic resonance spectroscopy. J Am Oil Chem Soc 2000;77(5):489-93.

[328] Knothe G. Analyzing biodiesel: standards and other methods. J Am Oil Chem Soc 2006;83(10):823-33.

[329] Nagy M, Alleman TL, Dyer T, Ragauskas AJ. Quantitative NMR analysis of partially substituted biodiesel glycerols. J Biobased Mater Bioeng 2009;3:1-4.

[330] Pu Y, Ragauskas AJ. Structural analysis of acetylated hardwood lignins and their photoyellowing properties. Can J Chem 2005;83(12):2132-9.

[331] Pu Y, Anderson S, Lucia L, Ragauskas AJ. Investigation of the photooxidative chemistry of acetylated softwood lignin. J Photochem Photobiol 2004; 163(1-2):215-21.

[332] AOCS. Official Methods and Recommended Practices of the AOCS. 5th ed. Champaign: American Oil Chemists' Society; 2000.

[333] Veljkovic VB, Lakicevic SH, Stamenkovic OS, Todorovic ZB, Lazic ML. Biodiesel production from tobacco (Nicotiana tabacum L.) seed oil with a high content of free fatty acids. Fuel 2006; 85(17-18):2671-5.

[334] Gerpen JV, Shanks B, Pruszko R, Clements D, Knothe G. Biodiesel analytical methods. NREL/SR-510-36240. Colorado: NREL; 2004.

[335] Knothe G. Dependence of biodiesel fuel properties on the structure of fatty acid alkyl esters. Biodiesel Proc Prod 2005;86(10):1059-70.

[336] Nagy M, Kerr BJ, Ziemer CJ, Ragauskas AJ. Phosphitylation and quantitative ^{31}P NMR analysis of partially substituted biodiesel glycerols. Fuel 2009;88(9):1973-7.

[337] Knothe G, Krahl J, Gerpen JV. The biodiesel handbook. Campaign: AOCS Press, 2005.

[338] Holcapek M, Jandera P, Fischer J, Prokes B. Analytical monitoring of the production of biodiesel by high-performance liquid chromatography with various detection methods. J Chromatogr A 1999; 858(1):13-31.

[339] Plank C, Lorbeer EJ. Simultaneous determination of glycerol, and mono-, di- and triglycerides in vegetable oil methyl esters by capillary gas chromatography. Chromatogr A 1995;697(1-2):461-8.

[340] ASTM International. Annual Book of ASTM Standards. West Conshohocken: ASTM International, 2007.

[341] Knothe, G. Monitoring a progressing transesterification reaction by fiber-optic near infrared spectroscopy with correlation to 1H nuclear magnetic resonance spectroscopy. J Am Oil Chem Soc 2000; 77(5):489-93.

[342] Knothe G. Analyzing biodiesel: standards and other methods. J Am Oil Chem Soc 2006; 83(10):823-33.

[343] Granata A, Argyropoulos DS. 2-Chloro-4,4,5,5-tetramethyl-1,3,2-dioxaphospholane, a reagent for the accurate determination of the uncondensed and condensed phenolic moieties in lignins. J Agric Food Chem 1995;43:1538-44.

[344] Nagy M, Alleman TL, Dyer T, Ragauskas AJ. Quantitative NMR analysis of partially substituted biodiesel glycerols. J Biobased Mater Bioen 2009;3(1):108-11.

[345] Mazur M, Argyropoulos DS. ^{31}P NMR spectroscopy in wood chemistry. VII. Studies toward elucidating the phosphorus relaxation mechanism of phosphitylated lignins. Cell Chem Tech 1995;29(5):589-601.

[346] Argyropoulos DSJ. Quantitative phosphorus-31 NMR analysis of lignins, a new tool for the lignin chemist. Wood Chem Technol 1994;14:45-63.

[347] Zawadzki M, Ragauskas AJ. N-Hydroxy Compounds as New Internal Standards for the ^{31}P-NMR Determination of Lignin Hydroxy Functional Groups. Holzforschung 2001;55:283-5.

[348] Pu Y, Ragauskas AJ. Structural analysis of acetylated hardwood lignins and their photoyellowing properties. Can J Chem 2005;83:2132-39.

[349] Chakar FS, Ragauskas AJ. The Effects of Oxidative Alkaline Extraction Stages After Laccase HBT and Laccase NHAA Treatments-An NMR Study of Residual Lignins. J Wood Chem Technol 2000;20(2):169-84.

[350] Argyropoulos DS. ^{31}P NMR in wood chemistry: A review of recent progress. Wood Chem Technol 1995;21(3-5):373-95.

[351]Holser, R. A.; Willett, J. L.; Vaughn, S. F. J. Thermal and Physical Characterization of Glycerol Polyesters. Biobased Mater Bioen 2008;2(1):94-6.

[352] Ma F, Hanna MA. Biodiesel production: a review. Bioresour Technol 1999;70(1):1-15.

[353] Gerpen JV, Shanks B, Pruszko R, Clements D, Knothe G. Biodiesel analytical methods. Colorado: NREL, 2004.

[354] Demirbas A. Biodiesel: A Realistic Fuel Alternative for Diesel Engines. London: Springer - Verlag London Ltd; 2008.

[355] AOCS. Official Methods and Recommended Practices of the AOCS. 5th ed. Champaign: American Oil Chemists' Society; 2000.

[356] Veljkovic VB, Lakicevic SH, Stamenkovic OS, Todorovic ZB, Lazic ML. Biodiesel production from tobacco (*Nicotiana tabacum L.*) seed oil with a high content of free fatty acids. Fuel 2006;85(17-18):2671-5.

[357] Al-Zuhair S. Production of biodiesel: possibilities and challenges. Biofuels Bioprod Bioref 2007; 1(1):57-66.

[358] NREL (National Renewable Energy Laboratory), PNNL (Pacific Northwest National Laboratory). Top value added chemicals from biomass Volume I – Results of screening for potential candidates from sugars and synthesis gas; Washington: U.S. Department of Commerce, 2004.

[359] Gierer J. Chemistry of delignification. Part 1. General concept and reactions during pulping. Wood Sci Technol 1985;19:289–312.